DIRECT DESIGN METHODS FOR ELECTRICAL FILTERS AND DIPLEXERS.

by

JOHN LESLIE HAINE, B.Sc.(Hons).

Submitted in fulfilment of the requirements of the degree of Doctor of Philosophy.

The University of Leeds,
Department of Electrical and Electronic Engineering.

December 1977.

Research carried out between September 1974 and September 1977, under the supervision of Professor J.D. Rhodes.

SUMMARY.

This thesis is concerned with developing design procedures for filters and diplexers. Its object is to present methods which the practicing engineer can use to design high-performance devices without necessarily being familiar with the technical details of circuit theory.

The basics of circuit and filter theory are reviewed and then several design methods for bandpass filters are examined. These include a new design procedure for single-sideband crystal filters.

Next, the thesis reviews the existing methods of diplexer design. Particular attention is given to those methods which use directly-interacting filters. These all share the disadvantage that only contiguous designs are possible.

A new method of designing non-contiguous bandpass diplexers is then developed. Computed and experimental results demonstrate the high performance possible with the new technique. Finally, the basic theory of the new method is applied to some other problems in diplexer and filter design.

Acknowledgements.

I would like to thank the many members of the Department of Electrical and Electronic Engineering at Leeds University who have helped in the research which led to this thesis. I should like especially to thank Mrs. G. Garbett for her expert typing.

I would like to tnank my wife for her help with the thesis, and her tolerance during many days of neglect.

The U.K. Science Research Council assisted with a studentship between 1974 and 1977.

The Marconi Company kindly provided photocopying facilities, for which I am very grateful.

Most of all, I am in debt to Professor David Rhodes of Leeds University for his expert advice, help, and encouragement during my time at the university.

Symbols and Abbreviations.

Algebraic quantities are defined as they arise in the text. The following special symbols occur in some of the derivations:

$A \Rightarrow B$ "A implies B"

$\{a_i\}$ "The set of elements a_i", the a_i in this case being a set of real frequencies with special significance for the networks being considered.

These abbreviations are used for labelling the ordinates of graphs of filter and diplexer performance:

L.R. Return Loss (measured in decibels)

I.L. Insertion Loss (measured in decibels).

Table of Contents.

	Summary	(i)
	Acknowledgements	(ii)
	Symbols and Abbreviations	(iii)
1	Introduction	1
	1·1 Electric Filters	1
	1·2 Filter Specifications	2
	1.3 Group Delay	4
	1.4 Outline of Thesis	5
2	Fundamentals of Linear Circuit Theory	7
	2·1 General Constraints	7
	2·2 Kirchoff's Laws	8
	2·3 Circuit Elements	8
	2·4 Laplace Transforms	10
	2·5 Nodal Analysis	11
	2·6 Driving-point and Transfer Quantities	13
	2·7 Rational Functions	14
	2·8 Properties of Driving-point Immittances	15
	2·9 Positive Real Functions	16
	2·10 Properties of Transfer Impedances	17
	2·11 Response to Real Excitation	18
	2·12 Hurwitz Polynomials	18
	2·13 Reactance Functions	19
	2·14 Ladder Networks	20
	2·15 Two-Port Networks	21

2·16 Darlington's Theorem 23

2·17 Scattering Parameters 24

2.18 Synthesis of Singly-Terminated Networks 29

2·19 Synthesis of Doubly-Terminated Networks 31

2·20 Circuit Properties of Transmission Lines 33

2·21 Conclusions 37

3 Fundamentals of Filter Design 39

3·1 Introduction 39

3·2 Maximally-Flat Response 41

3·3 Chebysnev Response 43

3·4 Synthesis of the Filter Networks 53

3·5 The Admittance Inverter 55

3.6 Explicit Formulae for Element Values 56

3·7 Distributed Low-pass Prototype 60

3·8 Frequency Transformations 62

3·9 Frequency Independent Reactances 66

3·10 Conclusions 67

4 Design of Coupled-Resonator Bandpass Filters 69

4·1 Introduction 69

4·2 Capacity Coupled Lumped Element Filters 72

4·3 Interdigital Filters 79

4·4 Combline Filters 85

4·5 Direct-Coupled-Cavity Filters 93

4·6 Single-Sideband Crystal Filters 98

4·7 Conclusions 113

5 Review of Diplexer Design 115

5·1 Introduction 115

5·2 Systems requirements on Diplexer Design 121

5·3 Methods of "Decoupled" Diplexer Design 125

5·4 Design of Directly Interacting Diplexers 137

5·5 Conclusions 155

6 Direct Design Formulae for Diplexers 158

6·1 Introduction 158

6·2 Design Philosophy 159

6·3 Derivation of Design Equations 165

6·4 Summary of Results 175

6·5 Discussion of Design Equations 176

6·6 Performance of Prototype Diplexers 179

6·7 Conclusions 185

7 Design and Performance of Experimental Waveguide Diplexers 189

7·1 Introduction 189

7·2 General Design Principles 189

7·3 A Narrow-Band Waveguide Diplexer 193

7.4 A Broadband Waveguide Diplexer 197

7·5 Conclusions 201

8 Extension and Further Applications 203

8·1 Introduction 203

8.2 Symmetrical Diplexer with Series Inductor 204

8.3 Design Theory for Non-Contiguous LP-HP Diplexers 212

8·4 Design Formulae for Interdigital Filters 218

8·5 Conclusions 224

9 Conclusions 225

9·1 Bandpass Filters 225

9·2 Diplexers 226

9·3 Direct Design of Non-Contiguous Diplexers 227

9.4 Further Work on Diplexers 230

9.5 Extension to Multiplexers 230

Bibliography 231

Published Papers 243

ADDENDA: pps 202A-G.

Appendices

1	244
2	246
3	249
4	252
5	254
6	256

CHAPTER 1. Introduction.

1.1 Electric Filters.

In electrical engineering, a FILTER is a circuit, generally with two access ports, which will pass energy between the ports in one or more well-defined frequency bands. Power at other frequencies will not be transmitted, or at any rate will be much attenuated.

The development of filters was strongly influenced by the needs of telecommunications, and in particular of frequency multiplex transmission over a common bearer. For example, modern high-capacity frequency-division-multiplex (f.d.m.) communication links, which are the backbone of trunk telephony, are entirely dependant on the existence of filters meeting extremely stringent specifications.

Even before inventing the telephone, Alexander Graham Bell experimented with tone-multiplex telegraphy [1.1] using tuned reed resonators. However, the development of successful filters awaited the coming of the thermionic valve, when devices such as oscillators and modulators became common and f.d.m. systems possible. Today, filter theory is in a highly developed state, and is an almost unique example of a highly mathematical subject of enormous practical power.

Being so mathematical, filter theory is a subject somewhat inaccessible to the practicing engineer. Filter design has become an area for specialists, and this is unfortunate, since the communication engineer should have a knowledge of what it is and is not possible to expect of a filter. Thus, design methods which he can

easily understand and apply, without sacrificing the optimum in performance, are very important. The ideal form of such a method is a set of explicit formulae which translate the initial specification into a physical design. This will be called a direct design method. It can be distinguished from a method which requires a special knowledge of network theory, and which might involve a synthesis or difficult transformation procedure.

1.2 Filter Specifications.

The typical form of a filter specification is shown in figure 1.1. This defines the required transmission loss through the filter in various frequency bands. For the moment the filter is assumed to be a two-port, and to be operating in a controlled impedance environment, such as a coaxial system.

The full line in the figure is a typical filter response which just meets the specification. The requirements specify the variation in transmission allowed in the PASSBAND, between f_1 and f_2, and the attenuation to be exceeded in the STOPBAND. In the case shown, another communication channel is supposed to exist between f_4 and f_5, which supplies the main stopband constraint. The possibility of the filter exhibiting spurious passbands has to be considered too, and a permissible limit on their transmission imposed.

Some of the power incident on the filter within the passband may be reflected. Many system components, such as amplifiers, are somewhat intolerant of reflecting loads on their output, and such considerations limit the permissible reflection from the filter. Thus a limit is set on the passband return loss (broken line).

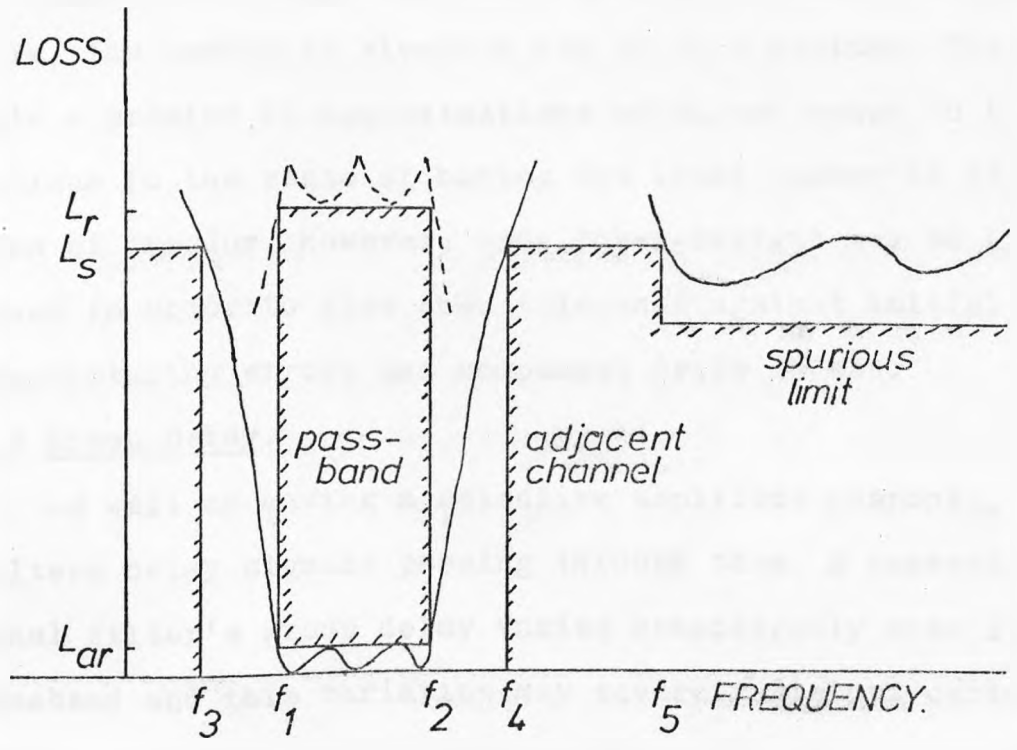

FIGURE 1.1 Filter Specification.

Given the specification, a mathematical function of frequency has to be found which will satisfy it. This is known as the approximation problem. The function has to do more than merely meet the specification. For one, it has to be realisable as the loss function of a real electric circuit using a finite number of elements.

Since the design has to be as cheap to make as possible, the number of elements has to be a minimum. This puts a premium on approximations which are known to be optimum in the sense of having the least number of degrees of freedom. However, some "over-design" may be allowed in order to give some tolerance against initial manufacturing errors and component drift in use.

1.3 Group Delay.

As well as having a selective amplitude response, filters delay signals passing through them. A conventional filter's group delay varies considerably over its passband and this variation may severely distort certain types of signal (for example, angle-modulated carriers). Measures have to be taken to "equalise" the variation with a separate network or design a special filter which does not exhibit the group delay variation. The latter approach has received a great deal of attention in recent years. Conventional filters have only a single path through which energy can flow and their responses are minimum-phase. New types of filter have been developed which use multipath structures and have non-minimum phase response. These can be designed to give good amplitude selectivity and nearly constant group delay. The design of this type of filter is rather specialised and is not "direct" in the sense discussed before. Further

discussion of this type of filter is beyond the scope of this thesis.

1.4 Outline of Thesis.

The aim of this thesis is to develop direct design methods for some type of bandpass filters and for bandpass diplexers.

Chapters two and three are concerned with the basis of circuit theory and with the development of the ideas of approximation, and the important notion of the lowpass prototype. Chapter four then derives some direct design procedures for bandpass filters. The filters considered are a type of lumped element filter, transmission line filters of the interdigital and combline type, direct-coupled cavity waveguide filters, and finally a new design procedure for high-performance crystal single-sideband filters.

Chapter five begins the study of diplexers. It reviews the main existing methods, in particular those which use interacting filters. Chapter six presents the main original material of the thesis, a new design procedure for asymmetric bandpass diplexers. Computed results are given for some trial designs which demonstrate the high performance possible with the new technique. Chapter seven considers the application of the design method to waveguide diplexers. Experimental results are given which show that the method is simple and direct to apply to narrow-band designs. Also, computed results show that it should be applicable to broadband designs.

Finally, chapter eight applies the basic theory of the method to another form of bandpass diplexer, lowpass-highpass diplexers, and to developing an improved design

method for broadband bandpass filters. Concluding comments and suggestions for future work are in chapter nine. Six appendices contain listings of various computer programs used in the research.

CHAPTER 2

FUNDAMENTALS OF LINEAR CIRCUIT THEORY

This review of linear circuit theory establishes the basic properties of electric circuits and the elementary methods of synthesis, as a basis for the review of filter theory in the next chapter. The material covered here is basic to all circuit theory, and references to proofs in existing literature are given where appropriate. A complete development of circuit theory from first principles would be a volume in itself. Thus a basic set of principles and concepts is assumed, and the object of this chapter is to establish the most important ideas behind filter theory and network synthesis. Certain concepts, such as the ideas of ideal voltage and current sources, resistive sources, insertion loss, and the basic theory of transmission lines, are assumed and appear in the text without comment.

There are a number of texts on circuit theory available and for convenience most of the references are to the treatment given by Scanlan and Levy [2.1], [2.4].

2.1

Let a stimulus function $s(t)$ be applied to an electric circuit, and a response $r(t)$ result. Then the networks of interest generally satisfy the following constraints [2.1];

Linearity If $s_1(t) \rightarrow$ ("leads to") $r_1(t)$
and $s_2(t) \rightarrow r_2(t)$
then $as_1(t) + bs_2(t) \rightarrow ar_1(t) + br_2(t)$

Time Invariance $s(t + \tau) \rightarrow r(t + \tau)$

Passivity If $s(t)$ is considered to be a driving point voltage $v(t)$, and $r(t)$ the resulting current $i(t)$, then passive networks only absorb or store energy, and thus $v(t)$ and $i(t)$ satisfy the condition

$$\int_{-\infty}^{t} v(\tau)\, i(\tau)\, d\tau \geqslant 0$$

Causality

For a linear circuit, if

$$s(t) = 0, \quad -\infty < t < t_o$$
$$= s_1(t), \quad t \geqslant t_o,$$

then

$$r(t) = 0, \quad -\infty < t < t_o$$
$$= r_1(t), \quad t \geqslant t_o$$

Real Time Function

If $s(t) = s_1(t) + j\, s_2(t)$

$r(t) = r_1(t) + j\, r_2(t)$

then

$$s_2(t) = 0 \rightarrow r_2(t) = 0$$

2.2

The fundamental quantities of interest in an electric network are voltages and currents. The fundamental rules they obey are called Kirchoff's laws. They are:

The algebraic sum of all current entering the junction of two or more circuit elements is zero.

The algebraic sum of all the voltages in any closed loop of an electric circuit is zero.

2.3

The elements of an electric circuit, of the class considered here, are shown in Figure 2.1(a). They are characterised by the relationships between their terminal voltages and currents

Resistor: $$v(t) = Ri(t) \qquad (2.1)$$

Inductor: $$v(t) = L\frac{di}{dt} \qquad (2.2)$$

Capacitor: $$v(t) = \frac{1}{C}\int_{-\infty}^{t} i(\tau)\, d\tau \qquad (2.3)$$

Ideal transformer: $$\left.\begin{aligned} v_1(t) &= n\, v_2(t) \\ i_1(t) &= i_2(t)/n \end{aligned}\right\} \qquad (2.4)$$

Mutual inductances have been excluded since they are not used in the

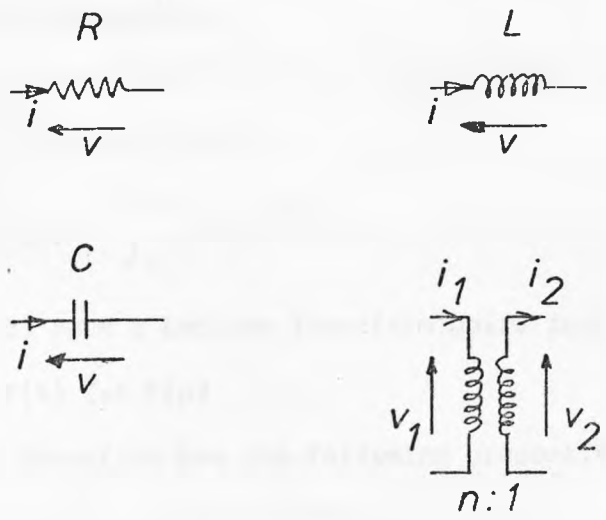

(a) Network Elements.

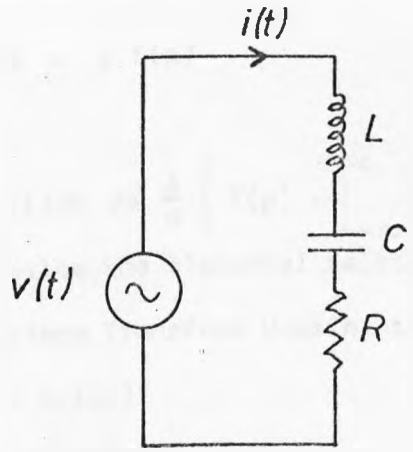

(b) LCR Network.

FIGURE 2.1

circuits considered. They can be accommodated by admitting negative inductor values [2.2].

2.4 Laplace Transforms

The Laplace Transform of a function f(t) is denoted F(p), $p = \sigma + j\omega$, and is defined by

$$F(p) = \int_0^\infty f(t)\, e^{-pt}\, dt \qquad (2.5)$$

F(p) and f(t) form a Laplace Transform pair, indicated

$$f(t) \Leftrightarrow F(p)$$

The Laplace Transform has the following properties [2.3].

Linearity $af_1(t) + bf_2(t) \Leftrightarrow aF_1(p) + bF_2(p)$ (2.6)

Scaling $f(at) \Leftrightarrow \frac{1}{a} F(\frac{p}{a})$ (2.7)

Shift $f(t)\exp(-at) \Leftrightarrow F(p + a)$ (2.8)

Differentiation

$$\frac{d}{dt} f(t) = p\,F(p) \qquad (2.9)$$

Integration

$$\int_{-\infty}^{t} f(t)dt \Leftrightarrow \frac{1}{p}\left[F(p) + \int_{-\infty}^{0} f(t)\, dt\right] \qquad (2.10)$$

(2.9) and (2.10) allow the elemental relationships (2.1)-(2.4) to be written in the Laplace Transform domain, thus:

Resistor $V(p) = R.I(p)$ (2.11)

Inductor $V(p) = Lp.I(p)$ (2.12)

Capacitor (assuming $i(t) = 0,\ t < 0$)

$$V(p) = \frac{1}{Cp}.I(p) \qquad (2.13)$$

Ideal transformer

$$V_1(p) = nV_2(p)$$
$$I_1(p) = I_2(p)/n \qquad (2.14)$$

The expressions (2.11) to (2.13) allow the generalisation of the concept of "resistance" to "impedance". Thus the impedance of an inductor of L henries is pL and of a capacitor of C farads 1/pC.

The dual of resistance is "conductance": of impedance, "admittance", and the admittances of an inductor and capacitor are $1/pL$ and pC.

Similarly with circuits, consider the series RLC network of Figure 2.1(b). The current and voltage in this circuit are related by the integro-differential equation

$$Ri(t) + L\frac{d}{dt}i(t) + \int_{-\infty}^{t}\frac{i(\tau)}{C}\,d\tau = v(t)$$

Assuming that $v(t)$ and $i(t)$ are zero for $t < 0$, taking the Laplace transform of this equation gives

$$\left[R + pL + \frac{1}{pC}\right] I(p) = V(p)$$

Thus the impedance of the RLC circuit, which by generalisation of (2.11) is just $V(p)/I(p)$ is given by

$$Z(p) = R + pL + \frac{1}{pC}$$

2.5 Nodal Analysis

The properties of electrical networks can be deduced from general node or mesh analysis. Only nodal analysis will be considered here, to develop the properties of driving point and transfer functions. The corresponding development in terms of mesh analysis is given in [2.4].

Refer to the general nodal analysis network of Figure 2.2. Each node except one is excited by a constant-current source of value $I_k(p)$, and there are $(n+1)$ nodes. One node has been arbitrarily given the index zero and is used as a reference node. The nodal voltages relative to the reference node, are $v_1, v_2, \ldots, v_n$. Each node K is connected to the ℓ'th node by a mutual admittance $y_{k\ell}$, and in general each node is connected to every other. The self admittance of the k'th node is defined as

$$y_{kk} = y_{k,o} + y_{K,1} + \cdots + y_{k,k-1} + y_{k,k+1} + \cdots + y_{k,n}$$

It is clear that the node voltages and currents are related by the

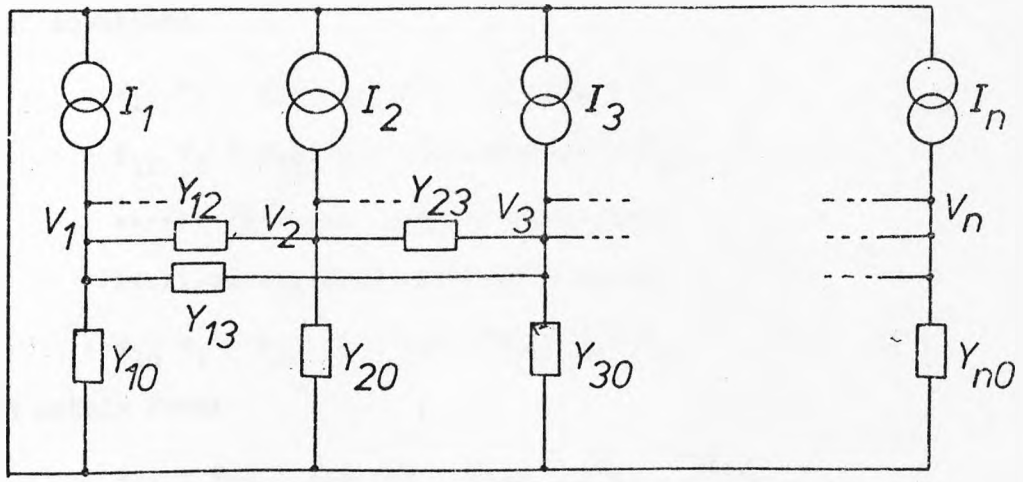

FIGURE 2.2 General Nodal Analysis Network.

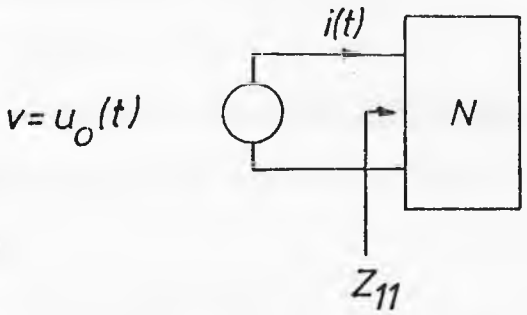

FIGURE 2.3 D.P. Impedance Excited by Unit Impulse.

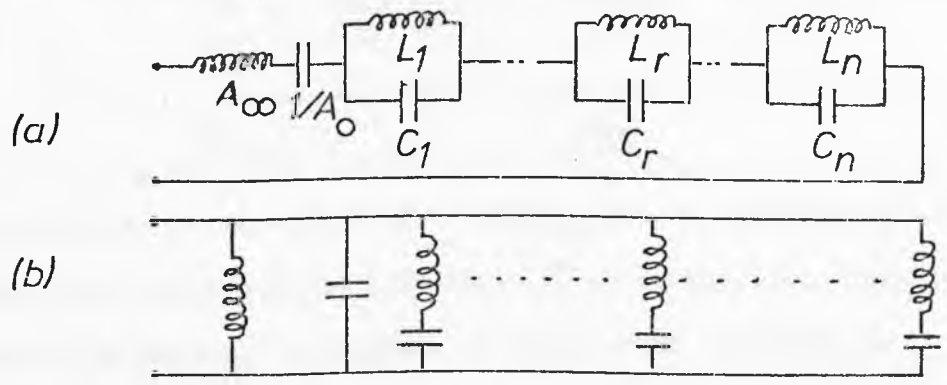

FIGURE 2.4 Foster Forms.

set of equations

$$y_{11} v_1 - y_{12} v_2 - \dots - y_{1n} v_n = I_1$$
$$- y_{12} v_1 + y_{22} v_2 - \dots\dots\dots\dots = I_2$$
$$\dots\dots\dots\dots\dots\dots\dots\dots\dots\dots$$
$$\dots\dots\dots\dots\dots\dots\dots\dots\dots\dots$$
$$- y_{1n} v_1 - y_{2n} v_2 - \dots + y_{nn} v_n = I_n$$

or in matrix form:

$$\begin{pmatrix} y_{11} & - y_{12} & - y_{13} \dots & - y_{1m} \\ - y_{12} & y_{22} & \dots\dots\dots\dots & \\ & & & \\ - y_{in} & & \dots\dots\dots\dots & y_{nn} \end{pmatrix} \begin{pmatrix} v_1 \\ v_2 \\ \vdots \\ v_n \end{pmatrix} = \begin{pmatrix} I_1 \\ \vdots \\ \vdots \\ I_n \end{pmatrix} \qquad (2.15)$$

(2.15) can be written compactly as;

$$[Y].(v) = (I) \qquad (2.16)$$

where $[Y]$ is known as the nodal admittance matrix.

Inverting (2.16), the column vector of node voltages can be found, i.e.

$$(v) = [Y]^{-1} (I)$$

and by the definition of the inverse of a matrix,

$$v_1 = \frac{\Delta_{11}}{\Delta} I_1 + \frac{\Delta_{12}}{\Delta} I_2 + \dots + \frac{\Delta_{1n}}{\Delta} I_n$$
$$\dots\dots\dots\dots\dots\dots\dots\dots\dots\dots$$
$$v_n = \frac{\Delta_{1n}}{\Delta} I_1 + \dots\dots\dots + \frac{\Delta_{nn}}{\Delta} I_n$$

where Δ is the determinant of Y, and $\Delta_{k\ell}$ is the cofactor of $- y_{k\ell}$. Notice that it is assumed here that $[Y]$ is symmetrical, which is the case if the network is composed of the elements considered.

2.6

Consider that one current source I_k is finite and all the others set to zero. Then the resulting node voltages are

$$v_\ell = \frac{\Delta_{k,\ell}}{\Delta} I_k, \quad \ell = 1, 2, \dots, n$$

Let the pair of terminals formed by node m and node zero be defined as port m. Then the impedance formed by looking into port k is

$$Z_{kk} = \frac{V_k}{I_k} = \frac{\Delta_{kk}}{\Delta} \qquad (.17)$$

and is known as the open-circuit driving-point impedance at port k.

The quantities $z_{k\ell}$, $\ell \neq k$, are known as the open circuit transfer impedances and

$$Z_{k\ell} = \frac{\Delta_{k\ell}}{\Delta} \qquad (2.18)$$

From mesh analysis the quantities Y_{kk} and $Y_{k\ell}$, known as the short-circuit driving-point and transfer admittances are defined [2.4].

2.7

A general admittance in Figure 2.2 can always be decomposed into a parallel combination of a resistor, inductor, and capacitor. If not, extra nodes can always be introduced into the network until the decomposition is possible. Thus, the general admittance $y_{k\ell}$ can be written

$$y_{k\ell} = p\,C_{k\ell} + G_{k\ell} + \frac{1}{pL_{k\ell}}$$

$$= \frac{p^2 L_{k\ell} C_{k\ell} + pL_{k\ell} G_{k\ell} + 1}{pL_{k\ell}} \qquad (2.19)$$

In (2.19), $G_{k\ell}$ is the reciprocal of the resistor $R_{k\ell}$.

Since the expressions for Z_{kk} and $Z_{k\ell}$ (2.17) and (2.18) were ratios of determinants, and the determinants are calculated by multiplying and adding rational functions of p of the form of (2.19), the determinants are themselves rational functions, as are their ratios.

Thus the driving-point and transfer impedances (and admittances) are rational functions in the complex variable p, i.e. the ratio of two polynomials in p. Since all the coefficients in (2.19) are real, the coefficients of each polynomial must also be real. The n'th degree polynomial has by the "fundamental theorem of alg ebra", exactly n roots,

and hence the $Z_{k\ell}$ can be written;

$$Z_{k\ell} = \frac{k(p-z_1)\ (p-z_2)\ (\ldots)\ (p-z_n)}{(p-p_1)\ (p-p_2)\ (\ldots)\ (p-p_m)} \qquad (2.20)$$

The points $\{z_i\}$ in the complex p-plane, where $Z_{k\ell} = 0$, are called zeros of the function, while the points $\{p_i\}$ where $Z_{k\ell} = \infty$ are called poles of the function. Since the coefficients of the numerator and denominator polynomials of (2.20) are real, the poles and zeros must be on the real axis or occur in complex-conjugate pairs.

2.8 Properties of Driving Point Immittances

A Driving Point Immittance may be an IMpedance or adMITTANCE. The driving point admittance of a network, $Y_{11}(p)$, is the reciprocal of its driving point impedance. The main properties of a driving point impedance can be seen by considering one port of a network excited by a unit impulse of current, as shown in Figure 2.3. The transform of the unit impulse is just unity, so the Laplace transform of the resulting current waveform is simply $Z_{11}(p)$. Now $Z_{11}(p)$ being of the form (2.20) can be expanded as a partial fraction, and since each pole of (2.20) may in fact be multiple, the partial fraction expansion about one pole P_j of order k will be a series of the form

$$V_j(p) = \sum_{r=1}^{k} \frac{A_r}{(p-p_j)^r} \qquad (2.21)$$

From [2.5], the inverse Laplace transform of (2.21) is

$$V_j(t) = \sum_{r=1}^{k} \frac{A_r}{(r-1)!}\, t^{r-1} \exp(p_j t) \qquad (2.22)$$

From the passivity restrictions, $v_j(t)$ must decay to zero as $t \to \infty$. If the pole p_j is given by

$$p_j = \sigma_j + j\omega_j$$

then, if ω_j and σ_j are zero (pole at the origin), r must be equal to one or zero. If σ_j is zero (pole on the imaginary axis), r must again

be equal to or less than unity. σ_j must be negative for a decaying $v_j(t)$, and if σ_j and ω_j are both finite, the pole can be of any order, i.e. r can have any positive value. This follows because

$$\lim_{t\to\infty} t^{r-1} e^{\sigma_j} t = 0$$

for $\sigma_j < 0$.

By considering the excitation of the network by a unit-impulse voltage source, the same properties can be shown to hold for the zeros of 2.20, which are the poles of $Y_{11}(p)$. To summarize:

A. The poles and zeros of an immittance function are either real or occur in complex conjugate pairs

B. All the poles and zeros must lie in the left half plane or on the jω-axis

C. Poles and zeros on the jω-axis are of multiplicity at most one

D. As a corrolary to C, the numerator and denominator of an immittance function differ by at most one, or there will be a non-simple pole at infinity.

2.9

In [2.6] it is further shown that the driving point immittance of a real network has the property of being POSITIVE REAL, and fulfils the conditions that:

$$R_e\, Z_{11}(p) > 0 \text{ for } R_e(p) > 0$$

$$Z_{11}(p) \text{ real for } p \text{ real}$$

These conditions apply also to $Y_{11}(p)$. The necessary and sufficient condition that a function Z(p) be realisable as the input impedance of a physical network is that Z(p) be positive real.

In addition to the properties of 2.8 A-D, positive real functions (p.r.f.) have the following properties:

E. The residues at any (simple) poles on the jω-axis are positive real.

F. If $Z(p)$ is a p.r.f. then

$$R_e(Z(p)) = 0 \text{ for } R_e(p) = 0$$

G. If $Z(p)$ is a p.r.f., then the function

$$Z_1(p) = Z(p) - \frac{2k_p}{p^2 + \omega_o^2}$$

is also p.r., if and only if $Z(p)$ has poles at $p = \pm j\omega_o$ with residues k', with $k' \geq k$.

A positive real function is analytic in the right-half-plane. If it further has no poles on the $j\omega$-axis, then its real and imaginary parts are related through the Hilbert Transform [2.13]. Thus, if the real part is, say, $R(\omega)$, then the imaginary part is given by

$$I(\omega) = -\frac{1}{\pi} \int_{-\infty}^{\infty} \frac{R(u)du}{\omega - u}$$

An impedance function with this property is said to be MINIMUM REACTIVE, an admittance function, MINIMUM SUSCEPTIVE.

2.10

Turning now to the properties of transfer impedances, the restrictions on a transfer impedance are not as stringent as on a driving-point impedance. Taking a function $Z_{12}(p)$ as a typical case, no physical meaning can be attached to $Z_{12}^{-1}(p)$, and hence, though passivity restricts the poles of $Z_{12}(p)$ to the left half plane, there is no such restriction on the zeros. However, note that poles on the $j\omega$-axis must be again simple, and hence the degree of the numerator of $Z_{12}(p)$ cannot exceed the denominator by more than one. To sum up:

H. The poles and zeros of $Z_{12}(p)$ are real or occur in complex conjugate pairs.

I. All the poles of $Z_{12}(p)$ lie in the left half plane, including the $j\omega$-axis

J. Poles on the $j\omega$-axis are simple

K. As a corrollary of J, the degree of the numerator of $Z_{12}(p)$ exceeds the degree of the denominator by, at most, one.

2.11

Of interest when calculating the response of a network to a real excitation is the response when the forcing function is a pure sinusoid, represented by the time function

$$v = V_o \cos(\omega_o t)$$

The response of a network for $p = j\omega$ is then of interest. For $p = j\omega$, a network function $F(p)$ can be written

$$F(j\omega) = E(\omega) + jO(\omega)$$

where E and O are even and odd functions of ω, respectively, i.e.

$$E(\omega) = E(-\omega)$$

$$O(-\omega) = -O(\omega)$$

This property follows from conditions A and H.

Furthermore, if $F(p)$ is a driving point function, then

$$E(\omega) \geq 0$$

2.12

A polynomial in p which has no zeros in the right-half p-plane is called HURWITZ. Thus, a p.r.f. is the ratio of two Hurwitz polynomials. Not all ratios of Hurwitz polynomials are p.r.f. They must also satisfy the condition that

$$R_e(Z(p)) \geq 0 \text{ for } R_e(p) = 0$$

If a function $Z(p)$ is p.r. and, further,

$$Z(p) + Z(-p) = 0$$

then $Z(p)$ is a REACTANCE function, and must obviously be the ratio of an even to an odd polynomial, or vice-versa.

Since $Z(p)$ is p.r., it has no poles or zeros in the right-half p-plane. Also, $Z(-p)$ has no left-half p-plane poles or zeros. Thus, since $Z(p) = -Z(-p)$, $Z(p)$ has no left- or right-half plane poles or zeros.

Thus, all the poles and zeros lie on the imaginary axis, and must therefore be simple.

2.13

If Z(p) is a reactance function, so that Z(p) can be written

$$Z(p) = \frac{E(p)}{O(p)}$$

(or Y(p) can), since all the poles and zeros lies on the jω-axis, Z(p) can be expanded in a partial fraction of the form

$$Z(p) = A\infty\ p + \frac{A_o}{p} + \sum_{i=1}^{r} \frac{2A_i\ p}{p^2 + \omega_i^2} \qquad (2.23)$$

where Z(p) is of degree 2r + 2. For p = jω, it is clear that

$$Z(j\omega) = jX(\omega),$$

$$X(\omega) = A\infty\ \omega - \frac{A_o}{\omega} + \sum_{i=1}^{r} \frac{2A_i\ \omega}{\omega_i^2 - \omega^2}$$

Differentiating with respect to ω,

$$\frac{dX(\omega)}{d\omega} = A\infty + \frac{A_o}{\omega^2} + \sum_{i=1}^{r} \frac{2A_i(\omega_i^2 + \omega^2)}{(\omega_i^2 - \omega^2)^2}$$

Since all the $\{A_i\}$ are positive (2.8E), the derivative is also positive, and thus it can be shown that the poles and zeros interlace along the imaginary axis.

The partial fraction expansion (2.23) is the key to the synthesis of the reactance function in the form shown in Figure 2.4(a), when it is recognised that the impedance of the i'th resonant circuit is

$$Z_i(p) = \frac{p/C_i}{p^2 + 1/L_iC_i}$$

From this the element values are as shown for the single inductor and capacitor, and

$$C_i = \frac{1}{2A_i}$$

$$L_i = \frac{2A_i}{\omega_i^2}$$

The dual form in Figure 2.4(b) can realise the admittance

$$Y(p) = \frac{1}{Z(p)}$$

These networks are known as the FOSTER forms for the driving-point immittance, and are CANONICAL in that they may realise any reactance function, and MINIMAL in that they use the minimum possible number of elements.

2.14

An alternative realisation of a reactance function follows from the form of (2.23). If the pole at infinity is removed by extracting series inductor of value A , the remaining function Z'(p) has a zero at infinity, and is also positive real by 2.9G. The reciprocal of Z'(p) thus has a pole at infinity which can be removed by extracting a shunt capacitor, leaving a function with a zero at infinity, also positive real. The process can be continued until the remainder function is zero, resulting in the Ladder structure shown in Figure 2.6(a). If the original Z(p) has no pole at infinity, the first inductor will be absent.

An alternative form results by successively removing the poles at the origin, resulting in the network shown in Figure 2.6(b). Note that the input impedance of the first network can be written

$$Z(p) = pL_1 + \cfrac{1}{pC_2 + \cfrac{1}{pL_3 + \cfrac{1}{pC_4 + \ddots}}}$$

and the input impedance of the second

$$Z(p) = \frac{1}{pC_1} + \cfrac{1}{\cfrac{1}{pL_2} + \cfrac{1}{\cfrac{1}{pC_3} + \cfrac{1}{\cfrac{1}{pL_4} + \cdots}}}$$

These forms are known as CONTINUED FRACTIONS, and the associated networks are the CAUER FORMS.

2.15

Two-port networks are of general importance in filter theory. A two-port network can be characterised by its port voltages and currents and by a set of two-port parameters. Various sets of parameters can be used: (refer to figure 2.5)

Admittance $$\begin{pmatrix} i_1 \\ i_2 \end{pmatrix} = \begin{pmatrix} y_{11} & y_{12} \\ y_{12} & y_{22} \end{pmatrix} \begin{pmatrix} v_1 \\ v_2 \end{pmatrix}$$

Impedance $$\begin{pmatrix} v_1 \\ v_2 \end{pmatrix} = \begin{pmatrix} z_{11} & z_{12} \\ z_{12} & z_{22} \end{pmatrix} \begin{pmatrix} i_1 \\ i_2 \end{pmatrix}$$

Transfer $$\begin{pmatrix} v_i \\ i_1 \end{pmatrix} = \begin{pmatrix} A & B \\ C & D \end{pmatrix} \begin{pmatrix} v_2 \\ -i_2 \end{pmatrix}$$

A number of other parameter sets can be used, and one, the scattering parameters, will be dealt with later. The transfer parameters are very useful in dealing with problems of cascading networks, since it is easily shown that if two networks are cascaded, the overall transfer matrix is given directly by the product of the individual transfer matrices.

It is important to note that both the [y] and [z] matrices are symmetrical about the leading diagonal, i.e.

$$Y_{12} = y_{21}, \quad z_{12} = z_{21}$$

and the networks are thus termed reciprocal. Reciprocity is a

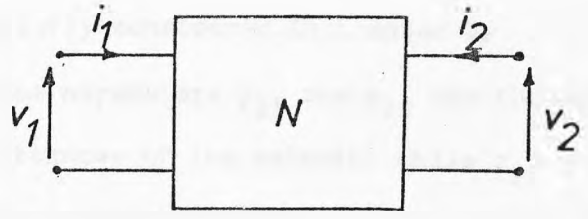

FIGURE 2.5 Two-Port Network.

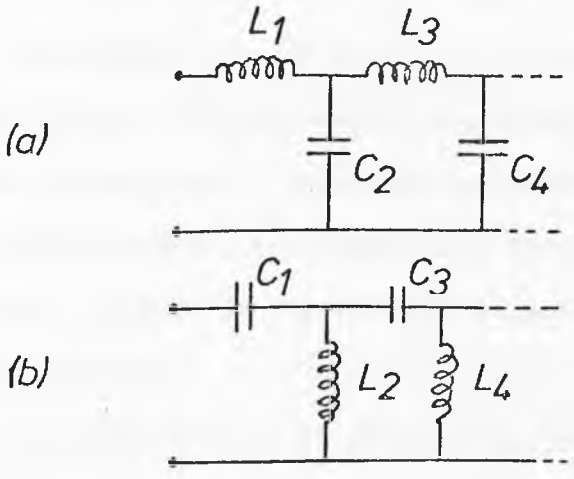

FIGURE 2.6 Cauer Forms.

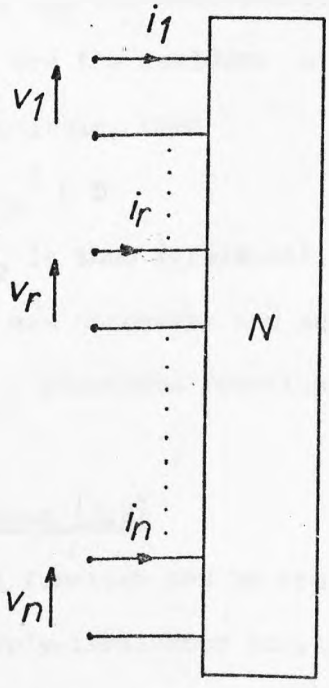

FIGURE 2.7

n-Port Network.

consequence of the elements used being bilateral. A non-reciprocal circuit will be briefly considered in Chapter 5.

The admittance parameters y_{11} and y_{22} are the short-circuit driving point admittances of the network, while z_{11} and z_{22} are the open-circuit driving-point impedances. It is clear from the form of the matrix equations that

$$\begin{pmatrix} y_{11} & y_{12} \\ y_{12} & y_{22} \end{pmatrix} = \begin{pmatrix} z_{11} & z_{12} \\ z_{12} & z_{22} \end{pmatrix}^{-1}$$

Considering the [z] matrix, if the network N is lossless, that is, contains only L, C, and ideal transformers, then z_{11} and z_{22} must be reactance functions. This case is particularly important because most filter circuits are essentially lossless. In this case, the poles of z_{12}, that is the transfer impedance, are restricted, as proved in [2.7].

L. All poles of z_{12} are poles of z_{11} and z_{22}. Poles of z_{11} and z_{22} not poles of z_{11} are called PRIVATE, and can be removed by a series Foster-like network. The resulting network, where z_{11}, z_{12}, z_{22} all have the same poles, is called COMPACT.

M. If k_{11}, k_{12}, k_{22} are the residues at a particular pole, of z_{11}, z_{12}, z_{22} respectively, then

$$k_{11}\, k_{22} - k_{12}^{2} \geq 0$$

The sign of k_{12} is thus irrelevant.

These conditions are necessary and sufficient for a given [z] matrix, with z_{11} and z_{22} reactance functions, to be realisable as a two-port LC network.

2.16 Darlington's Theorem [2.8]

Any positive real function can be realised as the driving-point impedance of a resistively-terminated lossless two-port network. If ideal transformers are admitted into the network, the value of the

termination may always be one ohm.

Associated with the theorem is a synthesis technique which permits the realisation of a p.r.f. in this form. Proof of the theorem is beyond the scope of this thesis and the technique is not explicitly required, so the theorem is merely quoted.

2.17 Scattering Parameters

The immittance parameters considered in section 2.15 are most useful for calculation when the networks being considered have their ports terminated in open- or short-circuits. In many practical cases, resistively terminated networks are important, especially when transmission-line systems are considered. In such cases the SCATTERING parameters are useful. A review of the scattering theory approach to networks is given by Carlin and Giordano [2.9].

Consider the general n-port network shown in Figure 2.7, with the port voltages and currents as defined. Let

$$(v) = \begin{pmatrix} v_1 \\ v_2 \\ \vdots \\ v_n \end{pmatrix}, \quad (i) = \begin{pmatrix} i_1 \\ i_2 \\ \vdots \\ i_n \end{pmatrix}$$

(v) and (i) are related through the immittance equation:

$$(i) = [Y](v) \qquad (2.24)$$

Now a set of "normalising numbers", R_1, R_2, ..., R_n is defined for the network, the R's being positive and (for present purposes) real. Now two new sets of port variables are defined:

$$(a) = \begin{pmatrix} a_1 \\ a_2 \\ \vdots \\ a_n \end{pmatrix} = \tfrac{1}{2} \left\{ \begin{vmatrix} R_1^{-\frac{1}{2}} & 0 & \cdots & 0 \\ 0 & R_2^{-\frac{1}{2}} & & \vdots \\ \vdots & & \ddots & \\ 0 & \cdots & & R_n^{-\frac{1}{2}} \end{vmatrix} (v) \right.$$

$$\left. + \begin{bmatrix} R_1^{\frac{1}{2}} & 0 & \cdots & 0 \\ 0 & R_2^{\frac{1}{2}} & & \vdots \\ \vdots & & \ddots & \\ 0 & \cdots & & R_n^{\frac{1}{2}} \end{bmatrix} (i) \right\} \qquad (2.25)$$

and

$$(b) = \begin{pmatrix} b_1 \\ b_2 \\ \vdots \\ b_n \end{pmatrix} = \tfrac{1}{2} \left\{ \begin{bmatrix} R_1^{-\frac{1}{2}} & 0 & \cdots & 0 \\ 0 & R_2^{-\frac{1}{2}} & & \vdots \\ \vdots & & \ddots & \\ 0 & \cdots & & R_n^{-\frac{1}{2}} \end{bmatrix} (v) \right.$$

$$\left. - \begin{bmatrix} R_1^{\frac{1}{2}} & \cdots & 0 \\ 0 & \ddots & \vdots \\ \vdots & & \\ 0 & \cdots & R_n^{\frac{1}{2}} \end{bmatrix} (i) \right\} \qquad (2.26)$$

For future reference, let

$$[R] = \operatorname{diag}\left[R_1^{\frac{1}{2}}, R_2^{\frac{1}{2}}, \ldots, R_n^{\frac{1}{2}}\right]$$

so that

$$[R]^{-1} = \operatorname{diag}\left[R_1^{-\frac{1}{2}}, R_2^{-\frac{1}{2}}, \ldots, R_n^{-\frac{1}{2}}\right]$$

Now (a) and (b) are two linearly independent vectors, which can be related through the matrix expression

$$(b) = [S]\,(a)$$

where

$$[S] = \begin{bmatrix} S_{11} & S_{12} & \cdots & S_{1n} \\ S_{21} & S_{22} & & S_{2n} \\ \vdots & \cdots & & \\ S_{n1} & \cdots & & S_{nn} \end{bmatrix}$$

is called the SCATTERING MATRIX of N.

Adding (2.25) and (2.26),

$$(a) + (b) = [R]^{-1}\,(v),$$

thus $(v) = [R]\left[(a) + (b)\right]$

$= [R]\left[[I] + [S]\right](a)$

where $[I]$ is the unit matrix.

Similarly, $(i) = [R]^{-1}\left[[I] - [S]\right](a)$

But, $(i) = [Y](v)$

thus $[R]^{-1}\left[[I] - [S]\right] = [Y][R]\left[[I] + [S]\right]$

and rearranging gives

$$[S] = \left[[I] - [R][Y][R]\right]\left[[I] + [R][Y][R]\right]^{-1} \qquad (2.27)$$

The product $[R][Y][R]$ is an interesting object. The operation of pre- and post-multiplying $|Y|$ by $|R|$ effectively multiplys the k'th row and column of $[Y]$ by $R_k^{\frac{1}{2}}$, and the product is thus effectively a normalised admittance matrix.

A number of different expressions are possible for $[S]$, similar to (2.27), in terms of different sets of immittance parameters. These are useful since one or more sets of immittance parameters may not exist. The particular importance of the $[S]$ matrix can perhaps be shown by considering the network shown in Figure 2.8. The n-port admittance matrix of this circuit is clearly

$$[Y] = \begin{bmatrix} R_1^{-1} & 0 & \cdots & 0 \\ 0 & R_2^{-1} & \ddots & \\ \vdots & \ddots & \ddots & \\ 0 & & & R_n^{-1} \end{bmatrix}$$

and hence the term $[R][Y][R]$ in (2.27) reduces to $[I]$. Hence $[S]$ is identically zero. Thus it can be seen that the vectors (a) and (b) can be considered as incident and reflected waves on a set of transmission lines of characteristic impedances $(R_1, R_2, \ldots, R_n)$. If the input impedance at the r'th port of a network is R_r, then the reflected wave is zero, and the port is said to be MATCHED.

Scattering parameters have several important properties, proved in [2.9]. For the purposes of this thesis, the most important are:

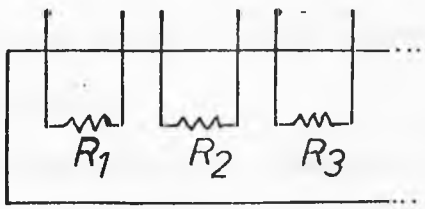

FIGURE 2.8 Matched Resistive Network.

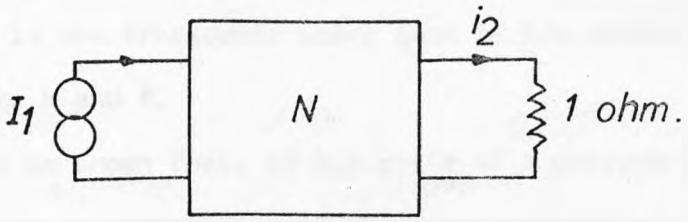

FIGURE 2.9 Singly-Terminated Network.

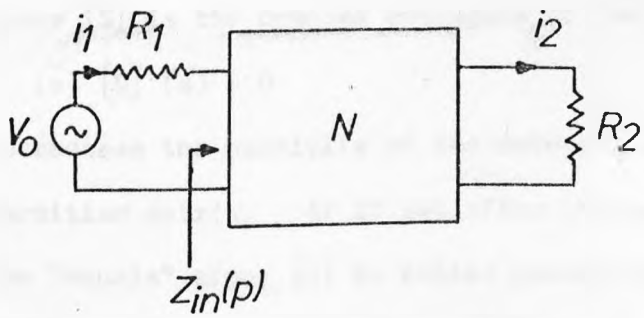

FIGURE 2.10 Doubly-Terminated Network.

N. The scattering matrix of every linear, passive, time invariant network exists.

P. The scattering matrix of a reciprocal network is symmetrical. (When N of Figure 2.7 is reciprocal, and Y exists, this follows from (2.27)).

Q. If a network is terminated with resistors equal to its port normalising numbers, then the modulus square of the off-diagonal term $S_{k\ell}$ is the transducer power gain of the network between ports k and ℓ.

R. It can be shown that, if all ports of a network are terminated with real loads, or real resistive sources, and an incident wave vector (a) excites the network, then the condition

$$(\tilde{a})\{[[I] - [\tilde{S}][S]]\}(a) \geq 0$$

or, if

$$[Q] = [I] - [\tilde{S}][S]$$

where $[\tilde{S}]$ is the complex conjugate of the transpose of $[S]$,

$$(\tilde{a})\ [Q]\ (a) \geq 0$$

guarantees the passivity of the network. $[Q]$ is then a Hermitian matrix. If it satisfies the condition without the "equals" sign, $[Q]$ is called positive definite, if with the equals sign positive semi-definite. If the network is lossless,

$$[Q] = [0],$$

and then $[S]$ is said to be UNITARY. For a unitary $[S]$,

$$[\tilde{S}][S] = [I]$$

and thus

$$[\tilde{S}] = [S]^{-1}$$

In the particular case of a lossless, reciprocal two-port network with the scattering matrix

$$\begin{pmatrix} S_{11} & S_{12} \\ S_{12} & S_{22} \end{pmatrix}$$

this results in the important condition

$$|S_{11}|^2 + |S_{12}|^2 = 1$$

For a lossless network there is thus a complementary relationship between the power transmitted through the network and that reflected, and thus between the insertion loss and the return loss. This is of particular importance in filter theory since most filters, being effectively lossless, reflect the power they do not transmit. Thus, the insertion loss of a filter in its passband is usually very low and difficult to measure, while the return loss is very high, and thus a sensitive indication of the filter's performance.

5. If the driving-point impedance at the k'th port of a network, all other ports being matched, is $Z_k(p)$, and this port is excited from a generator of internal resistance R_k, then the value of $S_{kk}(p)$ is given by

$$S_{kk}(p) = \frac{Z_k(p) - R_k}{Z_k(p) + R_k}$$

Furthermore, if $Z_k(p)$ is positive real, then $S_{kk}(p)$ satisfies the conditions [2.10]:

$S_{kk}(p)$ is real for p real

$0 \leq |S_{kk}(p)| < |, R_e(p) > 0$

and $S_{kk}(p)$ is called BOUNDED REAL.

2.18 Synthesis of Singly-Terminated Networks

Consider the resistively-terminated lossless two-port network N of Figure 2.9. Simple analysis gives

$$Z_{in} = z_{11} - \frac{z_{12}^2}{1 + z_{22}}$$

The output quantity of interest is the voltage V_2, and the excitation

is by the current I_1, and hence

$$Z_{21} = \frac{V_2}{I_1} = \frac{z_{12}}{1 + z_{22}} \tag{2.28}$$

Since N is lossless, z_{11}, z_{12}, z_{22} are odd functions of p. Consider the function

$$2E_v(Z_{in}(p)) = Z_{in}(p) + Z_{in}(-p)$$

$$= z_{11}(p) - \frac{z_{12}^2(p)}{1 + z_{22}(p)} + z_{11}(-p) - \frac{z_{12}^2(-p)}{1 + z_{22}(-p)}$$

$$\therefore \quad 2E_v(Z_{in}(p)) = -\frac{2z_{12}^2(p)}{1 - z_{22}^2(p)}$$

$$= 2Z_{21}(p)\, Z_{21}(-p) \tag{2.29}$$

Note that for $p = j\omega$, the right-hand side of (2.28) is just $2|Z_{21}(j\omega)|^2$. Thus (2.29) shows that the zeros of transmission of N are the zeros of the even part of the input impedance.

When the transfer function $Z_{21}(p)$ is known, it is of the form

$$Z_{21} = \frac{E(p)}{m(p) + n(p)} \text{ or } \frac{O(p)}{m(p) + n(p)}$$

where E(p), m(p) are even, O(p), n(p) odd functions. The numerator of $Z_{21}(p)$ is also the numerator of z_{12}, and hence must be pure even or pure odd. The denominator of $Z_{21}(p)$ must also be a Hurwitz polynomial.

Taking the first case,

$$Z_{21} = \frac{E(p)}{m(p) + n(p)} = \frac{E(p)/n(p)}{1 + m(p)/n(p)}$$

By comparison with (2.28), this can be realised by a lossless network with

$$Z_{22} = \frac{m(p)}{n(p)}, \quad z_{12} = E(p)/n(p) \tag{2.30}$$

Corresponding to the second case,

$$Z_{21} = \frac{O(p)/m(p)}{1 + n(p)/m(p)}$$

$$z_{22} = \frac{n(p)}{m(p)}, \quad z_{12} = O(p)/m(p) \tag{2.31}$$

An exact synthesis for z_{22} and z_{21} is then always possible if the zeros of Z_{21} lie at the origin or infinity. In that case, z_{22} is synthesised as a ladder network in one of the Cauer forms, and it can easily be shown (by induction) that the procedure simultaneously realises z_{12} in the prescribed form. This is the most important case in filter theory, as will emerge in the next chapter.

In many cases, the network has to be synthesised from the prescribed form of $|Z_{12}(j\omega)|^2$, that is, the magnitude response for real frequencies. In this case, $|Z_{21}|^2$ can be written

$$|Z_{21}(j\omega)|^2 = \frac{E^2(\omega)}{D(\omega^2)} \qquad (2.32)$$

assuming an even numerator of $Z_{21}(p)$. The corresponding odd case follows similarly.

Now (2.32) can be written

$$Z_{21}(j\omega)\, Z_{21}(-j\omega) = \frac{E^2(p)}{m^2(p) - n^2(p)}\Bigg|_{p = j\omega}$$

where m and n are even and odd respectively. Writing $-p^2$ for ω^2 in (2.32)

$$Z_{21}(p)\, Z_{21}(-p) = \frac{E^2(p)}{D(-p^2)}$$

Thus, the numerator of $Z_{21}(p)$ is known directly, while for the denominator

$$m^2(p) - n^2(p) = D(-p^2)$$

Since the denominator must be Hurwitz, $m(p) + n(p)$ must have only left-half-plane zeros. Thus $D(-p^2)$ can be factorised, and the left-half-plane zeros assigned to the function $m(p) + n(p)$. The synthesis of the network then follows as before.

2.19 Synthesis of Doubly-Terminated Networks

Doubly-terminated networks are generally synthesised by Darlington's

method referred to before in section 2.16. The response of interest is the modulus of the scattering transfer coefficient, $|S_{12}(j\omega)|$, specified on the real-frequency axis.

Consider Figure 2.10, which shows a lossless network embedded between a resistive source and load. For real frequencies, the power absorbed from the source is

$$P_{in} = |I_1(j\omega)|^2 \, E_v(Z_{in}(j\omega))$$

$$= \tfrac{1}{2} \, I_1(j\omega) \, I_1(-j\omega) \, [Z_{in}(j\omega) + Z_{in}(-j\omega)]$$

$$= \frac{V_o^2 \, [Z_{in}(j\omega) + Z_{in}(-j\omega)]}{2(R_1 + Z_{in}(j\omega) \, (R_1 + Z_{in}(-j\omega)}$$

Replacing $j\omega$ by p, the input power can be written

$$P_{in} = \frac{V_o^2 \, E_v(Z_{in}(p))}{(R_1 + Z_{in}(p) \, (R_1 + Z_{in}(-p))}$$

Now, since N is assumed lossless, all the input power is delivered to the load. Thus it can easily be shown that the transducer power gain of the network, and hence $|S_{12}(j\omega)|^2$, is just

$$|S_{12}(j\omega)|^2 = \frac{4R_1 \, E_v(Z_{in}(j\omega))}{(R_1 + Z_{in}(j\omega))(R_1 + Z_{in}(-j\omega))} \qquad (2.33)$$

From (2.33), the transmission zeros of $S_{12}(p)$ are the even-part zeros of $Z_{in}(p)$, plus any poles of $Z_{in}(p)$. Since these poles are simultaneously poles of $Z_{in}(-p)$, they must lie on the $j\omega$-axis.

The procedure for synthesising a specified $|S_{12}(j\omega)|^2$ is then as follows:

a) Provided that $|S_{12}(j\omega)|^2 \leq 1$ for all ω, the response can be realised by a physical network. Then $|S_{11}(j\omega)|^2$ can be formed because, if the resulting network is to be lossless its scattering matrix must be unitary. Thus, form

$$|S_{11}(j\omega)|^2 = 1 - |S_{12}(j\omega)|^2$$

b) Replace $j\omega$ by p, or $-\omega^2$ by p^2, to give $S_{11}(p)\,S_{11}(-p)$. Then $S_{11}(p)$ can be found by factorising the denominator of $S_{11}(p)\,S_{11}(-p)$ and assigning the left half-plane zeros to the denominator of $S_{11}(p)$. The zeros of the numerator of $S_{11}(p)$ can be assigned to either half-plane

c) In most cases a network with a one-ohm source resistance is required. In that case, $Z_{in}(p)$ can be found from 2.17S by rearranging as

$$Z_{in}(p) = \frac{1 + S_{11}(p)}{1 - S_{11}(p)}$$

and if the factorisation has been carried out so that $S_{11}(p)$ is bounded real, $Z_{in}(p)$ will be positive real.

d) $Z_{in}(p)$ is synthesised by Darlington's method as a lossless network terminated in a resistor, incorporating an ideal transformer if necessary if the resistor must be unity.

In the case where all the zeros of transmission of the network must be at the origin or infinity, a realisation as a ladder network is again possible.

2.20

This completes the survey of basic network theory. A final topic which will prove of importance in the next two chapters is the problem of the circuit properties of transmission lines.

The circuit elements of basic circuit theory, resistance, capacitance, and inductance, are all LUMPED, that is, they are implicitly considered to have zero extension in space. All real circuit elements are DISTRIBUTED, but at low frequency the lumped approximation is sufficiently valid for the lumped theory to be used for analysis and synthesis.

At "high" frequencies, that is, frequencies where the wavelength of propagation is significant compared to the size of the circuit, the

distributed nature of real elements becomes important, and at sufficently high frequencies, purely distributed elements are the only ones whose real behaviour can be predicted sufficiently accurately for filter design.

The properties of transmission lines as circuit elements can be deduced by considering the ideal lossless uniform line shown in Figure 2.11, of distributed inductance and capacitance L and C per unit length. Various text books show that the voltage and current at any point z along the line are related through the "telegraphists equations" [2.11]:

$$\frac{\partial v(t,z)}{\partial z} = - L \frac{\partial i(t,z)}{\partial t} \qquad (2.34)$$

$$\frac{\partial i(t,z)}{\partial z} = - C \frac{\partial v(t,z)}{\partial t} \qquad (2.35)$$

Differentiating (2.34) w.r.t. distance and (2.35) w.r.t. time, and combining gives the wave equation

$$\frac{\partial^2 v(t,z)}{\partial z^2} = \frac{1}{v^2} \frac{\partial^2 v(t,z)}{\partial t^2} \qquad (2.36)$$

where $v = 1/\sqrt{LC}$.

It can be shown that these equations are satisfied by any pair of functions f_1 and f_2, in the variables $t - z/v$ and $t + z/v$ respectively. f_1 represents a wave travelling in the positive, and f_2 in the negative z-direction. The solution for the voltage and current can then be written

$$v(t,z) = f_1(t - \frac{z}{v}) + f_2(t + \frac{z}{v}) \qquad (2.37)$$

$$i(t,z) = \frac{1}{Z_o} \left[f_1(t - \frac{z}{v}) - f_2(t + \frac{z}{v}) \right] \qquad (2.38)$$

where $Z_o = \sqrt{L/C}$, which must have the dimensions of resistance, is called the CHARACTERISTIC IMPEDANCE of the line.

(Equations (2.37) and (2.38) immediately demonstrate the physical basis of the definition of the scattering variables in (2.25) and (2.26).)

For the purposes of synthesis, the properties of the transmission line in the p-plane are required, and they can be obtained by Laplace

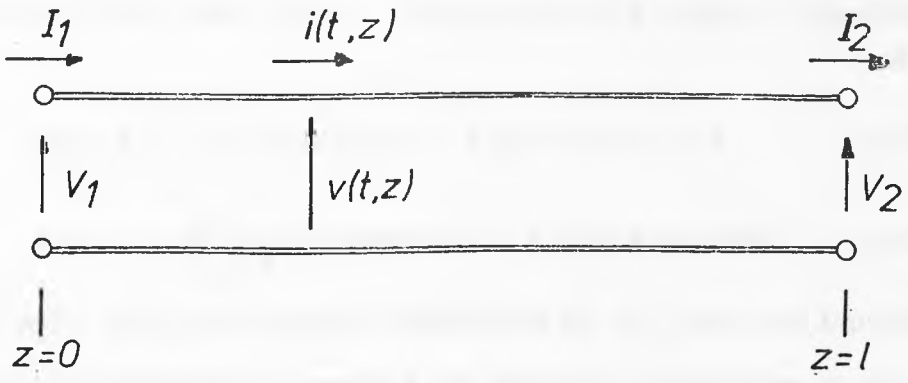

FIGURE 2.11 Transmission Line.

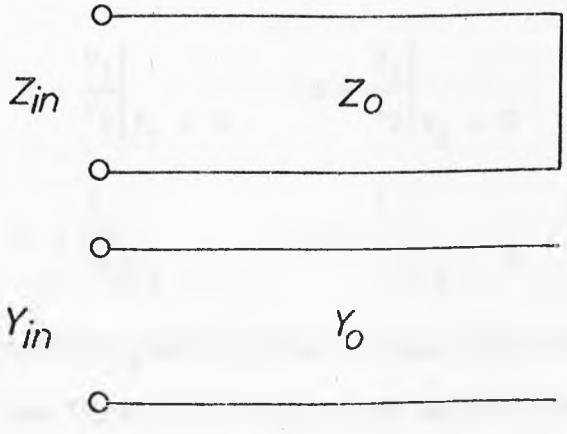

FIGURE 2.12 Short and Open Circuit Stubs.

transforming (2.37) and (2.38). Using the shift property immediately gives

$$V(p,z) = F_1(p)\exp(pz/v) + F_2(p)\exp(-pz/v) \qquad (2.39)$$

$$I(p,z) = \frac{1}{Z_o}\left[F_1(p)\exp(pz/v) - F_2(p)\exp(-pz/v)\right] \qquad (2.40)$$

In fact, only the terminal properties of the line are important, and thus it is necessary to specify the current and voltage at the accessible ports shown in Figure 2.12. The quantities of interest are V_1, I_1, V_2, I_2, and they are conveniently related by the transfer matrix

$$\begin{pmatrix} V_1 \\ I_1 \end{pmatrix} = \begin{pmatrix} A & B \\ C & D \end{pmatrix} \begin{pmatrix} V_2 \\ I_2 \end{pmatrix}$$

with

$$\left.\begin{aligned} A &= \left.\frac{V_1}{V_2}\right|_{I_2 = 0} & B &= \left.\frac{V_1}{I_2}\right|_{V_2 = 0} \\ C &= \left.\frac{I_1}{V_2}\right|_{I_2 = 0} & D &= \left.\frac{I_1}{I_2}\right|_{V_2 = 0} \end{aligned}\right\} \qquad (2.41)$$

It is a straightforward matter to apply the boundary conditions (2.41) to (2.39) and (2.40), to obtain the matrix elements A, B, C, D. The resulting matrix is;

$$\begin{bmatrix} \cosh(pT) & Z_o \sinh(pT) \\ Y_o \sinh(pT) & \cosh(pT) \end{bmatrix} \qquad (2.42)$$

where $Y_o = Z_o^{-1}$, and $T = \ell/v$ is the one-way delay along the line. In contrast to lumped networks, where the matrix elements are rational functions of p, the elements here are transcendental functions. For convenience, it is usual to assume that T is normalised to unity, so the matrix can be written

$$\begin{pmatrix} \cosh(p) & Z_o \sinh(p) \\ Y_o \sinh(p) & \cosh(p) \end{pmatrix}$$

Using identities between the hyperbolic functions it can be established

that the transfer matrix can be written in terms of the single variable $t = \tanh(p)$, as

$$\frac{1}{\sqrt{1 - t^2}} \begin{bmatrix} 1 & Z_o t \\ Y_o t & 1 \end{bmatrix} \qquad (2.43)$$

The transmission line of unit delay is the basic element in distributed network theory, called the UNIT ELEMENT. Also interesting are one-ports made of unit elements short- or open-circuited at their output ports, as shown in Figure 2.12. It is easily shown that

$$Z(t) = Z_o t$$

and $$Y(t) = Y_o t$$

Thus these elements, the short- and open-circuit STUBS, correspond to inductors of value Z_o and capacitors of value Y_o, in the t-plane. The variable t is called RICHARDS' variable, and Richards [2.12] has shown that networks composed of unit elements and stubs all with the same one-way delay (i.e. COMMENSURATE) have driving-point immittances which are positive real functions of t and of p. Conversely, positive real functions in the variable t are realisable as driving-point immittances of transmission line networks. However, the complexities of distributed network theory are not necessary for the purposes of this thesis.

2.21 Conclusions

This chapter has presented a brief summary of the principles of linear circuit theory. It has reviewed the realisability conditions under which a network with a given response can be synthesised, and referred to appropriate synthesis techniques.

From the point of view of filter theory, the key property of networks is Darlingtons' theorem, which permits the realisation of a two-port lossless network terminated with a resistor, with the required insertion-loss characteristics. Filter design then reduces to the

determination of a positive-real driving-point impedance function which will yield the required transfer response when realised as a resistively-terminated lossless network.

The properties of two-port, or in general n-port, resistively terminated networks which are to be fed from sources with finite interval resistance can be characterised conveniently using the scattering matrix. In the particular case of two-port lossless filter networks this leads to the convenient complementary relationship between reflected and transmitted power.

Finally, the terminal properties of transmission lines can be described by transcendental functions of the Laplace transform variable p, particularly in terms of the variable

$$t = \tanh(p)$$

Thus the properties of commensurate distributed networks can be described in terms of rational functions of the variable t. However, such techniques are not required for the distributed filters described in later chapters, and the technical details have not been fully explored here.

CHAPTER 3

FUNDAMENTALS OF FILTER DESIGN

3.1 Introduction

The last chapter considered the constraints a network must satisfy, and the basic methods of synthesis used in filter design. Given that the required network function is $|Z_{12}(j\omega)|$ or $|S_{12}(j\omega)|$, the methods generate the network functions ($z_{11}(p)$, $z_{12}(p)$, $Z_{in}(p)$) corresponding to a realisable network, giving the required modulus, and provide techniques of network synthesis. For the particular case where the zeros of transmission are all at the origin or infinity, the resulting network is a lossless, resistively terminated ladder.

The response of a filter is necessarily an approximation to some infinitely selective ideal. The ideal, lowpass filter response is shown in Figure 3.1, and is defined by

$$|H(j\omega) = 1, |\omega| < \omega_o$$
$$= 0 \quad |\omega| > \omega_o$$

If the phase response of the filter is also important, then the ideal response also satisfies

$$\arg|H(j\omega)| = - T_g \omega$$

It is well known that this response is not realisable by a physical network, being non-causal. All real filters have a response which approximates this ideal in a more or less optimum fashion. This thesis is particularly concerned with filters which are further restricted in that only the amplitude response is approximated, and all the transmission zeros of the filter occur at $\omega = \infty$.

Finding a function which approximates the ideal response is called the APPROXIMATION problem. The resulting function must be in a form which can be realised as a network function, generally by a network of degree n. Since the magnitude response is important, it is convenient

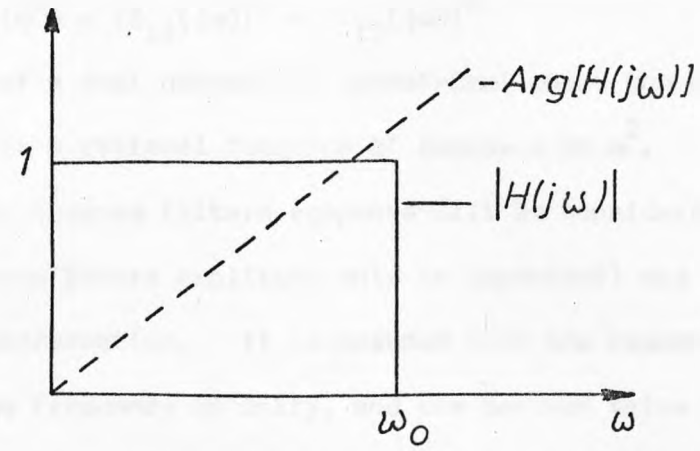

FIGURE 3.1 Ideal Filter Response.

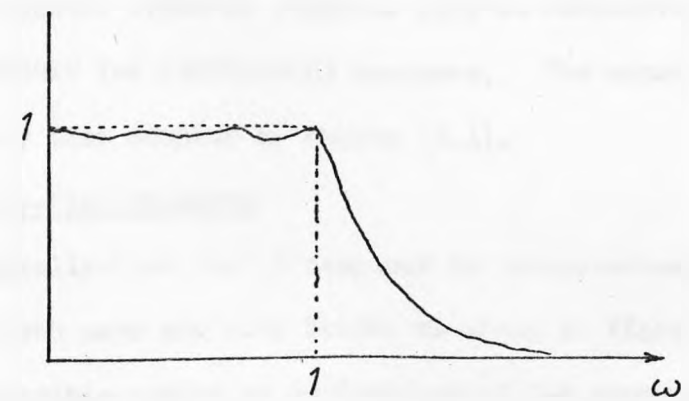

FIGURE 3.2 Approximation to Ideal Response.

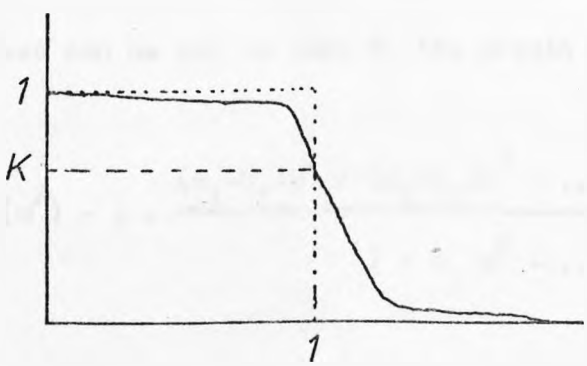

FIGURE 3.3 Maximally Flat Response.

to consider the function $F_n(x)$, where

$$F_n(\omega^2) = |S_{12}(j\omega)|^2 = |Z_{12}(j\omega)|^2$$

The response of a real network is symmetrical about the origin, and hence $F_n(\omega^2)$ is a rational function of degree n in ω^2.

Only the lowpass filters response will be considered; all other filter responses (where amplitude only is important) are obtainable by frequency transformation. It is assumed that the response is normalised to a band-edge frequency of unity, and the maximum value of transmission in the passband is unity. That is (referring to Figure 3.2)

$$F_n(\omega^2) \leq 1, \quad |\omega| \leq 1$$

$$F_n(\omega^2) \to 0, \quad |\omega| \to \infty$$

Two particular types of response will be considered, the MAXIMALLY-FLAT and CHEBYSHEV (or EQUIRIPPLE) response. The approach used follows closely that adopted by Rhodes [3.1].

3.2 Maximally-Flat Response

The Maximally-Flat (m.f.) response is characterised by being monotonic in both pass and stop bands, as shown in figure 3.3, and has the maximum possible number of derivatives of the response zero at both the origin and infinity. Let

$$F_n(\omega^2) = \frac{1 + a_1\omega^2 + a_2\omega^4 + \ldots + a_{n-1}\omega^{2n-2}}{1 + b_1\omega^2 + \ldots + b_n\omega^{2n}} \qquad (3.1)$$

2n-1 derivatives can be set to zero at the origin and infinity. From (3.1),

$$F_n(\omega^2) - 1 = \frac{(a_1-b_1)\omega^2 + (a_2-b_2)\omega^4 + \ldots + (a_{n-1}-b_{n-1})\omega^{2n-2} - b_n\omega^{2n}}{1 + b_1\omega^2 + \ldots + b_n\omega^{2n}} \qquad (3.2)$$

If (3.2) is to be zero, and its first 2n-1 derivatives, at the origin, then its power series expansion around $\omega = 0$ must be of the form

$$c_n\omega^{2n} + c_{n+1}\omega^{2n+2} + \cdots$$

which immediately gives

$$a_i = b_i,\ i = 1 \to n-1$$

To enforce the m.f. condition at $\omega = \infty$, numerator and denominator of (3.1) are divided by ω^{2n}, to give

$$F_n(\omega^2) = \frac{a_{n-1}\omega^{-2} + a_{n-2}\omega^{-4} + \cdots + a_1\omega^{2-2n} + \omega^{-2n}}{b_n + b_{n-1}\omega^{-2} + \cdots + \omega^{-2n}} \qquad (3.3)$$

To be maximally-flat about $\omega = \infty$, 3.3 must have a power series expansion of the form

$$\frac{d_n}{\omega^{2n}} + \frac{d_{n-1}}{\omega^{2n+2}} + \cdots$$

which gives

$$a_i = 0,\ i = 1 \to n-1$$

and hence

$$b_i = 0,\ i = 1 \to n-1$$

Then

$$F_n(\omega^2) = \frac{1}{1 + b_n\omega^{2n}},$$

and the coefficient b_n can have any convenient value. Usually b_n is set equal to unity, so that

$$F_n(\omega^2) = \frac{1}{1 + \omega^{2n}} \qquad (3.4)$$

The insertion-loss response of the corresponding filter is

$$L_A(\omega) = 10 \log_{10} (1 + \omega^{2n})\ \text{dB} \qquad (3.5)$$

and is always equal to 3dB for $\omega = 1$. As ω tends to infinity,

$$L_A(\omega) \to 10 \log_{10} (\omega^{2n})\ \text{dB} \qquad (3.6)$$

To construct $S_{12}(p)$ or $Z_{12}(p)$ from $F_n(\omega^2)$, the left-half plane poles of $F_n(p)\,F_n(-p)$ have to be selected. From (3.4), replacing ω^2

by $(-p^2)$ gives

$$F_n(p)\, F_n(-p) = \frac{1}{1 + (-p^2)^n}$$

The poles of $F_n(p)\, F_n(-p)$ then occur for

$$(-p^2)^n = -1$$

Let $-p^2 = \exp(j\theta)$

We require

$$\exp(jn\theta) = -1$$

$$= \exp[(2r-1)\pi], \quad r = 1,2,3 \ldots$$

Thus $n\theta = (2r-1)\pi$

or $-p^2 = \exp[(2r-1)j\pi/n]$

Thus the poles occur when

$$p = \exp[(2r-1+n)j\pi/2n]$$

Thus the n left-half-plane poles of $F_n(p)$ are equally spaced around the unit-semicircle as shown in Figure 3.4.

Note that, in the synthesis of doubly-terminated networks,

$$|S_{12}(j\omega)|^2 = \frac{1}{1 + \omega^{2n}}$$

thus

$$|S_{11}(j\omega)|^2 = \frac{\omega^{2n}}{1 + \omega^{2n}}$$

and

$$|S_{11}(p)S_{11}(-p) = \frac{(-p^2)^n}{1 + (-p^2)^n}$$

Thus all the zeros of $S_{11}(p)$ are at the origin. $S_{11}(p)$ has the left-half plane roots derived above, and thus $Z_{in}(p)$ can be formed explicitly.

3.3 Chebyshev Response

The Chebyshev response is an equiripple approximation to unity in the passband, and is maximally flat to zero in the stopband, as shown in Figure 3.5 for case n = 7.

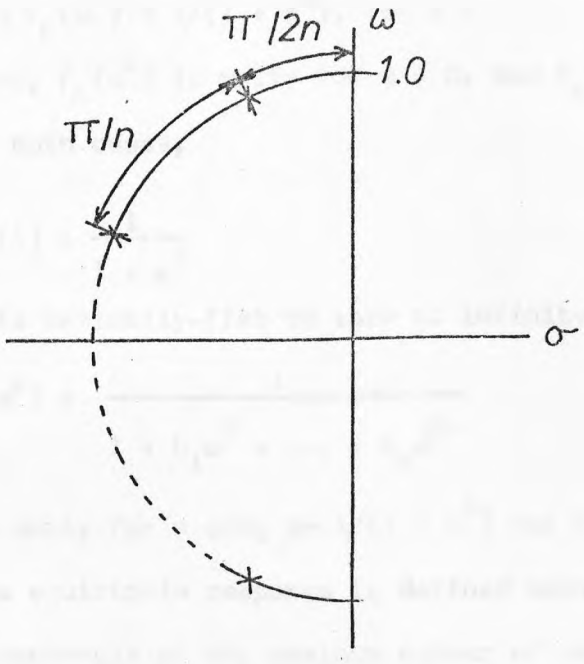

FIGURE 3.4 Poles of M.F. Response.

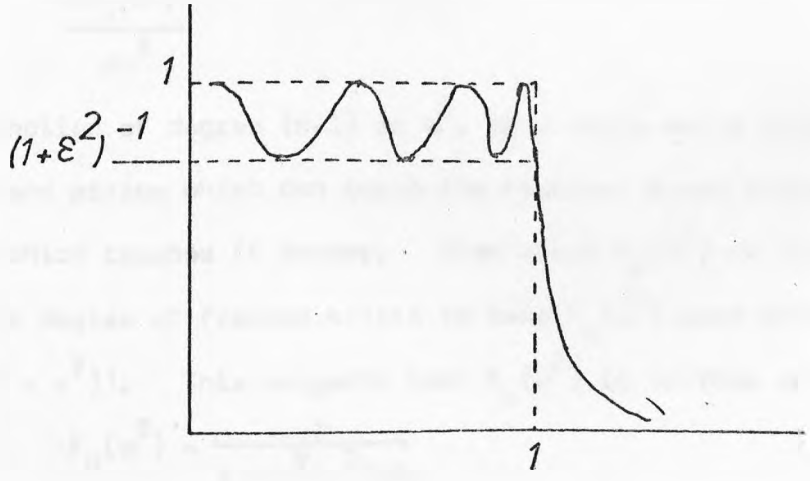

FIGURE 3.5 Equiripple Response.

Thus $1 \geq F_n(\omega^2) \geq 1/(1 + \varepsilon^2)$, $|\omega| \leq 1$

Also, for n odd, $F_n(\omega^2)$ is unity for $\omega = 0$, and $F_n(0) = 1/(1 + \varepsilon^2)$ for n even. For both cases,

$$F_n(1) = \frac{1}{1 + \varepsilon^2}$$

Since $F_n(\omega^2)$ is maximally-flat to zero at infinity, it can be written

$$F_n(\omega^2) = \frac{1}{1 + b_1\omega^2 + \ldots + b_n\omega^{2n}} \qquad (3.7)$$

A is equal to unity for n odd, or $1/(1 + \varepsilon^2)$ for n even.

Now, the equiripple response is defined such that $F_n(\omega^2)$ touches the boundary rectangle at the maximum number of points in the interval $0 \leq \omega \leq 1$. Thus all the maxima and minimum lie on this boundary rectangle. Now

$$\frac{dF_n(\omega^2)}{d\omega^2}$$

is a function of degree (n-1) in ω^2, thus there are a maximum of (n-1) maxima and minima which can touch the boundary apart from the one at $\omega = 0$, which touches it anyway. Also since $F_n(\omega^2)$ is of degree n, one more degree of freedom exists to make $F_n(\omega^2)$ pass through $(1, 1/(1 + \varepsilon^2))$. This suggests that $F_n(\omega^2)$ is written in the form

$$F_n(\omega^2) = \frac{1}{1 + \varepsilon^2 T_n^2(\omega)}$$

The function $T_n(\omega)$ has the form shown in Figure 3.6 for $n = 4$.

$T_n(\omega)$ clearly has turning points where the function is equal to ± 1, except for $\omega = \pm 1$. Thus, if $\{\omega_r\}$ are the points where $T_n(\omega_r) = \pm 1$,

$$\frac{d}{d\omega} T_n(\omega_r) = 0$$

Since the turning points occur when $T_n(\omega) = 1$, except for $\omega = 1$, and $T_n(\omega) = -1$, except for $\omega = -1$, $dT_n(\omega)/d\omega$ has the factors $(1 + T_n(\omega))/(1 + \omega)$ and $(1 - T_n(\omega))/(1 - \omega)$. However, $dT_n(\omega)/d\omega$ is of degree (n-1),

while the combined degree of the factors is (2_{n-2}), and thus $T_n(\omega)$ satisfies the differential equation

$$\frac{d}{d\omega} T_n(\omega) = C_n \sqrt{\frac{1 - T_n^2(\omega)}{1 - \omega^2}} \tag{3.7}$$

Separating the variables,

$$\frac{dT_n(\omega)}{\sqrt{(1 - T_n^2(\omega))}} = C_n \frac{d\omega}{\sqrt{(1 - \omega^2)}}$$

and noting that

$$\int \frac{dx}{\sqrt{(1 - x^2)}} = - \cos^{-1}(x),$$

$$\cos^{-1}[T_n(\omega)] = C_n \cos^{-1}(\omega)$$

The constant of integration must be zero, since $T_n(\omega)$ is either odd or even. Thus

$$T_n(\omega) = \cos[C_n \cos^{-1}(\omega)]$$

If ω is written "$\cos\theta$", then

$$T_n(\omega) = \cos(C_n\theta)$$

For $\omega = \infty$, $\theta = j\infty$, for only then

$$\omega = \cos j\infty$$

$$= \cosh \infty$$

$$= \infty$$

and $$T_n(\omega) = \infty$$

and thus all the poles of $T_n(\omega)$ are at infinity. Thus $T_n(\omega)$ is analytic in the finite plane (i.e., entire).

The zeros of $T_n(\omega)$ occur when $C_n\theta$ is an odd multiple of $\pi/2$, i.e.

$$C_n\theta = \frac{(2_{r-1})\pi}{2}, \quad r = 1, 2, \ldots$$

or $$\omega = \cos \frac{(2_{r-1})\pi}{2C_n}$$

The required polynomial has n distinct zeros for $|\omega| < 1$, and for this to be so, C_n must have the value n. Thus

$$T_n(\omega) = \cos(n \cos^{-1}\omega) = \cosh(n \cosh^{-1}(\omega)) \qquad (3.8)$$

and it remains to be shown that $T_n(\omega)$ is of exact degree n. Note that

$$T_o(\omega) = \cos(0)$$

$$= 1 \qquad (3.9)$$

$$T_1(\omega) = \cos(\cos^{-1}\omega)$$

$$= \omega \qquad (3.10)$$

Also $$T_{n+1}(\omega) = \cos([n + 1] \cos^{-1}\omega)$$

$$= \cos(n \cos^{-1}\omega) \cos(\cos^{-1}\omega) - \sin(n \cos^{-1}\omega) \sin(\cos^{-1}\omega)$$

$$T_{n-1}(\omega) = \cos(n \cos^{-1}\omega) \cos(\cos^{-1}\omega) + \sin(n \cos^{-1}\omega) \sin(\cos^{-1}\omega)$$

Thus

$$T_{n+1}(\omega) + T_{n-1}(\omega) = 2\omega T_n(\omega)$$

so that $$T_{n+1}(\omega) = 2\omega T_n(\omega) - T_{n-1}(\omega) \qquad (3.11)$$

The recurrence relation (3.11) with the initial conditions (3.9) and (3.10) show that $T_n(\omega)$ is a polynomial of exact degree n in ω.

Thus the equiripple response is given by

$$F_n(\omega^2) = \frac{1}{1 + \varepsilon^2 T_n^{\,2}(\omega)} \qquad (3.12)$$

The equiripple response is important because it has certain fundamental optimum properties. These can be appreciated by considering Figure 3.7. This shows an equiripple response curve of degree n which just satisfies a passband ripple and a minimum stopband attenuation specification. The question often arises; can a better approximation be found which has less deviation in the passband and greater attenuation in the stopband, with a lower degree than $F_n(\omega^2)$? Let this better function be $F_m'(\omega^2)$, with degree $m \leq n$, satisfying the specification, and let

$$F_m'(\omega^2) = \frac{1}{1 + \gamma^2 U_m^{\,2}(\omega)}$$

Now, the function $F_n(\omega^2)$ has n maxima and minima in the interval

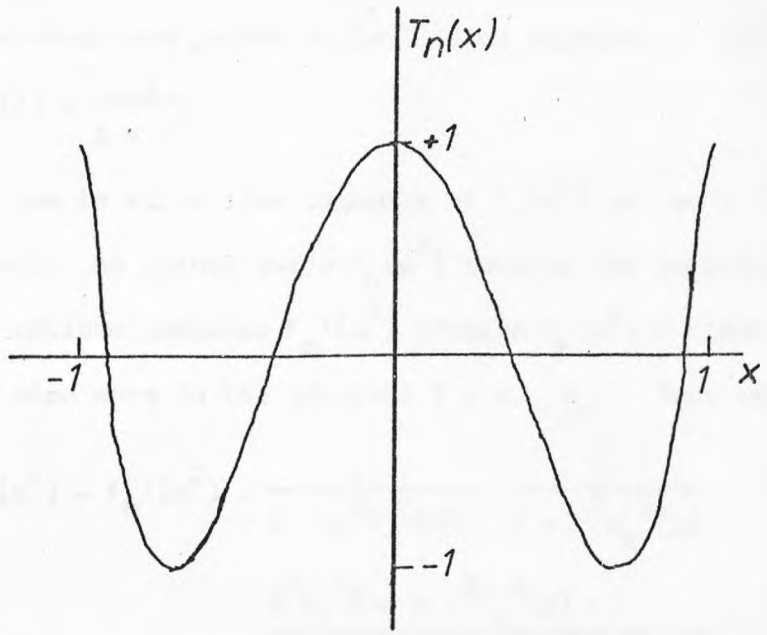

FIGURE 3.6 Chebyshev Function, n = 4.

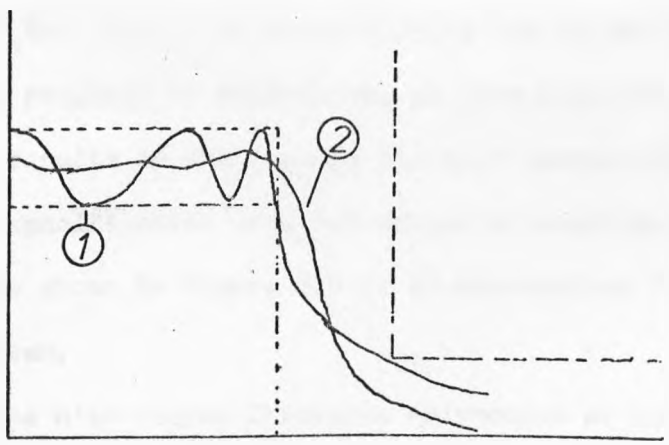

1 Equiripple function.
2 'More optimum' function.

FIGURE 3.7

$0 \leq \omega \leq 1$, and these are joined by (n-1) line segments. In addition,

$$F_n(1) = \frac{1}{1 + \varepsilon^2}$$

so that there are in all n line segments of $F_n(\omega^2)$ in the interval $0 \leq \omega \leq 1$ joining the points where $F_n(\omega^2)$ touches the defining rectangle. Thus the more optimum response $F_m'(\omega^2)$ crosses $F_n(\omega^2)$ n times in that interval, and once more in the interval $1 < \omega < \omega_c$. Thus the function

$$F_n(\omega^2) - F_m'(\omega^2) = \frac{1}{1 + \varepsilon^2 T_n^2(\omega)} - \frac{1}{1 + \gamma^2 U_m^2(\omega)}$$

$$= \frac{\gamma^2 U_m^2(\omega) - \varepsilon^2 T_n^2(\omega)}{(1 + \varepsilon^2 T_n^2(\omega))(1 + \gamma^2 U_m^2(\omega))}$$

has, in all, (n+1) zeros in $\omega < \infty$. But, the denominator of the function is entire, and hence the degree of $\gamma^2 U_m^2(\omega) - \varepsilon^2 T_n^2(\omega)$ is (n+1). Thus, either $U_m(\omega) = T_n(\omega)$, or $m > n$, contradicting the initial assumption. Notice that this property of equiripple, or more properly MINIMAX, approximations, results in their being the best approximations even if the form of the specification does not demand an equiripple function. Thus the response shown in Figure 3.8 is of the optimum form for the specification given.

$T_n(\omega)$ is the n'th degree Chebyshev Polynomial of the first kind, and the response is commonly referred to as "Chebyshev". The Insertion-Loss response is of the form

$$L_A(\omega) = 10 \log_{10}(1 + \varepsilon^2 T_n^2(\omega)) \text{ dB} \qquad (3.13)$$

For very large ω, the Chebyshev loss function tends to $10 \log_{10}(\omega^{2n}) + 10 \log_{10}(\varepsilon^2) + 6(n-1)$ dB, and thus the ultimate improvement over the m.f. case is approximately

$$10 \log_{10}(\varepsilon^2) + 6(n-1) \text{ dB}$$

Normally the passband specification is quoted as a maximum passband insertion loss, L_{AR}, normally of the order of 1 dB or less (0.01 dB

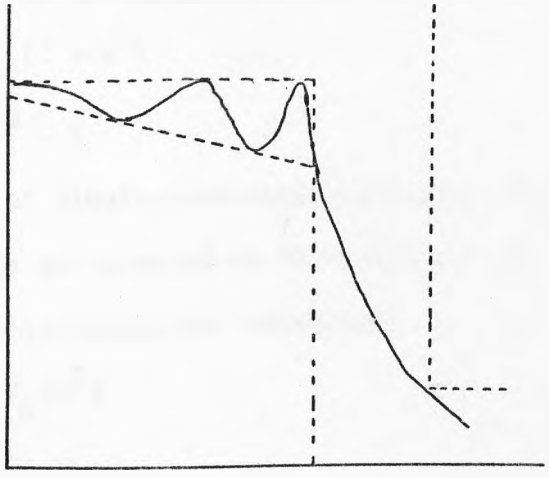

FIGURE 3.8 Minimax, but not Equiripple.

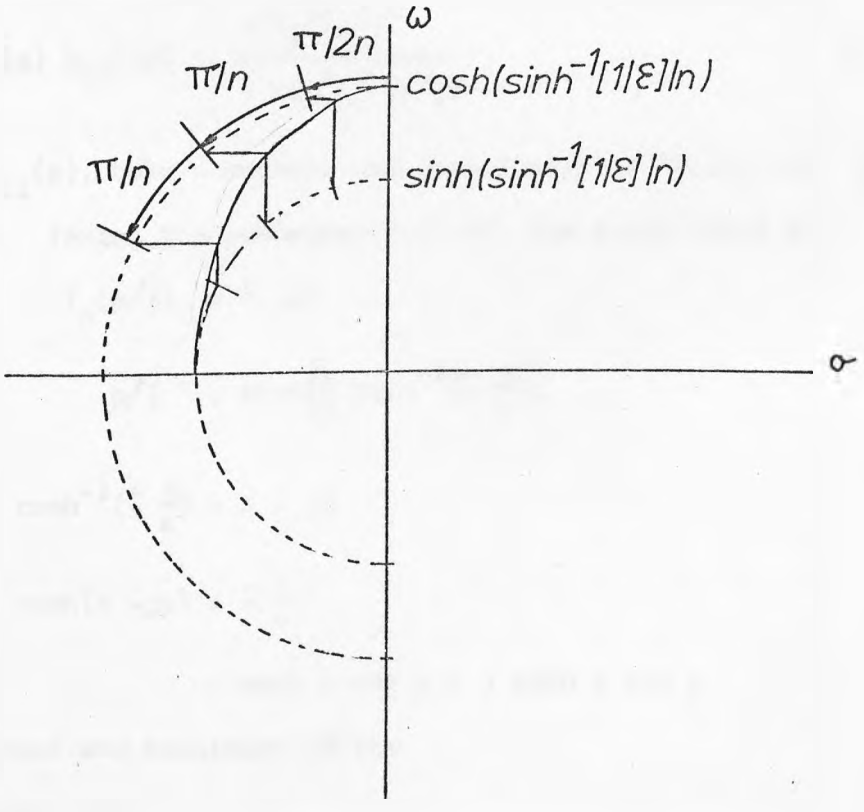

FIGURE 3.9 Poles of Chebyshev Response.

being not uncommon). Thus from (3.13),

$$L_{AR} = 10 \log_{10}(1 + \varepsilon^2)$$

or

$$\varepsilon^2 = 10^{L_{AR}/10} - 1 \qquad (3.14)$$

For the synthesis of singly-terminated networks, $|Z_{12}(j\omega)|^2 = F_n(\omega^2)$, and the synthesis can proceed as in section 2.18.

In the case of doubly-terminated networks,

$$|S_{12}(j\omega)|^2 = F_n(\omega^2)$$

so that

$$|S_{11}(j\omega)|^2 = 1 - \frac{1}{1 + \varepsilon^2 T_n^2(\omega)}$$

$$= \frac{\varepsilon^2 T_n^2(\omega)}{1 + \varepsilon^2 T_n^2(\omega)}$$

Thus

$$S_{11}(p)\, S_{11}(-p) = \frac{\varepsilon^2 T_n^2(p/j)}{1 + \varepsilon^2 T_n^2(p/j)} \qquad (3.15)$$

To form $S_{11}(p)$, both numerator and denominator of (3.15) must be factored. Taking the denominator first, the roots occur when

$$T_n(p/j) = \pm j/\varepsilon$$

or

$$p/j = \cosh\left[\frac{1}{n} \cosh^{-1}(\pm \frac{j}{\varepsilon})\right]$$

Let

$$\cosh^{-1}(\pm \frac{j}{\varepsilon}) = x + jy$$

so that

$$\cosh(x + jy) = \pm \frac{j}{\varepsilon}$$

$$= \cosh x \cos y + j \sinh x \sin y$$

Equating real and imaginary parts:

$$\cosh x \cos y = 0$$

$$\sinh x \sin y = \pm \frac{1}{\varepsilon}$$

These equations are only satisfied for y an odd multiple of $\pi/2$, i.e.

$$y = (2r-1)\pi/2, \quad r = 1,2,3, \ldots$$

when $\sin y = \pm 1$

Thus $$x + jy = \pm \sinh^{-1}\left(\frac{1}{\varepsilon}\right) + j\frac{(2r-1)\pi}{2}$$

Thus $$p = j\cosh\left[\pm\frac{1}{n}\sinh^{-1}\left(\frac{1}{\varepsilon}\right) + j\frac{(2r-1)\pi}{2n}\right]$$

$$= j\cosh\left[\pm\frac{1}{n}\sinh^{-1}\left(\frac{1}{\varepsilon}\right)\right]\cos\left[\frac{(2r-1)\pi}{2n}\right]$$

$$\pm j\sinh\left[\pm\frac{1}{n}\sinh^{-1}\left(\frac{1}{\varepsilon}\right)\right]\sin\left[\frac{(2r-1)\pi}{2n}\right]$$

$$= \sin\left[\frac{(2r-1)\pi}{2n}\right]\sinh\left[\frac{1}{n}\sinh^{-1}\left(\frac{1}{\varepsilon}\right)\right]$$

$$+ j\cos\left[\frac{(2r-1)\pi}{2n}\right]\cosh\left[\frac{1}{n}\sinh^{-1}\left(\frac{1}{\varepsilon}\right)\right] \quad (3.16)$$

In (3.16) the $\pm$ sign has been omitted, since both cases can be generated by a sufficient range of r.

Letting the r'th root p_r of (3.16) be

$$p_r = \sigma_r + j\omega_r,$$

then $$\frac{\sigma_r^2}{\sinh^2\left[\frac{1}{n}\sinh^{-1}\left(\frac{1}{\varepsilon}\right)\right]} + \frac{\omega_r^2}{\cosh^2\left[\frac{1}{n}\sinh^{-1}\left(\frac{1}{\varepsilon}\right)\right]}$$

$$= \sin^2\left[\frac{(2r-1)\pi}{2n}\right] + \cos^2\left[\frac{(2r-1)\pi}{2n}\right]$$

$$= 1$$

and thus the poles of $S_{11}(p)S_{11}(-p)$ lie on an ellipse as shown in Figure 3.9, and the poles of $S_{11}(p)$ are the left-half-plane poles.

For this unity-gain case, the zeros of $S_{11}(p)$ are the zeros of

$$T_n(p/j) = 0$$

or $$n\cos^{-1}(p/j) = \cos^{-1}(0)$$

$$= \frac{(2r-1)\pi}{2}, \quad r = 1,2,3, \ldots$$

Thus $$p = j \cos\left[\frac{(2r-1)\pi}{2n}\right] \qquad (3.17)$$

All the zeros of $S_{11}(p)$ thus lie on the $(j\omega)$-axis, in the interval $|\omega| < 1$.

At this stage it is instructive to consider the return-loss response of the Chebyshev filter. From above, the zeros of $S_{11}(p)$ occur for n distinct frequencies in the interval $|\omega| < 1$, and, assuming a source resistance of one ohm, the input impedance of the filter must be one ohm at this set of frequencies, and the return loss therefore infinite. This set of frequencies, denoted $\{\omega_i\}$, is of fundamental importance in the diplexer theory presented in Chapter 6.

The minimum return loss in the passband occurs when the insertion loss is maximum. From before,

$$|S_{11}|^2_{max} = \frac{\varepsilon^2}{1 + \varepsilon^2}$$

and thus the minimum value of return loss is

$$L_R = 10 \log_{10}\left(\frac{1}{|S_{11}|^2}\right)$$

$$= 10 \log_{10}\left(1 + \frac{1}{\varepsilon^2}\right)$$

This leads to an alternative form for ε, in terms of the minimum passband return loss;

$$1/\varepsilon^2 = 10^{L_R/10} - 1$$

The form of the return-loss response is then shown in Figure 3.10.

3.4 Synthesis of the Filter Networks

With the poles and zeros of $Fn(\omega^2)$ determined, $Z_{12}(p)$ and $S_{11}(p)$, $Z_{12}(p)$ and $S_{11}(p)$ are known to within a constant multiplier. For the maximally-flat and odd-degree Chebyshev cases, the multipler can be determined from the condition that

$$Fn(0) = 1$$

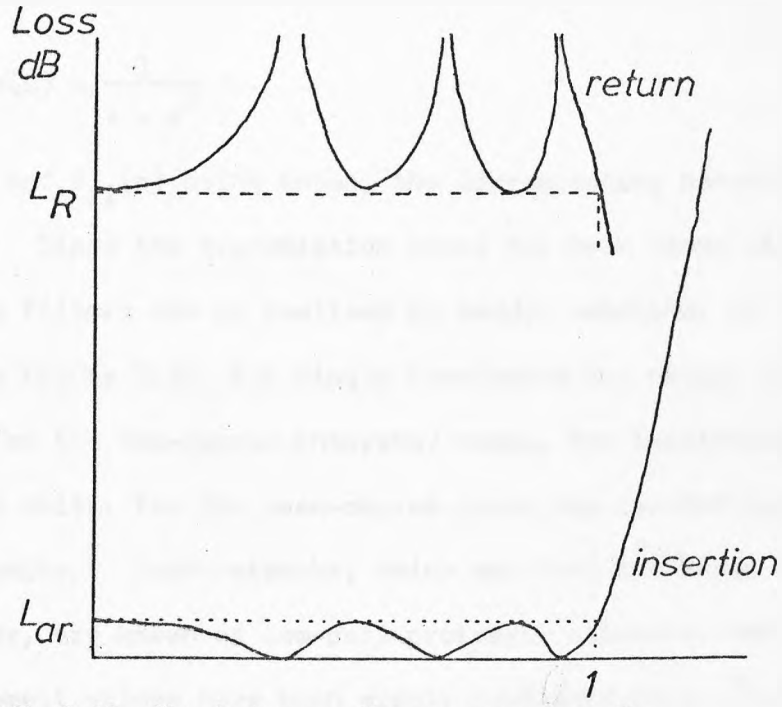

FIGURE 3.10 Prototype Response, n=6 .

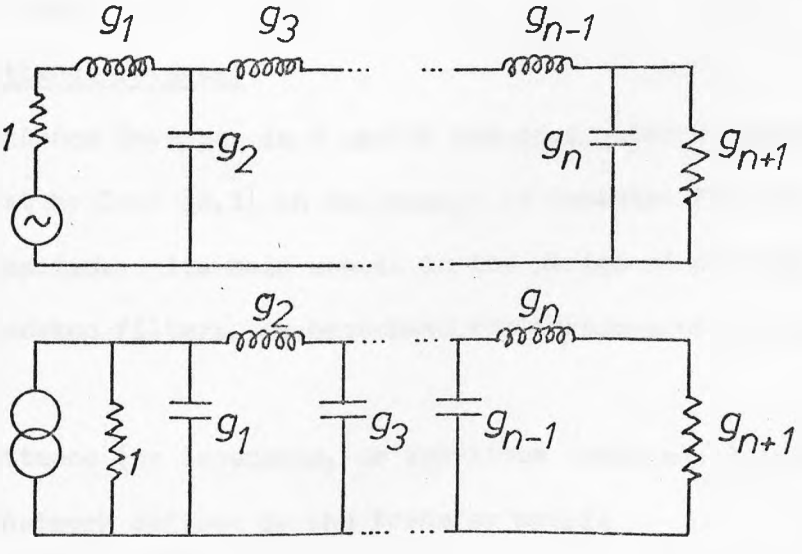

FIGURE 3.11 Prototype Ladder Networks .

and for the even-degree Chebyshev case that

$$Fn(0) = \frac{1}{1 + \varepsilon^2}$$

$Z_{12}(p)$ and $S_{11}(p)$ being known, the corresponding networks can be synthesised. Since the transmission zeros for both cases lie at infinity, the filters can be realised as ladder networks, of the general form shown in Figure 3.11, for singly terminated and doubly terminated networks. For the odd-degree Chebyshev cases, the terminating resistors are unity, for the even-degree cases the terminating resistors differ from unity. Such networks, which can form the basis of any type of filter, are known as low-pass-prototype networks, and tables for their element values have been widely published (e.g. [3.2]). Explicit formulae for the element values have also been derived, and are discussed later.

3.5 The Admittance Inverter

The Admittance Inverter is a useful two-port network concept introduced first by Cohn [3.3] in the design of bandpass filters, and later widely applied. Its main use is in the design of prototypes for bandpass or bandstop filters, as broadband realisations of the inverter do not exist.

The admittance (or impedance, or sometimes immittance) inverter is a two-port network defined by the transfer matrix

$$[T] = \begin{pmatrix} 0 & j/K \\ jK & 0 \end{pmatrix}$$

where K is called the "characteristic admittance" of inverter. If the output port of the network is terminated in an admittance Y, then the input admittance is clearly given by

$$Y_{in} = \frac{K^2}{Y}$$

Thus, for example, the input admittance of the network in

Figure 3.12(a) is given by the continued fraction;

$$Y_{in} = Y_1 + \cfrac{K_{12}^2}{Y_2 + \cfrac{K_{23}^2}{\ddots + \cfrac{K_{n-1,n}^2}{Y_n + G_n}}}$$

Similarly, if the K's are now the characteristic impedances of the inverters in Figure 3.12(b), then

$$Z_{in} = Z_1 + \cfrac{K_{12}^2}{Z_2 + \ddots + \cfrac{K_{n-1,n}^2}{Z_n + R_n}}$$

Thus, the circuit of Figure 3.12(a) can have an identical input admittance to that of a ladder network using shunt capacitors and series inductors, but only using shunt capacitors. Similarly, Figure 3.12(b) can have the same input impedance as a ladder, but using only series inductors. Introduction of the inverters has no effect on the transfer magnitude response, and also allows internal impedance scaling within the filter.

3.6 Explicit Formulae for Element Values

Explicit formulae for the element values in m.f. and Chebyshev ladder networks have been found by Orchard [3.4] and Takahasi [3.5], amongst others. Much of this thesis will be concerned with the design of bandpass filters, for which the alternative forms given by Rhodes [3.1] are more appropriate. The corresponding prototype circuits use shunt capacitors or series inductors coupled through admittance inverters, as shown in Figure 3.13(a) and (b). One consequence is that the end termination is always unity, because of the impedance scaling

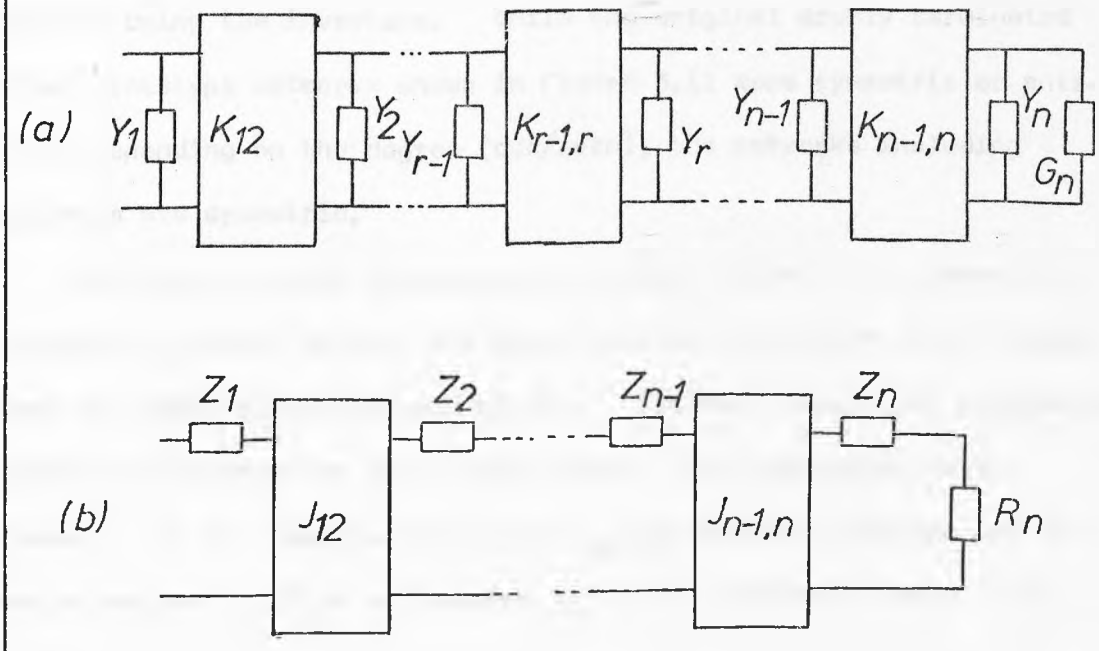

FIGURE 3.12 Ladder Networks with Immittance Inverters.

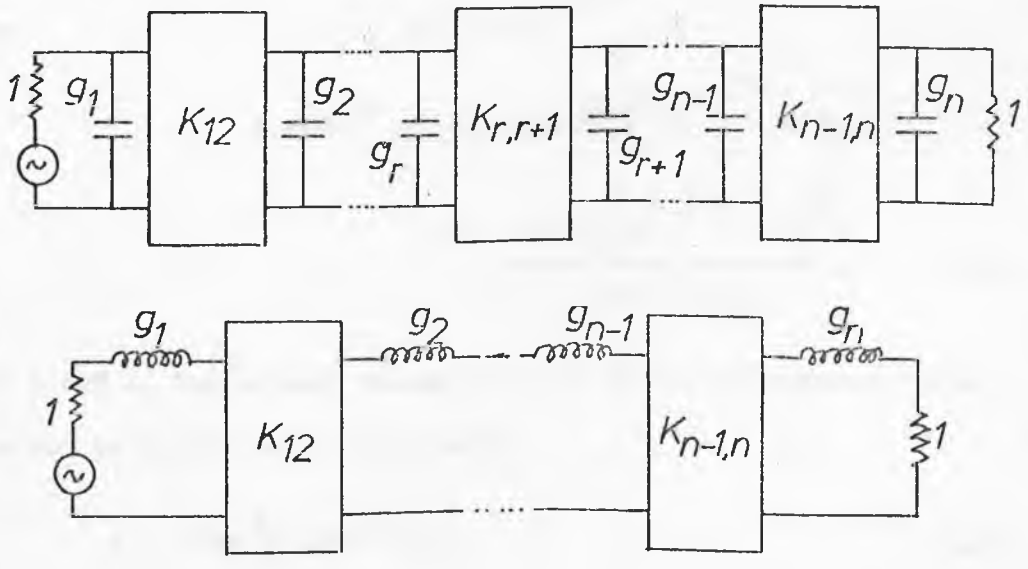

FIGURE 3.13 Lowpass Prototype Filters.

possible using the inverters. While the original doubly terminated ladder prototype networks shown in Figure 3.11 were symmetric or antimetric depending on the degree (odd/even), the networks including inverters are symmetric.

The first step in designing a prototype filter is to determine the degree required to meet the given stopband rejection specification given the permissible passband ripple. (In many cases, the permissible ripple is determined by the minimum return loss acceptable in the system.) If the required ripple is L_{AR} dB, and the response has to meet or exceed L_s dB at a frequency ω_c in the stopband, then, from (3.14),

$$\varepsilon^2 = 10^{L_{AR}/10} - 1$$

and $$10 \log_{10}(1 + \varepsilon^2 T_n^2[\omega_c]) \geq L_s$$

Hence $$\varepsilon^2 T_n^2[\omega_c] \geq 10^{L_s/10} - 1$$

$$n \cosh^{-1}[\omega_c] \geq \cosh^{-1}\left(\frac{1}{\varepsilon}\left[10^{L_s/10} - 1\right]^{\frac{1}{2}}\right)$$

$$n \geq \frac{\cosh\left(\frac{1}{\varepsilon}\left[10^{L_s/10} - 1\right]^{\frac{1}{2}}\right)}{\cosh^{-1}[\omega_c]} \qquad (3.18)$$

Given n and ε, the element values for the doubly-terminated filter are given by (3.20) and (3.21) below

$$\eta = \sinh\left[\frac{1}{n}\sinh^{-1}\left(\frac{1}{\varepsilon}\right)\right] \qquad (3.19)$$

$$g_r = \frac{2}{\eta}\sin\left[\frac{(2r-1)\pi}{2n}\right] \quad r = 1 \to n \qquad (3.20)$$

$$K_{r,r+1} = \frac{1}{\eta}\sqrt{(\eta^2 + \sin^2[r\pi/n])} \quad r = 1 \to n-1 \qquad (3.21)$$

$$g_{r+1} = 1 \qquad (3.22)$$

For some purposes an alternative form is useful, which occurs frequently in the design of bandpass filters:

$$g_o = \frac{2}{\eta} \sin\left[\frac{\pi}{2n}\right] \tag{3.23}$$

$$k_{r,r+1} = \sqrt{\frac{\eta^2 + \sin^2(r\pi/n)}{2[\cos(\pi/n) - \cos(2r\pi/n)]}} \quad , \; r = 1 \to n-1 \tag{3.24}$$

where the expression for $k_{r,r+1}$ is derived from (3.20) and (3.21), and

$$k_{r,r+1} = \frac{K_{r,r+1}}{\sqrt{(g_r g_{r+1})}}$$

For singly-terminated filters, the expressions given by Orchard [3.4] can be adapted to correspond to the network form of Figure 3.13, and are given in equations (3.25) to (3.28) below. Calculate

$$a_r = \sin\left[\frac{(2r-1)\pi}{2n}\right] \quad , \; r = 1 \to n$$

$$d_r = (\eta^2 + \sin^2[r\pi/2n]) \cos^2(r\pi/2n), \; r = 1 \to n-1$$

Then $$C_1 = \frac{a_1}{\eta}$$

$$C_r = \frac{a_r a_{r-1}}{d_{r-1} C_{r-1}} \quad , \; r = 2 \to n$$

and $$g_r = C_{n+1-r} \quad , \; r = 1 \to n \tag{3.25}$$

$$K_{r,r+1} = 1 \quad , \; r = 1 \to n-1 \tag{3.26}$$

$$g_{r+1} = 1 \quad , \; (r \text{ odd}) \tag{3.27}$$

$$g_{r+1} = \frac{1}{1 + \varepsilon^2} \quad (r \text{ even}) \tag{3.28}$$

The element values for the m.f. filter are obtainable by a limiting process from the Chebyshev form, and are, for the doubly-terminated filter,

$$g_r = 2 \sin\left[\frac{(2r-1)\pi}{2n}\right] \quad r = 1 \to n \tag{3.29}$$

$$K_{r,r+1} = 1, r = 1 \to n-1 \tag{3.30}$$

Correspondingly,

$$g_o = 2 \sin\left[\frac{\pi}{2n}\right] \tag{3.31}$$

$$k_{r,r+1} = \frac{1}{\sqrt{(2[\cos(\pi/2n)-\cos(2r\pi/n)])}} \qquad (3.32)$$

and for the singly-terminated case:

$$a_r = \sin\left[\frac{(2r-1)\pi}{2n}\right] , \quad r = 1 \rightarrow n$$

$$d_r = \cos^2\left(\frac{\pi r}{2n}\right) , \quad r = 1 \rightarrow n-1$$

Then $$C_1 = a_1$$

$$C_r = \frac{a_r a_{r-1}}{d_{r-1} C_{r-1}} \quad r = 2 \rightarrow n$$

and $$g_r = C_{n+1-r} , \quad r = 1 \rightarrow n \qquad (3.33)$$

$$K_{r,r+1} = 1 \qquad (3.34)$$

$$g_{r+1} = 1$$

3.7 Distributed Low-pass Prototype

The circuit of the basic distributed low-pass prototype filter is shown in Figure 3.14, and consists of tandem unit elements coupled through admittance inverters. When the inverters are scaled out of the circuit, the resulting filter is the stepped impedance filter. The distributed low-pass filter is important since it forms the prototype for both broadband waveguide and interdigital filters.

Because the elements of the filter are transmission lines it is convenient to discuss the behaviour of the filter in terms of the electrical length of the lines, θ, when

$$\theta = \frac{\pi}{2}\frac{f}{f_o} ,$$

f_o being the real frequency at which the lines are a quarter-wavelength of propagation.

In terms of the variable t, where t = tanh(p),

$$S_{12}(t) = \frac{(1-t^2)^{n/2}}{D_n(t)}$$

with $D_n(t)$ a Hurwitz polynomial. (For real frequencies, t = jtanθ.)

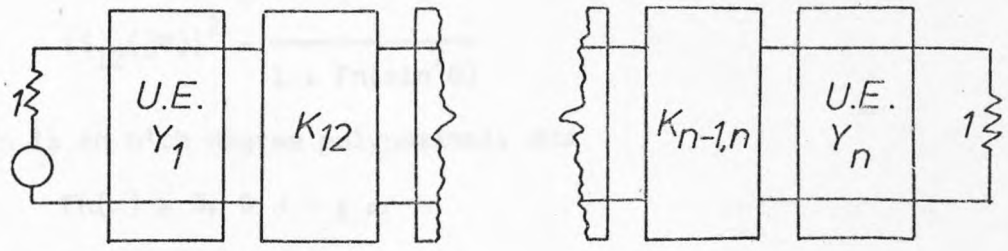

FIGURE 3.14 Stepped Impedance Prototype.

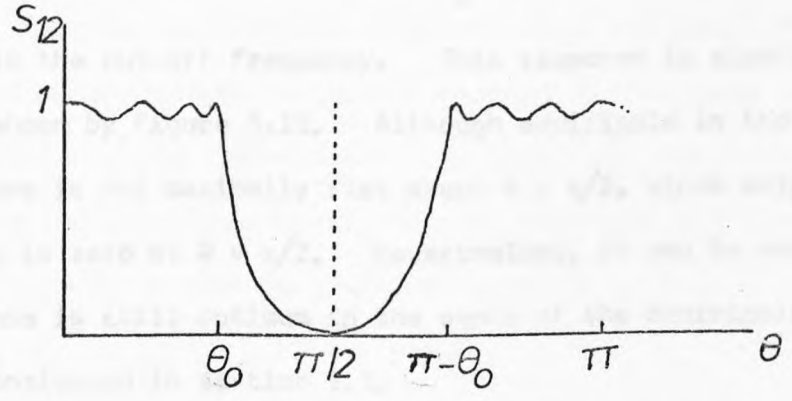

FIGURE 3.15 Response of Distributed Prototype.

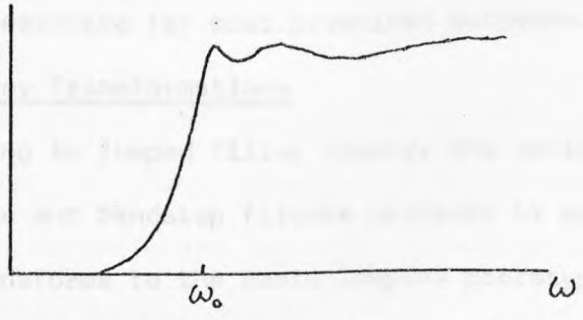

FIGURE 3.16 Highpass Filter Response.

Thus, $$|S_{12}(j\theta)|^2 = \frac{1}{1 + Fn(\sin^2\theta)}$$

where Fn is an n'th degree polynominal, and

$$Fn(x) \geq 0, \quad 0 \leq x \leq \infty$$

The particular equiripple solution is

$$|S_{12}(j\theta)|^2 = \frac{1}{1 + \varepsilon^2 T_n^2(\frac{\sin\theta}{\sin\theta_o})}$$

where θ_o is the cut-off frequency. This response is clearly periodic in θ, as shown by Figure 3.15. Although equiripple in the passband, the response is not maximally flat about $\theta = \pi/2$, since only one derivative is zero at $\theta = \pi/2$. Nevertheless, it can be shown that the response is still optimum in the sense of the equiripple approximations considered in section 3.3.

No closed-form explicit element value expressions have been found for the stepped impedance filter. However, Rhodes [3.1, p 139] derives explicit formulae in the form of a power series in the variable $\alpha = \sin \omega_o$. Since ω_o is usually less that $\pi/4$, these formulae are sufficiently accurate for most practical purposes.

3.8 Frequency Transformations

Returning to lumped filter theory, the design of lowpass, highpass, bandpass and bandstop filters proceeds by applying various frequency transforms to the basic lowpass prototype of Figure 3.13

a) Lowpass

The prototype lowpass filter has its cutoff frequency at unity. If the required cutoff frequency is ω_o, the corresponding frequency transform is

$$\omega \rightarrow \frac{\omega}{\omega_o}$$

Hence the reactance of an inductor, $X = \omega L$ is transformed by

$$\omega L \rightarrow \frac{\omega L}{\omega_o}$$

so that

$$L \rightarrow \frac{L}{\omega_o}$$

and similarly

$$C \rightarrow \frac{C}{\omega_o}$$

b) Highpass

The highpass transform is chosen so that the point of required infinite attenuation in the highpass filter, i.e. zero frequency, is transformed to infinity for the prototype. The required form of the highpass response is shown in Figure 3.16, and the transform used is

$$\omega \rightarrow -\frac{\omega_o}{\omega}$$

Thus a prototype inductor of reactance ωL is transformed by

$$\omega L \rightarrow -\frac{\omega_o L}{\omega}$$

which is a capacitor of value $1/\omega_o L$, while a capacitor transforms to an inductor of value $1/\omega_o C$.

c) Bandpass

The bandedges of the bandpass filter are ω_1 and ω_2, as shown in Figure 3.17. The transform required has to map the points $0, \omega_1, \omega_2, \infty$ in the "bandpass plane" to the points $-\infty$, -1, $+1$, $+\infty$ in the lowpass plane.

The transformation used is of the form

$$\omega \rightarrow B\left(\frac{\omega}{\omega_o} - \frac{\omega_o}{\omega}\right) \qquad (3.33)$$

Obviously this transforms the points $\omega = 0, \infty$ in the right way. From the other conditions,

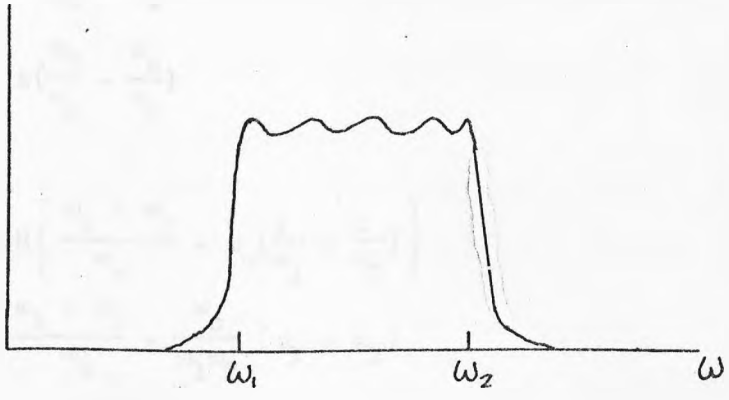

FIGURE 3.17 Bandpass Filter Response .

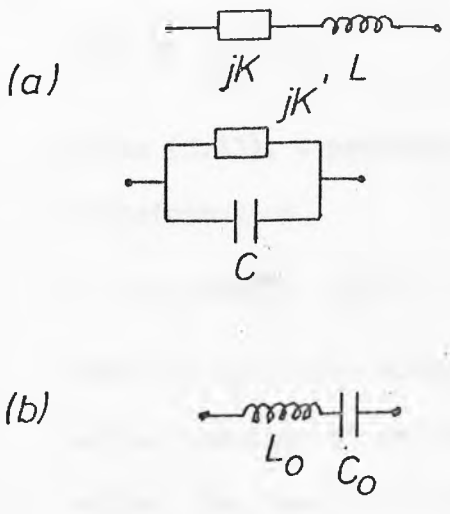

FIGURE 3.18 Realisation of Frequency-Invariant Immittances .

$$-1 = B\left(\frac{\omega_1}{\omega_o} - \frac{\omega_o}{\omega_1}\right)$$

$$1 = B\left(\frac{\omega_2}{\omega_o} - \frac{\omega_o}{\omega_2}\right)$$

Adding:

$$0 = B\left\{\frac{\omega_1 + \omega_2}{\omega_o} - \omega_o\left(\frac{1}{\omega_1} + \frac{1}{\omega_2}\right)\right\}$$

Thus $0 = \frac{\omega_1 + \omega_2}{\omega_o} - \frac{\omega_o}{\omega_1\omega_2}(\omega_1 + \omega_2)$

which is satisfied if

$$\omega_o^2 = \omega_1\,\omega_2.$$

Further,

$$-1 = B\left(\sqrt{\frac{\omega_1}{\omega_2}} - \sqrt{\frac{\omega_2}{\omega_1}}\right)$$

thus $B = \frac{\omega_o}{\omega_2 - \omega_1}$

Under (3.33), a prototype capacitor of susceptance ωC is transformed as

$$\omega C \rightarrow BC\left(\frac{\omega}{\omega_o} - \frac{\omega_o}{\omega}\right)$$

which is the shunt connection of a capacitor of value BC/ω_o and an inductor of value $1/\omega_o BC$. Similarly, an inductor of value L is transformed into the series connection of an inductor of value BL/ω_o and a capacitor of value $1/\omega_o BL$.

d) Bandstop

The bandstop transform can be obtained through a similar process to the bandpass, mapping the points 0, ω_1, ω_2, ∞ to 0, -1, +1, 0, with $\omega_o = \sqrt{\omega_1\omega_2}$ mapping to ∞ However, this is equivalent to applying, first the lowpass $\rightarrow$ highpass, then highpass $\rightarrow$ bandpass transforms to the lowpass filter. The resulting transform is

$$\omega \rightarrow \frac{-1}{B\left(\frac{\omega}{\omega_o} - \frac{\omega_o}{\omega}\right)}$$

with, again, $\omega_o = \sqrt{\omega_1 \omega_2}$

$$B = \frac{\omega_o}{\omega_2 - \omega_1}$$

3.9 Frequency Independent Reactances

Some of the design procedures developed later involve prototype filters which contain elements with reactances of the form

$$X = jK$$

with K independent of frequency. Such reactances are not realisable by any physical component, but are nevertheless useful in prototypes for relatively narrow band bandpass structures.

The driving-point immittances of circuits involving frequency-independent reactance are positive functions of p, i.e.

$$R_e[Z(p)] \geq 0 \text{ for } R_e(p) > 0$$

but not necessarily positive real.

Frequency-independent reactances usually occur in conjunction with real reactances such as shown in Figure 3.18(a). Considering the first case shown, this can be approximately realised in the bandpass case by a series tuned circuit, over a relatively narrow band, using the reactance slope technique.

The reactance of the first circuit shown in Figure 3.18(a) is

$$X = \omega L + K$$

Under the lowpass→bandpass transform, this becomes

$$X' = K + BL\left(\frac{\omega}{\omega_o} - \frac{\omega_o}{\omega}\right) \qquad (3.35)$$

Now the magnitude and first derivative of the reactance of the circuit of Figure 3.18(b) are equated to the magnitude and first derivative of (3.35) at $\omega = \omega_o$.

Thus $$\omega_o L_o - \frac{1}{\omega_o C_o} = K$$

and $$\frac{LB}{2\omega_o} = L_o + \frac{1}{\omega_o^2 C_o}$$

Solving for L_o and C_o gives:

$$L_o = \frac{1}{\omega_o}\left(LB + \frac{K}{2}\right) ,$$

$$C_o = \frac{1}{\omega_o \left(LB - \frac{K}{2}\right)}$$

A similar procedure can be adopted, using a parallel resonant circuit, to realise the second circuit of Figure 3.18(a).

Where a frequency-invariant reactance occurs in isolation, a narrow-band bandpass realisation is possible using an inductor or capacitor, according to its sign.

3.10 Conclusions

This chapter began by considering the problem of approximations in lowpass filter design, and derived the standard maximally-flat and equiripple approximations, in each case with all the zeros of the response lying at $\omega = \infty$. (Such approximations are often called "all-pole", and the corresponding filters are minimum phase.) The locations of the poles of the transfer functions, and for the doubly-terminated Chebyshev case, of the reflection zeros, were then derived.

After the introduction of the concept of the admittance inverter, the explicit element value formulae for the equally-terminated Chebyshev and Butterworth prototype filters, as derived by Rhodes, were quoted without proof. Also given were Orchard's formulae for the elements in singly-terminated filters. Then, the distributed low-pass prototype filter was introduced, and the approximate, explicit formulae for its elements, derived by Rhodes referred to.

The frequency transforms for the design of lowpass, highpass, bandpass and band-stop filters were derived, and the effect on the lowpass prototype of applying the transforms considered.

Finally, the significance of frequency-invariant reactances, which appear in some prototype design procedures for bandpass structures, was considered, and the "realisation" of such elements through the reactance-slope-parameter method introduced.

CHAPTER 4

DESIGN OF COUPLED-RESONATOR BANDPASS FILTERS

4.1 Introduction

This Chapter deals with the design methods available for bandpass filters of relatively narrow bandwidth, which can be designed from an appropriate lowpass prototype. The techniques are illustrated by deriving direct design formulas for the five types of bandpass filter shown in Figure 4.1(a)-(e).

The filter in (a) uses lumped, shunt-resonant circuits coupled by capacitors, and is suitable for use from low frequencies to VHF for bandwidths up to about ten percent. A design procedure based on the concept of admittance inverters was first given by Cohn [4.1]; the method here uses a substantially different procedure and is believed to be original.

In (b) is shown the interdigital filter, first described by Matthaei [4.2]: and improved design procedure was given by Cristal [4.14]. Physically, the device consists of parallel metal bars, forming transmission lines, symmetrically disposed between parallel metal ground plates. The bars are a quarter-wavelength long at the centre frequency of the filter, and shorted to the ground plates at alternate ends. For narrow and moderate bandwidths, the structure can be designed from a lumped prototype. The procedure given here is significantly different from Matthaei's and is implicit in techniques given by Rhodes [4.3] [4.4]. A similar method has also been considered by Pang [4.5].

The combline filter of 4(c) [4.2] uses a similar physical structure to the interdigital, except that the lines are all shorted to the ground plates at the same end. The lines are shorter than a quarter-wavelength at the passband centre, and are tuned by lumped capacitors at the open-circuit end. The design procedure given here

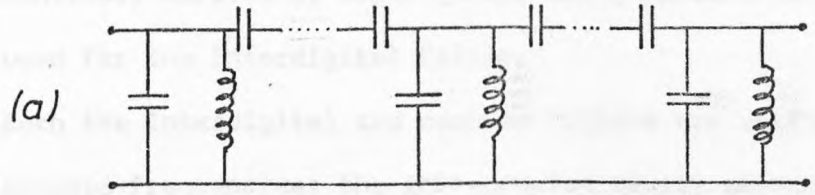

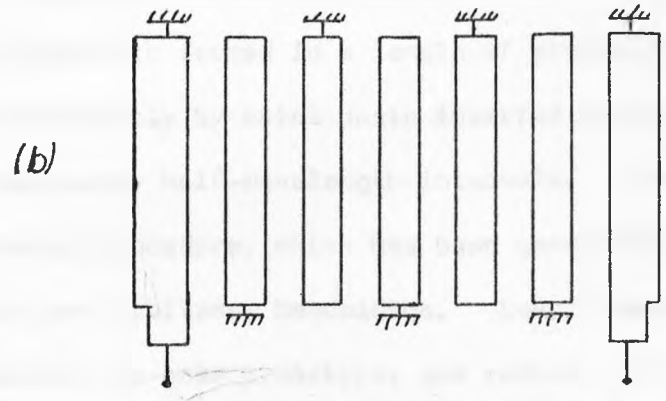

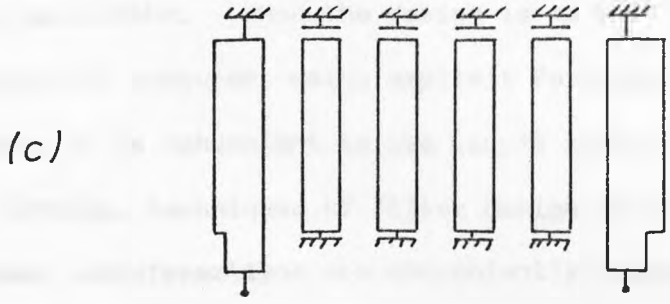

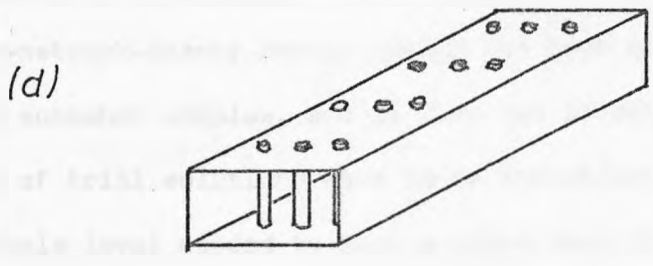

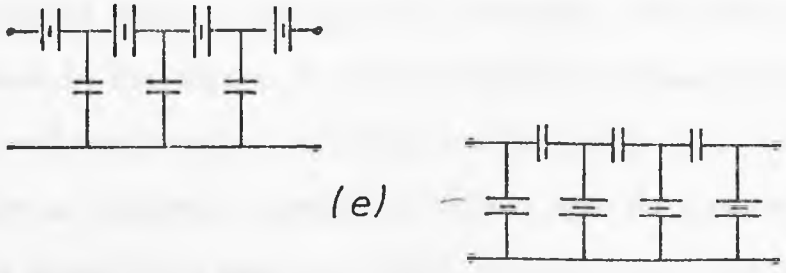

FIGURE 4.1 Some Bandpass Filters .

was essentially derived by Sayer [4.6], using similar techniques to those used for the interdigital filter.

Both the interdigital and combline filters are useful for UHF and low microwave frequencies: the iris-coupled cavity waveguide filter of 4.1(d) is useful from low microwave through to 20 GHz or even higher. The cavities are formed in a length of standard rectangular waveguide, most conveniently by metal posts inserted perpendicular to the broad-wall at roughly half-wavelength intervals. Cohn [4.1] gave a narrow-band design procedure, which has been generalised by Levy [4.7] for more-or-less arbitrary bandwidths. Levy's design is based on the distributed low-pass prototype, and reduces to Cohn's method for narrow bandwidths. When the design is carried out on a programmable calculator or computer, using explicit formulae for the prototype elements, it is convenient to use Levy's method, which is given here.

Finally, techniques of filter design and the derivation of frequency transformations are conveniently illustrated by the single-sideband (SSB) crystal filters of 4(e). These circuits were first described by Mason [4.8] and later considered by Sykes [4.9]. A modern-network-theory design method has been given by Dishal [4.10], but is somewhat complex, and is also not direct, in the sense that a number of trial solutions have to be investigated to find the degree and ripple level needed to meet a given specification. The method given here is based on the use of a frequency transform originally introduced in the design of active quadrature phase-shift networks [4.11], and also similar to Rhodes methods in [4.12]. The resulting procedure is extremely simple and direct, and the resulting filter circuits should have some advantages compared with existing methods of crystal filter design.

All the methods of design here are based on the transformation of a lowpass prototype network of the form given in Figure 3.13.

However, in most practical bandpass filters it is desirable to make all the resonators identical, and a modified form of the prototype is convenient, in which all the shunt capacitors or series inductors have the same value, in this case equal to "g_1" of the conventional prototype.

This can be achieved by nodal admittance scaling of all the internal nodes of the filter. Referring to Figure 3.13(a), using the definition of the admittance inverter (section 3.5) the nodal admittance matrix of the prototype is:

$$[Y] = \begin{bmatrix} pg_1 & -jK_{12} & 0 & \cdots & 0 \\ -jK_{12} & pg_2 & -jK_{23} & & \vdots \\ 0 & -jK_{23} & \ddots & & \\ \vdots & & -jK_{r-1,r} & pg_r & \ddots & -jK_{r,r+1} \\ 0 & & \cdots & & \ddots & pg_n \end{bmatrix}$$

This admittance matrix can be scaled by mutliplying any row and corresponding column except the first or last by a real, positive constant |4.13| within certain limits, without altering the transfer response of the network. In this case, the r'th row and column are multiplied by a constant k_r, where

$$k_r = \sqrt{\frac{g_1}{g_r}}, \quad r = 2 \rightarrow n$$

resulting in the equal-element prototype of Figure 4.2.

4.2 Capacity Coupled Lumped Element Filter

Figure 4.3 shows the r'th and r+1'th resonators of the filter of Figure 4.1(a), coupled through an admittance inverter composed of negative and positive capacitors. The negative shunt capacitors can generally be absorbed into the adjacent positive capacitor.

It is easily shown that the characteristic admittance of this

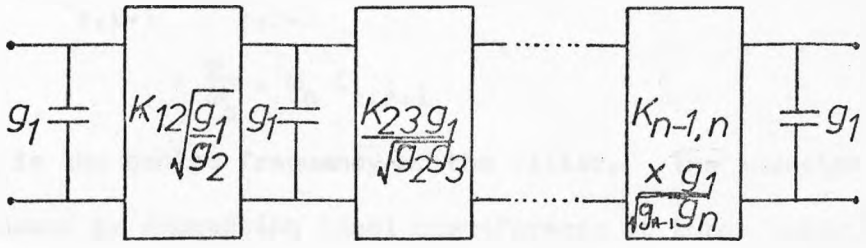

FIGURE 4.2 Modified Prototype for Coupled-Resonator Filters.

capacitive inverter is just

$$K_{r,r+1} = \omega C_{r,r+1}$$

$$= \frac{\omega}{\omega_o} \cdot \omega_o C_{r,r+1}$$

where ω_o is the centre frequency of the filter. The inverter can now be decomposed by extracting ideal transformers of turns ratio $\sqrt{\omega_o/\omega}$:1 and 1:$\sqrt{\omega_o/\omega}$ from its input and output, leaving an ideal inverter, as shown in Figure 4.4.

Turning to the resonator, its susceptance is given by

$$B_o = \omega C_o - \frac{1}{L_o \omega}$$

$$= \omega C_o(1 - \frac{\omega_o^2}{\omega^2})$$

where $$\omega_o^2 = \frac{1}{L_o C_o} \qquad (4.1)$$

is the centre frequency.

The shunt susceptance of each resonator can now be scaled through a neighbouring transformer. The resulting network is shown in Figure 4.5: all the transformers scale each other out of the network except at the input and output, and the resulting resonator susceptance is

$$B_o' = (\omega_o/\omega)B_o$$

$$= \omega_o C_o(1 - \frac{\omega_o^2}{\omega^2}) \qquad (4.2)$$

The appropriate lowpass to bandpass transform for the filter is hence

$$\omega \rightarrow A(1 - \frac{\omega_o^2}{\omega^2})$$

If the passband is to lie between ω_1 and ω_2, as in Figure 3.17,

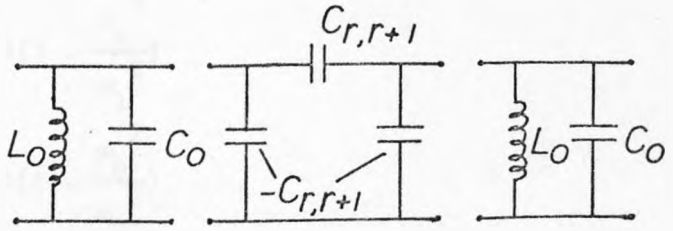

FIGURE 4.3 Decomposition of Capacitively Coupled Resonators.

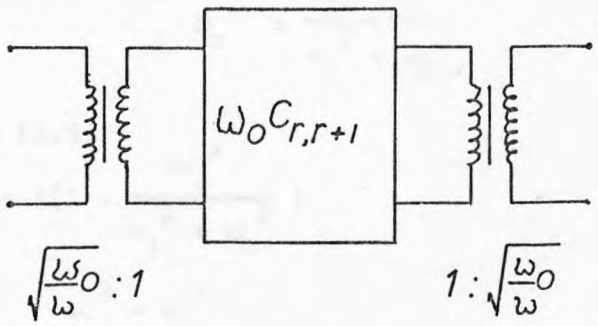

FIGURE 4.4 Decomposition of Frequency-Varying Admittance Inverter.

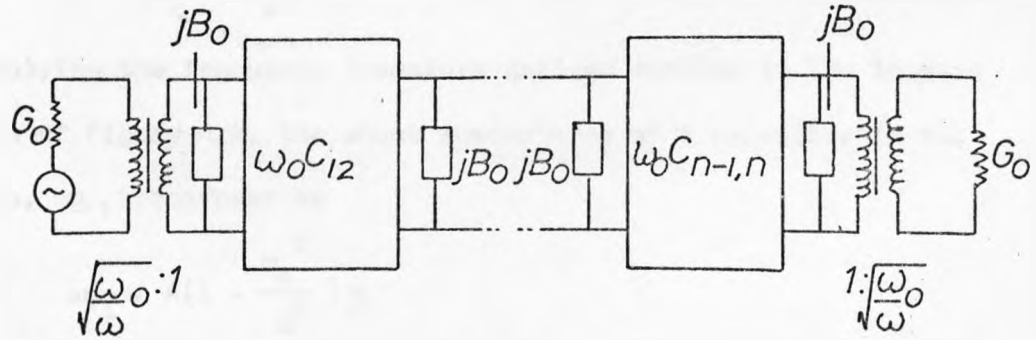

FIGURE 4.5 Frequency-Dependence of Couplings Scaled Out of Filter.

$$-1 = A\left(1 - \frac{\omega_o^2}{\omega_1^2}\right) \tag{4.3}$$

$$+1 = A\left(1 - \frac{\omega_o^2}{\omega_2^2}\right) \tag{4.4}$$

which requires, adding (4.3) and (4.4),

$$2 - \omega_o^2\left(\frac{1}{\omega_1^2} + \frac{1}{\omega_2^2}\right) = 0$$

or

$$\omega_o^2 = \frac{2\omega_1^2\,\omega_2^2}{\omega_1^2 + \omega_2^2} \tag{4.5}$$

Substituting in (4.3):

$$-1 = A\left(1 - \frac{2\omega_2^2}{\omega_1^2 + \omega_2^2}\right)$$

$$= A\left(\frac{\omega_1^2 - \omega_2^2}{\omega_1^2 + \omega_2^2}\right)$$

and thus

$$A = \frac{\omega_2^2 + \omega_1^2}{\omega_2^2 - \omega_1^2} \tag{4.6}$$

Applying the frequency transform derived earlier to the lowpass prototype of Figure 4.2, the shunt susceptance of a capacitor in the prototype, ωg_1, transforms as

$$\omega g_1 \rightarrow A\left(1 - \frac{\omega_o^2}{\omega^2}\right) g_1$$

Thus the terminating resistors of the prototype are scaled to a conductance of

$$G_o = \frac{\omega_o C_o}{A g_1}$$

and the admittance inverters scaled accordingly. The resulting admittance inverters required are

$$K_{12}' = K_{12}\sqrt{\frac{g_1}{g_2}} \cdot \frac{\omega_o C_o}{A g_1} = \frac{\omega_o C_o K_{12}}{A\sqrt{g_1 g_2}}$$

$$K_{r,r+1} = \frac{K_{r,r+1}\, g_1}{\sqrt{g_r\, g_{r+1}}} \cdot \frac{\omega_o C_o}{A g_1}$$

$$= \frac{\omega_o C_o\, K_{r,r+1}}{\sqrt{g_r\, g_{r+1}}}$$

$$K_{n-1,n} = \frac{\omega_o C_o\, K_{n-1,n}}{\sqrt{g_{n-1}\, g_n}}$$

Noting from Figure 4.5 that the admittance of the r'th inverter is $\omega_o\, C_{r,r+1}$,

$$C_{r,r+1} = C_o\, k_{r,r+1}$$

where the coupling parameter of equation (3.23) has been used.

Using the process developed above, the entire filter, within the frequency-varying transformers, is transformed exactly, and the input and output transformers are nearly unity for $\omega \approx \omega_o$, so that, at least for narrow bandwidths, they can be ignored.

The final filter circuit is shown in Figure 4.6, and the design procedure is as follows;

If the required band edges are ω_1 and ω_2, then the lowpass to bandpass transform is

$$\omega \to A\left(1 - \frac{\omega_o^2}{\omega^2}\right), \text{ with } A = \frac{\omega_2^2 + \omega_1^2}{\omega_2^2 - \omega_1^2} \text{ and } \omega_o^2 = \frac{2\omega_1^2\, \omega_2^2}{\omega_1^2 + \omega_2^2} \qquad (4.7)$$

which can be used to find the degree required for a given selectivity and ripple level, through (3.18). The required centre frequency is

$$\omega_o^2 = \frac{2\omega_1^2\, \omega_2^2}{\omega_1^2 + \omega_2^2} \qquad (4.8)$$

Either a convenient capacitor (C_o) or inductor (L_o) can be chosen for the frequency range. In either case,

$$C_o = \frac{1}{\omega_o^2 L_o} \text{ or } L_o = \frac{1}{\omega_o^2 C_o} \qquad (4.9)$$

Given the passband ripple and the required degree, use (3.22)

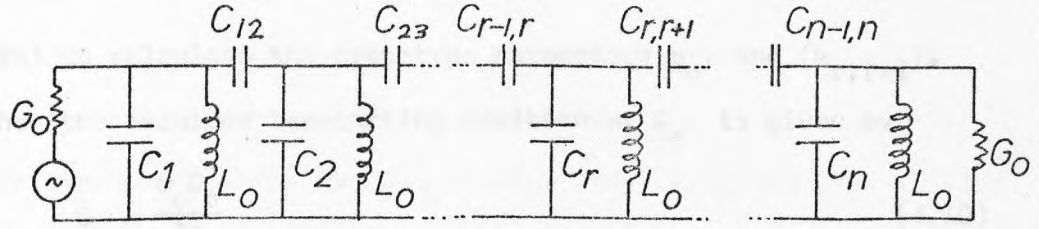

FIGURE 4.6 Final Filter Circuit.

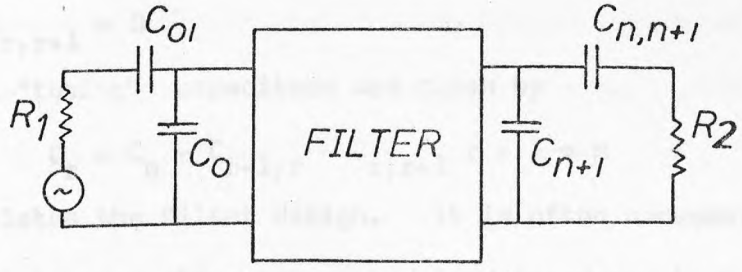

FIGURE 4.7 Matching to Other Impedances.

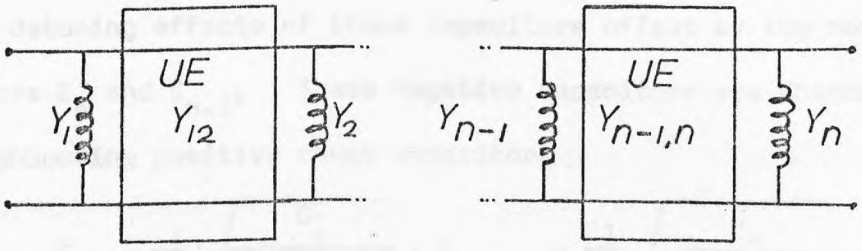

FIGURE 4.8 Equivalent Circuit of Interdigital Structure.

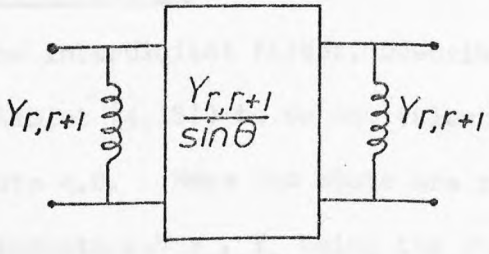

FIGURE 4.9 Extraction of Stubs from UE.

and (3.23) to calculate the prototype parameters g_o, and $\{k_{r,r+1}\}$.

Then the required terminating admittance, G_o, is given by

$$G_o = \frac{\omega_o C_o}{A g_o} \tag{4.10}$$

writing now "g_o" for "g_1" and the coupling capacitors by

$$\begin{aligned} C_{r,r+1} &= C_o\, k_{r,r+1}.\quad r = 1 \to n-1 \\ C_{r,r+1} &= 0 \end{aligned} \tag{4.11}$$

The nodal "tuning" capacitors are given by

$$C_r = C_o - C_{r-1,r} - C_{r,r+1} \quad r = 1 \to n \tag{4.12}$$

This completes the filter design. It is often necessary to match the filter to some other source and load impedance than $(1/G_o)$. In that case, the circuit of Figure 4.7 can be used, where the filter is matched to the terminations by the series capacitors C_{o1} and $C_{n,n+1}$, and the detuning effects of these capacitors offset by the negative capacitors C_o and C_{n+1}. These negative capacitors are absorbed into the neighbouring positive shunt capacitors

$$C_{o1} = \frac{1}{\omega_o}\sqrt{\frac{G_o}{R_1(1-R_1G_o)}}\,, \quad C_{n,n+1} = \frac{1}{\omega_o}\sqrt{\frac{G_o}{R_2(1-R_2G_o)}} \tag{4.13}$$

$$C_o = \frac{-C_{o1}}{1+\omega_o^2 C_{o1}^2 R_1^2}\,, \qquad C_{n+1} = \frac{-C_{n,n+1}}{1+\omega_o^2 C_{n,n+1}^2 R_2^2} \tag{4.14}$$

4.3 Interdigital Filters

The n-line interdigital filter, described in the introduction, can be shown (Riblet [4.15]) to be equivalent to the stub-unit-element cascade of Figure 4.8. Here the stubs are represented by t-plane inductors of "inductance" Y_r, Y_r being the characteristic admittance to ground of the r'th stub, coupled by unit elements equal in characteristic admittance to the mutual admittance between the stubs. The relationship between these characteristic admittances and the parameters of the physical structure (in this case the odd and even mode

capacitances per unit length between the lines) has been discussed by= Getsinger [4.16].

One immediate difficulty arises from this decompcsition: at near zero-frequency, the unit elements become effectively direct connections, the stubs coalesce into a single stub, and the structure posesses only a single transmission zero at the origin. Thus it is not possible to exactly equate this structure to a low-pass prototype with "n" zeros at the origin. As a result, two distinct design procedures exist for the interdigital filter. The method developed here, which applies for relatively narrow bandwidths, is based on the lumped element lowpass prototype. For broad bands, Rhodes has described a method based on the distributed prototype [4.17] which is valid even for the widest bandwidths physically possible with the device, and to some extent supersedes Wenzel's methods [4.18].

The interdigital filter's passband is centred on the frequency, f_c, at which the lines are quarter of a wavelength long, and the structure will be analysed in terms of the real frequency variable θ, where

$$\theta = \frac{\pi}{2}\frac{f}{f_c}$$

Then the transfer matrix of a unit element with characteristics admittance Y can be written and decomposed thus:

$$\begin{pmatrix} \cos\theta & j\sin\theta/Y \\ jY\sin\theta & \cos\theta \end{pmatrix} = \begin{pmatrix} 1 & 0 \\ -jY\cot\theta & 1 \end{pmatrix} \begin{pmatrix} 0 & j\frac{\sin\theta}{Y} \\ j\frac{Y}{\sin\theta} & 0 \end{pmatrix} \begin{pmatrix} 1 & 0 \\ -jY\cot\theta & 1 \end{pmatrix} \tag{4.15}$$

A shunt short-circuit stub has thus been extracted from the input and output of the unit element, to leave a frequency-variable ideal admittance inverter, shown in Figure 4.9, where the stubs extracted have been combined with the nodal stubs to give a combined stub characteristic

admittance

$$Y_{rr} = Y_r + Y_{r-1,r} + Y_{r,r+1} \qquad (4.16)$$

Next, an ideal transformer of turns ratio

$$\sqrt{\sin\theta}: 1$$

is extracted from each port of the ideal inverter, to leave an ideal frequency-independent inverter. As in the preceding section, these transformers can be scaled out of the network to leave the network shown in Figure 4.10, in which each shunt susceptance is of the form

$$B_r = - Y_{rr}\cos\theta$$

Once again, around $f \approx f_c$, $\theta \approx \pi/2$, and thus $\sin\theta \approx 1$, and, at least for narrow bandwidths, the frequency-varying transformer can be ignored (but see Chapter 8).

Now considering the equal-element low-pass prototype of Figure 4.2, it can be equated to the interdigital structure under the frequency transform

$$\omega \rightarrow - K \cos\theta$$

If the lower band edge of the interdigital filter is to be at f_o, so that

$$\theta_o = \frac{\pi}{2}\frac{f_o}{f_c} \qquad (4.17)$$

then $$-1 \rightarrow - K \cos\theta_o$$

or $$K = \frac{1}{\cos\theta_o} \qquad (4.18)$$

and the frequency transform becomes

$$\omega \rightarrow - \frac{\cos\theta}{\cos\theta_o}$$

Applying this transform to the low-pass prototype, the susceptance of a shunt capacitor, ωg_1, becomes

$$\omega g_1 \rightarrow - g_1 \frac{\cos\theta}{\cos\theta_o}$$

and thus $$Y_r = \frac{g_1}{\cos\theta_o} \qquad (4.19)$$

while the values of the coupling admittances are given directly by the

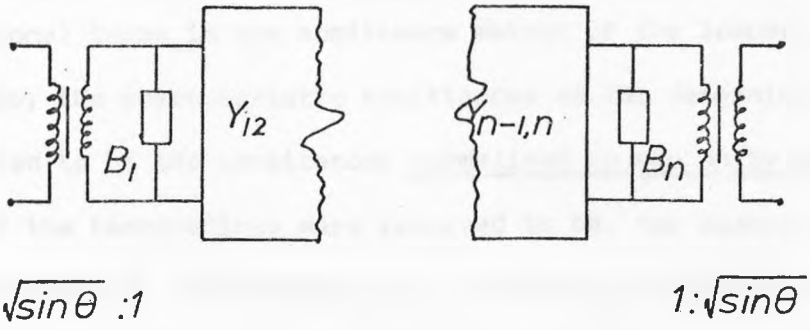

FIGURE 4.10 Transformers Scaled out of Network.

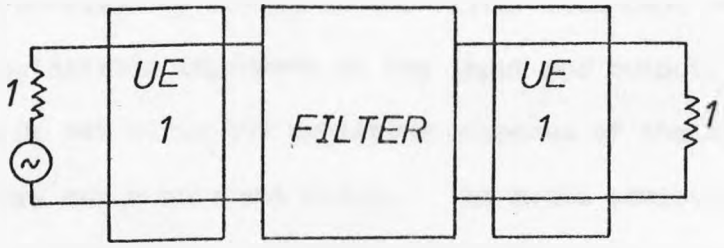

FIGURE 4.11 Introduction of redundant UE's for matching.

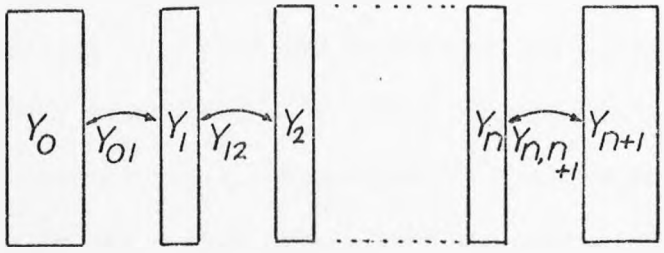

FIGURE 4.12 Definition of Interdigital Filter Parameters.

off-diagonal terms in the admittance matrix of the lowpass prototype.

Now, the characteristic admittances so far determined can be considered to be the admittances normalised to the unity terminations. Thus, if the terminations were required to be, for example, 50 ohms, then the corresponding admittances could be found by dividing the admittances determined above by 50. It happens, though, that the range of characteristic admittances easily realisable as the self-admittance of a line in an interdigital structure is restricted, and the most convenient value corresponds to about 50 ohms. However, the "Y_r" demanded by (4.19) is likely to be relatively much larger, being proportional to $(\cos\theta_o)^{-1}$, with $\theta_o \approx \pi/2$. Since most coaxial transmission systems in which the filter will be used are 50 ohm systems, it is convenient to modify the filter so that the normalised Y_r is around unity.

This is achieved by adding to the filter redundant unit elements of unity characteristic impedance at the input and output, as in Figure 4.11. These do not alter the amplitude response of the filter in any way, though they add a constant delay. The nodal admittance matrix of the resulting structure, using the admittance values found before,

is:

$$[Y] = \frac{1}{t}\begin{bmatrix} 1 & \sqrt{1-t^2} & 0 & \cdots & 0 \\ \sqrt{1-t^2} & 1+g_1/\cos\theta & K_{12}\frac{g_1}{g_2}\sqrt{1-t^2} & & \\ 0 & K_{12}\sqrt{\frac{g_1}{g_2}}\sqrt{1-t^2} & g_1/\cos\theta_o & \frac{K_{23}g_1\sqrt{1-t^2}}{\sqrt{g_2g_3}} & \vdots \\ 0 & 0 & \frac{K_{23}g_1\sqrt{1-t^2}}{\sqrt{g_2g_3}} & \ddots & \vdots \\ \vdots & & & & 0 \\ & & & 1+g_1/\cos\theta_o & \sqrt{1-t^2} \\ 0 & & & \sqrt{1-t^2} & 1 \end{bmatrix} \tag{4.20}$$

This matrix is an (n+2) x (n+2) matrix, though the original array had only n lines. It will be shown that this procedure effectively introduces extra coupling lines at the input and output, which will be numbered 0 and n+1.

Now rows and columns of (4.20) except for the first and last, can be scaled without changing the response of the network. The scaling factors are chosen to make the diagonal entries of the matrix unity. Thus the second and n'th row and column are multiplied by $1/\sqrt{1+g_1/\cos\omega_o}$ and the r'th row and column by $\sqrt{\cos\theta_o/g_1}$.

The resulting matrix is the admittance matrix of a new interdigital structure, and by reversing Riblet's procedure [4.15], the self and mutual admittances of the structure can be found, and thus the design equation established. Once again, the design equations are given in terms of the parameters of equations (3.23) and (3.24), g_o and $k_{r,r+1}$.

The design equations are, referring to Figure 4.12:

$$Y_{01} = Y_{n,n+1} = \frac{1}{\sqrt{1 + \frac{g_o}{\cos\theta_o}}} \qquad (4.21)$$

$$\left.\begin{aligned} Y_{12} &= \frac{g_o \cos\theta_o}{\sqrt{g_o + \cos\theta_o}}\, k_{12} \\ Y_{n-1,n} &= \frac{g_o \cos\theta_o}{\sqrt{g_o + \cos\theta_o}}\, k_{n-1,n} \\ Y_{r,r+1} &= k_{r,r+1} \cos\theta_o, \quad r = 2 \to n-2 \end{aligned}\right\} \qquad (4.22)$$

$$Y_o = Y_{n+1} = 1 - Y_{01} \qquad (4.23)$$

$$Y_r = 1 - Y_{r-1,r} - Y_{r,r+1}, \quad r = 1 \to n \qquad (4.24)$$

These characteristic admittances can be converted to cross-sectional dimensions using Getsingers data [4.16].

The design procedure here has been derived using techniques originally described by Rhodes [4.4]; similar design equations have been published in [4.19]. These equations and their derivation are substantially different from the original method of Matthaei [4.2].

4.4 The Combline Filter

The combline structure is represented in Figure 4.1c. It uses an array of parallel-coupled bars similar to the interdigital filter, but each bar is shorted to ground at the same end, and is tuned by a lumped capacitor at the other. The bars are again coupled by their fringing fields. An "open-wire" equivalent circuit for a section of the combline filter is shown in Figure 4.13 [4.2]. Considering the r'th bar, this behaves as a shunt short-circuited stub of characteristic

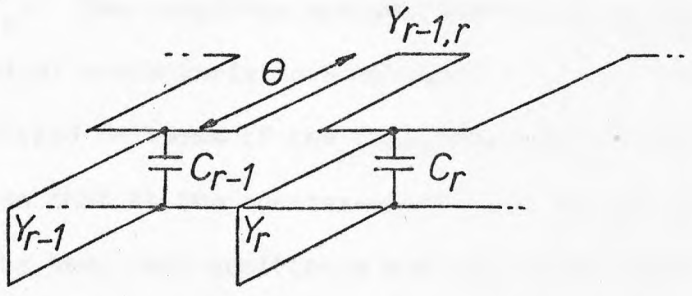

FIGURE 4.13 Part of a Combline Filter.

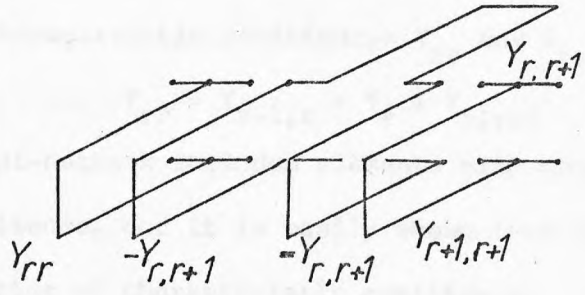

FIGURE 4.14 Decomposition of Coupling Admittance

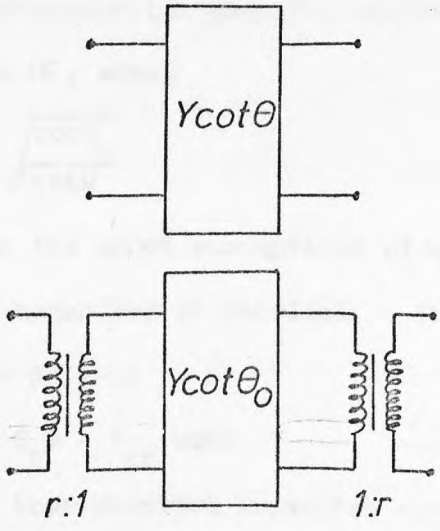

FIGURE 4.15 Decomposition of Frequency-Variant Admittance Inverter .

admittance Y_r. The couplings are represented as series short-circuited stubs of typical characteristic admittance $Y_{r,r+1}$. The structure will again be analysed in terms of the real-frequency variable θ. However, it can be seen that at the quarter-wavelength frequency ($\theta = \pi/2$) the coupling stubs have zero admittance and the filter therefore exhibits a transmission zero. The passband must therefore occur at a lower frequency, and lumped capacitors are provided to resonate the stubs.

The typical section of the filter can now be decomposed into the form shown in Figure 4.14: a pi-network of stubs couples shunt stubs of characteristic admittances Y_{rr} and $Y_{r+1,r+1}$, where

$$Y_{rr} = Y_{r-1,r} + Y_r + Y_{r,r+1} \qquad (4.25)$$

The pi-network includes elements with negative characteristic admittance, and it is easily shown that it behaves as an admittance inverter of characteristic admittance

$$K = Y_{r,r+1} \cot\theta$$

Now suppose that the filter is to be designed to work about a band-centre frequency of θ_o. The frequency-variation of the admittance inverter can be extracted by frequency-variable ideal transformers as shown in Figure 4.15, where

$$n = \sqrt{\frac{\cot\theta_o}{\cot\theta}} \qquad (4.26)$$

Now consider the shunt susceptance of a resonator, consisting of a stub and lumped capacitor in parallel. The shunt susceptance of the r'th resonator is thus

$$B_r = C_r\theta - Y_{rr} \cot\theta \qquad (4.27)$$

Here, C_r is not a true physical capacitor since it has the frequency variation θ instead of ω. However, this is convenient for the derivation, and the true value is easily determined after the physical design is completed.

C_r must resonate Y_{rr} at $\theta = \theta_o$, and thus

$$C_r\theta_o - Y_{rr}\cot\theta_o = 0$$

and

$$C_r = \frac{Y_{rr}\cot\theta_o}{\theta_o}$$

Substituting in (4.27), the resonator susceptance is

$$B_r = Y_{rr}\left(\frac{\theta\cot\theta_o}{\theta_o} - \cot\theta\right) \qquad (4.28)$$

Now the frequency-variable ideal transformers can be scaled out of the network and appear only at the terminations of the filter, as in the preceding sections. Once again, the effect of the transformers can be neglected near $\theta = \theta_o$. The resulting resonator susceptance, given by scaling (4.28) by the square of (4.26) is

$$B_r' = B_r \cdot \frac{\cot\theta_o}{\cot\theta}$$

$$= Y_{rr}\cot\theta_o\left[\frac{\theta\tan\theta}{\theta_o\tan\theta_o} - 1\right] \qquad (4.29)$$

Thus the appropriate frequency transform is

$$\omega \to B\left(\frac{\theta\tan\theta}{\theta_o\tan\theta_o} - 1\right) \qquad (4.30)$$

Figure 4.16 shows the shape of the required response and defines the band edges in relation to the quarter-wavelength frequency and the band-centre, θ_o. In practice, the quarter-wavelength frequency is fixed by the designer, and hence θ_1 and θ_2 are fixed by the required band-edge frequencies. Thus B and θ_o have to be determined from the specification.

When the frequency transform (4.30) is applied to the lowpass prototype, the lowpass band edges, $\pm$ 1, must be mapped to the bandpass band edges, θ_1 and θ_2. Hence

$$-1 = B\left[\frac{\theta_1\tan\theta_1}{\theta_o\tan\theta_o} - 1\right] \qquad (4.31)$$

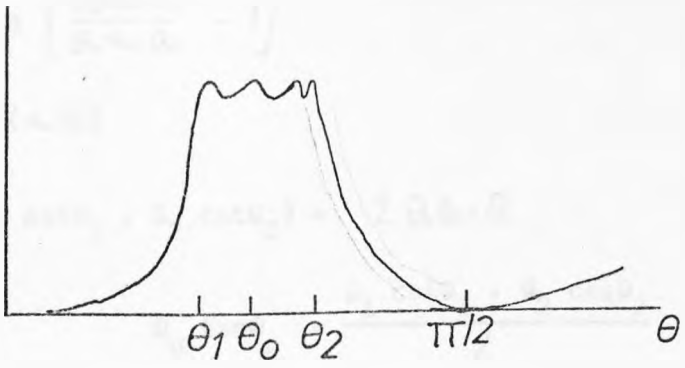

FIGURE 4.16 Response of Combline Filter.

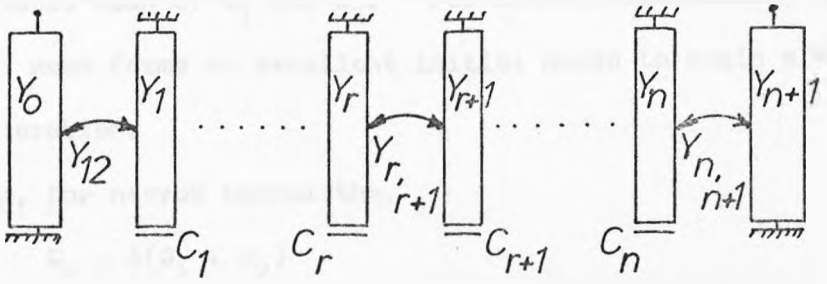

FIGURE 4.17 Definition of Combline Filter Parameters.

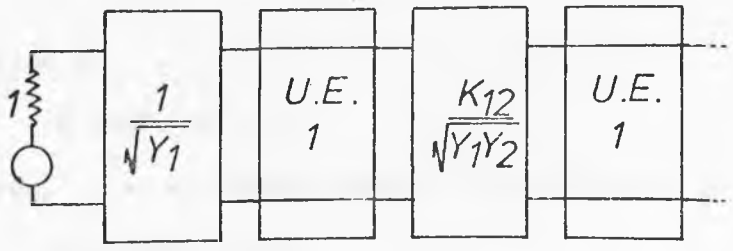

FIGURE 4.18 Modified Prototype for Waveguide Filter.

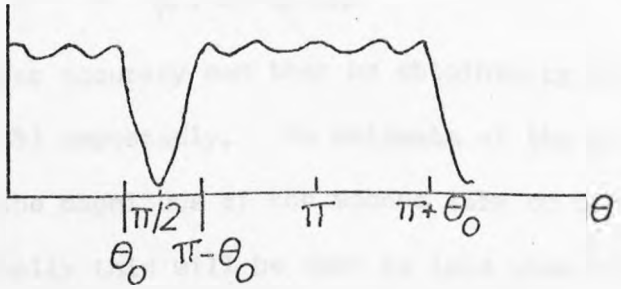

FIGURE 4.19 Half-Wave Filter Response.

$$+ 1 = B \left[\frac{\theta_2 \tan\theta_2}{\theta_o \tan\theta_o} - 1 \right] \qquad (4.32)$$

Adding (4.31) and (4.32)

$$(\theta_1 \cot\theta_1 + \theta_2 \cot\theta_2) = 2\theta_o \tan\theta_o$$

Thus
$$\theta_o \tan\theta_o = \frac{\theta_1 \cot\theta_1 + \theta_2 \cot\theta_2}{2} \qquad (4.33)$$

To find θ_o from (4.33) requires the solution of a transcendental equation. Fortunately, for narrow bandwidths a very close approximation for θ_o is the arithmetic mean of θ_1 and θ_2. For broader bandwidths, this arithmetic mean forms an excellent initial guess to begin a Newton-Raphson iteration.

Thus, for narrow bandwidths,

$$\theta_o = \tfrac{1}{2}(\theta_1 + \theta_2) \qquad (4.34)$$

For broader bandwidths, let

$$a = \frac{\theta_1 \cot\theta_1 + \theta_2 \cot\theta_2}{2}$$

The solution of

$$\phi \tan\phi - a = 0$$

is required. Let an initial guess to the solution be ϕ_1, where

$$\phi_1 = \tfrac{1}{2}(\theta_1 + \theta_2)$$

Then an improved approximation is

$$\phi_2 = \phi_1 - \frac{\cos\phi_1 (\phi_1 \sin\phi_1 - a\cos\phi_1)}{\phi_1 + \sin\phi_1 \cos\phi_1} \qquad (4.35)$$

An even greater accuracy can then be obtained by letting $\phi_1 = \phi_2$ and applying (4.35) repeatedly. An estimate of the accuracy at each step is given by the magnitude of the second term on the right-hand side of (4.35); typically this will be down to less than 0.01% of ϕ_1 within four to five iterations.

Having found θ_o by one means or other, B can be found from (4.32):

$$\frac{1}{B} = \frac{\theta_2 \tan\theta_2}{\theta_o \tan\theta_o} - 1$$

whence, using (4.33)

$$B = \frac{\theta_2 \tan\theta_2 + \theta_1 \tan\theta_1}{\theta_2 \tan\theta_2 - \theta_1 \tan\theta_1} \qquad (4.36)$$

Consider a shunt capacitor of the lowpass prototype of Figure 4.2. Under the frequency transform (4.30) the susceptance of this capacitor transforms as

$$\omega g_1 \rightarrow B \left(\frac{\theta \tan\theta}{\theta_o \tan\theta_o} - 1\right) g_1$$

and by comparison with (4.29),

$$Y_{rr} = B g_1 \tan\theta_o$$

Equating the admittance inverters to those of the prototype,

$$Y_{12} \cot\theta_o = K_{12} \sqrt{\frac{g_1}{g_2}}$$

thus $$Y_{12} = K_{12} \tan\theta_o \sqrt{\frac{g_1}{g_2}}$$

Similarly

$$Y_{r,r+1} = K_{r,r+1} \tan\theta_o \frac{g_1}{\sqrt{g_r\, g_{r+1}}} \qquad r = 2 \rightarrow n-2$$

$$Y_{n-1,n} = K_{n-1,n} \tan\theta_o \frac{g_1}{\sqrt{g_{n-1}\, g_n}}$$

Now, as with the interdigital filter, redundant unit elements are incorporated at the input and output of the filter, and nodal admittance scaling applied within the filter to adjust the self-admittances of the lines to a convenient value for realisation, again bearing in mind that the filter will generally be used in a 50 ohm system. The resulting normalised characteristic self- and mutual-admittances are defined in Figure 4.17 and are given by equations (4.37) to (4.42) with the

prototype parameters again in the form of (3.23) and (3.24):

$$Y_{01} = Y_{n,n+1} \tag{4.37}$$

$$= \frac{1}{\sqrt{1 + B g_0 \tan\theta_0}}$$

$$Y_{12} = k_{12}\sqrt{\frac{g_0 \tan\theta_0}{B(1 + B g_0 \tan\theta_0)}} \tag{4.38}$$

$$Y_{n-1,n} = k_{n-1,n}\sqrt{\frac{g_0 \tan\theta_0}{B(1 + B g_0 \tan\theta_0)}} \tag{4.39}$$

$$Y_0 = 1 - Y_{01} \tag{4.40}$$

$$Y_{n+1} = 1 - Y_{n,n+1} \tag{4.41}$$

$$Y_r = 1 - Y_{r-1,r} - Y_{r,r+1}, \quad r = 1 \to n \tag{4.42}$$

Finally, the lumped capacitors must be chosen to resonate the characteristic self-admittances of the lines at the real frequency, ω_0, corresponding to θ_0. Thus

$$C_r = \frac{\cot\theta_0}{\omega_0}, \quad r = 1 \to n \tag{4.43}$$

To conclude, a brief discussion of the choice of the quarter-wavelength frequency of the lines is necessary. The combline filter has a transmission zero at this frequency, and a stopband extending to at least an octave above that. Another resonance between the lumped capacitor and the line is possible when the line is slightly more than a half-wavelength long, and there may be a significant amount of transmission at that resonance. Thus, since the line is generally chosen to be about an eighth-wavelength long ($\theta_0 = \pi/4$), the combline filter has a stopband extending for at least two octaves above the passband. This contrasts with the interdigital filter, which has its first spurious

passband at three times the fundamental passband centre frequency. There are other considerations affecting the choice of θ_o. For example, if θ_o is made smaller the physical size of the filter can be reduced. Also, it has been found that a particular choice of θ_o (equivalent to 53^o) permits the resulting filter to be tuned over a wide range of centre frequencies while maintaining an acceptable response [4.20].

4.5 Direct-Coupled-Cavity Waveguide Filters

Figure 4.18 shows the distributed lowpass prototype introduced in Chapter 3, rearranged so that all the unit elements have unity characteristic admittance. This has been achieved by introducing redundant admittance inverters at input and output and then scaling all the unit element admittances into the inverters. This operation has no effect on the frequency response of the network beyond introducing an additional 180^o phase shift.

The amplitude response of this network is shown in Figure 4.19. Earlier, the "lowpass" passband was of interest; now, the second "harmonic" passband around $\theta = \pi$ is of interest, this being a "bandpass" characteristic.

The particular waveguide structure of interest is the inductive-post-coupled filter of Figure 4.1(d). An equivalent circuit of this is shown in Figure 4.20(a). The posts can be adequately described by shunt inductive susceptances, with an appropriate frequency variation proportional to guide wavelength. Thus a typical shunt admittance of a coupling post is

$$-jB_{r,r+1}\frac{\lambda_o}{\lambda g_o}$$

Here, $B_{r,r+1}$ is a constant equal to the susceptance at the "centre frequency" of the filter, λg_o. Because of the cut-off effect in waveguide and consequent dispersion, it is convenient to treat the filter in terms of the guide wavelength. In addition, the characteristic

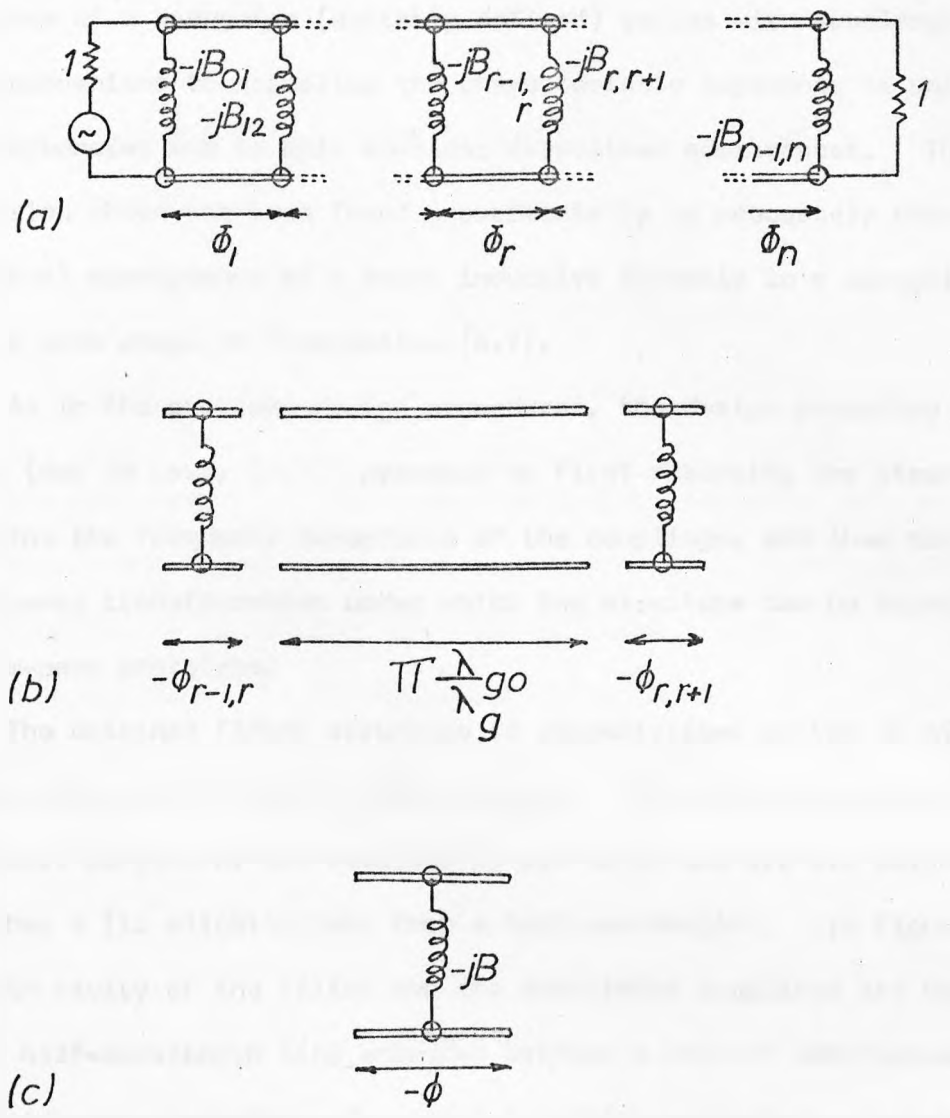

FIGURE 4.20 Decomposition of Waveguide Filter.

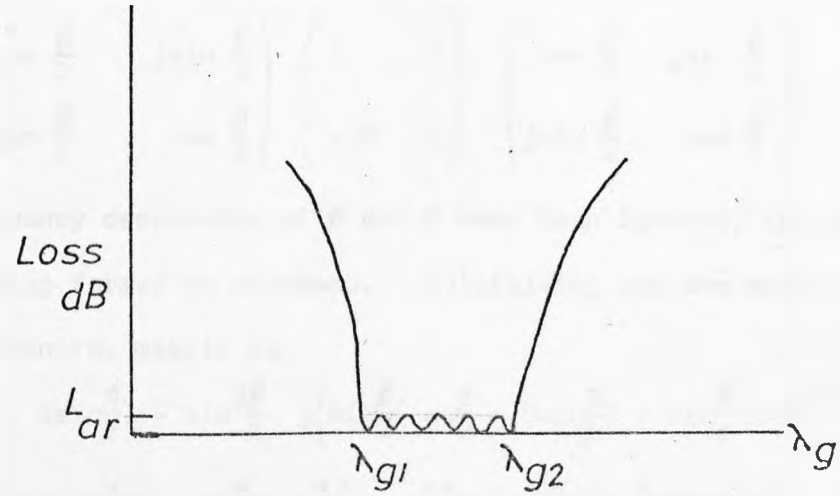

FIGURE 4.21 Response of Waveguide Filter.

impedance of a waveguide (suitably defined) varies with wavelength, so it is convenient to normalise the characteristic impedance to unity at all frequencies and to only consider normalised admittances. The expression above has been found experimentally to adequately characterise the actual susceptance of a shunt inductive obstacle in a waveguide over quite a wide range of frequencies [4.7].

As in the previous design procedures, the design procedure for this filter (due to Levy, [4.7]) proceeds by first analysing the structure to determine the frequency dependence of the couplings, and then determines a frequency transformation under which the structure can be equated to the low-pass prototype.

The original filter structure is characterised by the shunt post susceptances and the cavity phase-lengths. The phase-lengths are the electrical lengths of the cavities at mid band, and are all slightly less than π (ie slightly less than a half-wavelength). In Figure 4.20 (b) the r'th cavity of the filter and its associated couplings are decomposed into a half-wavelength line embedded between a pair of admittance inverters each consisting of a shunt inductive susceptance symmetrically located in a positive electrical length of line. The inverter circuit is shown again in Figure 4.20 (c).

The transfer matrix of the network of Figure 4.20 (c) is;

$$\begin{pmatrix} \cos\frac{\phi}{2} & j\sin\frac{\phi}{2} \\ j\sin\frac{\phi}{2} & \cos\frac{\phi}{2} \end{pmatrix} \begin{pmatrix} 1 & 0 \\ -jB & 1 \end{pmatrix} \begin{pmatrix} \cos\frac{\phi}{2} & j\sin\frac{\phi}{2} \\ j\sin\frac{\phi}{2} & \cos\frac{\phi}{2} \end{pmatrix}$$

Here the frequency dependence of ϕ and B have been ignored, the matrix implicitly being formed at mid-band. Multiplying out the matrices, the overall transfer matrix is

$$\begin{pmatrix} \cos\frac{\phi}{2}\left(\cos\frac{\phi}{2} + B\sin\frac{\phi}{2}\right) - \sin^2\frac{\phi}{2} & j\left\{\sin\frac{\phi}{2}\left(\cos\frac{\phi}{2} + B\sin\frac{\phi}{2}\right) + \sin\frac{\phi}{2}\cos\frac{\phi}{2}\right\} \\ j\left\{\cos\frac{\phi}{2}\left(\sin\frac{\phi}{2} - B\cos\frac{\phi}{2}\right) + \sin\frac{\phi}{2}\cos\frac{\phi}{2}\right\} & \cos^2\frac{\phi}{2} - \sin\frac{\phi}{2}\left(\sin\frac{\phi}{2} - B\cos\frac{\phi}{2}\right) \end{pmatrix}$$

For the circuit to behave as an inverter, "A" and "D" must be zero.

Hence

$$\cos^2\frac{\phi}{2} - \sin^2\frac{\phi}{2} + B\sin\frac{\phi}{2}\cos\frac{\phi}{2}$$

$$= \cos\phi + \frac{B}{2}\sin\phi$$

$$= 0$$

and hence

$$\phi = -\cot^{-1}\left(\frac{B}{2}\right) \qquad (4.45)$$

Thus the line lengths in the inverters must be negative, and can be absorbed in the neighbouring positive lengths. At the input and output, they can be absorbed into the convecting lines.

The admittance of the equivalent inverter, K, can be determined from the "C" term of the transfer matrix and is

$$K = 2\sin\frac{\phi}{2}\cos\frac{\phi}{2} - B\cos^2\frac{\phi}{2}$$

$$= \sin\phi - \frac{B}{2}(1 + \cos\phi)$$

However,

$$\cot\phi = -\frac{B}{2}$$

and hence

$$\sin\phi = \frac{1}{\sqrt{1 + B^2/4}}, \quad \cos\phi = -\frac{B/2}{\sqrt{1 + B^2/4}}$$

Thus

$$K = \frac{1}{\sqrt{1 + B^2/4}} - \frac{B}{2}\left(1 - \frac{B/2}{\sqrt{1 + B^2/4}}\right)$$

$$= \frac{1}{\sqrt{1 + B^2/4}}\left\{1 + B^2/4 - \frac{B}{2}\sqrt{1 + B^2/4}\right\}$$

$$= \sqrt{1 + B^2/4} - B/2$$

Now this can be recognised as one solution of the equation

$$B = \frac{1}{K} - K \qquad (4.46)$$

Thus (4.45) and (4.46) enable an inverter to be designed with a given admittance value.

It is important to note that the ϕ-variable in terms of which the waveguide structure was analysed is distinct from the θ-variable characterising the lowpass prototype.

Levy has shown that these inverters are relatively broad band, and that their characteristic admittance is approximately proportional to the guide wavelength. He has further shown that this frequency dependence can be scaled out of the network, to leave a new network which can be equated to the prototype of Figure 4.18.(a) under the frequency transform

$$\sin\theta \rightarrow \frac{\lambda g}{\lambda g_o} \sin\left(\pi \frac{\lambda g_o}{\lambda_g}\right) \qquad (4.47)$$

Thus, (4.47) must be used to determine the bandwidth variable $\sin\theta_o$ for the design of the prototype filter, in terms of the required band edge guide wavelengths.

Thus the design procedure can be summarised as follows. Let the required response in terms of guide wavelength be as shown in Figure 4. 21, with band-edge wavelengths λg_1 and λg_2.

Then the insertion-loss of the filter is of the form

$$L_A = 10 \log_{10} \left\{1 + \varepsilon^2 T_n^2 \left[\left[\frac{\lambda g}{\lambda g_o} \sin\left(\frac{\pi \lambda g_o}{\lambda g}\right)\right] / \sin\theta_o\right]\right\} \qquad (4.48)$$

where

$$\lambda g_o = \tfrac{1}{2}(\lambda g_1 + \lambda g_2) \qquad (4.49)$$

$$\varepsilon^2 = 10^{L_{AR}/10} - 1 \qquad (4.50)$$

Now, $\sin\theta_o$ must be determined by considering the frequency transform (4.47) and the required band-edge wavelengths. It can be shown that $\sin\theta_o$ can be determined to a close approximation from the equations:

$$x = \frac{\pi(\lambda g_2 - \lambda g_1)}{(\lambda g_2 + \lambda g_1)} \qquad (4.51)$$

$$\sin\theta_o = 1/(\frac{1}{x} + \frac{x}{6}) \qquad (4.52)$$

With $\sin\theta_o$ determined, Rhodes explicit formulae ([3.1], pp 139-147) may be used to determine the prototype parameters in Figure 4.20(b). The following equations then yield the required cavity lengths and post susceptances at mid-band (λg_o):

Let $\quad Y_o = Y_{n+1} = 1,\ K_{01} = K_{n,n+1} = 1$

then
$$B_{r,r+1} = \frac{\sqrt{Y_r\ Y_{r+1}}}{K_{r,r+1}} - \frac{K_{r,r+1}}{\sqrt{Y_r\ Y_{r+1}}}, \quad r = 0 \quad n \qquad (4.53)$$

$$\phi_{r,r+1} = \cot^{-1}(\frac{B_{r,r+1}}{2}), \quad r = 0 \rightarrow n \qquad (4.54)$$

$$\theta_r = \pi - \phi_{r-1,r} - \phi_{r,r+1}, \quad r = 1 \rightarrow n \qquad (4.55)$$

The dimensions of the posts can then be determined from standard experimental or theoretical data.

For narrow bandwidths (less than perhaps five percent) this procedure reduces essentially to that given by Cohn [4.1].

4.6 Single-Sideband Crystal Filters

A specially important filtering function in line and hf radio communication systems is the selection of a single sideband voice signal from a double-sideband suppressed carrier signal generated by a balanced modulator [4.21]. At carrier frequencies much higher than 100 KHz, the fractional bandwidth and unwanted-sideband rejection requirements are so severe that conventional lumped resonators cannot be used, because of their excessive loss. Quartz crystal resonators are widely used for this application for their extremely low loss and high stability.

A typical specific ation shape, in this case for a lower-sideband filter, is shown in Figure 4.22. The important requirements are that the ripple in the lower sideband does not exceed L_{AR} dB, and the rejection of the upper sideband should exceed L_s dB. The response shown

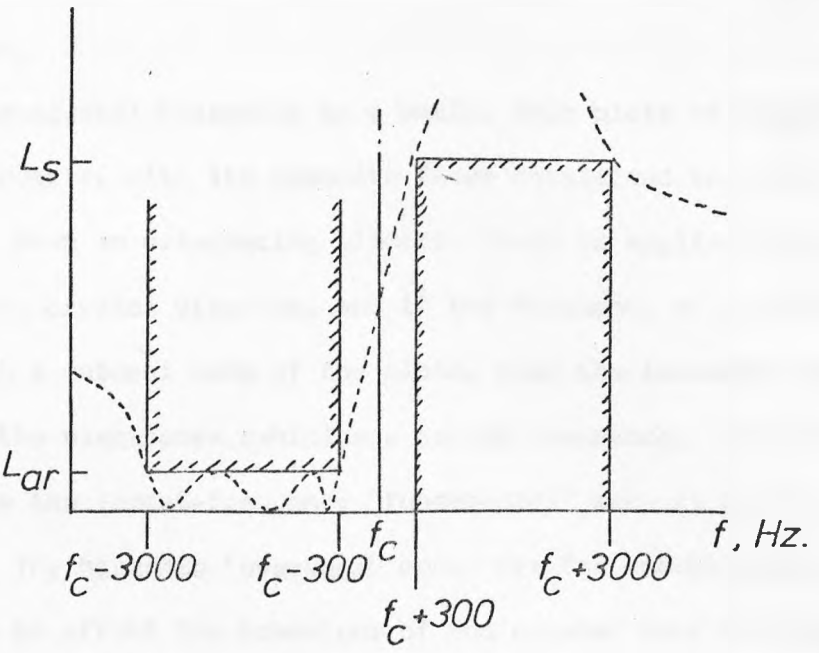

FIGURE 4.22 SSB Filter Response .

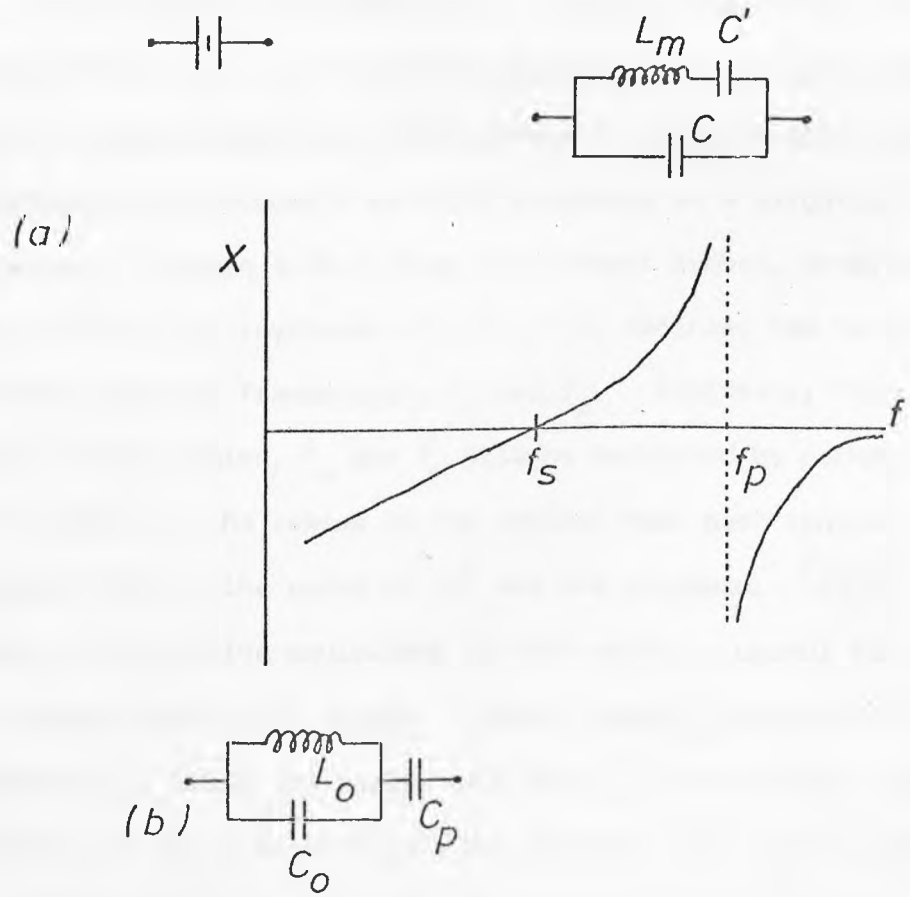

FIGURE 4.23 Properties of Crystal Resonator.

corresponds to a baseband of 300-3000 Hz, adequate for communication-quality speech.

A quartz-crystal resonator is a small, thin plate of suitably cut and polished quartz, with its opposite faces metallised to form two electrodes. When an alternating electric field is applied across the electrodes, the crystal vibrates, and if the frequency of alternation coincides with a natural mode of the plate, then the impedance seen "looking at" the electrodes exhibits a series resonance. For filter purposes, only the lowest-frequency "fundamental" mode is usually considered. The harmonic "overtone" modes are far enough removed in frequency not to effect the behaviour of the crystal near the fundamental resonance, With modern crystal design methods, an-harmonic modes of resonance can be almost entirely suppressed.

Near fundamental resonance, the crystal itself appears electrically to be a series tuned circuit. The parallel-plate capacity between the electrodes appears in parallel with the series resonator, and produces a parallel resonance at a slightly higher frequency. Figure 4.23(a) shows the circuit symbol, equivalent circuit, and a plot of the reactance of a crystal, defining the series and parallel resonant frequencies, f_s and f_p. Typically, for a crystal in the 10 MHz region, f_s and f_p will be separated by perhaps 20 KHz. In the diagram, the losses in the crystal have been ignored; typical crystal "Q's" of the order of 10^5 are not uncommon. Figre 4.23(b) shows an alternative equivalent circuit which is useful for the purposes of analysis and filter design. Here L_o and C'_o resonate at the parallel resonance f_p, while the series capacitor C_p is the actual total shunt capacity, as would be measured, for example, by a low-frequency bridge.

The double-resonance of a crystal is an embarrassment from the point of view of conventional filter design, which aims at achieving a

nearly symmetrical passband response. The conventional methods of crystal filter design use lattice and bridged-tee circuits extensively to circumvent this problem. However, the crystal is ideal for realising the highly asymmetric response needed for ssb, as in Figure 4.22. A suitable filter circuit is shown Figure 4.24(a), and uses capacitive impedance inverters to couple series crystals, and is designed from the prototype using series inductors and impedance inverters shown in Figure 4.24(b). The inverters in the crystal filter are realised with the capacitive tee-network shown in Figure 4.24(c). The negative capacitors have to be absorbed in the crystals; this is considered later.

The operation of this filter is simply explained. Around their series resonance, the crystals have nearly zero reactance and the filter exhibits a passband. Around their parallel resonance, the crystals have an almost infinite impedance, and the filter gives a very large attenuation. The art of designing the filter lies in choosing the series and parallel resonances of the crystals to just satisfy the specification.

Only the lower-sideband crystal filter will be considered in detail; the design procedure for the upper-sideband filter, which uses shunt crystals coupled by series capacitors, follow in a very similar fashion.

It is convenient to characterise the crystal in terms of three parameters, which in this case are chosen to be the parameters:

C_p (see Figure 4.23(b))

f_s, the series resonance frequency, or

ω_s, where $\omega_s = 2\pi f_s$

r_o, where

$$1 + r_o = \frac{f_p^2}{f_s^2}$$

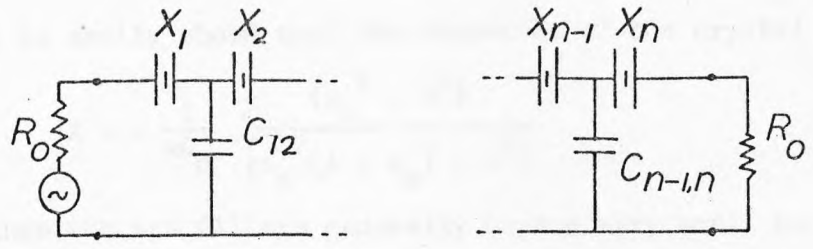

(a)

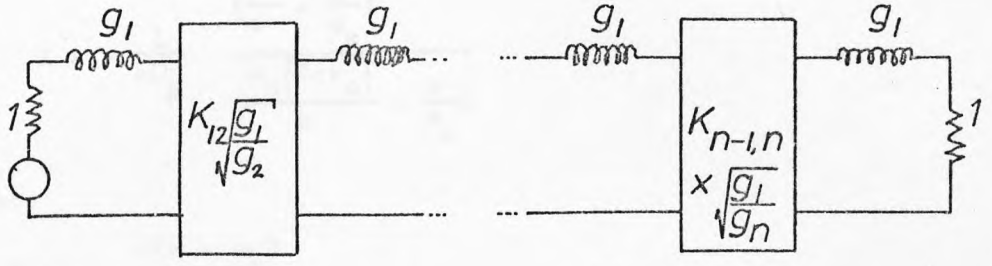

(b)

LSB Filter & Prototype .

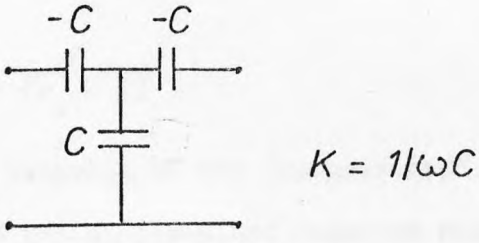

(c) Impedance Inverter.

FIGURE 4.24

It is easily shown that the reactance of the crystal is given by

$$X = -\frac{1}{\omega C_p} \cdot \frac{(\omega_s^2 - \omega^2)}{[\omega_s^2(1 + r_o) - \omega^2]} \qquad (4.56)$$

Since the ssb filters generally have a very small bandwidth, it is convenient to put (4.56) in an approximate, narrow-band form;

$$X = -\frac{1}{\omega C_p} \cdot \frac{(\frac{\omega_s}{\omega} - \frac{\omega}{\omega_s})}{(\frac{\omega_s[1+r_o]}{\omega} - \frac{\omega}{\omega_s})}$$

For $\omega \approx \omega_s$,

$$(\frac{\omega_s}{\omega} - \frac{\omega}{\omega_s}) \approx -\frac{2(\omega - \omega_s)}{\omega_s}$$

Let $$F = \frac{2(\omega - \omega_s)}{\omega_s}$$

then

$$X \approx \frac{1}{\omega_s C_p} \cdot \frac{F}{(r_o - F)} \qquad (4.57)$$

Consider now the response of the low-pass prototype filter, shown in Figure 4.25(a), and the single-sided response shown in Figure 4.25(b). A frequency transform will be derived which will map the passband of the prototype into the region -1 to - .1 (corresponding to (f_c - 3000) to (f_c - 300) Hertz), and the stopband to the region + .1 to + 1.0, so that the attenuation levels at each stopband edge are equal, and exceeded elsewhere in the stopband. This transform will be of the form:

$$\omega \rightarrow \frac{a\omega + \omega_1}{\omega + \omega_2} \qquad (4.58)$$

and it must map the prototype frequencies thus:

$$-1 \rightarrow -1$$

$$+1 \rightarrow -0.1$$

$$+x \rightarrow +0.1$$

$$-x \rightarrow +1$$

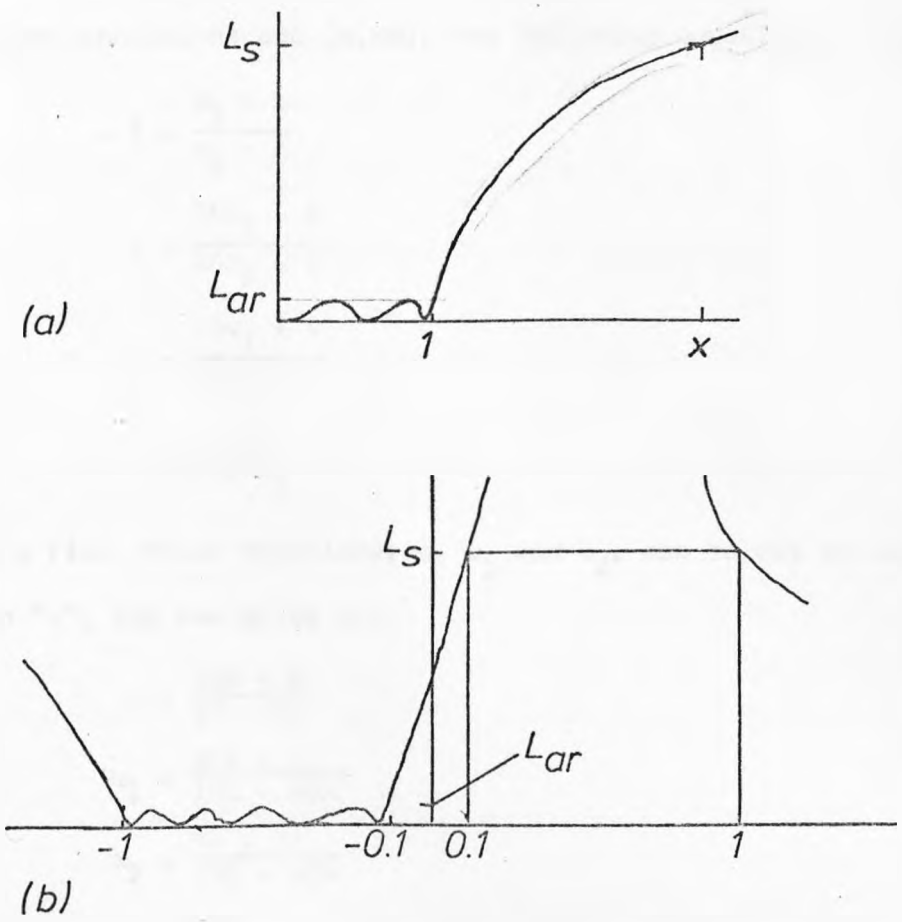

FIGURE 4.25 Single-Sided Transformation.

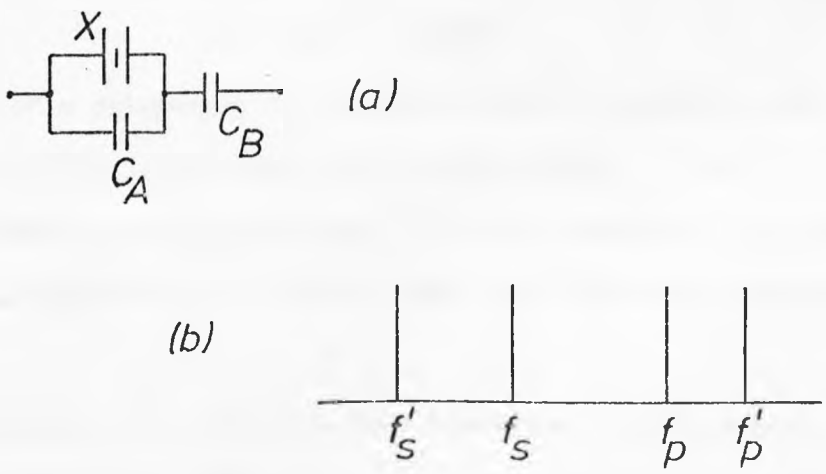

FIGURE 4.26 Pulling of Crystal Frequencies.

From these conditions and (4.58), the following equations follow:

$$-1 = \frac{\omega_1 - a}{\omega_2 - 1} \tag{4.59}$$

$$1 = \frac{10\omega_1 - a}{10\omega_2 - 1} \tag{4.60}$$

$$x = \frac{10\omega_1 + a}{10\omega_2 + 1} \tag{4.61}$$

$$-x = \frac{a + \omega_1}{1 + \omega_2} \tag{4.62}$$

From the first three equations, a, ω_1 and ω_2, can be put in terms of the unknown "x", and are given by:

$$a = \frac{13x - 9}{13 - 9x}$$

$$\omega_1 = \frac{31x + 9}{130 - 90x}$$

$$\omega_2 = \frac{9x + 31}{130 - 90x}$$

Substituting for a, ω_1, ω_2 in (4.62) and solving for x gives:

$$81x^2 - 322x + 81 = 0$$

whence $x = 3.705$ or 0.2699

Since the value of x determines the minimum stopband rejection, the largest possible value is desirable (see Figure 4.15). Thus $x = 3.705$; the smaller value corresponds to a case where the stopband is mapped to the region $(-1 < \omega < -0.1)$, and the filter is otherwise "all-pass".

With this value of x, the frequency transform (4.58) becomes

$$\omega \rightarrow \frac{1.926\omega + 0.6087}{0.3162 - \omega} \tag{4.63}$$

but for convenience it will be left in symbolic form until the final design equations are given, except for noting the sign of "ω" in the denominator of (4.63).

Now a further frequency transform will be introduced to map the

single-sided prototype response to an ssb response such as is dotted in Figure 4.22. This is of the form

$$\omega \rightarrow K(f - f_c) \tag{4.64}$$

where f_c is the required carrier frequency, K can be determined from the requirement that when

$$f = f_c + f_m$$

where f_m is the maximum modulating frequency (3000 Hz in Figure 4.22), f should map to $\omega = +1$.

Hence $\quad 1 = K(f_c + f_m - f_c)$

and $\quad K = 1/f_m$

Substituting (4.64) for ω in (4.58). gives the complete transform

$$\omega = \frac{aK(f - f_c) + \omega_1}{-K(f - f_c) + \omega_2}$$

Thus the reactance of a prototype inductor (Figure 4.24(b)), ωg_1, becomes

$$\omega g_1 \rightarrow g_1 \left\{ \frac{aK(f - f_c) + \omega_1}{-K(f - f_c) + \omega_2} \right\} \tag{4.65}$$

Now, if (4.65) can be put in the general form of (4.57), an equivalence can be drawn up between the transformed prototype and the crystal filter.

Equation (4.65) can be written

$$\omega g_1 \rightarrow \frac{2aK(f_c - \omega_1/aK)\left[f - (f_c - \omega_1/aK)\right]}{2(f_c - \omega_1/aK)\left[(\omega_2 + Kf_c) - Kf\right]} \; g_1$$

and thus it is possible to identify the variable "F" in (4.57) with

$$\frac{2(f - \left[f_c - \omega_1/aK\right])}{f_c - \omega_1/aK}$$

To complete the equivalence, let

$$\frac{aK(f_c - \omega_1/aK)}{2[\omega_2 + Kf_c - Kf]} = \frac{D}{r_o - F}$$

where D is an arbitrary constant. Thus it is required that

$$2[\omega_2 + Kf_c\ Kf] = \frac{aKr_o}{D}(f_c - \omega_1/aK) - \frac{2aK}{D}[f - (f_c - \omega_1/aK)]$$

from which $D = a$

and $$r_o = \frac{2(\omega_2 + \omega_1/a)}{Kf_c - \omega_1/a}$$

Thus, the required series resonant frequency f_s, and r_o, can be found:

$$f_s = f_c - (\frac{\omega_1}{a})\ f_m \tag{4.66}$$

$$r_o = \frac{2(\omega_2 + \omega_1/a)}{\frac{f_c}{f_m} - \frac{\omega_1}{a}} \tag{4.67}$$

(using $K = 1/f_m$).

Thus, the reactance of a prototype inductor, ωg_1, becomes, through the frequency transform,

$$\omega g_1 \rightarrow \frac{aF}{r_o - F} \cdot g_1 \tag{4.68}$$

Thus the series and parallel resonances of the required crystals can be found through (4.66) and (4.67); if the parallel capacity of the crystal is C_p, then from (4.57) its series reactance is

$$X = \frac{1}{2\pi\ F_s\ C_p} \cdot \frac{F}{(r_o - F)}$$

By comparison with (4.68) then, an equivalence can be drawn up between the crystal filter and the transformed prototype (see Figure 4.24) if the terminating resistors are raised to a value R_o, where

$$R_o = \frac{1}{2\pi\ f_s\ C_p\ ag_1} \tag{4.69}$$

and the impedance inverters are scaled accordingly. The values of the coupling capacitors are found by equating the capacitive inverters to the ideal inverters at the series resonant frequency f_s.

Before finally deriving the explicit design equations for the

crystal filter, it is necessary to descuss how the negative series capacitors of the inverters (Figure 4.24(c)) can be absorbed into the crystals. This can be conveniently done by embedding the crystals themselves within a capacitive network, as shown in Figure 4.26 (a). The capacitor C_A includes the "holder" capacitance of the crystal, and allows the parallel resonant frequency of the crystal to be set precisely, while C_B allows the negative inverter capacitance to be absorbed and the series resonance to be set precisely. Let the actual parallel capacitance of the crystal unit X be C_p', and the actual series and parallel resonant frequencies be f_s' and f_p'. The frequency relationships are shown in Figure 4.26 (b). Then it can easily be shown that, for the external resonances of X, C_A, C_B to be f_s, f_p, then

$$C_A = \frac{f_s'}{f_p'} \cdot \left(\frac{f_p - f_p'}{f_s' - f_p}\right) \cdot C_p' \qquad (4.70)$$

$$C_B = \frac{f_s'(f_p' - f_s')(f_s - f_p)}{f_p'(f_s' - f_p)(f_s - f_s')} \cdot C_p' \qquad (4.71)$$

The resulting parallel capacitance, C_p, is

$$C_p = \frac{f_p(f_p - f_s)(f_p' - f_s')}{f_p'(f_p - f_s')^2} \cdot C_p' \qquad (4.72)$$

Finally, the design formulae can be written explicitly, and the resulting filter circuit is shown in Figure 4.27. The design formulae are again given in terms of the parameters g_o and $k_{r,r+1}$ of equations (3.23) and (3.24).

If the passband ripple required is L_{AR} dB, the unwanted sideband rejection L_s dB, then the number of crystals required, n, is given by:

$$\varepsilon = \sqrt{10^{L_{AR}/10} - 1}$$

$$n \geq 0.504 \cosh^{-1}\left(\frac{1}{\varepsilon}\sqrt{10^{L_s/10} - 1}\right)$$

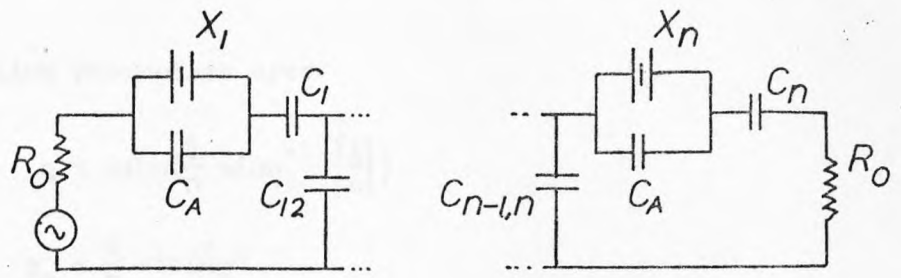

FIGURE 4.27 Lower Sideband Filter Circuit .

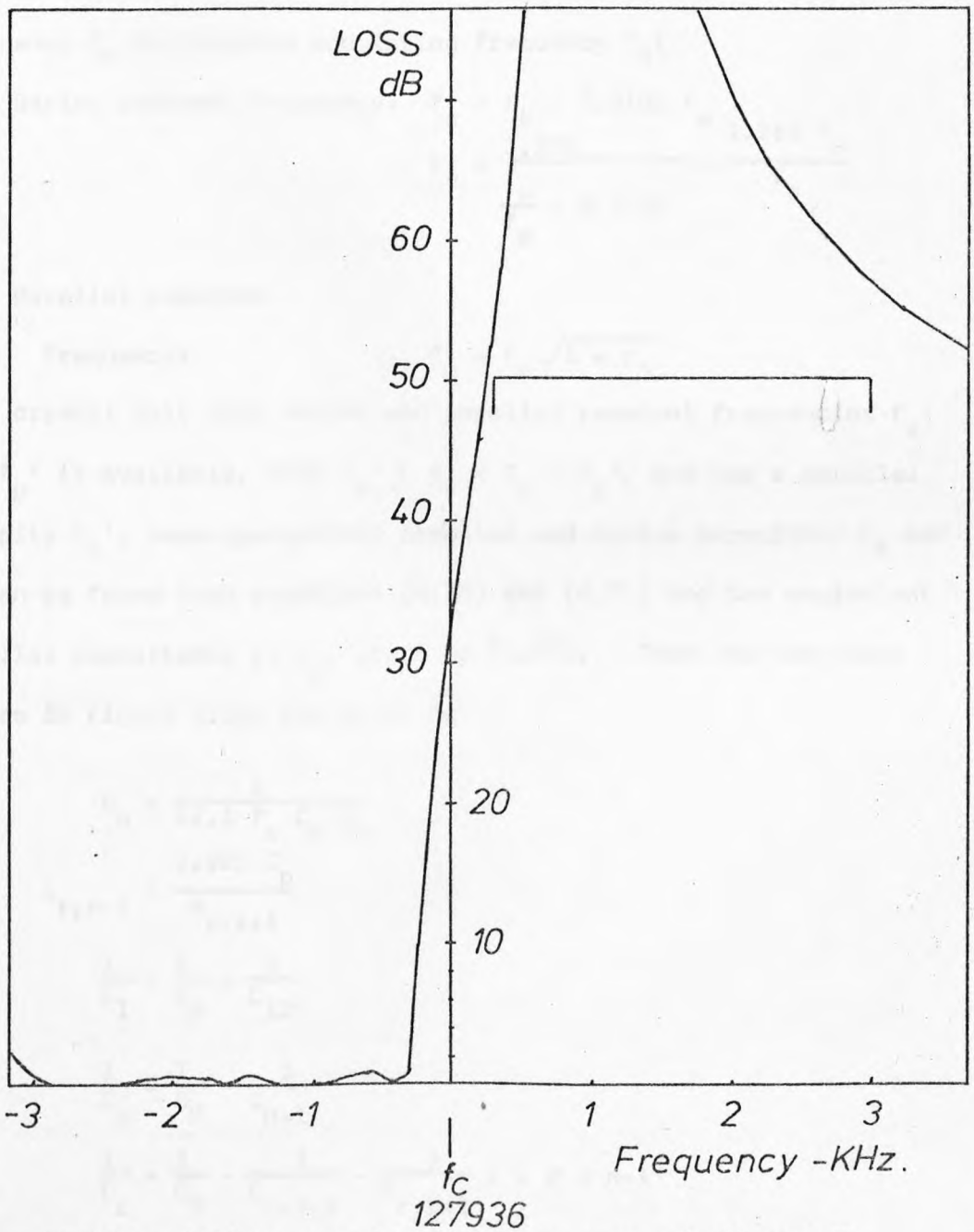

FIGURE 4.28 Computed Response of Example Design .

The coupling parameters are:

$$\eta = \sinh\left(\frac{1}{n}\sinh^{-1}\left[\frac{1}{\varepsilon}\right]\right)$$

$$g_o = \frac{2}{\eta}\sin\left(\frac{\pi}{2n}\right)$$

$$k_{r,r+1} = \sqrt{\frac{n^2 + \sin^2(r\pi/n)}{2[\cos(\pi/n) - \cos(2r\pi/n)]}}$$

Now the crystal parameters required can be found, given the carrier frequency f_c and maximum modulating frequency f_m:

Series resonant frequency: $f_s = f_c - 0.3162\, f_m$

$$r_o = \frac{1.265}{\frac{f_c}{f_m} - 0.3162} = \frac{1.265\, f_m}{f_s}$$

Parallel resonant frequency: $f_p = f_s\sqrt{1 + r_o}$

If a crystal unit with series and parallel resonant frequencies f_s' and f_p' is available, with $f_s' < f_s < f_p < f_p'$, and has a parallel capacity C_p', then appropriate parallel and series capacitors C_A and C_B can be found from equations (4.70) and (4.71) and the equivalent parallel capacitance is C_p, given by (4.72). Then the component values in Figure 4.27 are given by:

$$R_o = \frac{1}{12.1\, f_s\, C_p\, g_o}$$

$$C_{r,r+1} = \frac{1.925\, C_p}{k_{r,r+1}}$$

$$\frac{1}{C_1} = \frac{1}{C_B} - \frac{1}{C_{12}}$$

$$\frac{1}{C_n} = \frac{1}{C_B} - \frac{1}{C_{n-1}}$$

$$\frac{1}{C_r} = \frac{1}{C_B} - \frac{1}{C_{r-1,r}} - \frac{1}{C_{r,r+1}} \qquad r = 2 \rightarrow n-1$$

Design Example

Carrier Frequency, $f_c = 12.7936$ MHz

Maximum Baseband Frequency,

$$f_m = 3 \text{ KHz}$$

Passband Ripple $= 1$ dB

Minimum Sideband rejection

$$= 50 \text{ dB}$$

$$\varepsilon = \sqrt{10^{-1} - 1}$$

$$= 0.5088$$

$$n \geq 0.504 \cosh^{-1} \left(\frac{1}{.5088}\sqrt{10^5 - 1}\right)$$

$$n \geq 3.59$$

or $n = 4$

$$\eta = \sinh\left(\frac{1}{4} \sinh^{-1}\left[\frac{1}{.5088}\right]\right)$$

$$= 0.3646$$

$$g_o = 2.099$$

$$k_{12} = 0.6690 = k_{34}$$

$$k_{23} = 0.5761$$

Required crystal series resonance,

$$f_s = 12.7936 - 0.3162 \times 3 \times 10^{-3} \text{ MHz}$$

$$= 12.7927 \text{ MHz}$$

$$r_o = \frac{1.265}{\frac{12.7936}{3 \times 10^{-3}} - 0.3162}$$

$$= 2.967 \times 10^{-4}$$

$$f_p = 12.7946 \text{ MHz}$$

Crystals are available with

$$f_s' = 12.787 \text{ MHz}$$

$$f_p' = 12.807 \text{ MHz}$$

$$C_p' = 4.35 \text{ pF}$$

Thus
$$C_A' = \frac{12.787}{12.807}\left(\frac{12.7946 - 12.807}{12.787 - 12.7946}\right) \times 4.35$$

$$= 7.086 \text{ pF}$$

$$C_B = 3.81 \text{ pF}$$

$$C_p = 2.86 \text{ pF}$$

$$R_o = \frac{1}{12.1 \times 12.7927 \times 10^6 \times 2.86 \times 10^{-12} \times 2.099}$$

$$= 1076 \text{ ohms}$$

$$C_{12} = C_{34}$$

$$= \frac{1.925 \times 2.86}{0.669}$$

$$= 8.229 \text{ pF}$$

$$C_{23} = 9.557 \text{ pF}$$

$$\frac{1}{C_1} = \frac{1}{3.81} - \frac{1}{8.229}$$

$$C_1 = 7.095 \text{ pF}$$

$$= C_4$$

$$C_2 = \frac{1}{3.81} - \frac{1}{8.229} - \frac{1}{9.557}$$

$$C_2 = 27.54 \text{ pF}$$

$$= C_3$$

The insertion-loss response of this filter is plotted in Figure 4.28. This was computed assuming the crystals to have the "real" frequency variation (4.56), and the couplings to have a realistic frequency variation. The graph shows that the design procedure is virtually exact. The passband ripple level and the passband edges are exact. The insertion loss at the edges of the stopband are equal, and in fact exceed the specification by 5 dB, since the number of crystals used is, of course, integral!

Although the derivation of the design procedure was somewhat tedious, the resulting equations are very simple and easy to apply. The only

requirements placed on the crystals are that their series and parallel resonant frequencies should bracket the required resonant frequencies; the actual self-capacity of a practical crystal is then easily incorporated into the design. The resulting filter circuit uses only crystals and capacitors, and all the crystals are identical. This should allow an economy of scale in quantity manufacture, as well as simplifying store-keeping and reducing construction errors.

4.7 Conclusions

This Chapter has been concerned with developing design procedures for coupled-resonator bandpass filters. It has considered the design of what are essentially "microwave" filters, of the interdigital, combline and waveguide type, and lumped element filters which are essentially "low-frequency".

Broadly speaking, all the design procedures have been developed by the some method: the filter structure has been analysed in order to determine an appropriate lowpass to bandpass transformation; this transform is applied to the lowpass prototype; and the resulting network equated to the original structure. In the first four cases, the frequency dependence of the inter-resonator couplings were allowed for; however, this frequency dependence is not significant for the very narrow-band crystal single-sideband filters.

The emphasis has been on "direct" design methods, that is, methods which can be used by the engineer with no specialist knowledge of filter theory. This limits the designs to methods where explicit element values are obtainable for the prototype filters. Only in the design procedure for combline filters has a numerical procedure been introduced, and even that converges very rapidly and can be applied "by hand" using a non-programmable calculator.

The chapter finished by giving an original procedure for designing crystal single-sideband filters, using a filter circuit previously

considered by Mason, Sykes, and Dishal ([4.8] - [4.10]). The new method is extremely simple to apply, and the computed response of a typical filter showed it to be capable of very high performance.

CHAPTER 5

REVIEW OF DIPLEXER DESIGN

5.1 Introduction

In the context of this thesis, a diplexer is a passive device which is capable of splitting a signal on one path between two different paths, according to the frequency of the signal. The device is assumed linear, so an input signal with a broad spectrum of frequency components will divide between the outputs, according to the frequency of its components.

Diplexers are generally reciprocal, so they can equally well be used for combining signals in different frequency bands onto a common path. However, for the purposes of analysis, it is often convenient to consider the device as a "splitter" rather than a "combiner".

The diplexer is the simplest case of the multiplexer. Some of the methods of diplexer design described in this chapter can be extended to multiplexers, and the text indicates where this is so.

Diplexers should be distinguished from devices commonly called "power dividers", which merely divide their input power equally between two (or often more) output ports irrespective of frequency.

Communication systems use diplexers for a number of purposes, and Figure 5.1 shows some of these diagrammatically.

In Figure 5.1(a) a diplexer is used to divide the received signal from an antenna between two receivers, each handling a different band of frequencies. In (b) is shown the corresponding case, where the diplexer combines the outputs of two transmitters onto the feed to a common antenna. Diplexers are often used to allow a single medium to pass signals in both directions, distinguished from each other by their different frequencies. Figure 5.1(c) and (d) show this principle applied both to line and radio systems. In microwave radio systems a device performing this function is often referred to as a "diplexer".

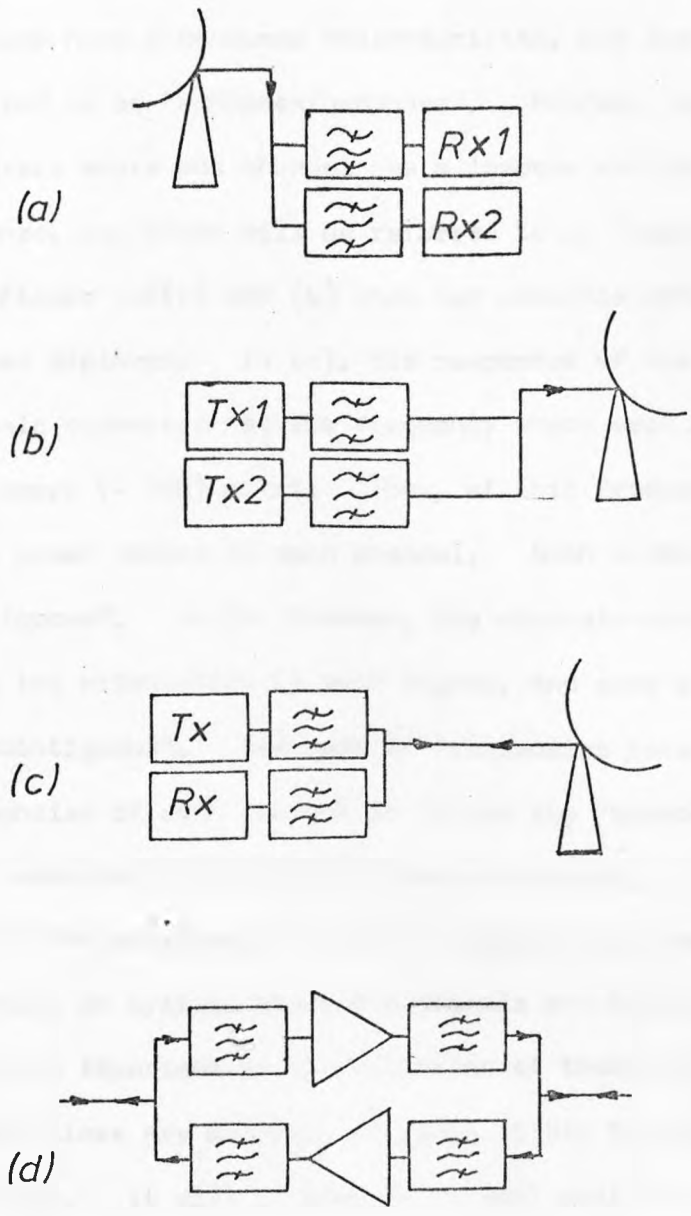

FIGURE 5.1 Some Diplexer Applications.

In all the applications shown in Figure 5.1, both channels of the diplexer have a bandpass characteristic, and such diplexers will be referred to as "bandpass/bandpass". However, some applications require diplexers where one channel has a lowpass and the other a highpass response, and these will be referred to as "highpass/lowpass" diplexers.

Figure 5.2(a) and (b) show two possible responses of a highpass/lowpass diplexer. In (a), the responses of the lowpass and highpass channels cross-over at the frequency where each response is at its half-power (- 3dB) point. Thus, at this frequency exactly half the input power passes to each channel. Such a diplexer is termed "contiguous". In (b) however, the channels cross-over at a frequency where the attenuation is much higher, and such a diplexer is termed "non-contiguous". The band of frequencies between the cut-off frequencies of each channel is called the "guard-band". These terms apply equally to bandpass/bandpass diplexers.

In the applications shown in Figure 5.1, the diplexers are operating in systems where the signals are borne on transmission lines, and it is important to the operation of these systems that these transmission lines are matched, at least within the individual channel passbands. It will be seen later that most of the fundamental problems in diplexer design stem from this requirement.

Because diplexers are selective devices, it is inevitable that their construction should involve filters in some way. One elementary form of diplexer is shown in Figure 5.3. It uses a pair of bandpass filters, each of which begins with a parallel resonant circuit, so that their stopband input impedances tend to a short circuit, or, equivalently, the filters are minimum reactive. The filters are connected in series at the "common port", and this forms the diplexer input. The impedance seen looking into the common port is, ideally, essentially resistive in the passband of each filter, and hence will match to a

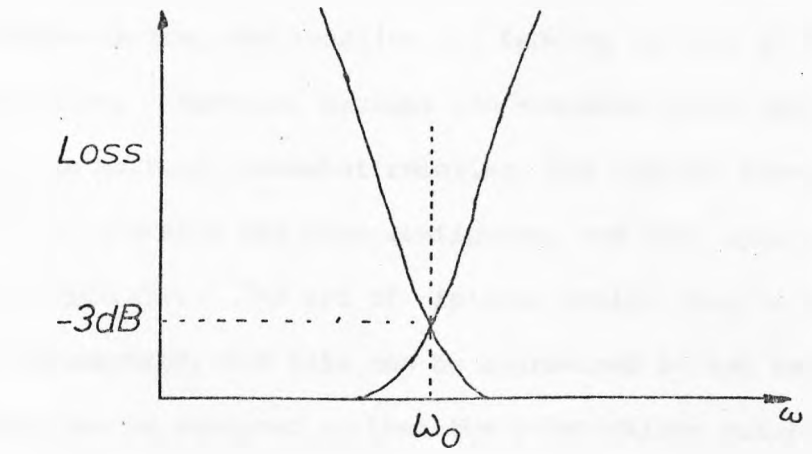

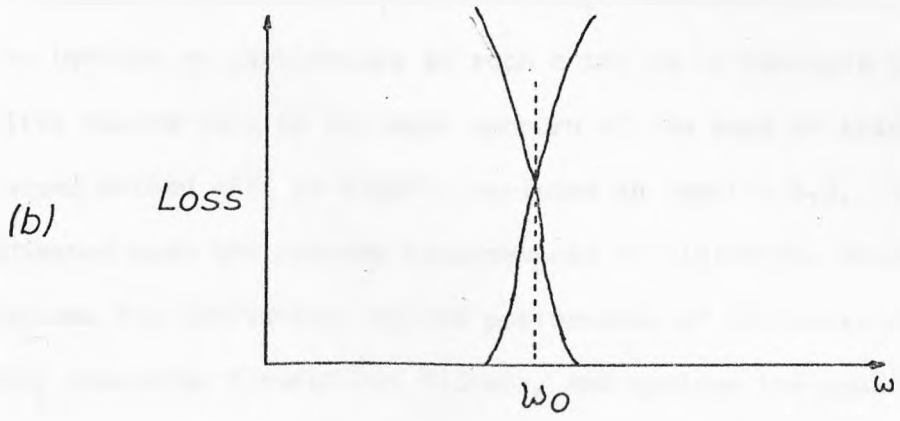

FIGURE 5.2 Contiguous (a) & Non-Contiguous (b) Responses .

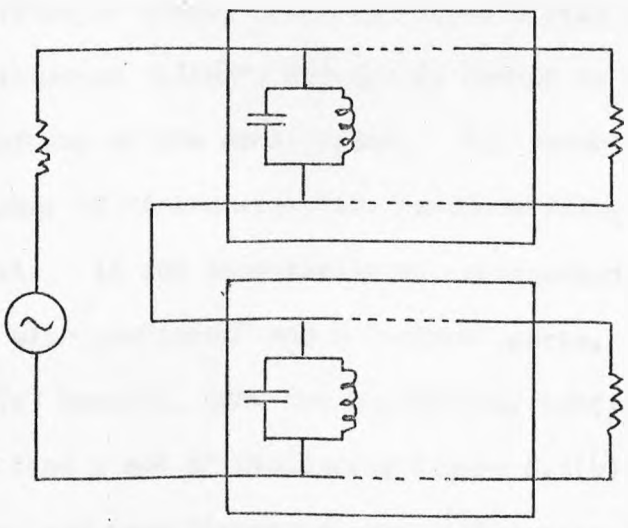

FIGURE 5.3 Èlementary Diplexer Circuit.

resistive source, and reactive and tending to zero at all other frequencies. However, because the stopband input impedance of a filter is actually somewhat reactive, the filters interact, especially if their passbands are near-contiguous, and this spoils the performance of the diplexer. The art of diplexer design lies in compensating for this interaction, and this can be approached in two ways; either the filters can be designed so that the interactions mutually cancel out, or the filters can be interconnected using additional passive devices such as hybrids or circulators in such a way as to decouple them. The first method will be the main concern of the rest of this thesis; the second method will be briefly reviewed in section 5.3. Section 5.2 is concerned with the systems requirements on diplexers, while section 5.4 reviews the limitations on the performance of diplexers which use directly connected interacting filters, and reviews the published methods of design.

It is perhaps appropriate at this stage to mention that there are a number of configurations into which multiplexers in general seem to fit. The first of these, shown in Figure 5.4(a) might be called a "true multichannel filter", because it cannot be decomposed into a combination of any of the other forms. For example, it could be composed of a number of minimum-reactive bandpass filters connected in series at one port. It can essentially be represented as an (n+1) port network, with one"input" and n "output" ports. Figures 5.4(b) and (c) however, show two multiplexer configurations which are assembled from a set of diplexers; Figure 5.4(b) might be termed a "tree" type, and uses highpass/lowpass diplexers (though bandpass/bandpass would be feasible); Figure 5.4(c) uses a cascade of "channel-dropping" diplexers.

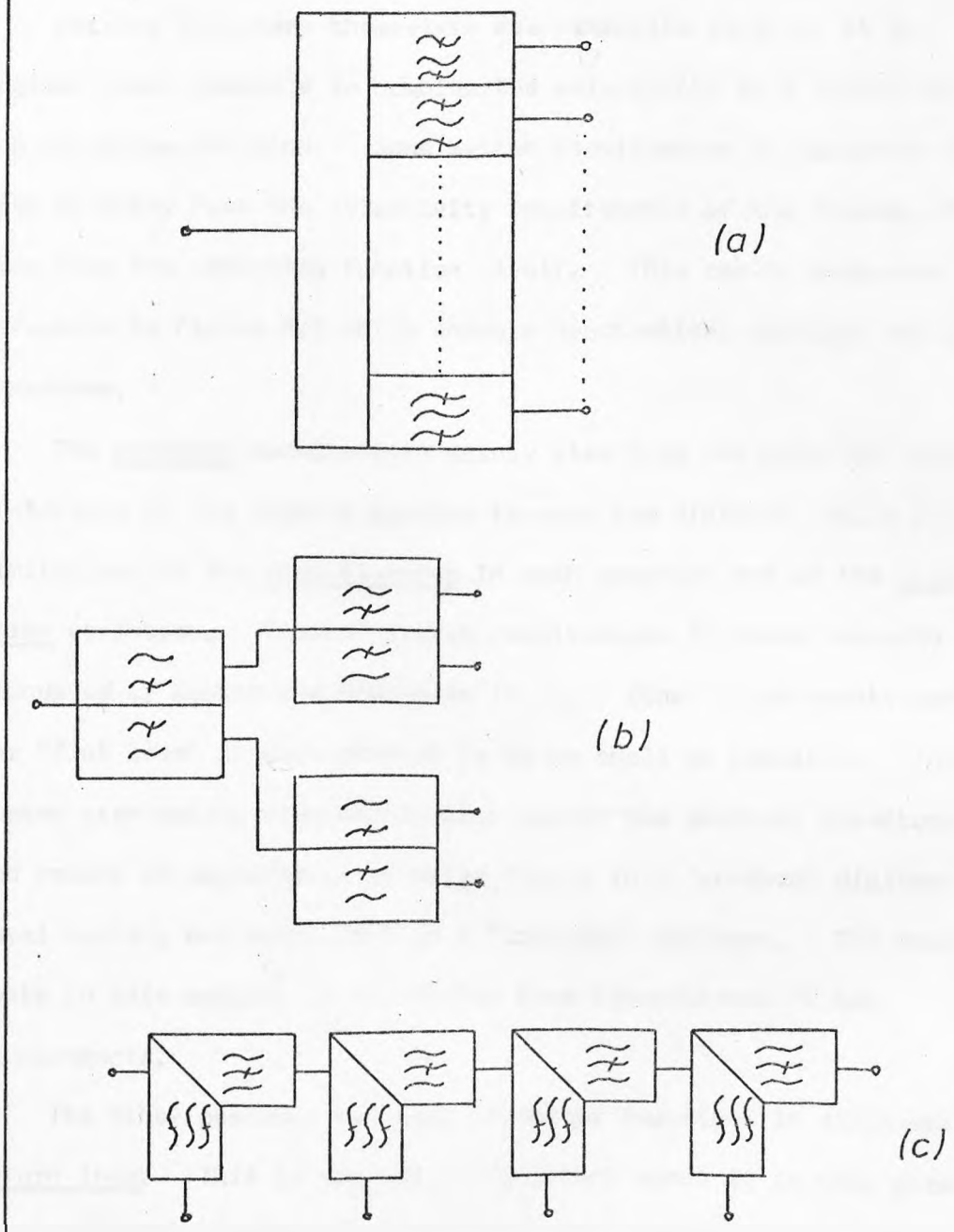

FIGURE 5.4 Multiplexer Configurations.

5.2 Systems Requirements on Diplexer Design

Because diplexers themselves are selective devices, it is logical where possible to combine the selectivity in a system with the diplexing function. Some system requirements on diplexers thus stem directly from the selectivity requirements of the system, others stem from the diplexing function itself. This can be discussed with reference to Figure 5.5 which shows a hypothetical diplexer and its responses.

The passband requirements mainly stem from the need for minimum distortion of the signals passing through the diplexer, which put limitations on the gain flatness in each passband and on the group delay variation. Typical system requirements in these respects are discussed by Kudsia and O'Donovan [5.1]. Other requirements are for "flat loss" in each channel to be as small as possible. These losses stem mainly from dissipation within the diplexer structure, and result in degradation of noise figure in a "receive" diplexer and local heating and power loss in a "transmit" diplexer. The requirements in this respect do not differ from conventional filter requirements.

The other passband response parameter important in diplexers is the return loss. This is especially important since it is this parameter which is mainly degraded when filters are interconnected. The passband return loss will be particularly important for diplexers destined for the multiplexer arrangements shown in Figure (5.4(b) and (c), since the diplexers have to be cascaded, and the limit of this "cascadeability" is governed by the quality of the impedance match at each port of the diplexer.

The passband response should also be discussed with reference to the stopband selectivity. The earlier discussion of the approximation

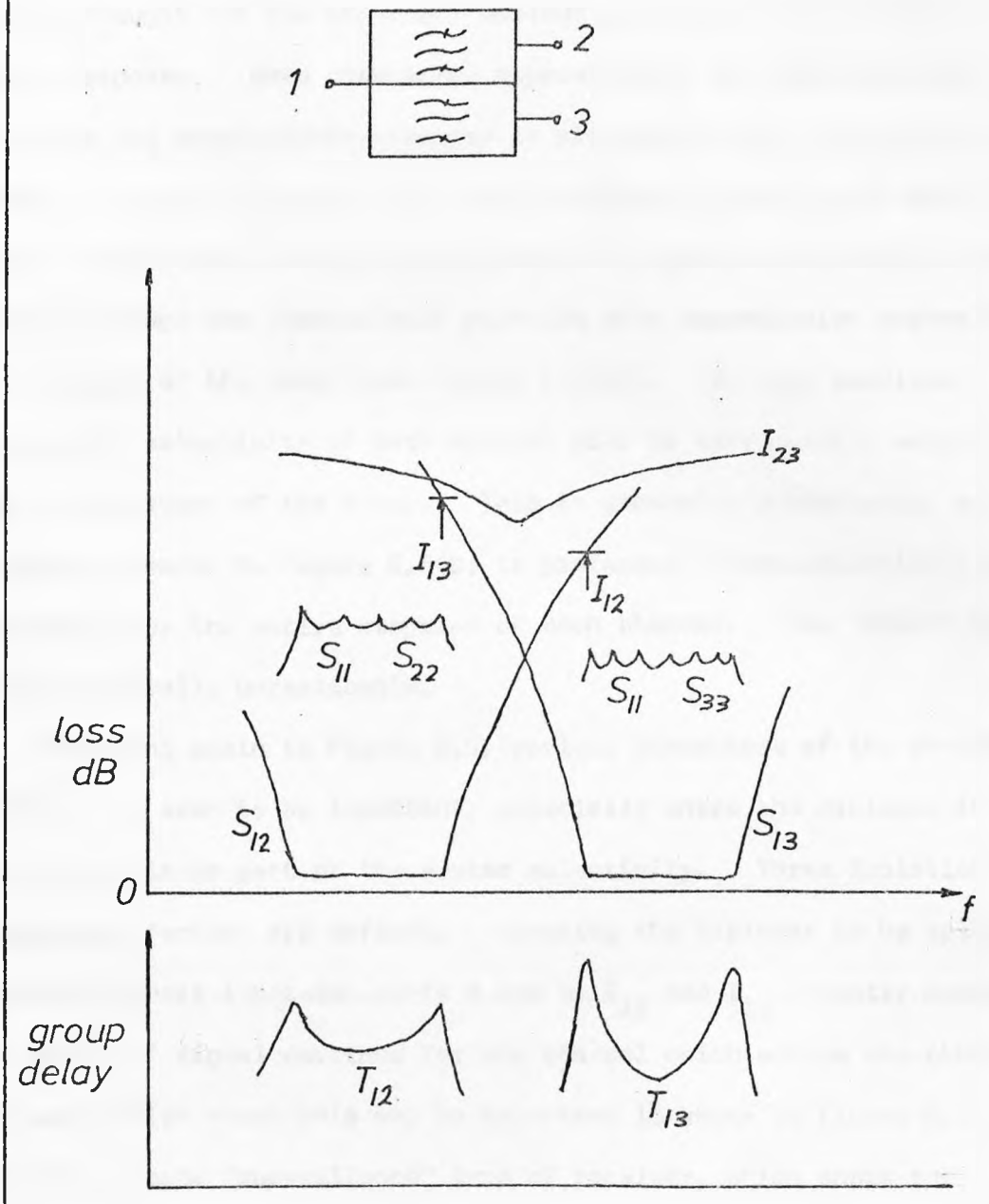

FIGURE 5.5 A Diplexer and its Responses .

problem brought out the important optimum properties of the equal-ripple response. When discussing approximation with reference to diplexers the equal-ripple response is also important. It will be shown in section 5.4 that, in an ideal lossless diplexer with equal-ripple transmission through each channel, the points of perfect transmission through one channel must coincide with transmission zeroes in the stopband of the other (see Figure 5.6(a)). If this condition is met, the selectivity of each channel will be very heavily weighted onto the passband of the other. This is generally undesirable, and a response nearer to Figure 5.6(b) is preferred, where selectivity is available over the entire stopband of each channel. The "ideal" case is also generally unrealisable.

Referring again to Figure 5.5, various parameters of the stopband response are seen to be important, especially where the diplexer is supplying a large part of the system selectivity. Three isolation attenuation factors are defined. Assuming the diplexer to be splitting a signal at port 1 between ports 2 and 3, I_{12} and I_{13} directly measure the amount of signal destined for one channel which enters the other. One application where this may be important is shown in Figure 5.7, which is a crude "surveillance" type of receiver, which shows the spectrum occupancy of two neigh bouring frequency bands. Here a strong signal in band 1 will also show up as a weak signal in band 2. The third important isolation figure is I_{23}, which would be important in the transmit-receive "duplexer" shown in Figure 5.8, and governs the amount of transmitter output power which enters the receiver and hence its dynamic range. This is of particular importance, for example, in satellite communication ground stations, where a highly sensitive receiver and very high power transmitter have to share a common antenna and feed.

Finally, a word on frequency plans is appropriate. Figure 5.9

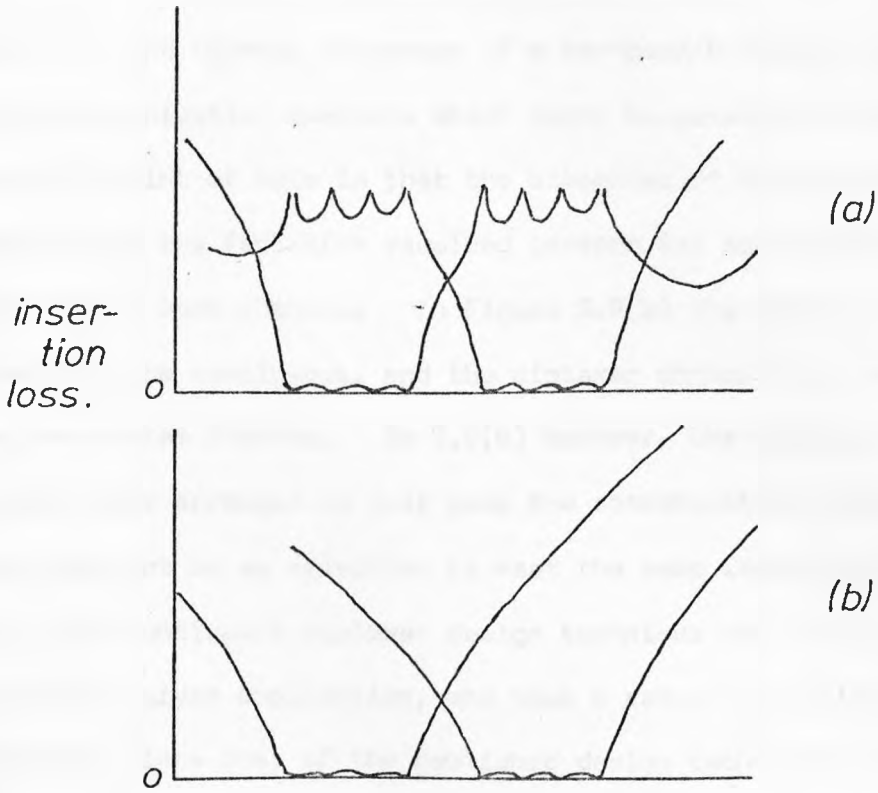

FIGURE 5.6 'Ideal'(a) and Non-Ideal (b) Diplexer Responses.

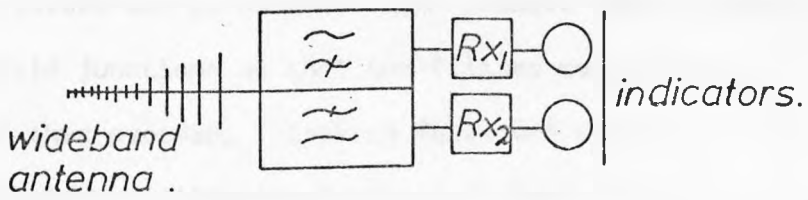

FIGURE 5.7 Surveillance Receiver.

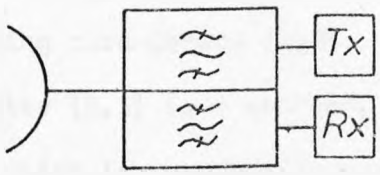

FIGURE 5.8 Diplexer used as 'Duplexer'.

represents the channel responses of a bandpass/bandpass diplexer relative to the communication channels which might be passing through it. The important point of note is that the closeness of the communication channels and the isolation required governs the selectivity requirements desirable in each channel. In Figure 5.9(a) the channel responses are arranged to be contiguous, and the diplexer channels are hence broader than the system demands. In 5.9(b) however, the diplexer channel responses are arranged to just pass the communication channels, and hence need not be so selective to meet the same isolation requirements. Thus a non-contiguous diplexer design technique may allow a saving of degree in a given application, and thus a reduction in loss. This is important, since most of the published design techniques using interacting filters, reviewed in section 5.4, apply only to contiguous diplexers. The main advance of the methods reported in later chapters of this thesis lies in their ability to produce non-contiguous designs.

5.3 Methods of "Decoupled" Diplexer Design

Filters can be combined with passive devices such as circulators or hybrid junctions so that the filters may be decoupled, and interaction thus avoided. Certain four-port structures exist which combine the hybrid and filtering functions; these are called "directional filters". Another diplexer structure involving hybrids but not using filters in the conventional sense is the "commutating filter".

a) Design using circulators [5.2]

A circulator [5.3] is a matched, lossless three- (or sometimes more) port network, which is necessarily non-reciprocal. Most circulators are also frequency-variant, and will only exhibit circulation, and remain matched, over a relatively narrow band of frequencies and are only matched within that band. For the purposes of this analysis, the circulator will be assumed frequency-independent.

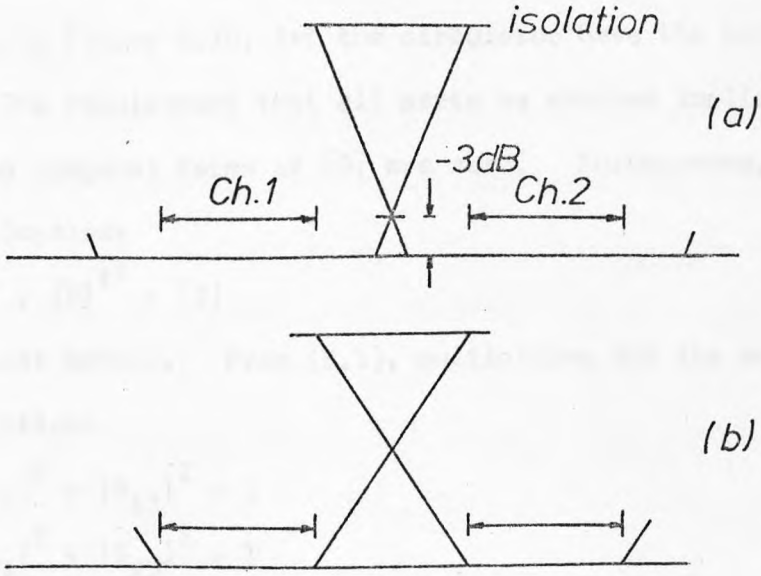

FIGURE 5.9 Meeting an Isolation Specification .

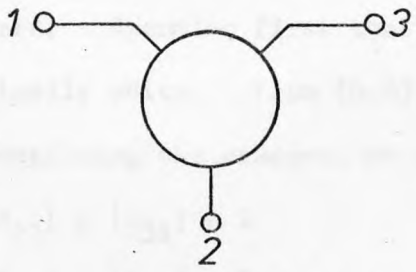

FIGURE 5.10 Circulator - Port Numbering .

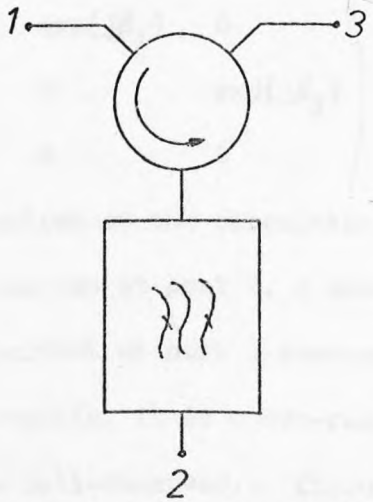

FIGURE 5.11 Circulator-type Diplexer .

Referring to Figure 5.10, let the circulator have the scattering matrix [S]. The requirement that all ports be matched implies that all the leading diagonal terms of [S] are zero. Furthermore, if the circulator is lossless

$$[S] \cdot [S]^{T^*} = [I] \tag{5.1}$$

with [I] the unit matrix. From (5.1), multiplying out the matrices, gives the conditions

$$|S_{12}|^2 + |S_{13}|^2 = 1 \tag{5.2}$$

$$|S_{21}|^2 + |S_{23}|^2 = 1 \tag{5.3}$$

$$|S_{31}|^2 + |S_{32}|^2 = 1 \tag{5.4}$$

$$S_{12}\, S_{23}^* = 0 \tag{5.5}$$

$$S_{12}\, S_{32}^* = 0 \tag{5.6}$$

$$S_{21}\, S_{31}^* = 0 \tag{5.7}$$

Each of (5.5) to (5.7) can be met only if at least one term on the LHS is identically zero. Assuming first that S_{13} is zero, then from (5.2) $|S_{12}|$ is identically unity. From (5.6) $S_{32} = 0$, and thus from (5.4) $|S_{31}| = 1$. Continuing the process, we obtain finally

$$|S_{12}| = |S_{23}| = |S_{31}| = 1$$

$$|S_{13}| = |S_{32}| = |S_{21}| = 0$$

and [S] can be written

$$\begin{pmatrix} 0 & \exp(j\phi_1) & 0 \\ 0 & 0 & \exp(j\phi_2) \\ \exp(j\phi_3) & 0 & 0 \end{pmatrix}$$

Physically, the operation of the circulator is as follows; a wave incident at port 1 emerges at port 2, a wave incident at port 2 emerges at port 3, a wave incident at port 3 emerges at port 1. It is clear that, [S] being asymmetric, it is a non-reciprocal device, and the name "circulator" is well-deserved. Circulators can be realised at microwave frequencies by ferrite Y-junctions, and at low frequency

using active circuits.

A diplexer using a circulator and bandpass filter is shown in Figure 5.11(a). (The conventional symbol for a circulator is as shown in Figure 5.11(a), the arrow indicating the direction of circulation.) It is clear that the scattering matrix of this arrangement is

$$\begin{pmatrix} 0 & S_{12}\exp(j\phi_1) & S_{11}\exp j(\phi_1+\phi_2) \\ 0 & S_{22} & S_{12}\exp(j\phi_2) \\ \exp(j\phi_3) & 0 & 0 \end{pmatrix}$$

where S_{11}, S_{12}, S_{22} are here the scattering coefficients of the filter. Now in its passband, essentially $|S_{12}| = 1$, $|S_{11}| = 0$, and thus power at port 1 within the passband emerges at port 2. In the filters stopband, $|S_{12}| = 0$ and $|S_{11}| \approx 1$, thus power incident at port 1 appears at port 3. Thus this circuit behaves as a channel-dropping filter. The responses of the device are shwon in Figure 5.11(b). Because of the circulator, the impedances at ports 1 and 3 are purely resistive, and the devices can be readily cascaded as shown in Figure 5.11(c).

This type of multiplexer has a number of disadvantages from a system viewpoint. When channels are reflected from a filter for which they are not intended, virtually all the power is reflected but the reflected signal suffers group-delay distortion. This can be minimised by careful choice of the order in which channels are dropped. Circulators are inevitably somewhat lossy, and since they generally use ferrite in their construction are prone to non-linearity at high power levels. These effects together limit dynamic range. The normal realisation of circulators involves a heavy magnet assembly for each circulator, so there may be a weight penalty when the multiplexer is to be used in, for example, a communication satellite. Despite these disadvantages, this method of design has great flexibility and

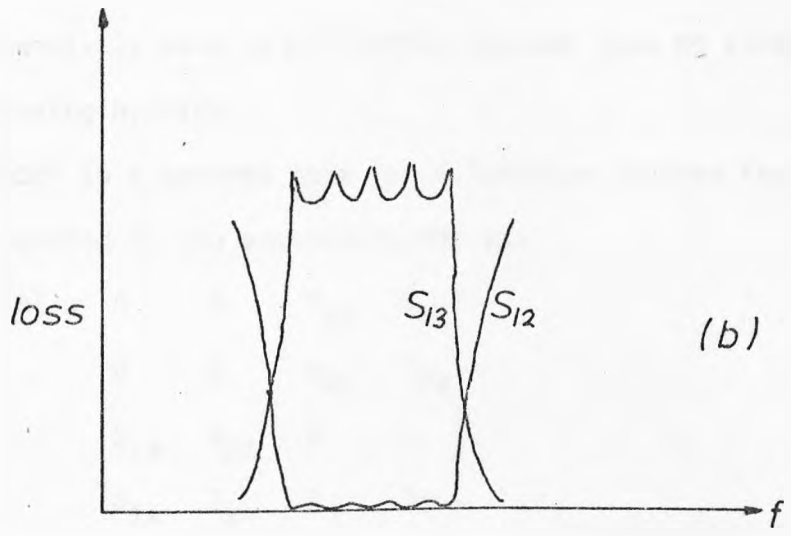

(b)

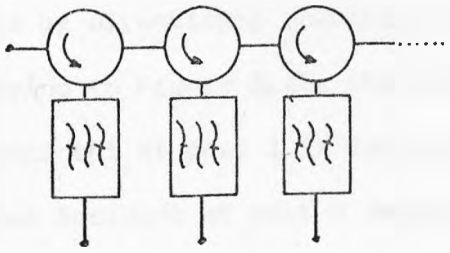

(c)

(figure 5.11 continued)

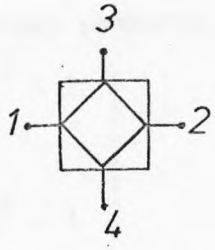

FIGURE 5.12 Four-port Hybrid.

has been extensively used in radio-relay systems (see eg reference [5.4]).

b) Design using hybrids

A "hybrid" is a general term for a lossless matched four-port network, described by the scattering matrix:

$$[S] = \begin{vmatrix} 0 & 0 & S_{13} & S_{14} \\ 0 & 0 & S_{23} & S_{24} \\ S_{13} & S_{23} & 0 & 0 \\ S_{14} & S_{24} & 0 & 0 \end{vmatrix} \qquad (5.8)$$

The theoretical limitations on such networks are fully discussed by Carlin and Giordano [2.1]. Hybrids are realisable by simple transformer networks [2.1] from audio frequency up to uhf, and at higher frequencies by directional couplers and waveguide "magic tees" [5.5].

Referring to Figure 5.12, the scattering matrix (5.8) imples that a signal incident at port 1 is decoupled from port 2 and vice-versa, and a signal incident at port 3 decoupled at port 4 and vice-versa. The network is matched and lossless, so an incident signal at port 1 is split according to the magnitudes of S_{13} and S_{14} between ports 3 and 4. The first elementary property which follows is thus

$$\left.\begin{aligned} |S_{13}|^2 + |S_{14}|^2 &= 1 \\ \text{and similarly} \qquad & \\ |S_{23}|^2 + |S_{24}|^2 &= 1 \end{aligned}\right\} \qquad (5.9)$$

The unitary condition also gives the relations

$$|S_{13}|^2 + |S_{23}|^2 = 1$$

and

$$|S_{14}|^2 + |S_{24}|^2 = 1$$

which taken in conjunction with (5.9) gives

$$\left.\begin{aligned} |S_{13}| &= |S_{24}| \\ \text{and} \qquad & \\ |S_{14}| &= |S_{23}| \end{aligned}\right\} \qquad (5.10)$$

There is thus a particular symmetry to the coupling coefficients of the hybrid. It is clear that there is no special requirement that the hybrid should split an input signal equally between its appropriate output ports. For example, directional couplers may give any degree of coupling.

Of particular interest in the design of diplexers are hybrids described by the scattering matrix (5.11):

$$[S] = \frac{1}{\sqrt{2}} \begin{pmatrix} 0 & 0 & 1 & j \\ 0 & 0 & j & 1 \\ 1 & j & 0 & 0 \\ j & 1 & 0 & 0 \end{pmatrix} \qquad (5.11)$$

Referring to Figure 5.12 again, this hybrid would split a signal at port 1 equally between ports 3 and 4, with a 90^{o} phase difference between them. Such hybrids are realisable by directional coupler circuits [5.5].

A diplexer configuration using hybrids is shown in Figure 5.13, where two identical filters are interconnected by a pair of identical 90^{o} hybrids. The four accessible ports of the diplexer are numbered and the number ringed, the other numbers are for reference. Let the filters be symmetrical and described by the scattering matrix

$$\begin{bmatrix} S_{11} & S_{12} \\ S_{12} & S_{11} \end{bmatrix}$$

Since both hybrids are matched, the filters are ideally terminated at each port. Thus, considering the coupling between ports 1 and 3, if waves a_1 and a_2 are incident on ports 1 and 3, we can find the waves reflected from the first hybrid straightforwardly as follows:

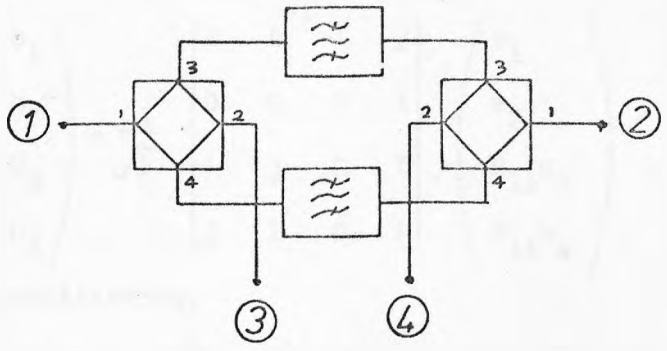

FIGURE 5.13 Hybrid-type Diplexer.

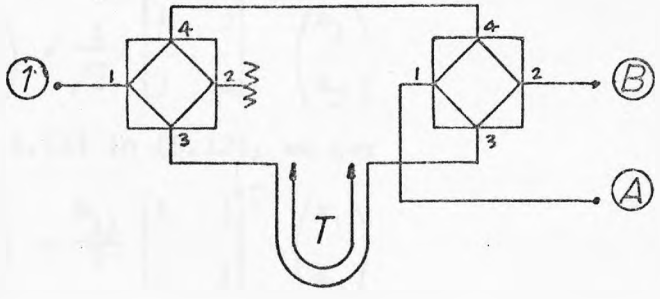

FIGURE 5.14 Commutating Filter.

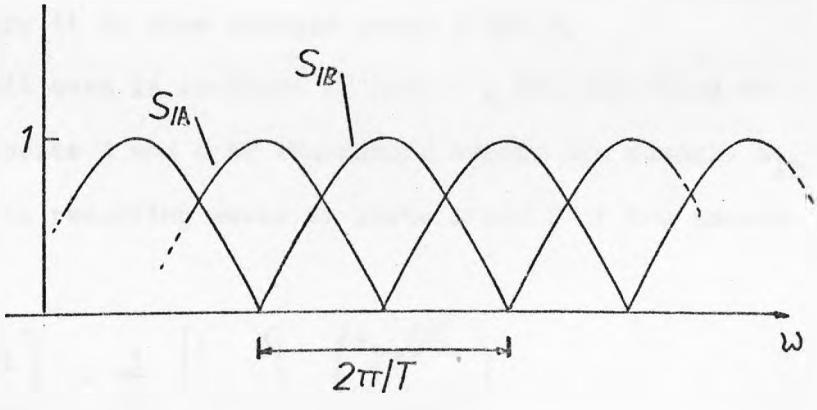

FIGURE 5.15 Response of Commutating Filter.

$$\begin{pmatrix} b_1 \\ b_2 \\ b_3 \\ b_4 \end{pmatrix} = \frac{1}{\sqrt{2}} \begin{bmatrix} 0 & 0 & 1 & j \\ 0 & 0 & j & 1 \\ 1 & j & 0 & 0 \\ j & 1 & 0 & 0 \end{bmatrix} \begin{pmatrix} a_1 \\ a_2 \\ S_{11}b_3 \\ S_{11}b_4 \end{pmatrix}$$

By simple partitioning,

$$\begin{pmatrix} b_1 \\ b_2 \end{pmatrix} = \begin{bmatrix} 0 & 0 \\ 0 & 0 \end{bmatrix} \begin{pmatrix} a_1 \\ a_2 \end{pmatrix} + \frac{S_{11}}{\sqrt{2}} \begin{bmatrix} 1 & j \\ j & 1 \end{bmatrix} \begin{pmatrix} b_3 \\ b_4 \end{pmatrix} \qquad (5.12)$$

$$\begin{pmatrix} b_3 \\ b_4 \end{pmatrix} = \frac{1}{\sqrt{2}} \begin{bmatrix} 1 & j \\ j & 1 \end{bmatrix} \begin{pmatrix} a_1 \\ a_2 \end{pmatrix} \qquad (5.13)$$

Substituting (5.13) in (5.12), we get

$$\begin{pmatrix} b_1 \\ b_2 \end{pmatrix} = \frac{S_{11}}{2} \begin{bmatrix} 1 & j \\ j & 1 \end{bmatrix}^2 \begin{pmatrix} a_1 \\ a_2 \end{pmatrix}$$

$$= \begin{bmatrix} 0 & jS_{11} \\ jS_{11} & 0 \end{bmatrix} \begin{pmatrix} a_1 \\ a_2 \end{pmatrix}$$

and thus the coupling coefficient between ports 1 and 3 is just jS_{11}, as by symmetry it is also between ports 4 and 2.

If a unit wave is incident on port 1 , the resulting waves incident on ports 3 and 4 of the second hybrid are clearly $S_{12}/\sqrt{2}$ and $jS_{12}/\sqrt{2}$. The resulting waves at ports 1 and 2 of the second hybrid are thus

$$\begin{pmatrix} b_1 \\ b_2 \end{pmatrix} = \frac{1}{\sqrt{2}} \begin{bmatrix} 1 & j \\ j & 1 \end{bmatrix} \begin{pmatrix} S_{12}/\sqrt{2} \\ jS_{12}/\sqrt{2} \end{pmatrix}$$

$$= \frac{S_{12}}{2} \begin{pmatrix} 1 + j^2 \\ j + j \end{pmatrix}$$

$$= \begin{pmatrix} 0 \\ jS_{12} \end{pmatrix}$$

Thus port 1 is decoupled from port 2 and coupled to port 4 by the coefficient jS_{12}. Thus the scattering matrix of the hybrid diplexer is

is

$$j\begin{bmatrix} 0 & 0 & S_{11} & S_{12} \\ 0 & 0 & S_{12} & S_{11} \\ S_{11} & S_{12} & 0 & 0 \\ S_{12} & S_{11} & 0 & 0 \end{bmatrix}$$

It is clear that his network fulfils the conditions of equations (5.8)-(5.10) and is thus itself a hybrid.

In Figure 5.13 the filters shown are bandpass types, but it is clear that lowpass, highpass or bandstop types could be used. In use, port 1 would be regarded as the "input", and port 2 terminated by a resistive "dummy" load. The unit then functions as a channel-dropping filter, the dropped channel emerging from port 4 and the remainder of the input from port 3. The responses of the diplexer are thus essentially similar to the circulator type discussed in the preceding section, and it is subject to the same disadvantages in respect of group-delay distortion. Since two filters are used rather than one, there is again a weight penalty, though hybrids are commonly lighter than circulators. In addition it may be noted that if the filters used are of n'th degree the response is also of n'th degree, but the overall network is of 2n'th degree, so the network is highly redundant. The performance is also critically dependent on maintaining exact balance in each hybrid and each filter path. On the other hand the network can handle high powers, and has found application for transmitting combiners.

An equivalent device to the hybrid diplexer just described is the directional filter, in which the functions of the hybrid junctions and the filters are combined. A good review of directional filters can be found in Cohn and Coal [5.12].

The hybrid diplexer seems to have been first described by Lewis and Tillotson [5.6], similar ideas having been put forward by Vos and Ianvent [5.7] and Bobis [5.8]. Another application for the hybrid

diplexer appears in [5.9]. The first appearance of the directional filter is from Carlin [5.10]. Both devices are then developed by a number of authors [5.11]-[5.42]. High-power diplexers have been described by Young and Owen [5.16]. The hybrid diplexer has been considered as a channel-dropping filter in trunk waveguide systems by Marcatili [5.18] and Marcatili and Bisbee [5.19], Saha [5.28], and Shimada et al [5.30], amongst many others.

c) Waveguide commutating filters

The waveguide commutating filter [5.43], [5.44], is likely to become numerically a very important type of multiplexer because of its adoption as the channelling filter in millimetric waveguide trunk systems. Superficially it resembles the hybrid diplexer discussed in the previous section, but its operating principles are very different. Figure 5.14 shows a simple form of commutating filter. It consists of a pair of 90° hybrids interconnected by matched transmission lines, such that the path lengths differ by a time delay T seconds. In the following analysis, it will be assumed for simplicity that there is no phase shift in the interconnecting lines apart from the time delay in one of them.

Assume that a unit wave is incident on port 1 of hybrid 1. Since the hybrid is matched at all its ports, the wave is decoupled from port 2, and the waves at ports 3 and 4 are given by

$$\begin{pmatrix} b_3 \\ b_4 \end{pmatrix} = \frac{1}{\sqrt{2}} \begin{bmatrix} 1 & j \\ j & 1 \end{bmatrix} \begin{pmatrix} 1 \\ 0 \end{pmatrix}$$

$$= \frac{1}{\sqrt{2}} \begin{pmatrix} 1 \\ j \end{pmatrix}$$

These waves are incident on ports 3 and 4 of the second hybrid after the wave b_3 has been delayed by a time T. Since the second hybrid is matched there are no reflections from ports 3 and 4, and the waves emerging from ports 1 and 2 of the second hybrid are given by

$$\begin{pmatrix} b_1 \\ b_2 \end{pmatrix} = \frac{1}{\sqrt{2}} \begin{bmatrix} 1 & j \\ j & 1 \end{bmatrix} \frac{1}{\sqrt{2}} \begin{pmatrix} e^{-j\omega T} \\ j \end{pmatrix}$$

$$= \frac{1}{2} \begin{pmatrix} e^{-j\omega T} - 1 \\ je^{-j\omega T} + j \end{pmatrix} \qquad (5.14)$$

and these form the outputs b_A and b_B of the system.

From (5.14) the modulus of the output at port A for a unit wave at port 1 of the first hybrid, which is the appropriate transfer coefficient modulus, is given by:

$$|S_{1A}|^2 = 1/4\ [(\cos\omega T - 1)^2 + \sin^2\omega T]$$

$$= 1/4\ [\cos^2\omega T - 2\cos\omega T + 1 + \sin^2\omega T]$$

$$= 1/2\ [1 - \cos\omega T]$$

$$= \sin^2(\frac{\omega T}{2}) \qquad (5.15)$$

while

$$|S_{1B}|^2 = 1/4\ [(\cos\omega T + 1)^2 + \sin^2\omega T]$$

$$= 1/2\ [1 + \cos\omega T]$$

$$= \cos^2(\frac{\omega T}{2}) \qquad (5.16)$$

Thus the division of power between the output ports varies periodically with frequency, with a period of $\omega = 2\pi/T$, as shown in Figure 5.15. Note that

$$|S_{1A}|^2 + |S_{1B}|^2 = \sin^2(\frac{\omega T}{2}) + \cos^2(\frac{\omega T}{2})$$

$$= 1$$

as expected.

From equation (5.14) again, the phase shift can be determined, and for example

$$\text{ang}(S_{1A}) = \tan^{-1}\left[-\frac{\sin\omega T}{\cos\omega T - 1}\right]$$

$$= \tan^{-1}\left[\frac{2\sin(\frac{\omega T}{2})\ \cos(\frac{\omega T}{2})}{2\sin^2(\frac{\omega T}{2})}\right]$$

$$= \tan^{-1}\left[\cot(\frac{\omega T}{2})\right]$$

$$= \frac{\pi}{2} - (\frac{\omega T}{2})$$

This is a linear function of ω, and hence the response of the commutating filter is inherently linear phase.

For applications such as in the trunk waveguide scheme the commutating filter is very suitable for several reasons. Firstly, its periodic responses can be used to advantage in planning the multiplexer configuration, and the fact that the commutating filter is matched simplifies cascading. Second, it has a very low loss, since no resonant elements are used, and an intrinsically linear-phase response. It is easy to fabricate in large numbers using numerically controlled machine tools.

The commutating filters main disadvantage is its poor selectivity in comparison with conventional filter responses. The selectivity can be improved by replacing the delay line with all-pass networks with a larger rate of change of phase with frequency in the transition region between bands [5.45], but at the expense of sacrificing the linear-phase response. Nevertheless, the group delay distortion remains small.

The commutating filter type of diplexer is also attractive when high power handling capacity is needed [5.45]; since there is no resonance and therefore little stored energy, local heating and ionisation leading to breakdown are less of a problem than in conventional filters.

5.4 Design of Directly Interacting Diplexers

a) Lowpass/highpass diplexers

Consider the input impedance of a doubly-terminated lowpass filter, which for the sake of argument can have a Chebyshev insertion-loss response. At a finite set of frequencies within the passband, the insertion loss of the filter is zero. These frequencies are the zeros of the insertion loss function L_A, where

$$L_A = 10 \log_{10} (1 + \varepsilon^2 T_n^2 (\omega))$$

Thus the frequencies of zero insertion loss are the zeros of the Chebyshev polynomial $T_n(\omega)$. At the zero-loss frequencies, the input impedance of the filter is purely real, and equal to the designed source impedance. Thus, in essence, in its passband the filters input impedance is real and constant, while, if the filter is a minimum reactance network, the stopband input impedance is approximately zero, and mainly imaginary. Under these conditions, if two filters are connected in series at one port as in Figure 5.3, the input impedance will be real in the passband of each filter and thus present a match to a resistive source, and so the device will function as a diplexer.

However, the behaviour of real filters complicates the situation. This is shown by Figure 5.16, which shows the input impedance characteristics of lowpass and highpass filters. Although the reactive part of the input impedance of one filter is nearly zero in its passband, it has a large peak just beyond cutoff, lying within the passband of the other, and thus the filters will interact severely if they are connected directly in series.

This interaction can be avoided if the filters are designed so that their input impedances are actually complex in the passbands, so that their imaginary parts are equal and opposite and the real parts sum to a constant. Such networks are termed "complementary" [5.46]. One example of complementary filters which can be used in a diplexer is the maximally-flat singly-terminated lowpass/highpass filter pair [5.47]. Singly-terminated filters were discussed briefly in Chapter 3; briefly, the n'th-degree singly-terminated maximally flat prototype lowpass filter has an input impedance of the form

$$Z_L(j\omega) = \frac{1}{1 + \omega^{2n}} + jX_L(\omega) \qquad (5.17)$$

Thus, if the filter is excited by a current source of one amp, the real power absorbed by the filter has the form of the real part on

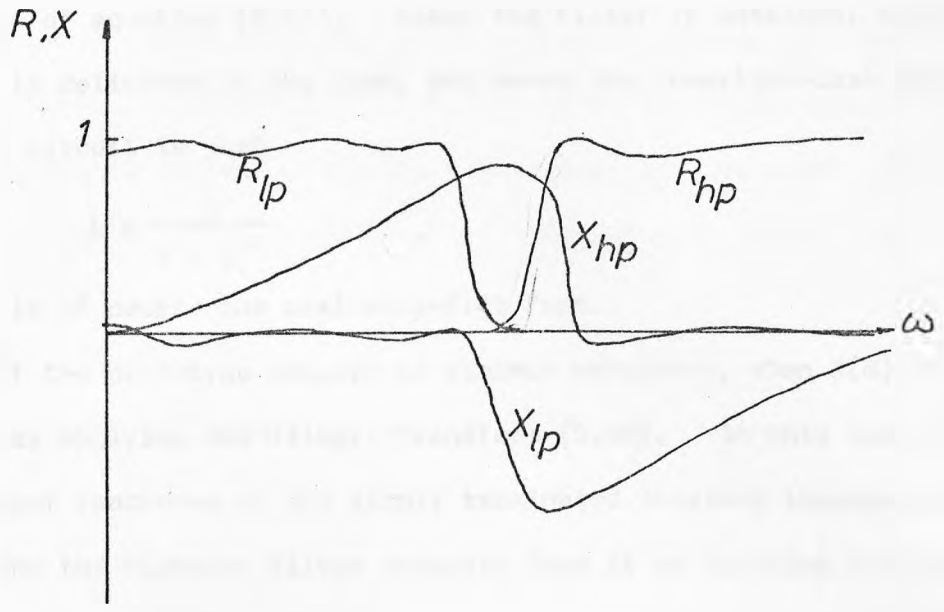

FIGURE 5.16 Input Impedance of HP/LP Filter Pair.

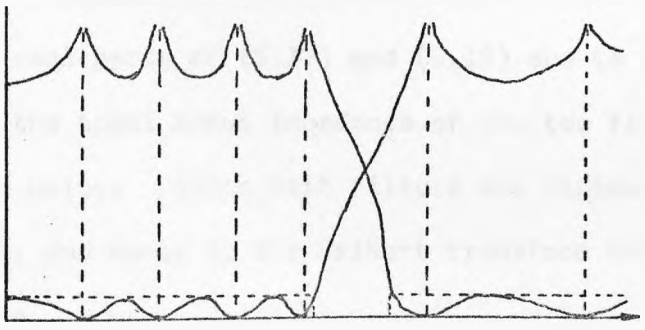

FIGURE 5.17 Responses of 'Ideal' Diplexer.

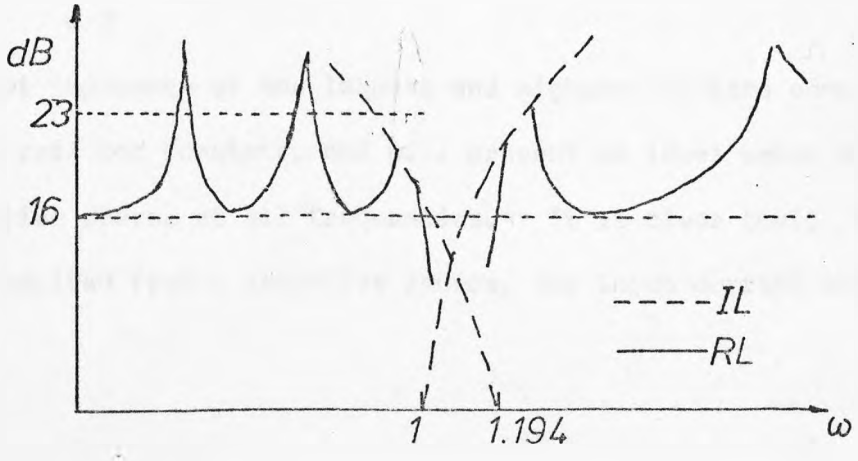

FIGURE 5.18 'Approximate' Diplexer Response.

the rhs of equation (5.17). Since the filter is lossless, all this power is delivered to the load, and hence the insertion-loss ratio of the circuit is just

$$L = \frac{1}{1 + \omega^{2n}}$$

which is of course the maximally-flat form.

If the prototype network is minimum reactance, then $X(\omega)$ can be found by applying the Hilbert transform [5.48]. In this case consider the input reactance of the singly terminated lossless lowpass prototype and the highpass filter obtained from it by applying the frequency transform $\omega \to -1/\omega$. The input impedance of the highpass filter is found by substituting for ω in (5.17), and is of the form

$$Z_H(j\omega) = \frac{\omega^{2n}}{1 + \omega^{2n}} + jX_H(\omega) \qquad (5.18)$$

Clearly the real parts of (5.17) and (5.18) sum to unity, and thus the real part of the total input impedance of the two filters connected in series will be unity. Since both filters are minimum reactance their sum is also, and hence by the Hilbert transform the input reactance of the diplexer is

$$\begin{aligned} X(\omega) &= -\frac{1}{\pi}\int_{-\infty}^{\infty}\frac{du}{\omega - u} \\ &= \frac{1}{\pi}\left[\log(\omega - u)\right]_{-\infty}^{\infty} \\ &= 0 \end{aligned}$$

Thus the input impedance of the lowpass and highpass filters connected in series is real and constant, and will present an ideal match to a unit resistive source at all frequencies. It is clear that, if the diplexer is excited from a resistive source, the input current will

therefore be constant, and thus the transfer response of each filter will have the maximally-flat form. If port 1 is defined as the common port where the filters are connected in series, port 2 the output port of the lowpass filters, and port 3 of the highpass filter, it is clear that:

$$|S_{11}| = 0$$

$$|S_{12}|^2 = \frac{1}{1 + \omega^{2n}}$$

$$|S_{13}|^2 = \frac{\omega^{2n}}{1 + \omega^{2n}}$$

and further that

$$|S_{11}|^2 + |S_{12}|^2 + |S_{13}|^2 = 1$$

The resulting diplexer, having a maximally-flat amplitude response, is not sufficiently selective for many applications. If an equal ripple response is sought, the fact that an ideal match is required at the input places restrictions on the type of response that is physically possible. For, if the diplexer is lossless, the unitary condition implies that

$$|S_{11}|^2 + |S_{12}|^2 + |S_{13}|^2 = 1$$

and thus, if S_{11} is zero,

$$|S_{12}|^2 + |S_{13}|^2 = 1 \qquad (5.22)$$

Thus, at any frequency where the insertion loss in one channel is zero there must be a transmission zero in the other channel. Thus the frequency responses of an equi-ripple ideal lowpass/highpass diplexer will be of the form shown in Figure 5.17 and Norton [5.47] has shown that the appropriate filters must be elliptic-function. It may be noted that the form of the responses is restricted by equation (5.22) even if the input match requirement is relaxed, and an exact input match required only at the finite set of frequencies where either filter has zero insertion loss.

This restriction on the form of the responses possible in an ideal diplexer is particularly arduous in the case of a bandpass/bandpass diplexer. In this case, the responses will have the form already seen in Figure 5.6(a), with the selectivity of each channel heavily weighted onto the passband of the other; in fact, the response of each channel resembles more the single-sideband responses of Chapter 4. Thus selectivity is not available in the remainder of the stopband where it is usually required. In addition, if one channel has greater degree than the other, the diplexer will be unrealisable. For these reasons, and recognising that the maximally-flat response is insufficiently selective, approximate realisations of diplexers are of great importance.

To show that approximate realisations may give acceptable performance, consider the design of a "typical" lowpass-highpass diplexer using conventional Chebyshev response channel filters, where each filter has a passband ripple of 0.1 dB and a degree of 6, and the filters responses cross-over at the -3 dB frequencies, ie the diplexer is contiguous. Assuming that the lowpass channel is normalised for a cutoff frequency of unity, the cutoff frequency of the highpass channel is then at $\omega = 1.194$. The approximate insertion-loss responses of these two filters are shown in Figure 5.18. Now suppose that the filters are connected in series and a method found to reduce the interaction to acceptable proportions. Consider the return-loss response in the lowpass channel. A 0.1 dB ripple Chebyshev filter will normally have a minimum return loss of approximately 16 dB, and it is clear that the maximum return loss can exceed 23 dB for over 85% of the lowpass channel. From this simple treatment it can be seen that the adverse affect of the interactions in an approximately designed diplexer may not be very serious from a simple "power-flow" point of view, as long as the interaction between the input impedances

can be minimised. It also appears that the proportion of the band over which the return-loss peaks can reach an acceptable level decreases as the ripple level of the filters decreases; however, it will be seen that filters connected in a diplexing configuration exhibit a considerable apparent increase in selectivity.

The problem of designing Chebyshev lowpass/highpass diplexers with a nearly constant and real input impedance has been considered by Wenzel [5.49]. He has shown that a lowpass/highpass Chebyshev filter pair can be very nearly complementary if they are designed on a singly-terminated prototype and if:

a) The cut-off frequency of the highpass filter is scaled so that the filters insertion-loss responses cross-over at the -3 dB point. Since the filters are singly terminated, this implies that the input (real-port) impedances (assuming unit termination) are equal at the same frequency to 0.5 ohm.

b) The filter cut-off slopes are equal and opposite at the cross-over frequency.

Wenzel has shown that both conditions are satisfied by the singly-terminationed Chebyshev lowpass prototype when the highpass filter is obtained by directly transforming the lowpass prototype by the frequency transformation

$$\omega \rightarrow -\frac{k}{\omega} \tag{5.23}$$

where k is given by

$$k = \cosh^2\left[\frac{1}{n}\cosh^{-1}\left(\frac{1}{\varepsilon}\right)\right] \tag{5.24}$$

ε being the prototype ripple factor. Since element values are obtainable for the singly-terminated prototype from explicit formulae [5.50] this method of design is very simple and direct. One matter not yet treated is the relationship between the ripple factor

of the singly-terminated prototypes and the resulting ripple of the diplexer.

Consider a singly terminated prototype filter with a Chebyshev transfer response, for which

$$R_e(Z_{in}) = \frac{1}{1 + \varepsilon^2 T_n^2(\omega)}$$

The minimum value of $R_e(Z_{in})$ within the lowpass passband is just

$$R_{min} = \frac{1}{1 + \varepsilon^2}$$

If it is assumed that the imaginary part of the input imedpance is exactly cancelled in the diplexer arrangement, then the corresponding maximum value of the reflection coefficient at the common port of the diplexer is just

$$S_{11max} = \frac{-\varepsilon^2}{2 + \varepsilon^2}$$

$$\approx \frac{-\varepsilon^2}{2}$$

in the usual case for which $\varepsilon << 1$. Thus

$$|S_{11}|^2_{max} = \frac{\varepsilon^4}{4} \qquad (5.25)$$

and thus

$$|S_{12}|^2_{min} = 1 - \frac{\varepsilon^4}{4} \qquad (5.26)$$

(Here it is assumed that port 2 is the output port of the lowpass filter and that the insertion loss of the highpass filter is very high, so that effectively all the power transmitted is to port 2.)

Thus, as shown by (5.25), the return-loss ripple measured at the diplexer input is considerably smaller than might be expected from the prototype ripple level. For example, consider the 0·5 dB ripple singly terminated prototype. The corresponding value of ε is

$$\varepsilon = \sqrt{10^{0.05} - 1}$$

$$= 0.349$$

and thus $|S_{11}|^2_{max} = 3.72 \times 10^{-3}$

corresponding to a return-loss of about 24 dB (for a conventional doubly-terminated prototype, a 0.5 dB ripple corresponds to a return loss of about 9.6 dB). At the same time, this decrease in the passband ripple is not accompanied by a decrease in the stopband selectivity; since the input impedance of the diplexer is sensibly constant, the stopband rejection of either filter is not affected since the excitation is effectively from a constant-current source.

Quantifying this, let the effective ripple factor of one channel of the diplexer be ε'. Then, from (5.26) we have

$$\frac{1}{1 + \varepsilon'^2} \approx 1 - \varepsilon'^2$$

$$= 1 - \frac{\varepsilon^4}{4}$$

whence $$\varepsilon' = \frac{\varepsilon^2}{2}$$

By considering the effective asymptotic passband attenuation of the Chebyshev filter (see Chapter 3) it is easily shown that the stopband attenuation of one channel of the diplexer exceeds that of a conventional doubly-terminated filter with the same passband ripple by, in the limit as $\omega \to \infty$,

$$6 + 10 \log_{10} \left(\frac{1}{\varepsilon^2}\right)$$

For the example considered before, this apparent increase in attenuation is

$$6 + 10 \log_{10} \left(\frac{1}{0.349^2}\right)$$

$$= 15.1 \text{ dB}$$

which is very significant.

With these considerations, the design procedure emerges, and will

be discussed with reference to the form of specification given in Figure 5.18. Attenuation and return-loss levels are quoted only for the lowpass channel, since those for the highpass channel are identical through the frequency transform (5.23) and (5.24).

The passband return-loss level required is L_R dB. Thus, from (5.25),

$$\varepsilon^2 = 2 \times 10^{-L_R/20} \tag{5.27}$$

Now the stopband attenuation has to exceed L_s dB at a frequency ω_o, and thus

$$n \geq \frac{\cosh^{-1}\left[\frac{1}{\varepsilon}\sqrt{10^{L_s/10} - 1}\right]}{\cosh^{-1}[\omega_o]} \tag{5.28}$$

In conjunction with (5.23) and (5.24) and the explicit element-value formulae these are the design equations for the Chebyshev lowpass/highpass diplexer.

A computer program has been written (Appendix 1) to design these diplexers using explicit formulae for the element values given the degree, and the required return-loss level of the diplexer, and to analyse the performance of the resulting circuit. Figure 5.19 shows the performance of a diplexer in which each channel has a degree of 7 and the designed return-loss level is 22 dB. The performance is clearly very good. The only visible degradation in the common-port return loss is the absence of the peaks nearest the cross-over frequency; however, an extra return-loss pole has appeared at the cross-over frequency to offset this. The lowpass channel insertion-loss response, also plotted, shows that, though the in-channel response meets the 22 dB return-loss level, the stopband attenuation is characteristic of a much higher ripple filter, being some 16 dB more selective than a 22 dB return-loss doubly-terminated filter.

These results demonstrate that Wenzel's method permits the rapid

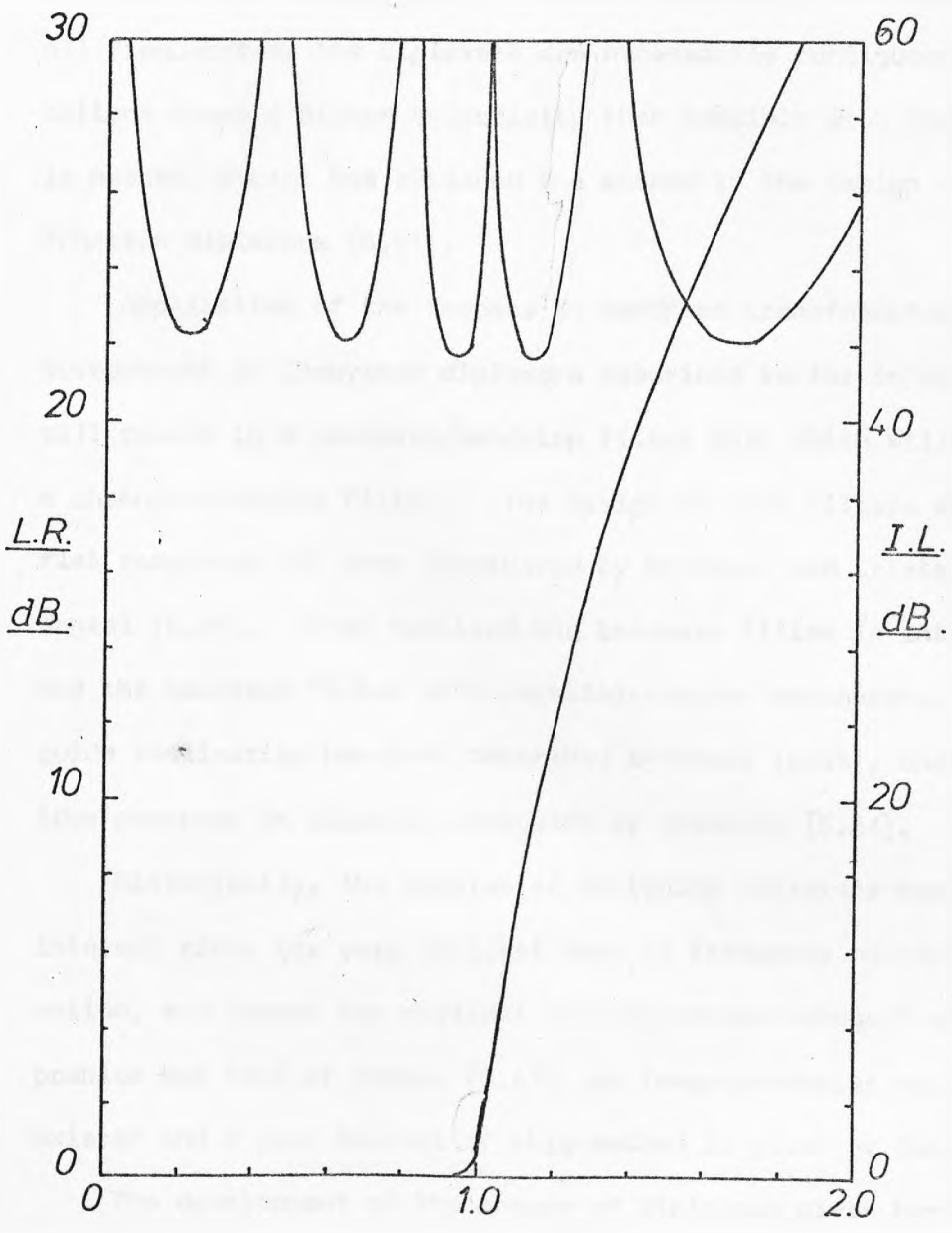

FIGURE 5.19 Response of LP/HP Example.

and accurate design of high performance nearly equi-ripple diplexers. Because of the requirements of making the input match almost exact at all frequencies, the diplexers are necessarily contiguous. For applications where a higher selectivity than possible with Chebyshev filters is needed, Wenzel has extended the method to the design of elliptic-function diplexers [5.51].

Application of the lowpass to bandpass transformation to the Butterworth or Chebyshev diplexers described so far in this section will result in a bandpass/bandstop filter pair which will behave as a channel-dropping filter. The design of such filters with maximally-flat responses has been considered by Matthaei and Cristal [5.52], and Wenzel |5.64|. They realised the bandpass filter in interdigital form and the bandstop filter with parallel-coupled resonators. A waveguide realisation has been described by Abele [5.53], and a similar idea proposed in circular waveguide by Standley [5.54].

Historically, the problem of designing diplexers has been of interest since the very earliest days of frequency multiplex communication, and though the earliest "modern-network-theory" attack on the problem was that of Norton [5.47], an image-parameter design method existed and a good account of this method is given by Guillemin [5.55].

The development of the theory of diplexers given here has been in terms of series-connected minimum-reactance filters, but it should be clear that a development in terms of shunt connected minimum susceptance networks is equally valid.

b) Bandpass/bandpass diplexers

With little modification the methods worked out in section (a) can be applied to the design of bandpass/bandpass diplexers. The argument is simplified if the "quasi-bandpass" diplexer prototype of Figure 5.20 is considered. Here, the two channels of the diplexer are shifted to

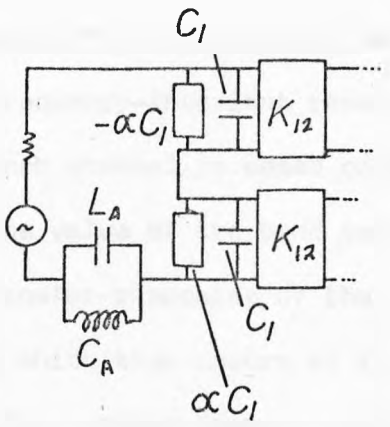

FIGURE 5.20 'Prototype' Bandpass Diplexer.

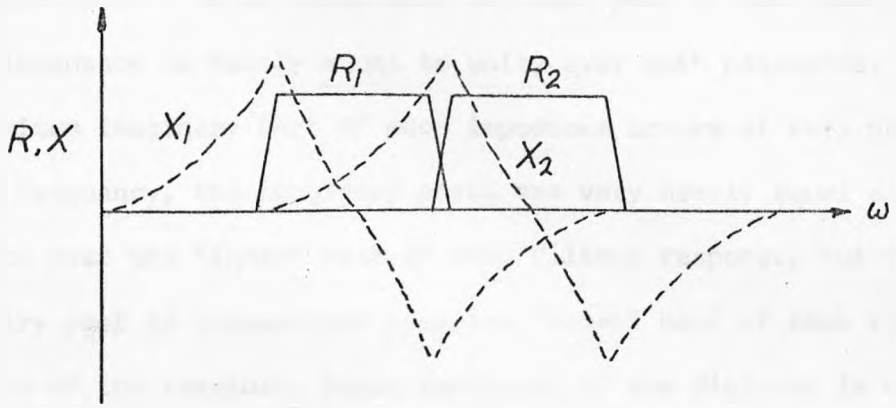

FIGURE 5.21 Impedance Characteristics of Filters.

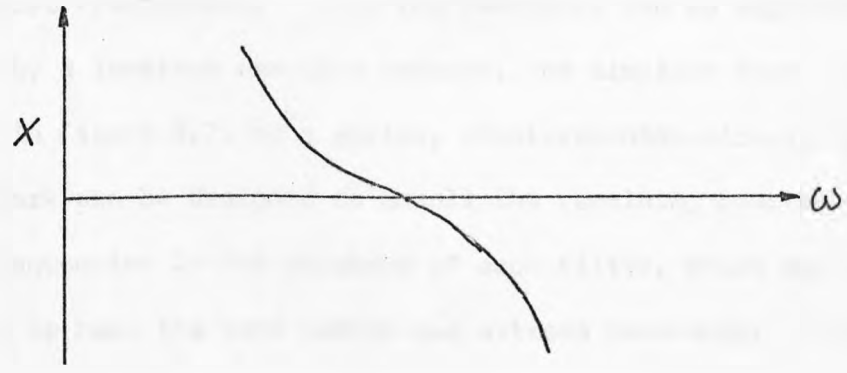

FIGURE 5.22 Reactance to be Annulled.

frequencies $\pm \alpha$ by shunting each capacitor in the lowpass prototype by a frequency-invariant reactance of value $\mp \alpha C_r$. It is assumed that each channel is based on the same singly-terminated prototype.

The value of the band separation factor "α" is chosen so that the transfer responses of the two filters cross-over at the - 3 dB point, which thus occurs at zero frequency. The value of α is thus fixed for a given degree n and ripple factor ε, and n and ε are found as in the last section. α is then given by

$$\alpha = \cosh\left(\frac{1}{n} \cosh^{-1} \frac{1}{\varepsilon}\right) \qquad (5.29)$$

The input impedance characteristics of the two filters are shown in Figure 5.21. It is clear that the real part of the total diplexer input impedance is nearly equal to unity over both passbands. Since the maximum imaginary part of each impedance occurs at very nearly the - 3 dB frequency, the imaginary parts are very nearly equal and opposite over the "inner" half of each filters response, but the total imaginary part is substantial over the "outer" half of each response. The form of the remaining input reactance of the diplexer is therefore as shown in Figure 5.22. Within the passband of each filter the slope of this remaining reactance is negative, and the reactance is positive for negative frequencies. Thus the reactance can be approximately annulled by a lossless reactive network, the simplest form of which is shown in Figure 5.21 as a series, shunt-resonant circuit, L_A, C_A. This network can be designed to annull the remaining reactance exactly at two frequencies in the passband of each filter, which are usually chosen to be near the band centre and extreme band-edge. Because of symmetry, the annulling need only be worked out for one channel. The resulting diplexer prototype can be directly transformed into a real bandpass/bandpass filter pair using the reactance slope technique.

The design of a diplexer prototype will be illustrated by an

example. Consider a specification for a bandpass/bandpass diplexer which requires a 5th-degree filter in each channel, to meet an in-channel return-loss requirement of 26 dB. From equation (5.27) the corresponding value of ε^2 is

$$\varepsilon^2 = 2 \times 10^{-1.3}$$

so $$\varepsilon = 0.317$$

Now from equation (5.29), α is given by

$$\alpha = \cosh\left(\frac{1}{5}\cosh^{-1}\left[\frac{1}{0.317}\right]\right)$$

$$= 1.067$$

A computer program was written to calculate the real and imaginary parts of the input impedance of the two bandpass filters connected in series, and the result plotted in Figure 5.23. The important parameters are the band-centre and band-edge reactances X_1 and X_2, which determine the series annulling reactance. Because the channels are contiguous, it is convenient in most cases, for ease of calculation, to consider the reactance at the frequencies $\omega_1 = 1$ and $\omega_2 = 2$.

From the graph,

$$X_1 = -0.2896 \text{ at } \omega = 1,$$

$$X_2 = -1.0104 \text{ at } \omega = 2$$

The reactance of the annulling network is

$$jX_A = \frac{1}{j\omega C_A + \frac{1}{j\omega L_A}}$$

thus $$X_A = \frac{\omega L_A}{1 - \omega^2/\omega_A^2}$$

where $$\omega_A^2 = \frac{1}{L_A C_A} \qquad (5.30)$$

So $$\frac{L_A}{1 - 1/\omega_A^2} = -X_1 \qquad (5.31)$$

and $$\frac{2L_A}{1 - 4/\omega_A^2} = -X_2 \qquad (5.32)$$

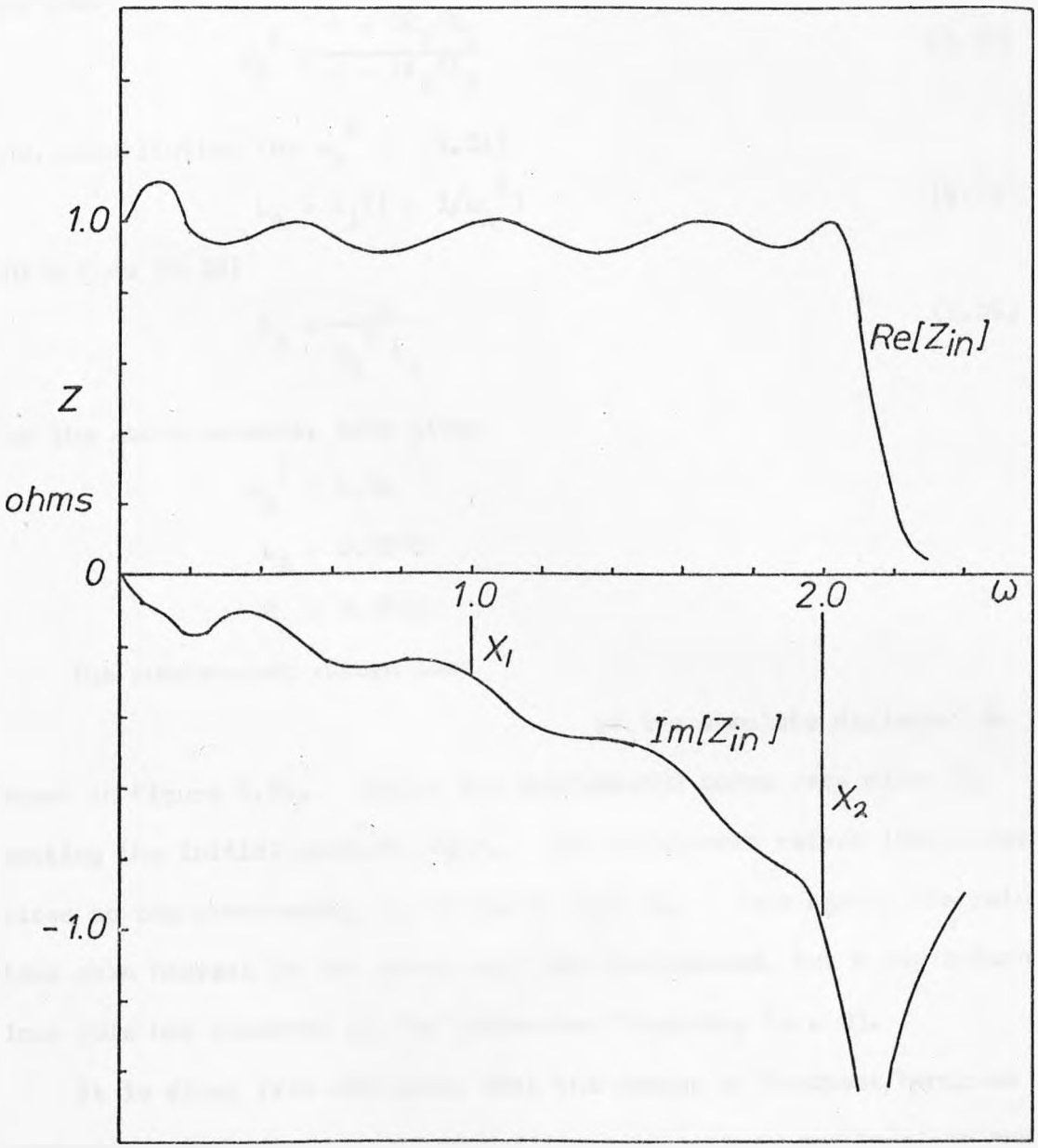

FIGURE 5.23 Input Impedance of BP/BP Pair.

Dividing (5.30) by (5.31),

$$\frac{1 - 4/\omega_A^2}{1 - 1/\omega_A^2} = \frac{2X_1}{X_2}$$

and thus

$$\omega_A^2 = \frac{4 - 2X_1/X_2}{1 - 2X_1/X_2} \qquad (5.33)$$

and, substituting for ω_A^2 in (5.31)

$$L_A = X_1(1 - 1/\omega_A^2) \qquad (5.34)$$

while from (5.30)

$$C_A = \frac{1}{\omega_A^2 L_A} \qquad (5.35)$$

For the above example, this gives

$$\omega_A^2 = 8.02$$

$$L_A = 0.2535$$

$$C_A = 0.4913$$

The common-port return loss of the complete diplexer is shown in Figure 5.24. Again, the performance comes very close to meeting the initial specification. The worst-case return loss occurs close to the cross-over, and is about 23.5 dB. Once again, the return-loss pole nearest to the cross-over has disappeared, but a new return loss pole has appeared at the cross-over frequency ($\omega = 0$).

It is clear from the above that the design of bandpass/bandpass diplexers using singly terminated filters is rather more involved than the design of lowpass/highpass types, involving steps of what are, in effect, optimisation. The performance of the diplexer can be improved by increasing the degree of the annulling network, complicating the design process further, and making the final structure more complex. However, the method can be extended to multiplexer design, as indicated

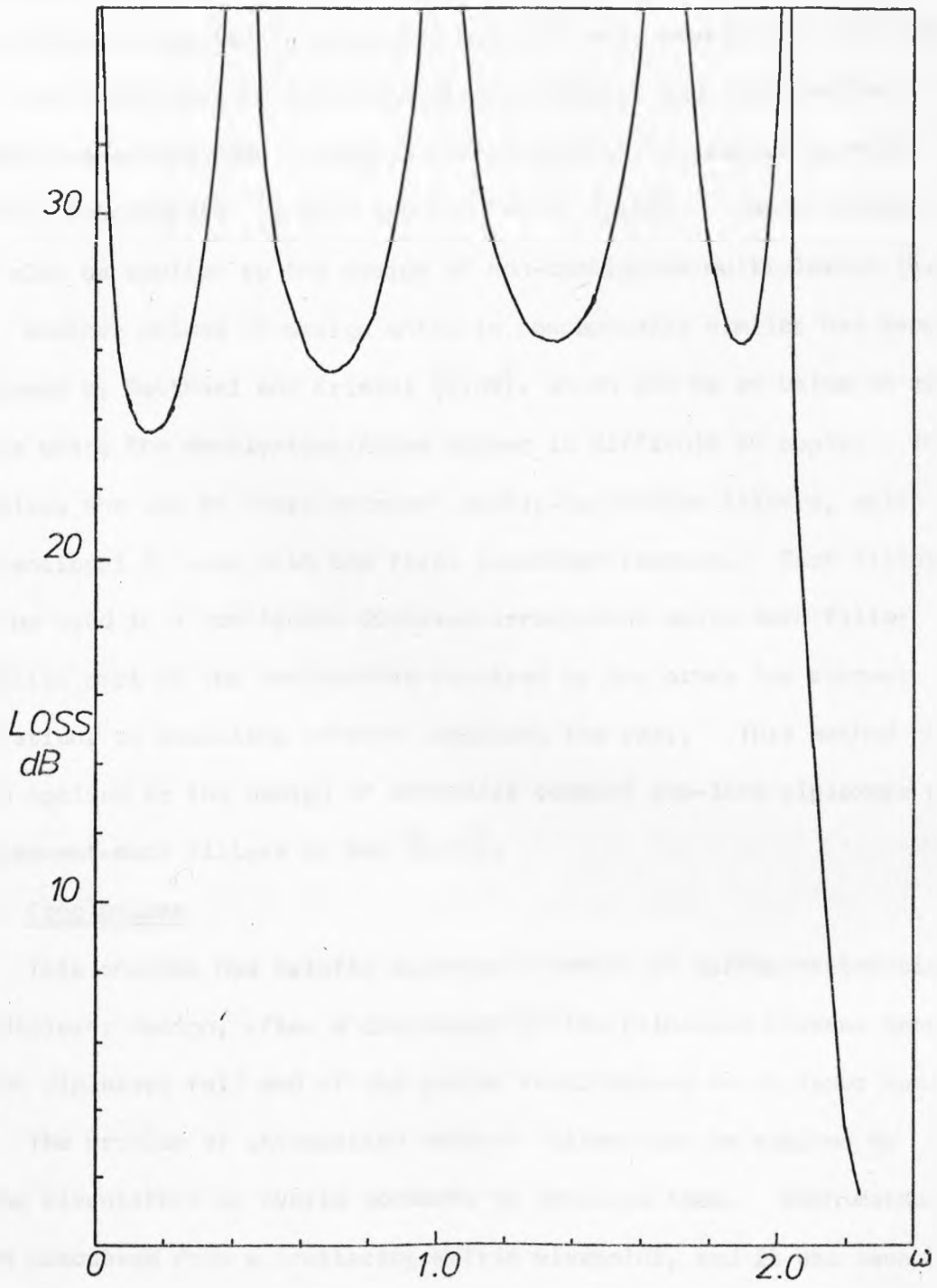

FIGURE 5.24 Common-Port Return-Loss of Contiguous BP|BP Design Example.

by Cristal and Matthaei [5.56] and Wenzel and Erlinger [5.57]. When the method is applied to waveguide multiplexers, waveguide manifolds are frequently used to interconnect the filters, and optimisation methods have been used to design the manifold, for example by Atia [5.58], Pfitzenmaier [5.59], and Chen et al [5.60]. These methods can also be applied to the design of non-contiguous multiplexers [5.61].

Another method of design which is conceptually similar has been proposed by Matthaei and Cristal [5.62], which can be of value in some cases where the doubly-terminated method is difficult to apply. This involves the use of "forshortened" doubly-terminated filters, which are conventional filters with the first resonator removed. Such filters can be used in a contiguous diplexer arrangement where each filter supplies part of the susceptance required by the other for correct operation, an annulling network supplying the rest. This method has been applied to the design of extremely compact low-loss diplexers using evanescent-mode filters by Mok [5.63].

5.5 Conclusions

This chapter has briefly surveyed a number of different techniques of diplexer design, after a discussion of the principle classes into which diplexers fall and of the system requirements on diplexer design.

The problem of interaction between filters can be avoided by using circulators or hybrid networks to decouple them. Both methods were discussed from a scattering matrix viewpoint, and it was seen that the responses of the resulting "channel-dropping" units were essentially similar, though the hybrid type was a reciprocal, and the circulator type a non-reciprocal, device. These methods have the advantage that all the ports of the diplexer are ideally matched and they can therefore be readily cascaded. Both methods introduce group-delay distortion into the "reflected" channels, and carry a weight penalty; one because of

the circulator needed, the other using two identical filters as well as two hybrids. The performance of the hybrid-type network also depends on the maintenance of exact balance in two parallel paths.

Another method using hybrids is the "commutating filter". This device provides selectivity using phase cancellation between two parallel paths of different time-delay rather than conventional filters. The selectivity thus tends to be poorer than conventional devices, and it is again dependent on maintaining balance between two parallel paths. The device has an intrinsically linear phase response and low-loss, and has been adopted for multiplexing in millimetric trunk waveguide schemes. Its selectivity can be improved at the expense of linear phase by using all-pass delay networks rather than simple delay lines, and it can handle high powers, being less prone to breakdown than conventional resonant filters.

The classical solution to the problem of designing lowpass/highpass diplexing filter pairs using singly-terminated maximally flat filters was outlined using Hilbert transforms to prove that these filters were complementary. This solution results in a diplexer which is not selective enough for many applications, and Wenzel's solution for designing approximately complementary Chebyshev diplexers was given. Using explicit formulae for the element values in singly terminated Chebyshev filters, Wenzel's method provides a very direct and simple solution to the design of lowpass/highpass diplexers. The design formulae were given, and a trial design, analysed on a computer, showed the high performance obtainable. These diplexers are also suitable prototypes for transformation to bandpass/bandstop channel-dropping filters.

Finally, the design of bandpass/bandpass diplexers was briefly considered, using singly terminated filters in conjunction with a reactance annulling network. The design procedure was much less straightforward, and computer aid is desirable in determining the

design of the annulling network.

The introductory remarks to the chapter mentioned that non-contiguous design methods are desirable to meet system requirements with minimum degree. There is obviously no restriction on the channel spacing using the circulator or hybrid-type diplexers. The commutating filter is, however, necessarily contiguous. The design methods using directly connected interacting filters result in convenient and simple structures which tend to be light and compact since they use no additional decoupling devices. The design methods given here result in contiguous diplexers, this condition being necessary for the cancellation of the reactive part of the common-port input impedance. Though a non-contiguous image parameter method was mentioned by Guillemin [5.55], no coherent "modern network theory" design procedure for non-contiguous diplexers has appeared in the literature until very recently. The next chapter of this thesis develops a general design theory for non-contiguous bandpass diplexers, while Chapter 8 applies the theory to lowpass/highpass diplexers.

DIRECT DESIGN FORMULAE FOR DIPLEXERS.

6·1 Introduction.

The last chapter reviewed several methods of designing diplexers, emphasising those where the the filters were connected in series or parallel at a common junction. The designers's problem is then to compensate for the undesirable interactions between the filters. The discussion can be summarised:

1. The available design methods are applicable only to cases where the diplexer passbands are contiguous, even though this may be undesirable for the system using the diplexer. This leads to designs using more selective filters, with higher degree and therefore higher group-delay distortion and loss, than the channels themselves demand. For this reason a circulator is often used to isolate the filters in a non-contiguous design even though this has a large weight, power handling, and cost penalty.

2. A direct design procedure, due to Wenzel, is available for contiguous lowpass/highpass diplexers using Chebyshev (and, indeed, elliptic) filters. A similar procedure can be used to design contiguous bandpass-bandpass diplexers, but a computer analysis is needed to determine the input impedance characteristics of the filter pair in order to determine the design of the reactance annulling network necessary. The design method cannot be considered to be "direct".

This chapter presents the derivation of direct design equations for bandpass diplexers. They allow an engineer to design high performance contiguous or non-contiguous diplexers which can be realised using coup-

led resonator filters of the type considered in chapter 4.

The key property of doubly-terminated filters used in the derivation was first applied to the design of symmetrical diplexers (in which the channel filters are identical except in centre frequency) by J.D. Rhodes 6·1 . The work presented here extends the derivation to the general asymmetric case 6·2 .

Following the derivation, computed performance curves are given for several prototype diplexers. The performance of a practical waveguide diplexer based on one of these examples is given in the next chapter.

6·2 Design Philosophy.

The "ideal" bandpass diplexer was described in chapter 5, where it was shown that each channel filter would have to have transmission zeros coinciding with the required reflection zeros in the passband of the other. Such a channel filter would be very difficult to realise, and if one channel needed to have a higher degree than the other the lower degree channel would be unrealisable. For these reasons it is desirable to to use conventional filters in a diplexer and to accept the need to compensate for their interactions.

To obtain designs where the channels may be close but not necessarily contiguous internal modifications are made to the filters, resulting in optimum performance when the filters are diplexed. It is found unnecessary to modify every element in each filter; only the first two or three resonators need to be altered, to obtain a very high performance design.

To begin with, only the first two resonators of

each filter will be modified for clarity of exposition. In the final result, modifications are extended to the first three resonators.

Let the channel filters be based on the normalised, unit-doubly-terminated prototypes shown in Figure 6.1. Each prototype begins with a pair of shunt capacitors coupled through an admittance inverter, and each filter hence has at least a second-order transmission zero at infinity. The remainder of the prototypes, N1 and N2, is arbitrary and the prototypes could realise conventional minimum-phase responses or certain types of linear-phase response.

As in Chapter 5, the prototypes will be transformed to bandpass channel filters at centre frequencies "$\pm\alpha$".* The networks N_1 and N_2 are transformed by the direct frequency transforms:

$$N1: \quad \omega \rightarrow \omega - \alpha \tag{6.1}$$

$$N2: \quad \omega \rightarrow \omega + \alpha \tag{6.2}$$

and the resulting diplexer circuit is shown in Figure 6.2. The frequency transform applied to each of the first two capacitors of each prototype is more complex, and of the form

$$\omega \rightarrow \omega \mp [\alpha + f_r(\alpha)] \tag{6.3}$$

Also, the coupling admittance inverters are modified by a factor

$$\sqrt{1 + k_r(\alpha)} \tag{6.4}$$

and matching transformers of turns ratio

$$N = \sqrt{1 + n_r(\alpha)} \tag{6.5}$$

are introduced at the input of each channel. A frequency invariant annulling reactance X_o where

$$X_o = x_r(\alpha) \tag{6.6}$$

is connected in series with the common port of the diplexer. The unknown functions f_r, k_r, n_r, x_r, which represent the required modifications, can be found when it is recognised that these functions have certain symmetry and limiting properties, and that the input

* α now being arbitrary.

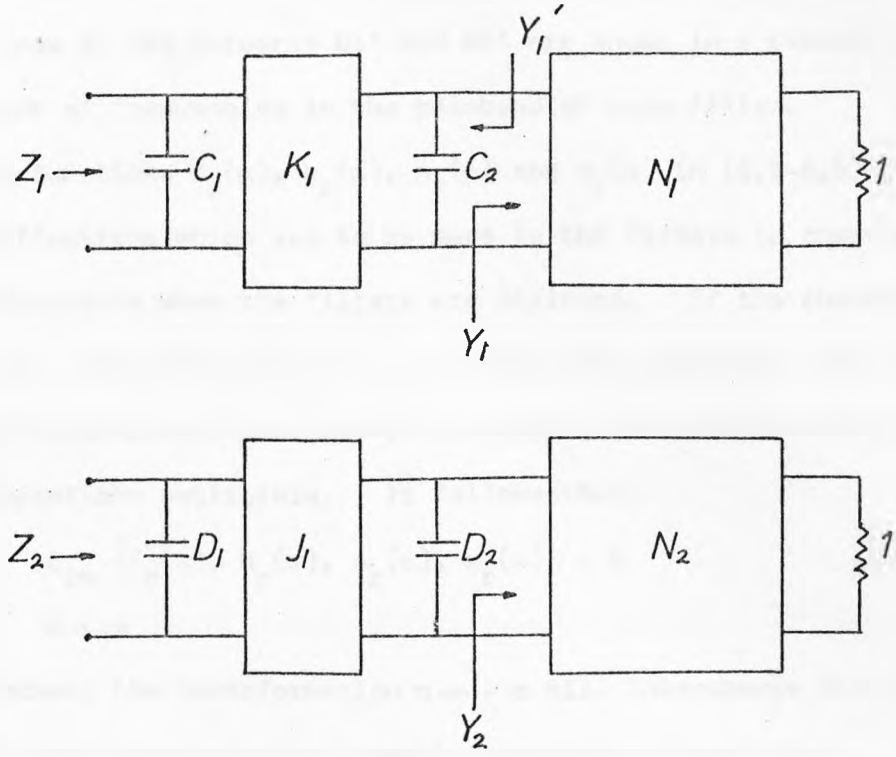

$$Z_1(j\omega_i) = Z_2(j\sigma_i) = 1$$

FIGURE 6.1 Prototypes for Channel Filters.

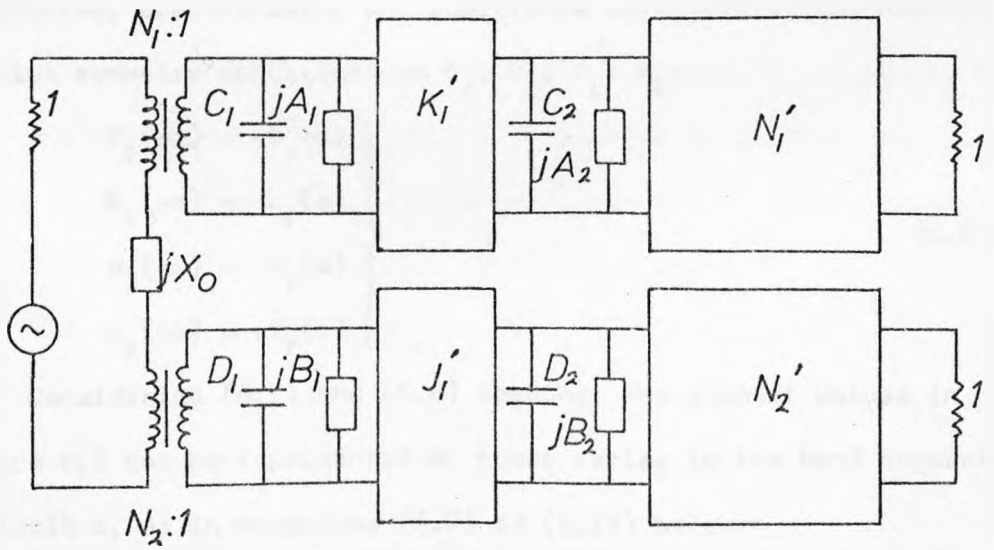

FIGURE 6.2 Prototype Diplexer.

admittances of the networks N1' and N2' are known in a closed form at a finite set of frequencies in the passband of each filter.

The functions $f_r(\alpha)$, $k_r(\alpha)$, $n_r(\alpha)$ and $x_r(\alpha)$ in (6.3-6.5) represent the modifications which are to be made to the filters to compensate for the the interactions when the filters are diplexed. If the channels are very widely separated, that is, α is very large, the input impedance of each filter in the passband of the other will be virtually zero and the interactions negligible. It follows that:

$$\lim_{\alpha \to \infty} \left[f_r(\alpha),\ k_r(\alpha),\ n_r(\alpha),\ x_r(\alpha) \right] = 0 \qquad (6.7)$$

Further, the transformation $\alpha \rightarrow -\alpha$ will interchange the channels, and the transformation $\omega \rightarrow -\omega$ will interchange them again. Application of both transformations will therefore result in a network with the same magnitude response as the original; considering the effects which each transform must have on the frequency-invariant reactances, transformers, and admittance inverters of the network implies symmetry conditions on f_r, k_r, n_r, x_r:

$$\left.\begin{aligned} f_r(-\alpha) &= -f_r(\alpha) \\ k_r(-\alpha) &= k_r(\alpha) \\ n_r(-\alpha) &= n_r(\alpha) \\ x_r(-\alpha) &= -x_r(\alpha) \end{aligned}\right\} \qquad (6.8)$$

Considering (6.7) and (6.8) together the element values in Figure 6.2 can be represented by power series in the band separation variable α, as in equations (6.9) to (6.17) below:

$$X_o = \frac{x_1}{\alpha} + \frac{x_3}{\alpha^3} \qquad (6.9)$$

$$A_1 = -C_1\left(\alpha + \frac{a_{11}}{\alpha} + \frac{a_{13}}{\alpha^3} + \frac{a_{15}}{\alpha^5} + \ldots\right) \qquad (6.10)$$

$$A_2 = -C_2\left(\alpha + \frac{a_{21}}{\alpha} + \frac{a_{23}}{\alpha^3} + \frac{a_{25}}{\alpha^5} + \ldots\right) \qquad (6.11)$$

$$B_1 = D_1\left(\alpha + \frac{b_{11}}{\alpha} + \frac{b_{13}}{\alpha^3} + \frac{b_{15}}{\alpha^5} + \ldots\right) \tag{6.12}$$

$$B_2 = D_2\left(\alpha + \frac{b_{21}}{\alpha} + \frac{b_{23}}{\alpha^3} + \frac{b_{25}}{\alpha^5} + \ldots\right) \tag{6.13}$$

$$N_1^2 = 1 + \frac{n_{12}}{\alpha^2} + \frac{n_{14}}{\alpha^4} + \ldots \tag{6.14}$$

$$N_2^2 = 1 + \frac{n_{22}}{\alpha^2} + \frac{n_{24}}{\alpha^4} + \ldots \tag{6.15}$$

$$K_1'^2 = K_1^2\left(1 + \frac{k_{12}}{\alpha^2} + \frac{k_{14}}{\alpha^4} + \ldots\right) \tag{6.16}$$

$$J_1'^2 = J_1^2\left(1 + \frac{h_{12}}{\alpha^2} + \frac{h_{14}}{\alpha^4} + \ldots\right) \tag{6.17}$$

Let the original prototype filters have passband reflection zeros at the sets of frequencies $\{\omega_i\}$, $\{\sigma_i\}$, as indicated in Figure 6.1, and thus perfect transmission at these sets of frequencies. It follows that, at these sets of frequencies, referring to Figure 6.1,

$$Z_1(j\omega_i) = 1$$

$$Z_2(j\sigma_i) = 1$$

Since there is perfect transmission, hence maximum power-transfer, through the prototypes at these sets of frequencies, the impedances seen looking to left and right from any plane sectioning a prototype must be complex conjugate, and hence, again referring to Figure 6.1,

$$\begin{aligned} Y_1(j\omega_i) &= Y_1'^*(j\omega_i) \\ &= Y_1'(-j\omega_i) \\ &= -j\omega_i C_2 + \frac{K_1^2}{-j\omega_i C_1 + 1} \end{aligned} \tag{6.18}$$

and similarly

$$Y_2(j\sigma_i) = -j\sigma_i D_2 + \frac{J_1^2}{-j\sigma_i D_1 + 1} \tag{6.19}$$

Equations (6.18) and (6.19) are the required closed-form expressions for the input admittance of the unmodified part of each filter.

The derivation of the design equations reduces to finding the undetermined coefficients in Equations (6.9) to (6.17), and proceeds

as follows. Using (6.9) to (6.19) the input impedance of each filter is found at the set of frequencies $\{\omega_i + \alpha\}$ in the passband of channel 1, noting that the expression (6.18) for the input admittance of N_1 at $\{\omega_i\}$ is valid for the input admittance of the transformed network N1' at the set of frequencies $\{\omega_i + \alpha\}$. The input impedances are found as a power series in α^{-1}, and their sum is the input impedance of the diplexer in the passband of channel 1, which is of the form, referring to Figure 6.2:

$$Z_{in}(j[\omega_i + \alpha]) = 1 + z_1(\alpha^{-1}) + z_2(\alpha^{-2}) + z_3(\alpha^{-3}) + \varepsilon(\alpha^{-4}) \tag{6.20}$$

where $\varepsilon(-)$ means "an error of the order of (-)". The coefficients $\{z_i\}$ are, in general, functions of $\{\omega_i\}$. A similar expansion can be made for the input impedance of the diplexer in the passband of channel 2, that is at the set of frequencies $\{\sigma_i - \alpha\}$, resulting in an expansion of the form:

$$Z_{in}(j[\sigma_i - \alpha]) = 1 + z_1'(\alpha^{-1}) + z_2'(\alpha^{-2}) + z_3'(\alpha^{-3}) + \varepsilon'(\alpha^{-4}) \tag{6.21}$$

where the $\{z_i'\}$ in general are functions of $\{\sigma_i\}$. From these expansions can be derived a set of simultaneous equations in the unknown coefficients whose solution forces the $\{z_i$ and $z_i'\}$ to zero. Thus the passband input impedance of the diplexer is a match to a one-ohm source up to a degree of approximation of α^{-4}. It will be seen that this approach concentrates its "compensating ability" on those frequencies where the independent filters would normally have reflection zeros, and attempts to force this condition on the filters when diplexed. Making modifications to the first two resonators it is possible to force up to the third-order error terms to zero; the modifications made are then of third and lower order. If the first three resonators are modified, it is also possible to force the

fourth and fifth order error terms to nearly zero, and fourth and fifth order modifications are then made.

6.3 DERIVATION OF DESIGN EQUATIONS

Expanding first the input impedance of channel 1 in its passband, that is at the set of frequencies $\{\omega_i + \alpha\}$, referring to Figure 6.2 and neglecting coefficients of degree higher than 3:

$$Z_1(j[\omega_i + \alpha]) = \frac{1 + n_{12}/\alpha^2 + \ldots}{j(\omega_i+\alpha)C_1 - jC_i(\alpha+a_{11}/\alpha+a_{13}/\alpha^3)} + \frac{K_1^2(1+k_{12}/\alpha^2+\ldots)}{\left\{ j(\omega_i+\alpha)C_2 - jC_2(\alpha+a_{21}/\alpha+a_{23}/\alpha^3) - j\omega_i C_2 + \frac{K_1^2}{1 - j\omega_i C_1} \right\}}$$

$$= \frac{1 + n_{12}/\alpha^2 + \ldots}{j\omega_i C_1 - \frac{jC_1 a_{11}}{\alpha} - \frac{jC_1 a_{13}}{\alpha^3} + \ldots + \frac{K_1^2(1+k_{12}/\alpha^2+\ldots)}{\frac{K_1^2}{1-j\omega_i C_1} - \frac{jC_2 a_{21}}{\alpha} - \frac{jC_2 a_{23}}{\alpha^3} + \ldots}}$$

$$= \frac{1 + n_{12}/\alpha^2 + \ldots}{1 - \frac{j}{\alpha}\left[C_1 a_{11} - \frac{C_2 a_{21}}{K_1^2}(1-j\omega_i C_1)^2\right] + \frac{(1-j\omega_i C_1)}{K_1^2 \alpha^2}\left[K_1^2 k_{12} - \frac{C_2^2 a_{21}^2}{K_1^2}(1-j\omega_i C_1)^2\right]}$$

$$- \frac{j}{\alpha^3}\left\{C_1 a_{13} - \frac{C_2}{K_1^2}\left\{a_{23} + \frac{C_2 a_{21}}{K_1^2}\left[K_1^2 k_{12} - \frac{C_2^2 a_{21}^2}{K_1^2}(1-j\omega_i C_1)^2\right]\right.\right.$$

$$\left.\left. \times (1-j\omega_i C_1)^2 \right\}\right\} + \varepsilon(\alpha^{-4}) \qquad (6.22)$$

The next step in the expansion will be given in full, to demonstrate the general method used. The expression (6.22) has to be expanded as a power series of the form

$$z_{10} + \frac{z_{11}}{\alpha} + \frac{z_{12}}{\alpha^2} + \frac{z_{13}}{\alpha^3} + \varepsilon(\alpha^{-4}) \qquad (6.23)$$

Multiplying (6.22) and (6.23) by the denominator of (6.22), and equating equal-degree terms in α, we get:

In α^0, $z_{10} = 1$ (6.24)

In α^{-1}, $z_{11} - j\left[C_1 a_{11} - \frac{C_2 a_{21}}{K_1^2}(1 - j\omega_i C_1)^2\right] = 0$

$$\Rightarrow z_{11} = j\left[C_1 a_{11} - \frac{C_2 a_{21}}{K_1^2}(1 - j\omega_i C_1)^2\right] \quad (6.25)$$

In α^{-2}, $z_{12} + \left[C_1 a_{11} - \frac{C_2 a_{21}}{K_1^2}(1 - j\omega_i C_1)\right]^2 + \frac{(1-j\omega_i C_1)}{K_1^2}$

$$\times \left[K_1^2 k_{12} - \frac{C_2^2 a_{21}^2}{K_1^2}(1 - j\omega_i C_1)^2\right] = n_{12}$$

$$\Rightarrow z_{12} = n_{12} - \left[C_1 a_{11} - \frac{C_2 a_{21}}{K_1^2}(1 - j\omega_i C_1)\right]^2 - \frac{(1-j\omega_i C_1)}{K_1^2}$$

$$\times \left[K_1^2 k_{12} - \frac{C_2^2 a_{21}^2}{K_1^2}(1-j\omega_i C_1)^2\right] \quad (6.26)$$

In α^{-3}, $z_{13} - j\left[C_1 a_{11} - \frac{C_2 a_{21}}{K_1^2}(1-j\omega_i C_1)^2\right] z_{12} + \frac{(1-j\omega_i C_1)}{K_1^2}$

$$\times \left[K_1^2 k_{12} - \frac{C_2^2 a_{21}^2}{K_1^2}(1-j\omega_i C_1)^2\right] z_{11}$$

$$- j\left\{C_1 a_{13} - \frac{C_2}{K_1^2}\left\{a_{23} + \frac{C_2 a_{21}}{K_1^2}\left[K_1^2 k_{12} - \frac{C_2^2 a_{21}^2}{K_1^2}(1-j\omega_i C_1)^2\right]\right\}\right.$$

$$\left. \times (1-j\omega_i C_1)^2\right\} = 0 \quad (6.27)$$

The expression (6.27) for z_{13} has not been written in full for clarity, as some simplification will be possible at a later stage.

An expression can be formed for the input impedance of channel 2 in the passband of channel 1, as in (6.28)

$$Z_2(j[\omega_i+\alpha]) = \frac{1 + n_{22}/\alpha^2 + \dots}{j(\omega_i+\alpha)D_1 + jD_1(\alpha + \frac{b_{11}}{\alpha} + \frac{b_{13}}{\alpha^3} + \dots)} + \frac{J_1^2(1+h_{12}/\alpha^2 + \dots}{j(\omega_i+\alpha)D_2(\alpha + \frac{b_{21}}{\alpha} + \frac{b_{23}}{\alpha^3} + \dots)} + \dots \quad (6.28)$$

$$= \frac{1 + n_{22}/\alpha^2 + \dots}{2j\alpha D_1 + j\omega_i D_1 + jD_1(\frac{b_{11}}{\alpha} + \frac{b_{13}}{\alpha^3} + \dots)} + \frac{J_1^2(1+n_{12}/\alpha^2 + \dots)}{2j\alpha D_2 + j\omega_i D_2 + jD_2(\frac{b_{21}}{\alpha} + \frac{b_{23}}{\alpha^3} + \dots)} + \dots \quad (6.29)$$

Now it may be noted that each partial denominator of the continued fraction (6.29) is of maximum degree α, and thus contributes to the term in α^{-1} in the previous partial denominator. Further inspection thus shows that if the expansion of (6.29) is required only to degree α^{-3}, only the terms shown will contribute. Thus, equating (6.29) to the power series

$$\frac{z_{21}}{\alpha} + \frac{z_{22}}{\alpha^2} + \frac{z_{23}}{\alpha^3} + \varepsilon(\alpha^{-4})$$

as before, the coefficients z_{21} , z_{23} can be found:

$$2jD_1 z_{21} = 1$$

$$\Rightarrow z_{21} = -\frac{j}{2D_1} \quad (6.30)$$

$$2jD_1 z_{22} + \frac{\omega_i}{2} = 0$$

$$\Rightarrow \quad z_{22} = \frac{j\omega_i}{4D_1} \tag{6.31}$$

$$2jD_1 z_{23} - \frac{\omega_i^2}{4} + \frac{1}{2}\left(b_{11} - \frac{J_1^2}{2D_1D_2}\right) = n_{22}$$

$$\Rightarrow \quad z_{23} = -\frac{j}{2D_1}\left\{ n_{22} + \frac{\omega_i^2}{4} - \frac{1}{2}\left(b_{11} - \frac{J_1^2}{2D_1D_2}\right) \right\} \tag{6.32}$$

The expansions for $Z_1(j[\omega_i+\alpha])$ and $Z_2(j[\omega_i+\alpha])$ can now be combined to give an expansion for the input impedance of the diplexer in the passband of channel 1. An exactly analogous procedure yields the input impedance of the diplexer at the set of frequencies $\{\sigma_i - \alpha\}$ in the passband of channel 2. Considering each term of the expansions a set of simultaneous equations can be derived whose solution yields the required coefficients in (6.9) to (6.17). Before considering this step in detail, notice that the total α^{-1} input impedance in channel 1 is, combining (6.30) and (6.25),

$$z_1 = j\left[C_1 a_{11} - \frac{C_2 a_{21}}{K_1^2}(1-j\omega_i C_1)^2\right] - \frac{j}{2D_1} + jx_1 \tag{6.33}$$

The only way for this expression to be zero independent of ω_i is if $a_{21} = 0$, and similarly $b_{21} = 0$ from considering the corresponding equation in the other passband. Using this allows a considerable simplification in the equations. The detailed derivation of the expansions at the frequencies $\{\sigma_i - \alpha\}$ will not be carried out. The resulting equations are; from the α^{-1} terms:

$$jC_1 a_{11} - \frac{j}{2D_1} + jx_1 = 0 \tag{6.34a}$$

$$-jD_1 b_{11} + \frac{j}{2C_1} + jx_1 = 0 \tag{6.34b}$$

from the α^{-2} terms:

$$n_{12} - C_1^2 a_{11}^2 - (1-j\omega_i C_1)k_{12} + \frac{j\omega_i}{4D_1} = 0 \qquad (6.35a)$$

$$n_{22} - D_1^2 b_{11}^2 - (1-j\sigma_i D_1)h_{12} + \frac{j\sigma_i}{4C_1} = 0 \qquad (6.35b)$$

The ω_i and σ_i dependent terms in (6.35) give independent equations for k_{12} and h_{12}:

$$j\omega_i C_1 k_{12} + \frac{j\omega_i}{4D_1} = 0, \quad j\sigma_i D_1 h_{12} + \frac{j\sigma_i}{4C_1} = 0$$

$$\Longrightarrow \qquad k_{12} = h_{12} = -\frac{1}{4C_1 D_1} \qquad (6.36)$$

From the α^{-3} terms:

$$jC_1 a_{11}\left\{ n_{12} - C_1^2 a_{11}^2 + \frac{(1-j\omega_i C_1)}{4C_1 D_1} \right\} + \frac{jC_1 a_{11}}{4C_1 D_1}(1-j\omega_i C_1)$$

$$+ j\left\{ C_1 a_{13} - \frac{C_2 a_{23}}{K_1^2}(1-2j\omega_i C_1 - \omega_i^2 C_1^2) \right\}$$

$$- \frac{j}{2D_1}\left\{ n_{22} + \frac{\omega_i^2}{4} - \tfrac{1}{2}\left(b_{11} - \frac{J_1^2}{2D_1 D_2}\right) \right\} + jx_3 = 0 \qquad (6.37a)$$

$$- jD_1 b_{11}\left\{ n_{22} - D_1^2 b_{11}^2 + \frac{(1-j\sigma_i D_1)}{4C_1 D_1} \right\} - \frac{jD_1 b_{11}}{4C_1 D_1}(1-j\omega_i C_1)$$

$$- j\left\{ D_1 b_{13} - \frac{D_2 b_{23}}{J_1^2}(1-2j\sigma_i D_1 - \sigma_i^2 D_1^2) \right\}$$

$$+ \frac{j}{2C_1}\left\{ n_{12} + \frac{\sigma_i^2}{4} - \tfrac{1}{2}\left(a_{11} - \frac{K_1^2}{2C_1 C_2}\right) \right\} + jx_3 = 0 \qquad (6.37b)$$

Taking first the ω_i^2 and σ_i^2 dependent terms of (6.36 a and b), gives;

$$\frac{jC_2 a_{23} C_1^2}{K_1^2} - \frac{j}{8D_1} = 0$$

$$\Longrightarrow \quad a_{23} = \frac{K_1^2}{8C_1^2 C_2 D_1} \qquad (6.38)$$

$$-\frac{jD_2b_{23}D_1^2}{J_1^2}+\frac{j}{8C_1}=0$$

$$\Rightarrow b_{23}=\frac{J_1^2}{8D_1^2D_2C_1} \tag{6.39}$$

Substituting for a_{23} and b_{23} in (6.37) and taking the resulting ω_i-dependent terms, gives;

$$\frac{C_1a_{11}}{2D_1}-\frac{1}{4C_1D_1}=0$$

$$\Rightarrow a_{11}=\frac{1}{2C_1^2} \tag{6.40}$$

$$-\frac{D_1b_{11}}{2C_1}+\frac{1}{4C_1D_1}=0$$

$$\Rightarrow b_{11}=\frac{1}{2D_1^2} \tag{6.41}$$

and thus from (6.34a) we get

$$\frac{j}{2C_1}-\frac{j}{2D_1}+jx_1=0$$

which is satisfied if

$$x_1=\tfrac{1}{2}\left(\frac{1}{D_1}-\frac{1}{C_1}\right)$$

This result also follows from (6.34b).

Substituting for a_{11}, b_{11}, k_{12}, h_{12}, in (6.35) we get

$$n_{12}-\frac{1}{4C_1^2}+\frac{1}{4C_1D_1}=0$$

$$\Rightarrow n_{12}=\frac{1}{4C_1}\left(\frac{1}{C_1}-\frac{1}{D_1}\right) \tag{6.42}$$

$$n_{22}-\frac{1}{4D_1^2}+\frac{1}{4C_1D_1}=0$$

$$\Rightarrow n_{22}=\frac{1}{4D_1}\left(\frac{1}{D_1}-\frac{1}{C_1}\right) \tag{6.43}$$

Finally, taking the terms in (6.37a) not dependent on ω_i, we get;

$$\frac{j}{2C_1}\left\{\frac{1}{4C_1}\left(\frac{1}{C_1}-\frac{1}{D_1}\right)-\frac{1}{4C_1^{\,2}}\right\}+\frac{j}{8C_1^{\,2}D_1}+jC_1a_{13}-\frac{j}{8C_1^{\,2}D_1}$$

$$-\frac{j}{2D_1}\left\{\frac{1}{4D_1}\left(\frac{1}{D_1}-\frac{1}{C_1}\right)-\tfrac{1}{2}\left(\frac{1}{2D_1^{\,2}}-\frac{J_1^{\,2}}{2D_1D_2}\right)\right\}+jx_3=0$$

$$\Rightarrow\quad a_{13}=\frac{1}{8D_1^{\,2}C_1}\left(\frac{J_1^{\,2}}{D_2}-\frac{1}{C_1}\right) \qquad (6.44)$$

while $x_3 = 0$

Similarly, from (6.36b)

$$b_{13}=\frac{1}{8C_1^{\,2}D_1}\left(\frac{K_1^{\,2}}{C_2}-\frac{1}{D_1}\right) \qquad (6.45)$$

also with $x_3 = 0$

This completes the derivation of the third-ordered corrections. Before discussing the results, however, the procedure for deriving the approximate fourth- and fifth-order corrections will be outlined and the results given.

Throughout the preceding work a symmetry between the results for the two channels has been obvious. This symmetry makes it unnecessary to explicitly consider the derivation of the corrections for one channel; they can be obtained by inspection. In making fourth and fifth-order corrections it will be assumed that the lower-order corrections are independent, and can be assumed to be made before deriving the fourth and fifth order error terms. Additional corrections will be made to (referring to Figure 6.3);

The input transformers, and the first and second admittance inverters of each filter (fourth-order).

Fifth-order corrections to the third frequency-invariant susceptance of each filter.

N_1	C_1 A_1	K_1	C_2 A_2	K_2	C_3 A_3
N_2	D_1 B_1	J_1	D_2 B_2	J_2	D_3 B_3

FIGURE 6.3 Parameters of Fifth-order Corrections.

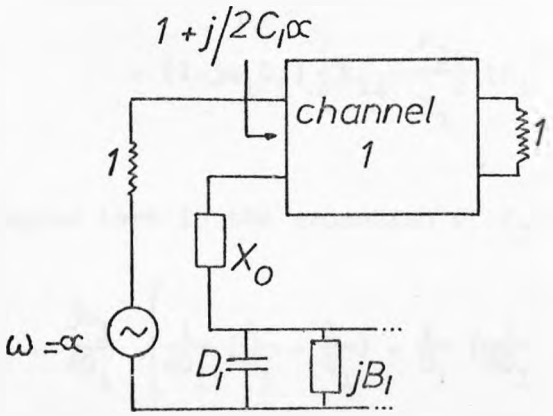

FIGURE 6.4 Calculation of Insertion-loss Increase.

Note that corrections are now made to the first three resonators of each filter, and the prototypes must therefore posses at least a third-ordered transmission zero at infinity.

Assuming the first- to third-order corrections, the fourth-degree term in the expansion of $Z_1(j[\omega_i + a])$ can be written:

$$z_{14} = n_{14} - \frac{1}{2C_1}\left\{\frac{J_1^2}{4D_1^2}\left(\frac{J_1^2}{D_2} - \frac{1}{C_1}\right) + \frac{\omega_i^2}{8D_1}\right\} - \frac{j\omega_i(1-j\omega_i C_1)}{16C_1D_1^2}$$

$$+ \frac{(1 - 2j\omega_i C_1 - \omega_i^2 C_1^2)}{16\, C_1^3 D_1}$$

$$- (1-j\omega_i C_1)\left\{k_{14} - \frac{k_{24}}{K_1^2}(K_1^2 - j\omega_i C_2 - \omega_i^2 C_1 C_2)\right\} \qquad (6.46)$$

The fourth degree term in the expansion of $Z_2(j[\omega_i+a])$ is;

$$z_4' = \frac{j\omega_i}{4D_1}\left[\frac{1}{4D_1}\left(\frac{1}{D_1} - \frac{1}{C_1}\right) - \frac{1}{D_1}\left(\frac{1}{2D_1} - \frac{3J_1^2}{4D_2}\right) + \frac{\omega_i^2}{4}\right] \qquad (6.47)$$

Inspection of (6.46) shows that there are four error terms to eliminate, in ω_i^0, ω_i, ω_i^2, ω_i^3, with only three parameters to control (n_{14}, k_{14}, k_{24}). The ω_i^0 and ω_i terms can always be nulled, and one of the ω_i^2 or ω_i^3 terms. With the element values usually met in practice, the ω_i^3 error is generally the most significant, and the following derivation therefore eliminates the ω_i^0, ω_i, and ω_i^3 terms.

The total ω_i^3 - dependent error is

$$j\omega_i^3 \frac{k_{24}}{K_1^2} C_1^2 C_2 + \frac{j\omega_i^3}{16D_1} = 0$$

$$\Rightarrow \quad k_{24} = \frac{K_1^2}{16C_1^2 C_2 D_1} \qquad (6.48)$$

Substituting for k_{24} in (6.46), the ω_i-dependent terms are

$$-\frac{j\omega_i}{16C_1D_1^2}-\frac{j\omega_i}{8C_1^2D_1}+j\omega_iC_1k_{14}+\frac{j\omega_iK_1^2}{16C_1C_2D_1}+\frac{j\omega_i}{16C_1^2D_1}$$

$$+\frac{j\omega_i}{4D_1}\;\frac{1}{4D_1}\left(\frac{1}{D_1}-\frac{1}{C_1}\right)-\frac{1}{D_1}\left(\frac{1}{2D_1}-\frac{3J_1^2}{4D_2}\right)=0$$

which after some rearrangement yields

$$k_{14}=\frac{1}{16C_1D_1}\;\frac{1}{C_1}\left(\frac{K_1^2}{C_2}-\frac{1}{C_1}-\frac{2}{D_1}\right)+\frac{1}{D_1}\left(\frac{3J_1^2}{D_2}-\frac{1}{D_1}\right)\qquad(6.49)$$

Again substituting back for k_{14} in (6.46), the ω_i^0 dependent terms yield

$$n_{14}+\frac{J_1^2}{16C_1D_1^2D_2}-\frac{1}{16C_1D_1^3}=0$$

$$n_{14}=\frac{1}{16C_1D_1^2}\left(\frac{J_1^2}{D_2}-\frac{1}{D_1}\right)\qquad(6.50)$$

The complete expression for the fifth order error terms is extremely unwieldy. To simplify the derivation, a fifth-order correction is made to only the third resonator, and only the ω_i^4 error term is eliminated. The resulting equation for the fifth-order coefficient a_{35} is

$$\frac{C_1^2C_2^2C_3a_{35}}{K_1^2K_2^2}-\frac{1}{32D_1}=0$$

$$a_{35}=\frac{K_1^2K_2^2}{32C_1^2C_2^2C_3D_1}\qquad(6.51)$$

The corresponding corrections in the other channel are found analogously, and are:

$$h_{24}=\frac{-J_1^2}{16D_1^2D_2C_1}\qquad(6.52)$$

$$h_{14}=-\frac{1}{16C_1D_1}\;\frac{1}{D_1}\left(\frac{J_1^2}{D_2}-\frac{1}{D_1}-\frac{2}{C_1}\right)+\frac{1}{C_1}\left(\frac{3K_1^2}{C_2}-\frac{1}{C_1}\right)\qquad(6.53)$$

$$n_{24} = \frac{1}{16D_1C_1^2}\left(\frac{K_1^2}{C_2} - \frac{1}{C_1}\right) \tag{6.54}$$

$$b_{35} = \frac{J_1^2 J_2^2}{32D_1^2 D_2^2 D_3 C_1} \tag{6.55}$$

6.4 Summary of Results

Combining the results of the foregoing derivation and substituting for the unknown coefficients in equation (6.9-6.17), the following set of equations results, which are the basic design equations for the bandpass channel diplexer. Equations (6.69) and (6.70) are derived in a later section, and refer to an improvement in the stopband insertion loss of each channel over the passband of the other. They are included here as they form part of the necessary design information. The formulae given below include fourth and fifth order corrections, and the element values refer to Figure 6.3.

$$X_o = \frac{1}{2\alpha}\left(\frac{1}{D_1} - \frac{1}{C_1}\right) \tag{6.56}$$

$$A_1 = -C_1\left(\alpha + \frac{1}{2C_1^2\alpha} + \frac{1}{8D_1^2C_1\alpha^3}\left[\frac{J_1^2}{D_2} - \frac{1}{C_1}\right]\right) \tag{6.57}$$

$$A_2 = -C_2\left(\alpha + \frac{K_1^2}{8C_1^2C_2D_1\alpha^3}\right) \tag{6.58}$$

$$A_3 = -C_3\left(\alpha + \frac{K_1^2K_2^2}{32C_1^2C_2^2C_3D_1\alpha^5}\right) \tag{6.59}$$

$$B_1 = D_1\left(\alpha + \frac{1}{2D_1^2\alpha} + \frac{1}{8C_1^2D_1\alpha^3}\left[\frac{K_1^2}{C_2} - \frac{1}{D_1}\right]\right) \tag{6.60}$$

$$B_2 = D_2\left(\alpha + \frac{J_1^2}{8D_1^2D_2C_1\alpha^3}\right) \tag{6.61}$$

$$B_3 = D_3\left(\alpha + \frac{J_1^2 J_2^2}{32 D_1^2 D_2^2 D_3 C_1 \alpha^5}\right) \tag{6.62}$$

$$N_1^2 = 1 + \frac{1}{4C_1\alpha^2}\left(\frac{1}{C_1} - \frac{1}{D_1}\right) - \frac{1}{16 D_1^2 C_1 \alpha^4}\left(\frac{J_1^2}{D_2} - \frac{1}{D_1}\right) \tag{6.63}$$

$$N_2^2 = 1 + \frac{1}{4D_1\alpha^2}\left(\frac{1}{D_1} - \frac{1}{C_1}\right) - \frac{1}{16 C_1^2 D_1 \alpha^4}\left(\frac{K_1^2}{C_2} - \frac{1}{C_1}\right) \tag{6.64}$$

$$K_1'^2 = K_1^2\left(1 - \frac{1}{4C_1 D_1 \alpha^2} - \frac{1}{16 C_1 D_1 \alpha^4}\left\{\frac{1}{C_1}\left[\frac{K_1^2}{C_2} - \frac{1}{C_1} - \frac{2}{D_1}\right] + \frac{1}{D_1}\left[\frac{3J_1^2}{D_2} - \frac{1}{D_1}\right]\right\}\right) \tag{6.65}$$

$$K_2'^2 = K_2^2\left(1 - \frac{K_1^2}{16 C_1^2 C_2 D_1 \alpha^4}\right) \tag{6.66}$$

$$J_1'^2 = J_1^2\left(1 - \frac{1}{4C_1 D_1 \alpha^2} - \frac{1}{16 C_1 D_1 \alpha^4}\left\{\frac{1}{D_1}\left[\frac{J_1^2}{D_2} - \frac{1}{D_1} - \frac{2}{C_1}\right] + \frac{1}{C_1}\left[\frac{3K_1^2}{C_2} - \frac{1}{C_1}\right]\right\}\right) \tag{6.67}$$

$$J_2'^2 = J_2^2\left(1 - \frac{J_1^2}{16 D_1^2 D_2 C_1 \alpha^4}\right. \tag{6.68}$$

$$\Delta L_L = 6 + 10 \log_{10}\left(1 + \frac{1}{4D_1^2\alpha^2}\right) \tag{6.69}$$

$$\Delta L_u = 6 + 10 \log_{10}\left(1 + \frac{1}{4C_1^2\alpha^2}\right) \tag{6.70}$$

6.5 Discussion of Design Equations

What effect does application of the diplexer design procedure have on the independent bandpass filter designs?

It can be seen that all even-order (in α) corrections change

the values of the input matching transformers (normally 1:1) and the coupling admittance inverters. The odd-order corrections effect the frequency-invariant susceptances of each filter, and since the odd-order correction terms are all positive, it can be seen that the main affect is to push the resonant frequencies of the first two or three resonators away from the centre frequency of the diplexer.

The design procedure forces the reflection coefficient at the diplexer input to approximate zero at the sets of real frequencies where the independent channel filter would normally have reflection zeroes: what effect does it have on the passband insertion-loss of the channels, and the return loss at the other ports?

Identifying the common port as port 1, and the channel 1 and 2 ports as 2 and 3 respectively, the effect of the modifications the design procedure generates is to force

$$\begin{aligned} \left|S_{11}(\omega_i+\alpha)\right| &= 0 + \varepsilon(\alpha^{-4}) \\ \left|S_{11}(\sigma_i-\alpha)\right| &= 0 + \varepsilon(\alpha^{-4}) \end{aligned} \qquad (6.71)$$

and thus there is to at least this degree of precision, maximum power transfer from the source to the entire network. Consider the diplexer at the frequencies $\{\omega_i+\alpha\}$: there is maximum power transfer from the source to the entire network up to the third degree in α; up to this degree in α the input impedance of channel 2 is purely reactive and thus no power enters channel 2; therefore to the same degree of approximation there is maximum power transfer into channel 1. Also, the network N1 is entirely lossless; thus it follows that

$$\left[S_{12}(\omega_i+\alpha)\right] = 1 - \varepsilon(\alpha^{-4}) \qquad (6.72)$$

$$\left[S_{22}(\omega_i+\alpha)\right] = 0 + \varepsilon(\alpha^{-4}) \qquad (6.73)$$

and analôgously for channel 2 at $\{\sigma_i-\alpha\}$. Thus the design procedure

optimises the common-port and the other port return losses, and the passband insertion loss of each channel, simultaneously and automatically.

In addition, the diplexing of the filters combined with the modifications produces a significant <u>increase</u> in the stopband insertion loss of each channel over the passband of the other. To calculate the approximate magnitude of this increase, consider the circuit of Figure 6.4. This shows the first-order equivalent circuit of the diplexer input near the centre of the passband of channel 1. If the channels are sufficiently separated, the contribution of D_1 to the insertion loss of channel 2 can be found approximately by simple potential-divider theory. On this basis, the contribution of D_1 is given by

$$L_D(j[\omega_i+\alpha]) = \frac{-(\frac{j}{2D_1\alpha})}{1 + 1 + \frac{jC_1}{\alpha} \cdot \frac{1}{2C_1^2} + \frac{j}{2\alpha}(\frac{1}{D_1} - \frac{1}{C_1}) - \frac{j}{2D_1\alpha}}$$

$$= \frac{-j}{4D_1\alpha}$$

$$\therefore |L_D|^2 = \frac{1}{16D_1^2\alpha^2}$$

In isolation, at the same frequency (2α) the contribution of D_1 is given by

$$L_D' = \frac{-\frac{j}{2D_1\alpha}}{1 - \frac{j}{2D_1\alpha}}$$

$$\therefore |L_D'|^2 = \frac{1}{4D_1^2\alpha^2 + 1}$$

The ratio

$$\left|\frac{L_D}{L_D'}\right|^2 = \frac{4D_1^2\alpha^2 + 1}{16D_1^2\alpha^2}$$

and, expressed in decibels, this is the increase in insertion loss required, of channel 2 over the passband of channel 1. A similar argument follows for channel 1 over the passband of channel 2. Thus

$$\Delta L_L = 6 + 10 \log_{10} \left(1 + \frac{1}{4D_1^2\alpha^2}\right) \qquad (6.74)$$

and similarly

$$\Delta L_U = 6 + 10 \log_{10} \left(1 + \frac{1}{4C_1^2\alpha^2}\right) \qquad (6.75)$$

The estimate of the increase given by (6.74) and (6.75) is asymptotically correct in the limit as $\alpha \to \infty$, when the increase is 6 dB. For normal values of α, the actual increase is larger, typically by about 0.5-2 dB, so these equations give a conservative estimate. The additional increase is due to higher-order interactions. This increase in stopband attenuation is most worthwhile, and may allow a saving of degree to meet a given specification, with the benefit of reduced dissipation loss in a practical diplexer.

6.6 Performance of Prototype Diplexers

To investigate the performance available using the new design method, a computer program has been written (Appendix 2) which designs prototype diplexers using Chebyshev channel filters and analyses the resulting design.

Figure 6.5(a)-(c) shows the response of a diplexer with the following specification:

	Bandwidth	Centre Frequency	Degree
Channel 1	2 rads/sec	1.5 rads/sec	5
Channel 2	2 rads/sec	-1.5 rads/sec	5

The original return-loss specification of the channels was 26 dB. This example is also considered in [6.1].

Figure 6.5(a) shows (full line) the common-port return loss over

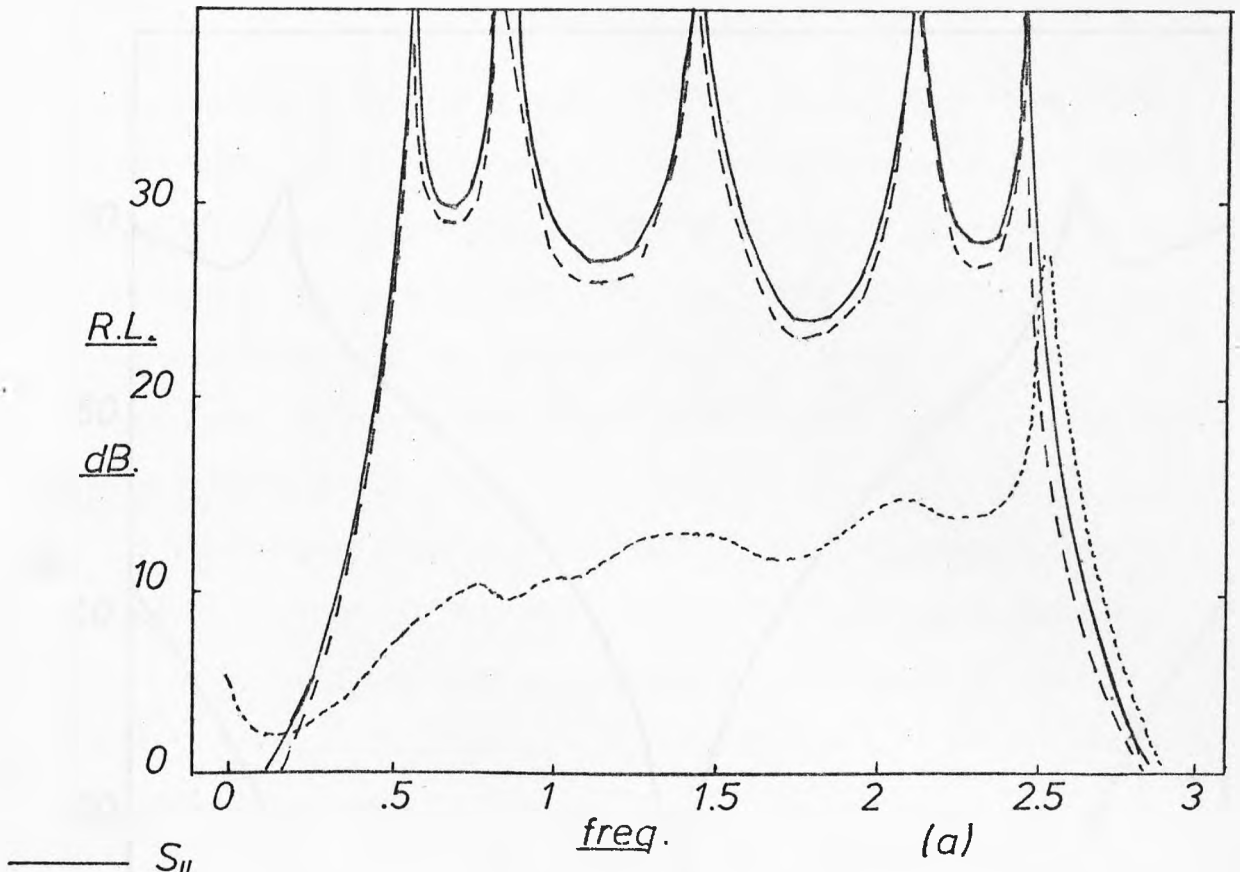

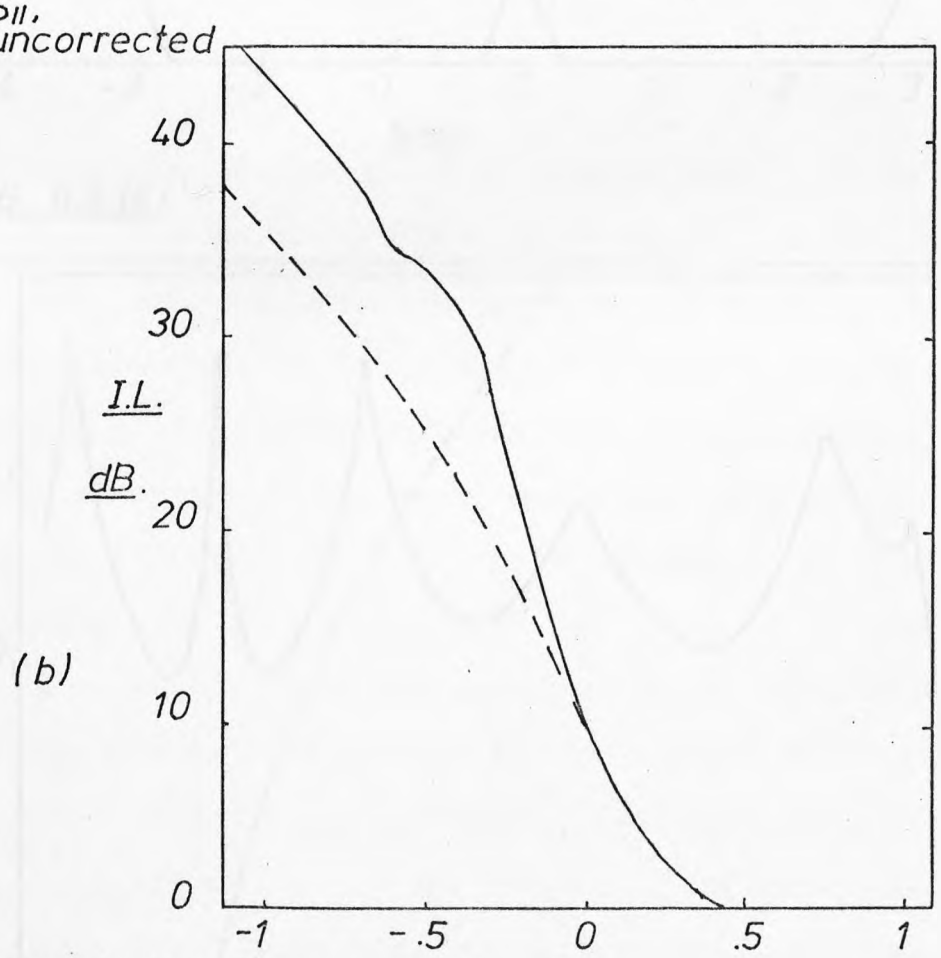

FIGURE 6.5 Response - Ex. I.

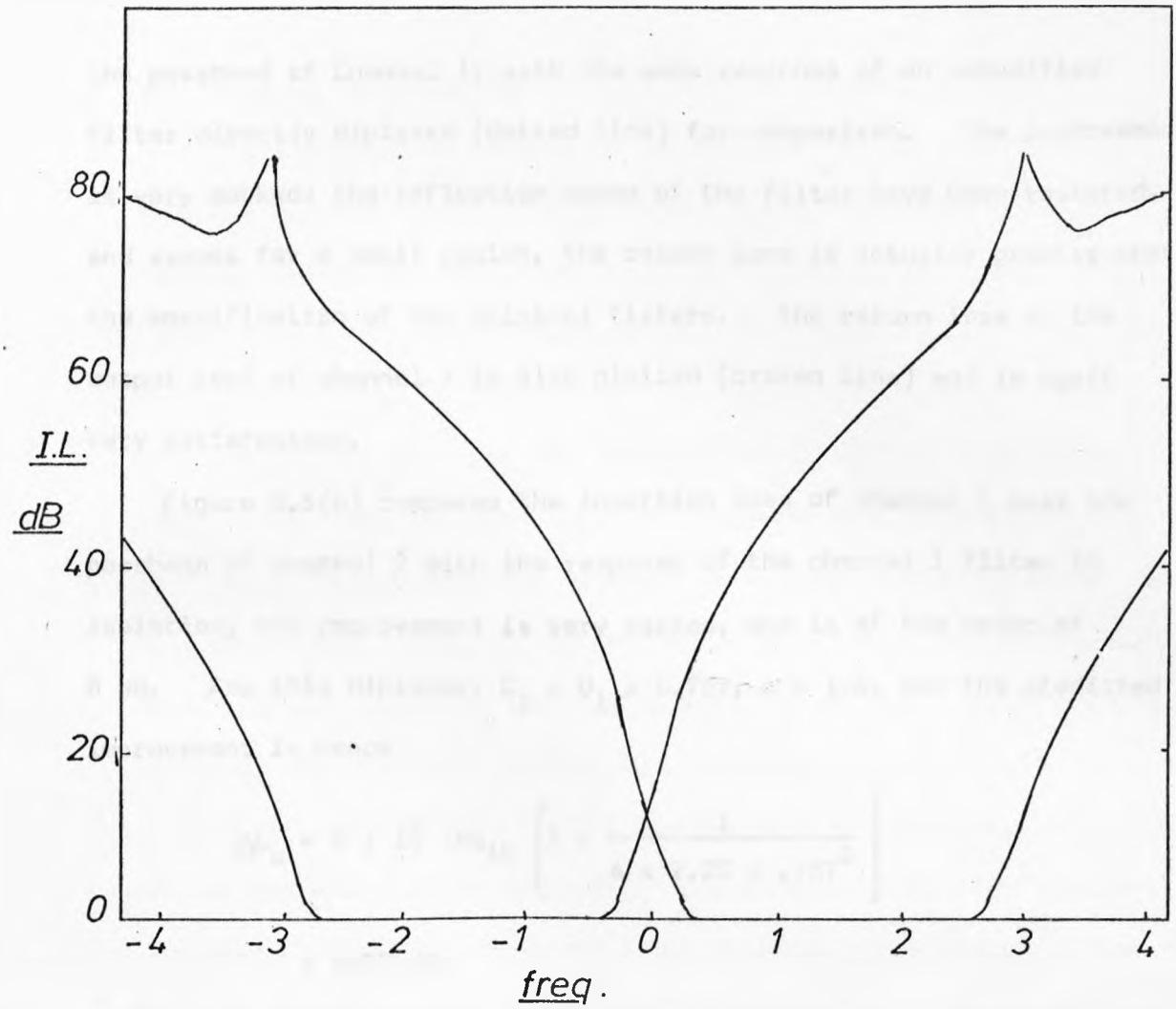

FIG. 6.5 (c)

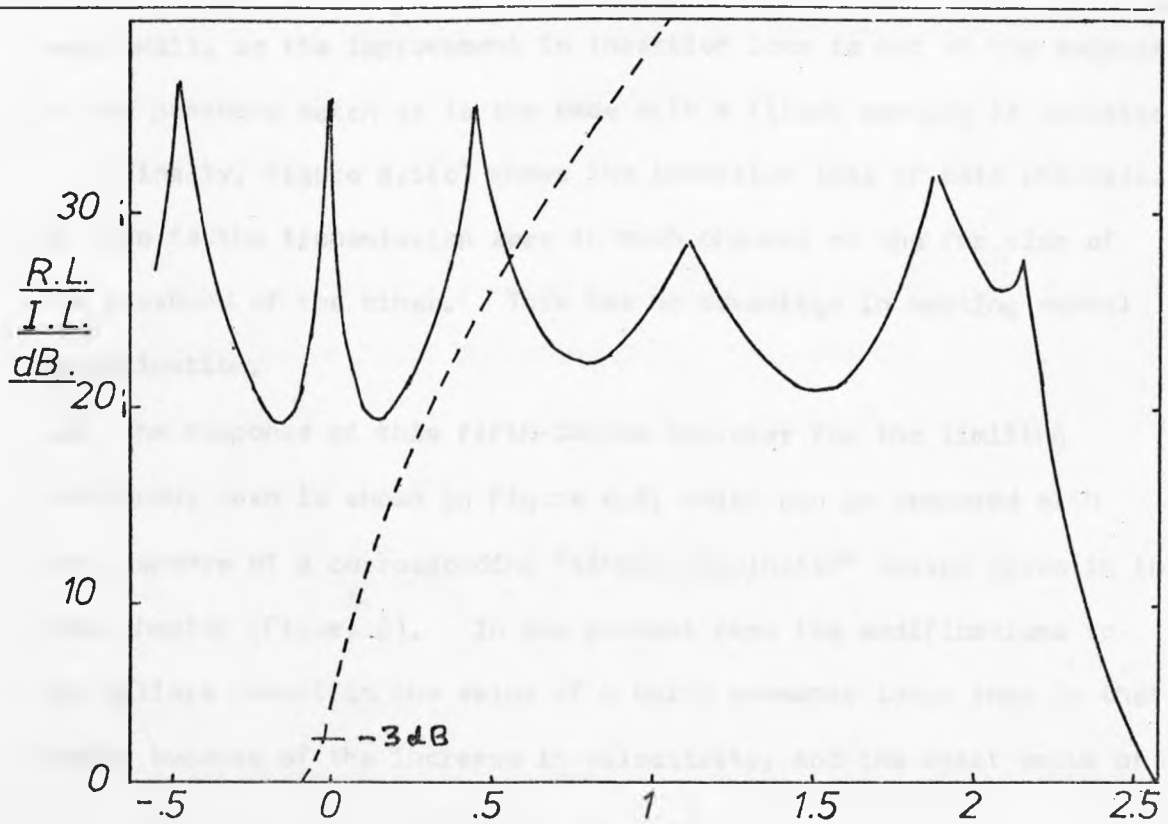

FIGURE 6.6 Response-Ex.II.

the passband of Channel 1, with the same response of an unmodified filter directly diplexed (dotted line) for comparison. The improvement is very marked: the reflection zeros of the filter have been restored, and except for a small region, the return loss is actually greater than the specification of the original filters. The return loss at the output port of channel 1 is also plotted (broken line) and is again very satisfactory.

Figure 6.5(b) compares the insertion loss of channel 1 over the passband of channel 2 with the response of the channel 1 filter in isolation; the improvement is very marked, and is of the order of 8 dB. For this diplexer, $C_1 = D_1 = 0.767$, $\alpha = 1.5$, and the predicted improvement is hence

$$\Delta L_u = 6 + 10 \log_{10} \left[1 + \frac{1}{4 \times 2.25 \times .767^2} \right]$$

$$= 6.75 \text{ dB}$$

which is an under-estimate of the actual improvement. It can be seen that the degradation of the return loss of channel 1 in the passband is very small, so the improvement in insertion loss is not at the expense of the passband match as is the case with a filter working in isolation.

Finally, Figure 6.5(c) shows the insertion loss of both channels. Of note is the transmission zero in each channel at the far side of the passband of the other. This has no advantage in meeting normal specification.

II The response of this fifth-degree diplexer for the limiting contiguous case is shown in Figure 6.6, which can be compared with the response of a corresponding "singly terminated" design given in the last chapter (Figure 5). In the present case the modifications to the filters result in the value of α being somewhat lower than in that design because of the increase in selectivity, and the exact value of α

was found by trial and error to be 1.2 (as compared with 1.067).

The return-loss performance of the diplexer is clearly acceptable and thus the new design technique is a viable alternative to the "singly terminated" design even for the limiting contiguous case. However, it may be noted that, because the channel filters are based on doubly-terminated prototypes, the increase in stopband insertion loss of each channel over the passband of the other is considerably less. The computed value is 9 dB, compared with a theoretical value of 7.17 dB (Equation 6.75), whereas the singly terminated design gave 16.2 dB. This should be considered in the context of the argument developed in Chatper 5, that contiguous designs will frequently not be necessary where non-contiguous design methods are available.

When the bandwidths of the two channels are unequal, the performance of the diplexer suffers because of the unequal interactions between the channels. This can be corrected by increasing the degree of the broader channel, hence increasing its selectivity. One criterion for this is to increase the degree until the insertion losses of each channel at the passband edge of the other are equal, but it has been found that best results are obtained by iteration, testing different designs using a computer analysis program to obtain the desired response.

The next two examples give the prototype responses of the waveguide diplexers fully described in the next chapter.

Figure 6.7 shows the responses of a diplexer to the following specification:

III	Bandwidth (Rads/sec)	Degree	Centre Frequency (Rads/sec)	Return-Loss (dB)
Channel 1	2.0	3	-2.5	26
Channel 2	4.0	7	+2.5	27.31

Here the degree and ripple-level of channel 2 have been chosen so that

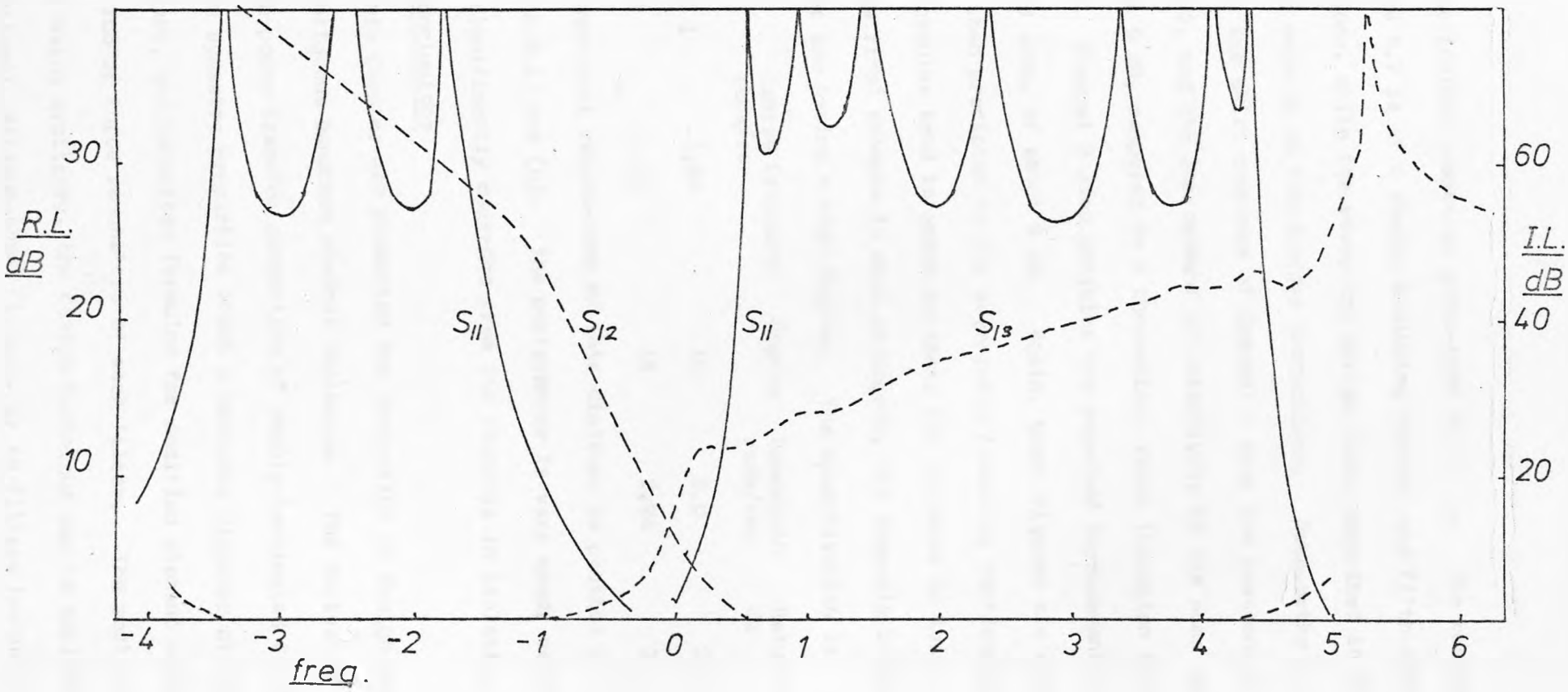

FIGURE 6.7 Response - Ex. III .

the insertionloss responses cross-over at $\omega = 0$. The response shown in Figure 6.7 is of a design including fourth- and fifth-order corrections, while the waveguide design (also described in [6.2]) included only up to third-order corrections. Noteworthy are the kinks in the skirt response of Channel 1 over the passband of Channel 2, and the improvement in selectivity in the same region, which is about 9 dB, compared to a theoretical value (Equation 6.75) of 6.4 dB. Channel 2 also exhibits the expected improvement in its stopband loss, of about 8 dB. Again, these figures are somewhat larger than predicted by the asymptotic formulae, confirming that these formulae tend to under-estimate the increase in loss.

The final example is more stringent, the channels being closer together and having a high degree. The specification is:

IV	Centre Frequency rads/sec	Degree	Bandwidth rads/sec	Return-Loss dB
Channel 1	-1.59	15	2.0	22
Channel	+1.59	15	2.94	22

The common-port return-loss of this diplexer is plotted in Figure 6.8(a) and (b). The performance is very good, neither channel being significantly degraded from its response in isolation.

6.7 Conclusions

This Chapter has presented the derivation of design equations for non-contiguous bandpass channel diplexers. The derivation depends on certain power transfer properties of doubly-terminated filters, and certain symmetry properties which a bandpass diplexer prototype possesses, and generates formulae for modified element values in the first two or three resonators of each filter. The rest of the filter being arbitrary, the design technique can be applied to conventional, minimum-phase filters, or to filters having linear-phase response.

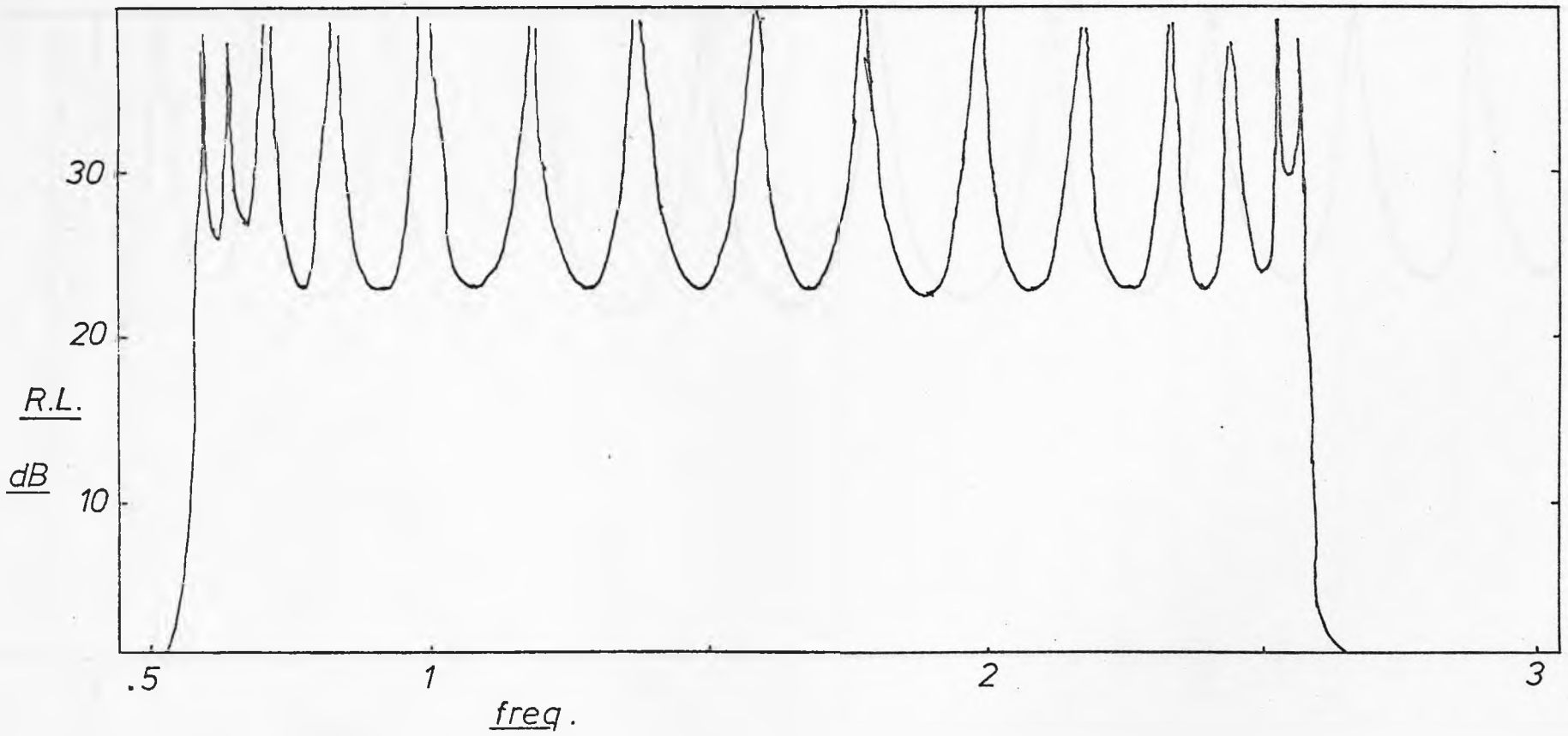

FIGURE 6.8 Response -Ex. IV. (a)

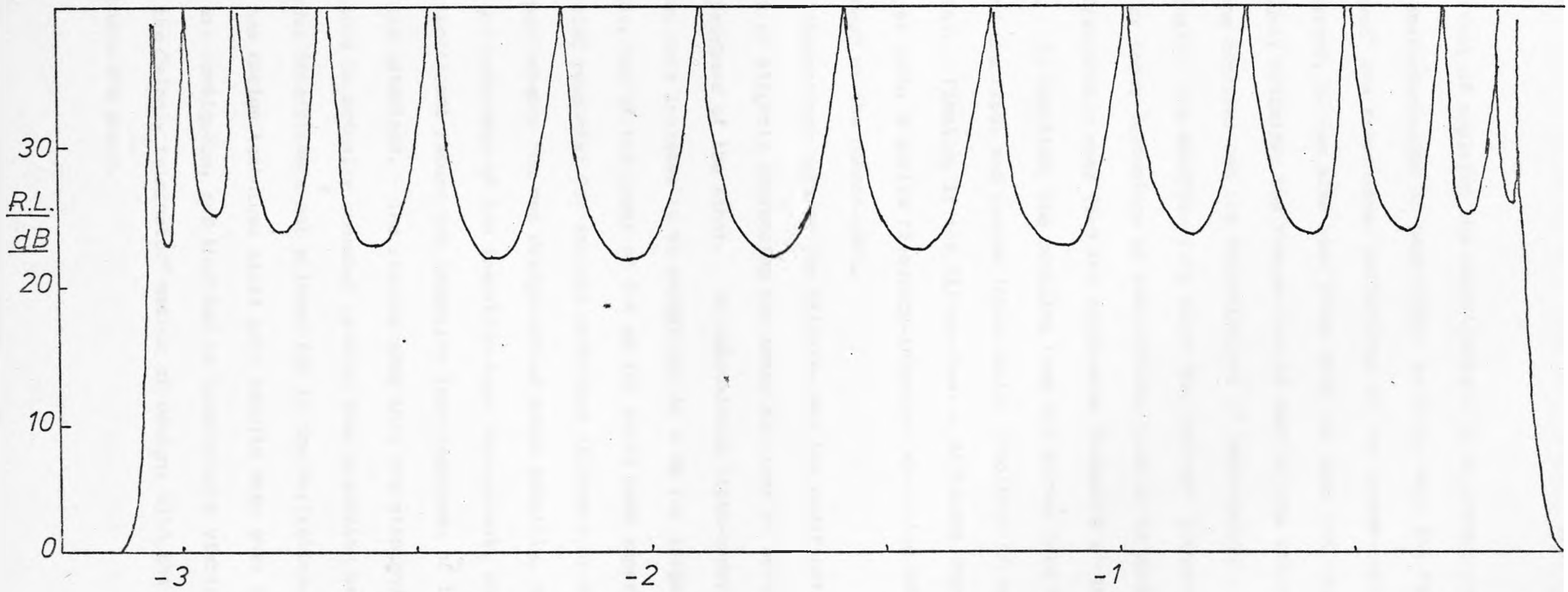

FIGURE 6.8 (b)

The effect of applying the modifications is to change the input impedance characteristics of each filter so that, when the filters are "diplexed" the return-loss performance at the common-port is optimised. However, it has also been shown that the same procedure simultaneously optimises the return-loss at each of the other two ports of the diplexer and the insertionloss of each channel.

Physically, the modifications alter the resonant frequencies of the first two or three resonators of each filter, such as to push the resonant frequencies away from the cross-over frequency of the diplexer responses. In addition, the coupling from the source into the first cavity, and the first and second inter-cavity couplings of each filter are modified. Finally, if the filters have a different degree or bandwidth or both, a series frequency-invariant annulling susceptance is introduced at the common-port.

The interactions between the filters, and the modifications, have the effect of slightly increasing the insertion loss of each filter over the passband of the other. An approximate first-order calculation shows this increase to be asymptotic to 6 dB for large band separations, and of the order of 7-8 dB for small band separations.

Computed responses for several prototype diplexers have shown the high performance the new design method makes possible, and confirms the existence of the insertion-loss improvement, and that all the significant return and insertion loss responses of the diplexer are optimised. The results show that the stopband insertion-loss increase is actually somewhat greater than predicted because of second-order interation s not allowed for in the derivation.

The new design technique gives good results even when the diplexer channels are contiguous, and thus can be considered a viable alternative to the "singly terminated" method of design, with the advantage of directness and speed.

CHAPTER 7. Design and Performance of Experimental Waveguide Diplexers.

7.1 Introduction

This chapter briefly describes the application of the new theory developed in the last chapter to the design of real diplexers using direct-coupled cavity waveguide filters. Rhodes [6·1] has reported successful results for a symmetrical diplexer: here the theory is applied to two asymmetric designs. One is a very narrow band diplexer around 5.8Ghz, the other a broad-band design between 7.25 and 8.4Ghz.

7.2 General Design Principles.

The design process for a diplexer begins with a specification which defines the band edges of the channels or their band centres and bandwidths, the selectivity and the insertion- or return-loss ripple. From the latter, the degree needed can be calculated, bearing in mind the improvement in insertion-loss experienced when filters are diplexed. The design equations derived in the last chapter were given in terms of a prototype diplexer, and the prototype has to be related to the real bandpass filters. This is very easy to do for narrow-band diplexers.

Consider the channels of a diplexer shown in figure 7·1(a), which defines the centre frequencies and bandwidths. The degree and ripple factors have been for the moment ignored; it is assumed that suitable low-pass prototypes are available.

Now, this channel layout has to be related to the prototype channel layout shown in figure 7·1(b). Here, the band separation is "2α", and the bandwidth of the upper

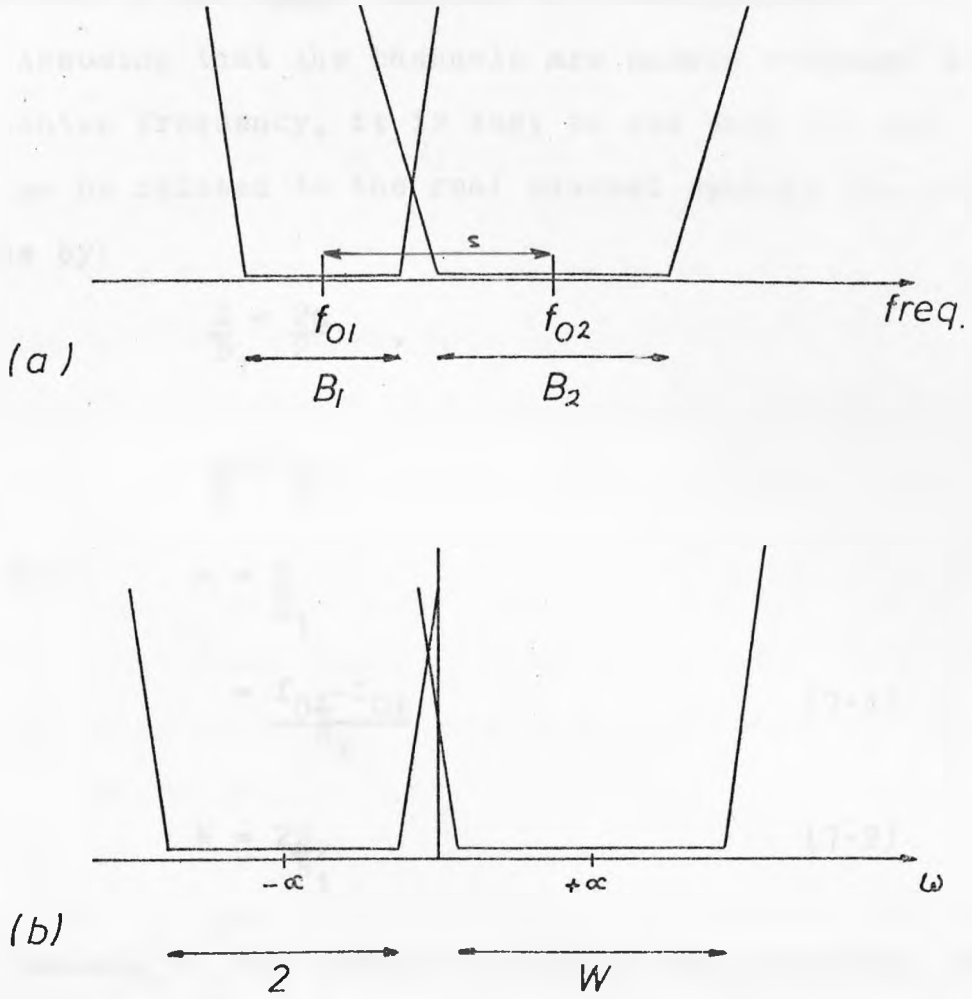

FIGURE 7.1 Relating 'Real' and 'Prototype' Diplexer Responses.

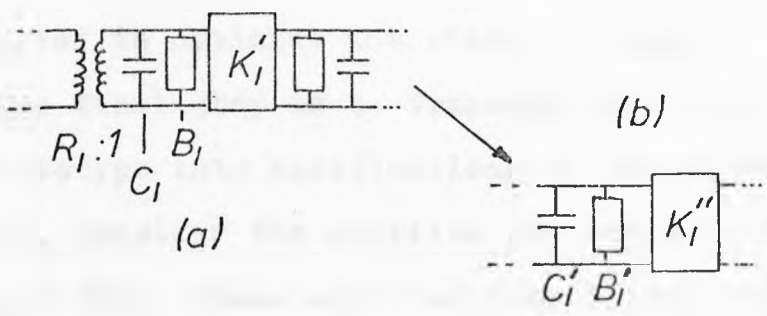

FIGURE 7.2 Absorbing Input Transformer.

channel is "W". It is convenient to assume that the bandwidth of the lower channel is 2 radians/sec.

Assuming that the channels are narrow compared to the centre frequency, it is easy to see that "αc" and "W" can be related to the real channel spacing and bandwidths by:

$$\frac{S}{B_1} = \frac{2\alpha c}{2} \quad ,$$

$$\frac{W}{2} = \frac{B_2}{B_1}$$

and thus

$$\alpha = \frac{S}{B_1}$$

$$= \frac{f_{02} - f_{01}}{B_1} \qquad (7\cdot1)$$

$$W = \frac{2B_2}{B_1} \qquad (7\cdot2)$$

Knowing W, the element values in the prototype for the lower channel can be scaled accordingly, so that the lower channel of the prototype diplexer has a bandwidth W. The design formulae given in the last chapter can now be applied to optimise the element values.

The final step is to translate the modifications to the prototype into modifications of the actual bandpass filters. Consider the modified prototype filter shown in figure 7·2(a). Since most bandpass filter design procedures are given in terms of the prototype capacitors and admittance inverters, it is perhaps simplest to eliminate the input transformer by scaling it into the first admittance inverter, to give the circuit of figure 7.2(b), with

$$C_1' = \frac{C_1}{1+r(\alpha)}$$

$$B_1' = \frac{B_1}{1+r(\alpha)} \qquad (7\cdot3)$$

$$K_1'' = K_1' / \sqrt{1+r(\alpha)} \qquad (7\cdot4)$$

Turning now to the frequency-invariant susceptances in the prototype diplexer, these could be realised through the reactance-slope technique discussed in chapter 3. However, it is simplest to allow for them by a direct perturbation of the resonant frequencies of the first three resonators.

Consider the r'th shunt capacitor and its associated frequency-invariant susceptance of one of the filters in the prototype diplexer. From chapter 6, the susceptance of the combination is

$$B_r = \omega C_r - C_r(\alpha + \delta(\alpha))$$

where $\delta(\alpha)$ represents the modifications made to the susceptance. The resonant frequency of the combination occurs when its susceptance is zero, that is when

$$\omega = \alpha + \delta(\alpha)$$

Thus the shift in the resonant frequency is just $\delta(\alpha)$. In order to apply this shift to the real bandpass filter this shift has to be related to the channel separation. It is clear that the actual shift in the resonant frequency of the corresponding resonator is

$$\delta' = \frac{\delta(\alpha)}{2\alpha} \cdot S \qquad (7\cdot5)$$

where s is again the channel separation. This procedure is valid as long as the reactance slope of the bandpass resonators is nearly constant over the total band of the diplexer. This is true, in particular, for waveguide resonators over a fairly broad band.

7.3 A Narrow-Band Waveguide Diplexer.

The initial specification of this diplexer is given below.

	Return-loss Ripple (dB)	Degree	Centre frequency (Ghz)	Bandwidth (Mhz)
Channel 1	26	3	5·975	20
Channel 2	27·31	7	6·025	40

The different degrees and return loss levels of the channels were chosen so that the insertion-loss responses of the filters should cross-over at 6 Ghz.

Applying (7·1) and (7.2),

$$\alpha = \frac{(6\cdot025-5.975).10^3}{20}$$

$$= 2\cdot5$$

$$W = \frac{2x40}{20}$$

$$= 4$$

Thus this example corresponds to the third case analysed in chapter 6, and the corresponding prototype performance was plotted in figure 6·7. However, the waveguide diplexer was designed before the approximate fourth and fifth order corrections were worked out, and incorporated only up to third-order corrections.

Figure 7.3 snows the waveguide diplexer, made in waveguide WG14 (WR137). The series connection of the filters was made with a simple H-plane Tee-junction. The filters themselves used single posts for the input and output couplings, and triple posts for the internal couplings. Tuning screws were located at the centre of each cavity. The design procedure used was essentially that given in chapter 4, but using the lumped-element prototype since the bandwidth was very narrow. The modifications were incorporated into the waveguide structure as described in section 7·2, except that the resonant frequency correct-

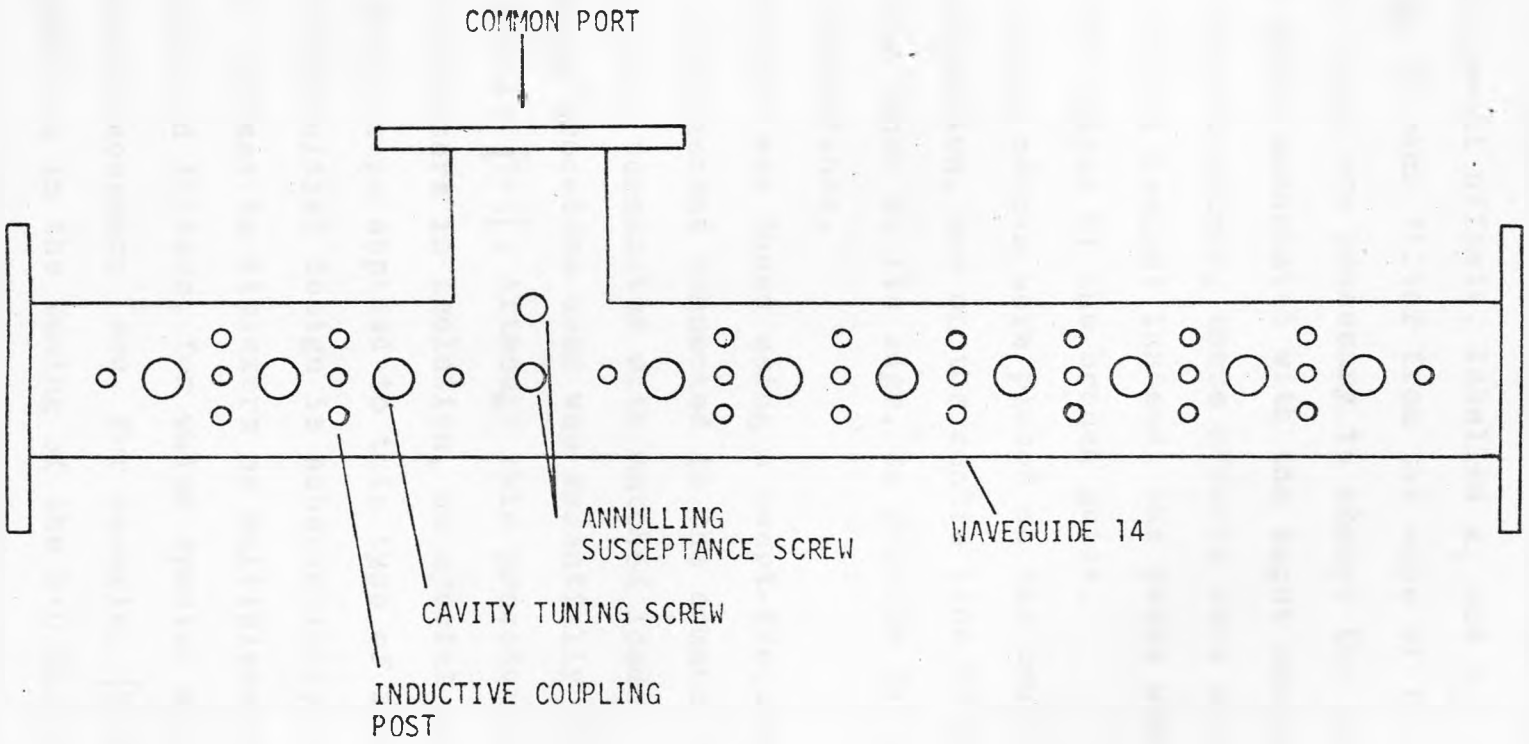

FIGURE 7.3 Construction of Waveguide Diplexer.

ions, being very small, were not explicitly allowed for but taken up by the tuning screws.

Figure 7·4 shows a "close-up" of the Tee-junction. It shows the small offsets, labelled x_1 and x_2, of the first couplings of each filter from the edge of the branch wave guide. These are necessary to absorb the negative lengths of guide associated with the input admittance inverters. Unfortunately, these offsets were not included in the initial design! Instead, the posts were placed level with the edges of the branch guide.

Large tuning screws were placed on the centre line of the Tee-junction, one on the centre line of the main guide and the other at its edge, to provide the junction annulling susceptance.

The diplexer was tuned using a swept-frequency reflectometer arrangement connected to the common port. The other ports were terminated with matched loads.

The tuning procedure used was essentially that described by Dishal [7·1]. Although this procedure is really intended for filters in isolation, no special difficulties arise when it is applied to this type of diplexer as long as the initial design is substantially correct. This is in contrast to diplexers or multiplexers using singly-terminated filters, for which special alignment procedures are necessary (see, for example, [5·60]).

Very early on in the tuning of the 6·0 Ghz. diplexer it was found that the filters interacted in a peculiar way, the resonant frequencies of the first cavity of the two filters being interdependent. Careful investigation of the phase of the reflection coefficient using a Hewlett-Packard network analyser indicated that this seemed to be because the negative lengths of guide at the

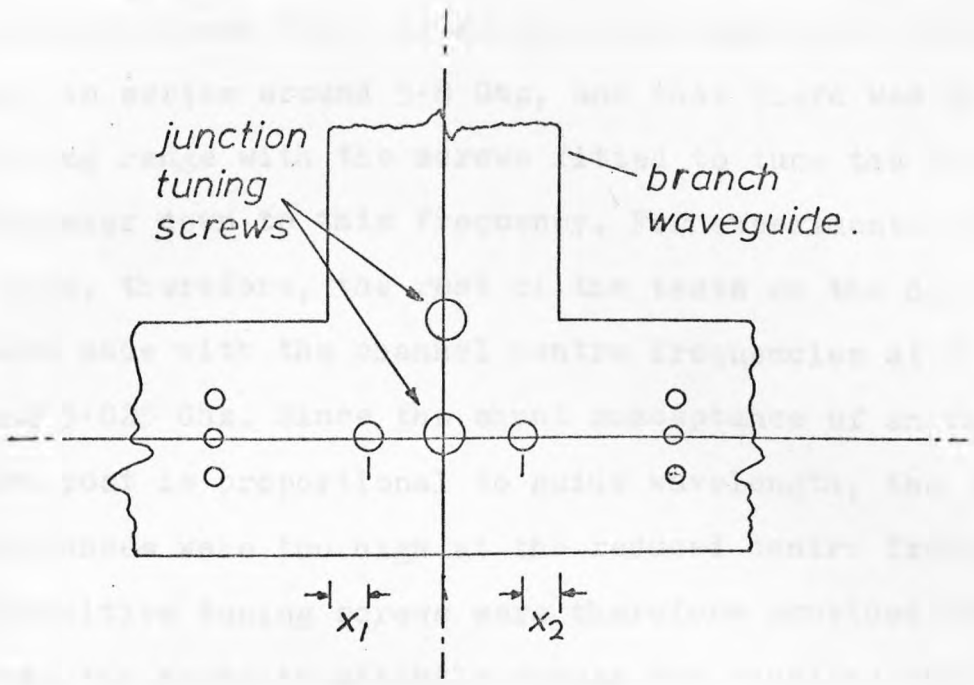

FIGURE 7.4 'Close-Up' of Tee-Junction.

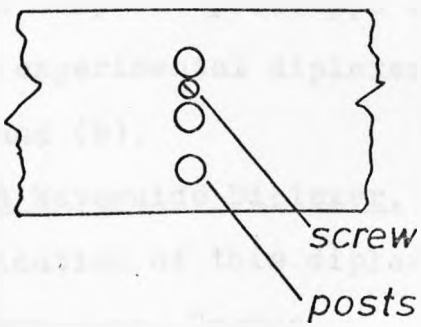

FIGURE 7.5 Reducing Iris Susceptances.

filter inputs had not been allowed for. Further investigation showed that the filters did seem to be effectively in series around 5·8 Ghz, and that there was enough tuning range with the screws fitted to tune the entire diplexer down to this frequency. For experimental purposes, therefore, the rest of the tests on the diplexer were made with the channel centre frequencies at 5·775 and 5·825 Ghz. Since the shunt susceptance of an inductive post is proportional to guide wavelength, the susceptances were too high at the reduced centre frequency. Capacitive tuning screws were therefore provided between the posts to slightly reduce the coupling susceptances (figure 7.5).

With these modifications, the diplexer proved relatively easy to tune, and gave performance gratifyingly close to the computed prototype response. The performance of the experimental diplexer is plotted in figure 7·6(a) and (b).

7·4 A Broadband Waveguide Diplexer.

The specification of this diplexer is given below.

	Return-loss Ripple (dB)	Degree	Bandedges (Ghz.) Lower	Upper
Channel 1	22	15	7·25	7·75
Channel 2	22	15	7.9	8.4

Waveguide: WG15 (WR112).

Since the channels are rather wide, the band edges have to be found in terms of guide wavelength to determine W and α. Also, the individual filters have to be based on distributed rather than lumped prototypes. This introduces an interesting problem, since the original design equations werederived for filters whose input impedances could be described as continued fractions in their

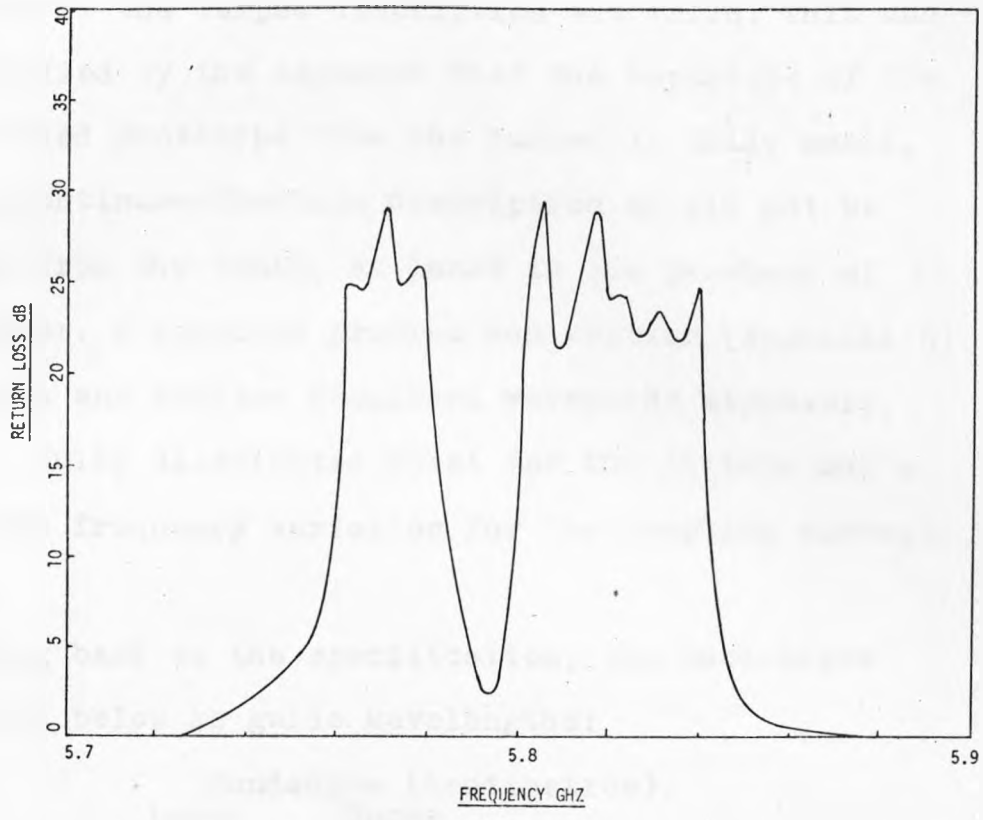

(a)

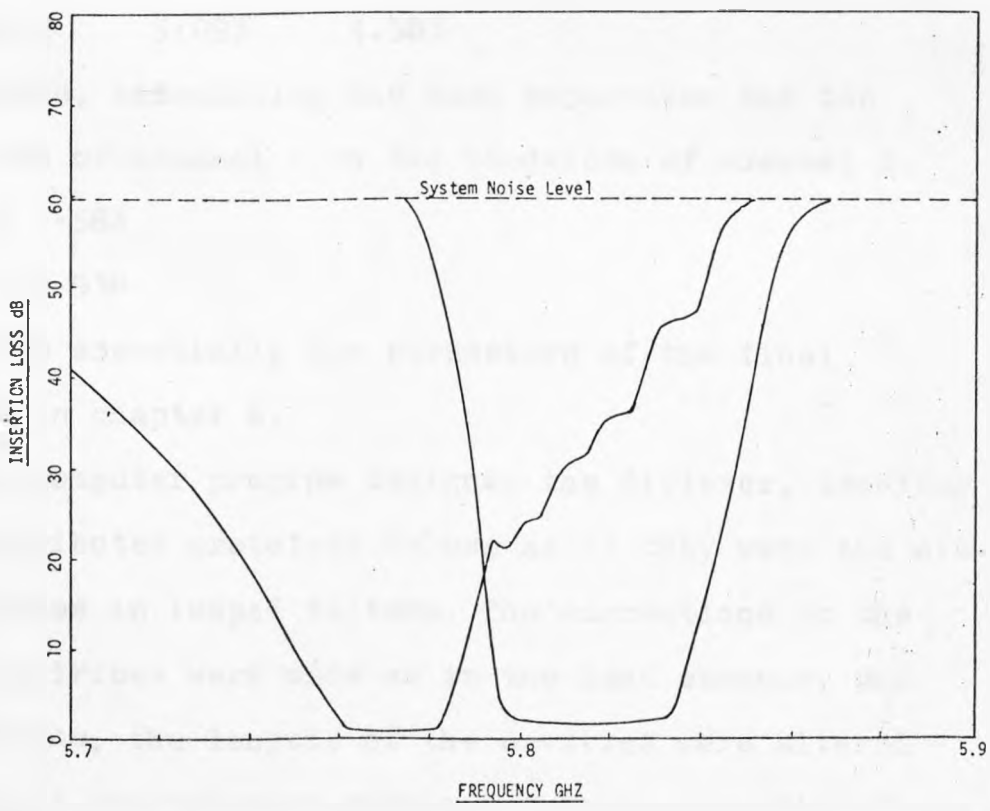

(b)

FIGURE 7.6 Response of the waveguide diplexer. (a) Return loss. (b) Insertion loss.

element values. This is not the case for distributed filters, but it was decided to try designing the diplexer as if the lumped description was valid. This can be justified by the argument that the departure of the distributed prototype from the lumped is faily small, so the continued-fraction description should not be too far from the truth, at least in the passband of the filter. A computer program was written (Appendix 6) to design and analyse broadband waveguide diplexers, using a fully distributed model for the filters and a realistic frequency variation for the coupling susceptances.

Going back to the specification, the band-edges are given below as guide wavelengths:

	Bandedges (centimetres). Lower	Upper
Channel 1	6·018	5·274
Channel 2	5·093	4.583

From these, normalising the band separation and the bandwidth of channel 1 to the bandwidth of channel 2,

$\alpha = 1{\cdot}584$

$W = 2{\cdot}918$

These are essentially the parameters of the final example in chapter 6.

The computer program designed the diplexer, treating the distributed prototype values as if they were the element values in lumped filters. The corrections to the coupling irises were made as in the last example, and in addition, the lengths of the cavities were altered to produce the relative resonant frequency shifts. For the computation of the performance, it was assumed that the cavities could be treated as simple lengths of trans-

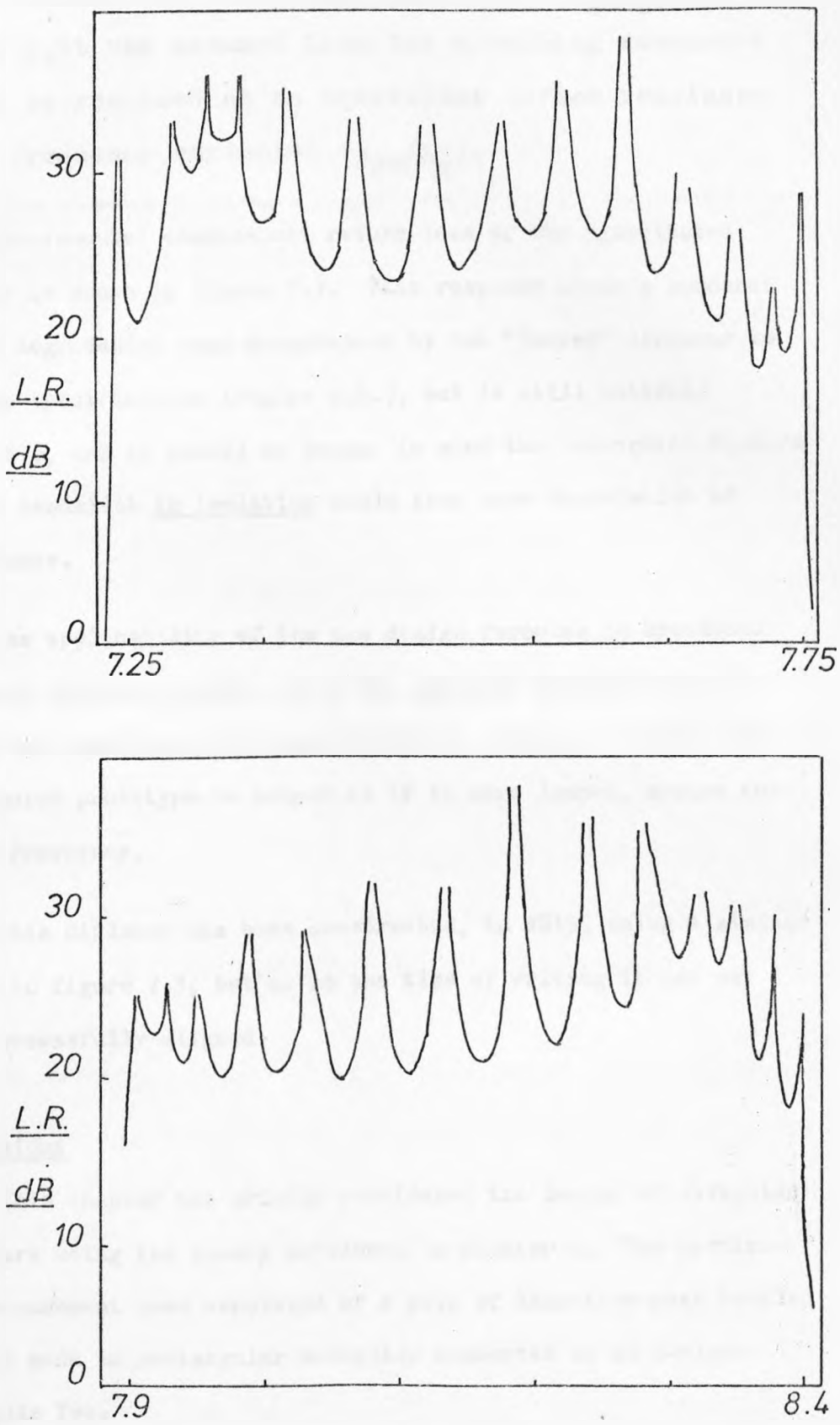

FIGURE 7.7 Broadband Waveguide Diplexer Response .

The computed common-port return loss of the distributed diplexer is shown in figure 7.7. This response shows a someshat greater degradation than experienced by the "lumped" diplexer to the same specification (figure 6.8.), but is still entirely acceptable, and it should be borne in mind that waveguide filters of this bandwidth in isolation would show some degradation of performance.

The applicability of the new design formulas to broadband waveguide diplexers arises since the explicit formular used to design the broadband prototypes themselves attempt to force the distributed prototype to behave as if it were lumped, around the centre frequency.

This diplexer has been constructed, in WG15, using a similar layout to figure 7.3, but up to the time of writing it has not been successfully aligned.

7.5 Conclusions

This chapter has briefly considered the design of waveguide diplexers using tne theory developed in chapter 6. The particular arrangement used consisted of a pair of inductive-post coupled filters made in rectangular waveguide connected by an H-plane waveguide Tee.

After an initial design error had been allowed for, a narrow-band diplexer gave excellent performance, con -

mission line, and the coupling posts as inductive susceptances with frequency variation (λ_g/λ_{g0}). Finally, it was assumed that the annulling reactance could be realised as an equivalent series reactance with frequency variation (λ_{g0}/λ_g).

The computed common-port return-loss response of the distributed diplexer is plotted in figure 7·7. Not only is this response acceptable, but considering that the design theory should not strictly apply to the distributed diplexer, it is remarkable.

This diplexer has been built in WG15 using the same layout as the narrow band diplexer, but making allowance for the negative length of guide at the inputs of the filters. Up to the time of writing, it has not been possible to tune up this diplexer correctly. However, from the experience gained with it so far, it seems that the filters are interacting in the right way and the main problem is to get the filters aligned. It is well-known that broadband waveguide filters are much more difficult to tune than narrow-band types.

7·5 Conclusions.

This chapter has briefly considered the design of waveguide diplexers with the theory developed in chapter 6. The particular arrangement used consisted of a pair of inductive-post coupled filters made in rectangular waveguide connected together by an H-plane waveguide Tee. This is a convenient arrangement for experimental purposes, but may not be convenient in a practical application.

After an initial design error had been allowed for, a narrow-band diplexer gave excellent performance, con-

sistent with theoretical predictions. With the results already obtained by Rhodes [6·1], this indicates that the direct design of narrow-band diplexers can be regarded as routine.

The design theory has also been applied to broadband waveguide diplexers. The theoretical basis of the method would indicate that it should not strictly apply to such diplexers as they must be designed from a distributed prototype while the theory assumes a lumped one. Nevertheless, the computed response shows that the method should be capable of excellent results even for broadband diplexers. It has not yet been possible to confirm this with experimental results.

ADDENDA

1. Table 1 gives the prototype values for the narrow-band waveguide diplexer. From these values, the relative significance of the modifications to the cavity resonant frequencies will be assessed. Considering the l.f. channel filter first, only the first two cavities were modified (only up to third-order corrections being made). Thus comparing B_1 and B_3 indicates the shift of the first cavity resonance, which is seen to be at

$$-2.5 \times \frac{1.907}{1.601} = -2.98 \text{ rads/sec.}$$

Thus the resonance has been shifted away from the diplexer's centre frequency by about 10% of the band separation or 25% of the filter's bandwidth. Similarly, it can be shown that the second cavity resonance is shifted away from the diplexer centre frequency by approximately 2.5% of the band separation.

For the high frequency channel filter, comparing A_1 with A_7, the first cavity resonant frequency is shifted from +2.5 to +3.76 rads/sec., a shift of 25% of the channel separation and 32% of the fitler's bandwidth. The second resonant frequency is shifted upward in frequency by 12% of the band separation.

Table 2 gives the normalised coupling susceptance required in the waveguide realisation of the diplexer. Comparing the input (i.e. common-port) and output (un-modified) susceptances of the l.f. filter, the input coupling susceptance B_{01}, has been increased by 3.5%, while the greatest change is to the first inter-resonator coupling, B_{12}, which in increased by 9.2%.

For the h.f. channel, the first coupling susceptance has been decreased by 5%, and the first inter-resonator coupling susceptance increased by 9%. The input coupling susceptance of the two filters behave differently because of the asymmetry of the diplexer. If the channels and filters were symmetrical both susceptances would be equally modified.

In this narrowband diplexer the resonant frequency corrections were small compared to the centre frequency and made by adjustment of the cavity tuning screws. The modifications to the coupling susceptances were substantial and had to be allowed for in the physical design of the coupling posts.

2. The difficulties with the electrical characterisation of the Tee-junction of the filters in the narrow-band diplexer were not adequately resolved. An experimental approach was used to investigate the junction properties and determine a centre frequency for the diplexer around which the filters interacted correctly. For design purposes though, a theoretical characterisation is necessary.

In the experimental approach, a network analyser was set up to obtain a swept-frequency display of the common-port reflection-coefficient phase of the diplexer over the frequency range of interest (Figure 7.8). All the cavities of each filter were completely detuned except for the first cavity of each. Each of these cavities then produced its own "kink" in the phase display, as shown in figure 7.9. If the filters are effectively connected in series at the common-port, each kink can be tuned independantly

of the other as the resonances of the two cavities are then essentially uncoupled. With the diplexer, it was found that the cavity tunings interacted severely around 6 GHz, but that the resonances were independent around 5.8 GHz, over a band large enough to cover the filter passbands. 5.8 GHz was therefore chosen as the diplexer centre freqneucy.

LOWER CHANNEL	
N_2	0.9674
D_1	0.6402
B_1	1.9069
J_1'	1.0469
D_2	1.2805
B_2	3.2672
J_2'	1.1434
D_3	0.6402
B_3	1.6006

$X_0 = -0.2053$

UPPER CHANNEL.	
N_1	1.0518
C_1	0.3863
A_1	-1.4529
K_1'	1.1463
C_2	1.0825
A_2	-2.8374
K_2	1.6860
C_3	1.5642
A_3	-3.9106
K_3	1.9660
C_4	1.7362
A_4	-4.3404
K_4	1.9660
C_5	1.5642
A_5	-3.9106
K_5	1.6860
C_6	1.0825
A_6	-2.7062
K_6	1.2520
C_7	0.3863
A_7	-0.9658

TABLE 1 - MODIFIED ELEMENT VALUES FOR PROTOTYPE NARROW-BAND DIPLEXER. (SEE FIGURE 6.2).

	L.F. CHANNEL (3 CAVITY)		H.F. CHANNEL (7 CAVITY)
B_{01}	7.837	← COMMON PORT →	5.513
B_{12}	80.15		52.27
B_{23}	73.38		71.11
B_{34}	7.574		77.23
B_{45}	|		77.23
B_{56}	|		71.11
B_{67}	|		47.85
B_{78}	|		5.917

TABLE 2 - NORMALISED POST SUSCEPTANCES FOR NARROW-BAND DIPLEXER IN WG 14

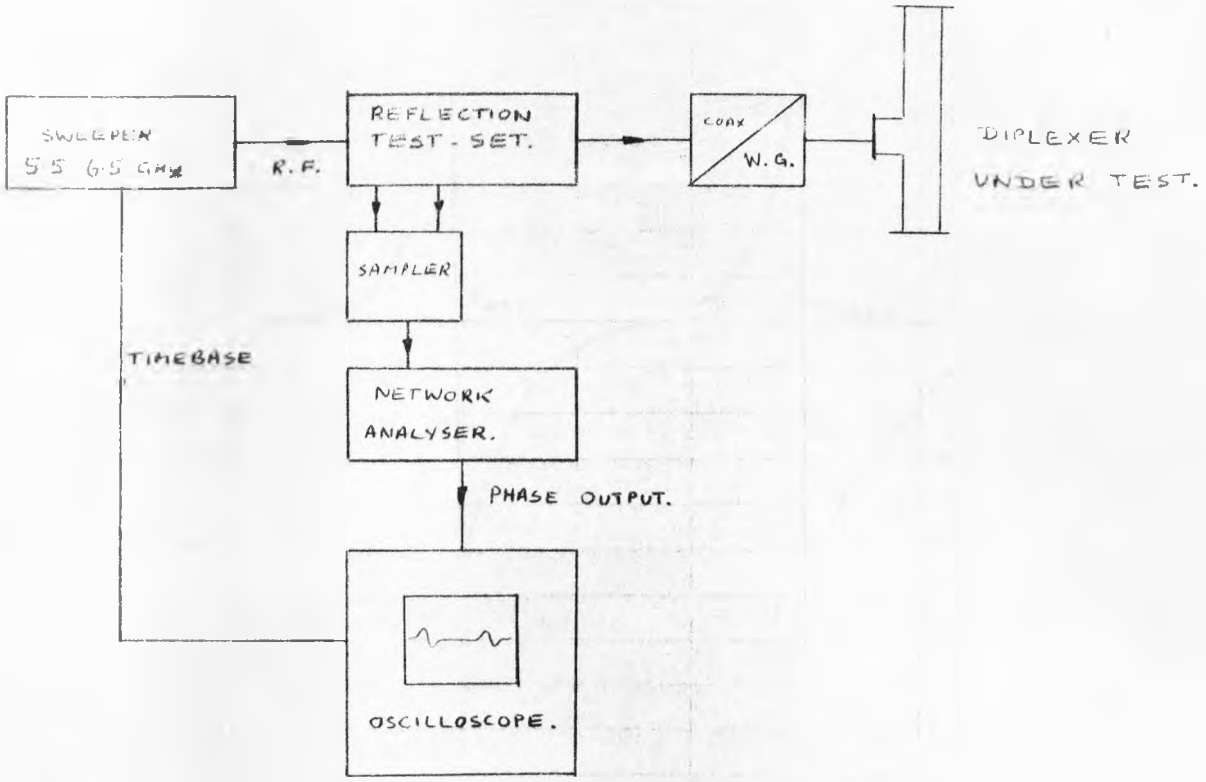

FIGURE 7·8 - TEST ARRANGEMENT.

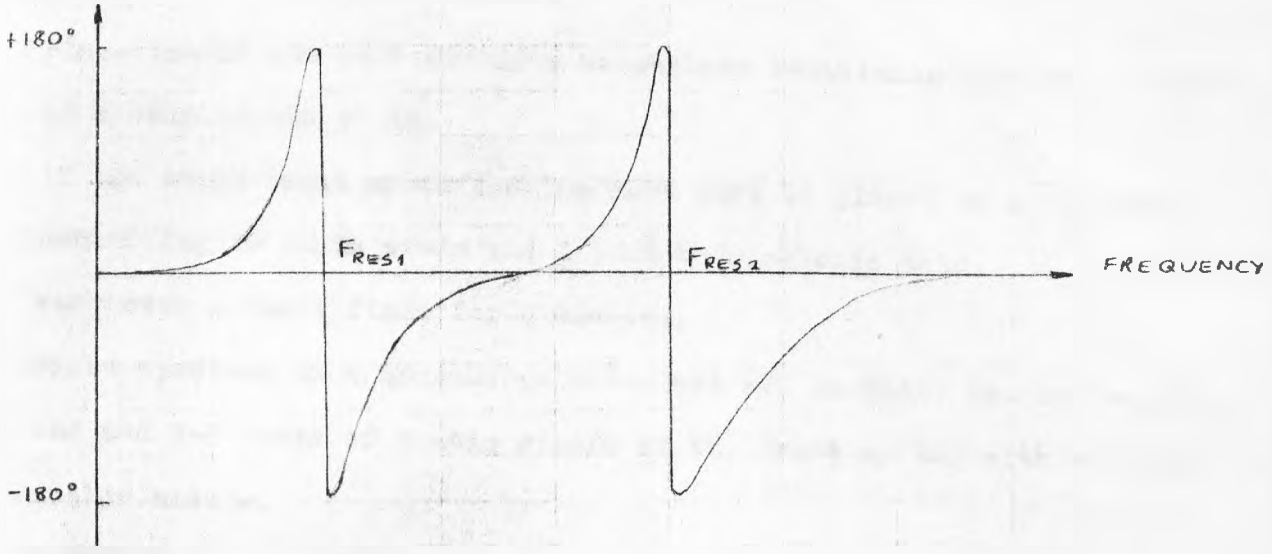

FIGURE 7.9 - APROXIMATE SKETCH OF REFLECTION-PHASE OF TWO INDEPENDENT SERIES-CONNECTED RESONATORS.

Observation of Mitosis in root tip cells.

Procedure -

1. Place 1cm of the root tip in a watchglass containing approx. 10 drops of acetic orcein stain.
   If the stain isnot acidified the root must be placed in a solution containing 10 parts stain and 1 part hydrochloric acid.
   Warm over a small flame for 5 minutes.
2. Place specimen on a microscope slide and cut in half. Retain the tip, and add 2-3 drops of acetic orcein stain, Break up tip with a blunt seeker needle.
3. Lower on a coverslip, cover with a layer of filter paper and GENTLY squash against the slide.
   Warm for 10 seconds.
4. View the onion root tip with low and high power of a light microscope.

Observation -

Acetic orcein shows up the chromosomes in dividing cells. Most of the dividing cells will be found near the very tip of the root.
It may also be possible to count the number of chromosomes in the nucleus.
Are there the same numbers in each cell?
Draw accurate diagrams of any stages visible.

CHAPTER 8

EXTENSION AND FURTHER APPLICATIONS

8.1 INTRODUCTION

This chapter deals with three further applications of the basic theory introduced in Chapter 6, to diplexer and filter design.

Section 8.2 develops a different solution for the bandpass/bandpass diplexer for the special symmetrical case. It is shown that, in the symmetrical case, another solution to the equations defining the modifications (equations 6.34-6.50) exis ts where an annulling inductor is connected in series with the common port. This solution does not exist for the more general asymmetrical case, but is presented for completeness and because it corresponds to a useful practical arrangement with diplexers using filters which show a common ground connection.

Although much of Chapter 5, and Chapter 6, concentrated on bandpass diplexers, lowpass/highpass diplexers are important, and the conventional methods of design again are only applicable to contiguous diplexers. Section 8.3 presents a design theory for general non-contiguous lowpass/highpass diplexers, using filters constrained to have at least two transmission zeros at the origin or infinity.

One way of looking at the design theory is that each filter is modified so that its passband input impedance is a conjugate match for the stopband reactance of the other filter in series with the source resistance. An obvious application is then to filters which must operate with frequency-varying load impedances. An example is an interdigital filter, which was shown in Chapter 4 to be equivalent to a conventional lumped lowpass filter operating between source and load resistors with a cosine-dependence on frequency. Section 8.4 develops a design theory for broadband interdigital filter prototypes,

where the first and last two elements of the conventional lowpass prototypes are modified to partly compensate for this frequency-dependence, and indicates further extensions of the idea.

8.2 SYMMETRIC DIPLEXER WITH SERIES INDUCTOR

If an inductor in series with the common port is included in the diplexer solution, the symmetry considerations of Section 6.2 indicate that the inductor value must be an even function of the band separation variable α. Furthermore, in the symmetric case the frequency-invariant annulling reactance X_o (refer to Figure 6.2) must be exactly zero. The diplexer circuit now is shown in Figure 8.1; the expansions for the input impedances can be derived directly from the expressions in Chapter 6 substituting

$$D_1 = C_1,\ D_2 = C_2,\ D_3 = C_3$$

$$J_1 = K_1,\ J_2 = K_2$$

The symmetry of the problem makes the expansion in channel 2 passband redundant. Let the element values of Figure 8.1 be given by:

$$B_1 = C_1 \left[\alpha + \frac{a_{11}}{\alpha} + \frac{a_{13}}{\alpha^3}\right] \tag{8.1}$$

$$B_2 = C_2 \left[\alpha + \frac{a_{23}}{\alpha^3}\right] \tag{8.2}$$

$$B_3 = C_3 \left[\alpha + \frac{a_{35}}{\alpha^5}\right] \tag{8.3}$$

$$R^2 = 1 + \frac{n_2}{\alpha^2} + \frac{n_4}{\alpha^4} \tag{8.4}$$

$$K_1'^2 = K_1^2 \left[1 + \frac{k_{12}}{\alpha^2} + \frac{k_{14}}{\alpha^4}\right] \tag{8.5}$$

$$K_2'^2 = K_2^2 \left[1 + \frac{k_{24}}{\alpha^4}\right] \tag{8.6}$$

$$L_o = \frac{\ell_2}{\alpha^2} \tag{8.7}$$

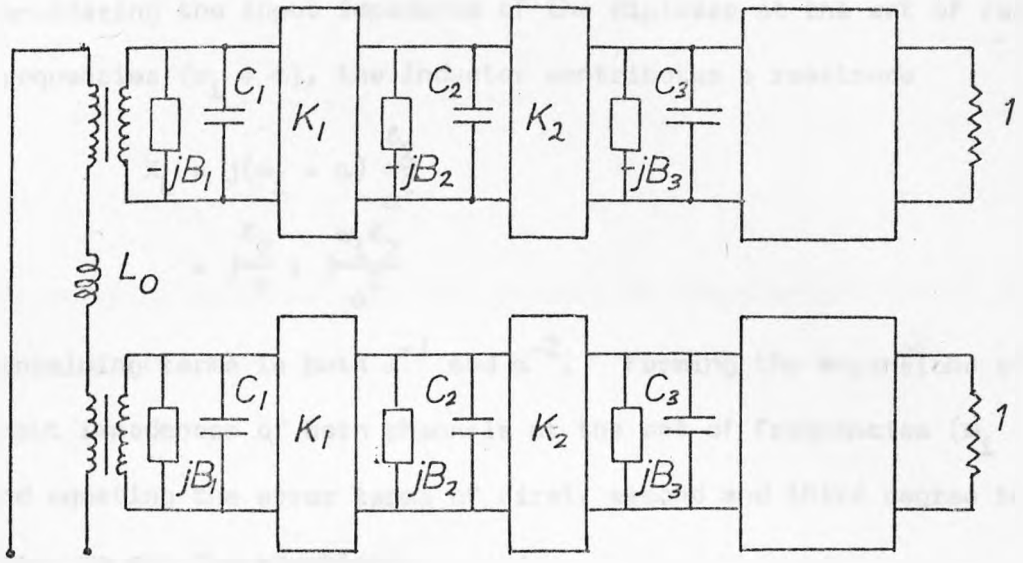

FIGURE 8.1 Diplexer with Series Inductor.

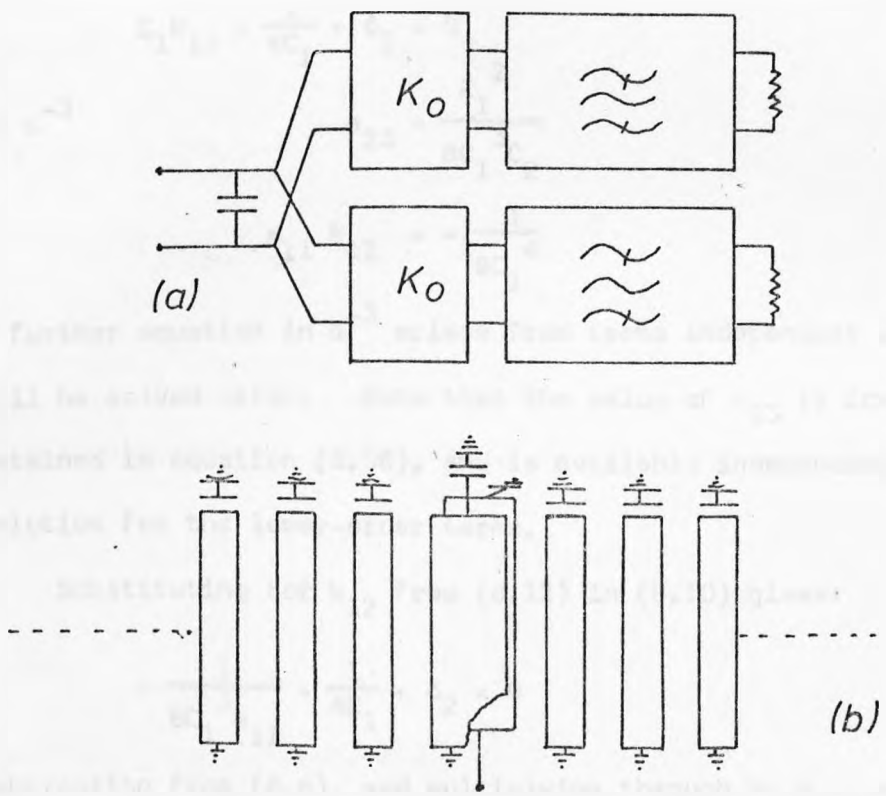

FIGURE 8.2 (a) Alternative Arrangement
(b) Combline Diplexer.

Considering the input impedance of the diplexer at the set of real frequencies $\{\omega_i + \alpha\}$, the inductor contributes a reactance

$$X_L = j(\omega_i + \alpha)\frac{\ell_2}{\alpha^2}$$
$$= j\frac{\ell_2}{\alpha} + j\frac{\omega_i \ell_2}{\alpha^2}$$

containing terms in both α^{-1} and α^{-2}. Forming the expansions of the input impedances of both channels at the set of frequencies $\{\omega_i + \alpha\}$, and equating the error terms of first, second and third degree to zero, we get the equations:

In α^{-1} $$C_1 a_{11} - \frac{1}{2C_1} + \ell_2 = 0 \qquad (8.8)$$

In α^{-2} $$n_2 - C_1^2 a_{11}^2 - k_{12} = 0 \qquad (8.9)$$

$$C_1 k_{12} + \frac{1}{4C_1} + \ell_2 = 0 \qquad (8.10)$$

In α^{-3} $$a_{23} = \frac{K_1^2}{8C_1^3 C_2} \qquad (8.11)$$

$$a_{11} k_{12} = -\frac{1}{8C_1^4} \qquad (8.12)$$

A further equation in α^{-3} arises from terms independent of ω_i, which will be solved later. Note that the value of a_{23} is identical to that obtained in equation (6.38), and is available independently of the solution for the lower-order terms.

Substituting for k_{12} from (8.12) in (8.10) gives:

$$-\frac{1}{8C_1^3 a_{11}} + \frac{1}{4C_1} + \ell_2 = 0$$

Subtracting from (8.8), and multiplying through by a_{11}, elminates ℓ_2 and gives a quadratic in a_{11}:

$$C_1 a_{11}^2 - \frac{3a_{11}}{4C_1} + \frac{1}{8C_1^3} = 0$$

whence $$a_{11} = \frac{\frac{1}{4C_1} \pm \sqrt{\frac{9}{16C_1^2} - \frac{1}{2C_1^2}}}{2C_1}$$

Thus $$a_{11} = \frac{1}{2C_1^2} \text{ or } \frac{1}{4C_1^2} \qquad (8.13)$$

The first solution is identical to that obtained before, where the corresponding value of ℓ_2 is found by substituting in (8.8):

$$\frac{1}{2C_1} - \frac{1}{2C_1} + \ell_2 = 0$$

or $$\ell_2 = 0$$

as expected. The value of ℓ_2 corresponding to the second solution is found from;

$$C_1 \frac{1}{4C_1^2} - \frac{1}{2C_1} + \ell_2 = 0$$

whence $$\ell_2 = \frac{1}{4C_1} \qquad (8.14)$$

Now from (8.10),

$$C_1 k_{12} + \frac{1}{4C_1} + \frac{1}{4C_1} = 0$$

thus $$k_{12} = -\frac{1}{2C_1^2} \qquad (8.15)$$

Substituting for a_{11} and k_{12} in (8.9),

$$n_2 - C_1^2 \frac{1}{16C_1^4} + \frac{1}{2C_1^2} = 0$$

whence $$n_2 = -\frac{7}{16C_1^2} \qquad (8.16)$$

Finally, it can be shown that

$$a_{13} = \frac{1}{8C_1^3}\left(\frac{K_1^2}{C_2} - \frac{9}{4C_1}\right) \qquad (8.17)$$

The fourth- and fifth-order corrections are made as before, and

are found to be;

$$k_{14} = -\frac{1}{4C_1^3}\left(\frac{K_1^2}{C_2} - \frac{27}{16C_1}\right) \tag{8.18}$$

$$k_{24} = -\frac{K_1^2}{16C_1^3 C_2} \tag{8.19}$$

$$n_4 = \frac{1}{4C_1^3}\left(\frac{K_1^2}{C_2} - \frac{1}{C_1}\right) \tag{8.20}$$

$$a_{35} = \frac{K_1^2 K_2^2}{32C_1^3 C_2^2 C_3} \tag{8.21}$$

It is interesting to note that k_{24} and a_{35} have precisely the values found previously.

If the solution is attempted for the asymmetric case, it is found impossible to simultaneously null both the first and third-order terms. Thus the solution with a series inductor is less general than the previous asymmetric solution. It may have practical importance, as indicated in Figure 8.2(a), which shows an alternative arrangement electrically equivalent to Figure 8.1. Here the filters are paralled through admittance inverters, and the series inductor replaced with a shunt capacitor at the common junction. Figure 8.2(b) shows a microwave stripline equivalent, using combline filters coupled to a common resonator at the centre. It may be noted that the "series" connection of stripline filters may present considerable difficulty at high frequencies.

The computed performance (see Appendix 3) of a prototype diplexer incorporating a series inductor, with a similar specification to the first example in section 6.6, is plotted in Figure 8.3(a) and (b). Figure 8.3(a) shows that the degradation of the common-port return-loss is rather large. One reflection zero has been lost and the others much attenuated. The overall return-loss level is, however, still fairly high.

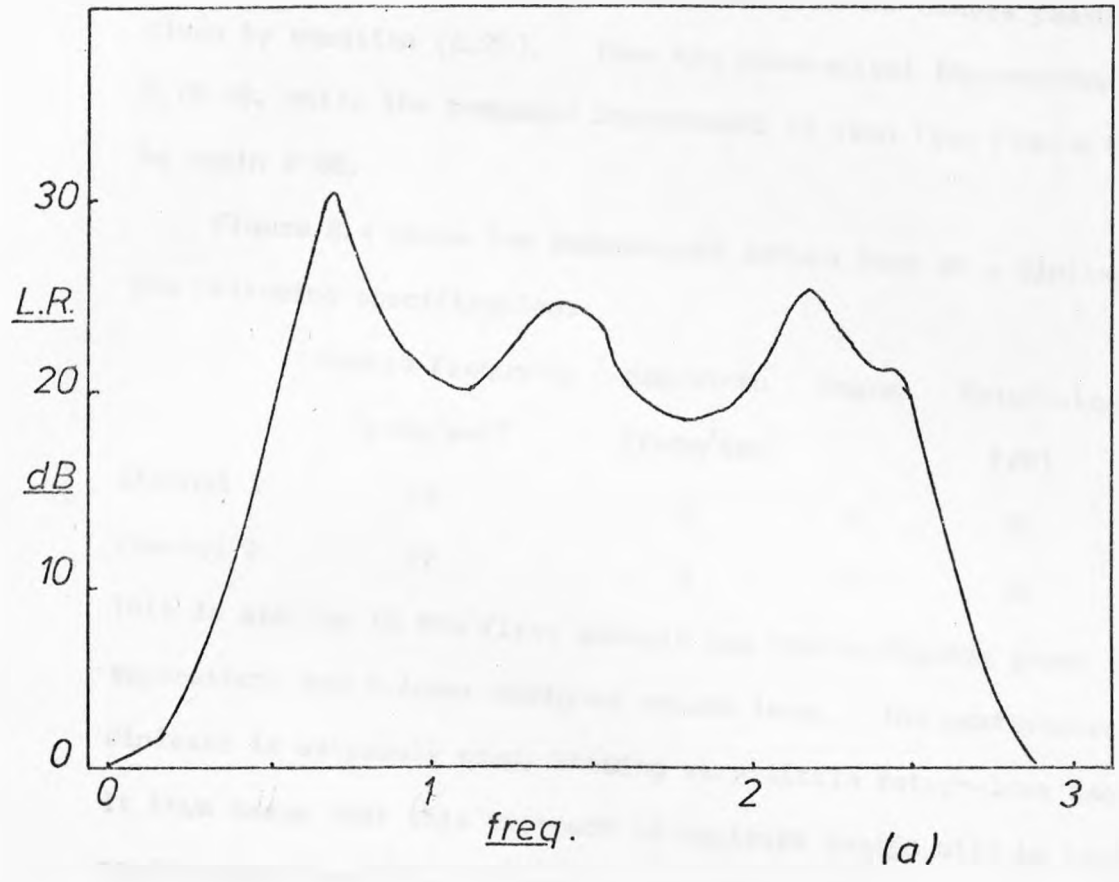

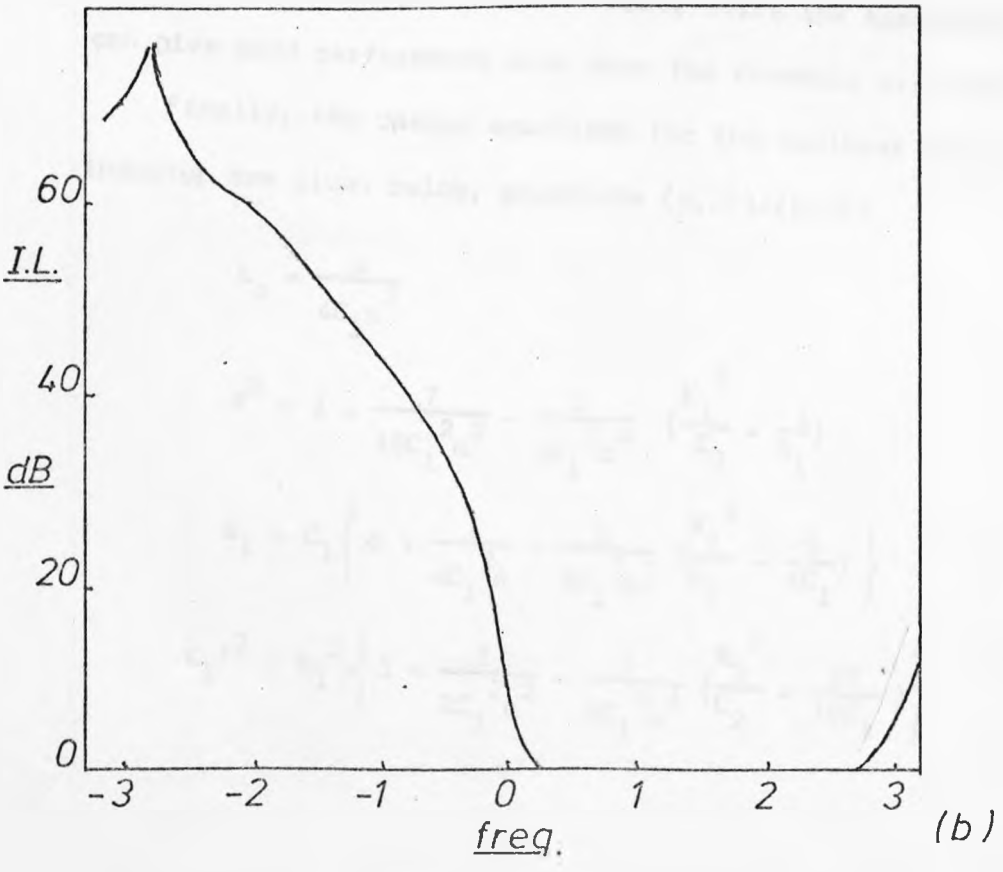

FIGURE 8.3 Response of Diplexer, $\alpha = 1.5$.

It can easily be shown that the theoretical insertion-loss improvement of one channel at the centre of the others passband is still given by equation (6.75). Thus the theoretical improvement is again 6.75 dB, while the computed improvement is seen from Figure 8.3(b) to be again 8 dB.

Figure 8.4 gives the common-port return loss of a diplexer to the following specification:

	Centre Frequency (rads/sec)	Bandwidth (rads/sec)	Degree	Return-Loss (dB)
Channel 1	-2	2	5	22
Channel 2	+2	2	5	22

This is similar to the first example but has a slightly great channel separation, and a lower designed return loss. The performance of this diplexer is extremely good, showing very little return-loss degradation. It thus seems that this approach to diplexer design will be useful for applications where the convenient physical arrangement is preferable and channel separation not too small, while the approach of Chapter 6 can give good performance even when the channels are contiguous.

Finally, the design equations for the diplexer using the series inductor are given below, equations (8.22)-(8.28).

$$L_o = \frac{1}{4C_1\alpha^2} \tag{8.22}$$

$$R^2 = 1 - \frac{7}{16C_1^2\alpha^2} - \frac{1}{4C_1^3\alpha^4}\left(\frac{K_1^2}{C_2} - \frac{1}{C_1}\right) \tag{8.23}$$

$$B_1 = C_1\left\{\alpha + \frac{1}{4C_1^2\alpha} + \frac{1}{8C_1^3\alpha^3}\left(\frac{K_1^2}{C_2} - \frac{9}{4C_1}\right)\right\} \tag{8.24}$$

$$K_1'^2 = K_1^2\left\{1 - \frac{1}{2C_1^2\alpha^2} - \frac{1}{4C_1^3\alpha^4}\left(\frac{K_1^2}{C_2} - \frac{27}{16C_1}\right)\right\} \tag{8.25}$$

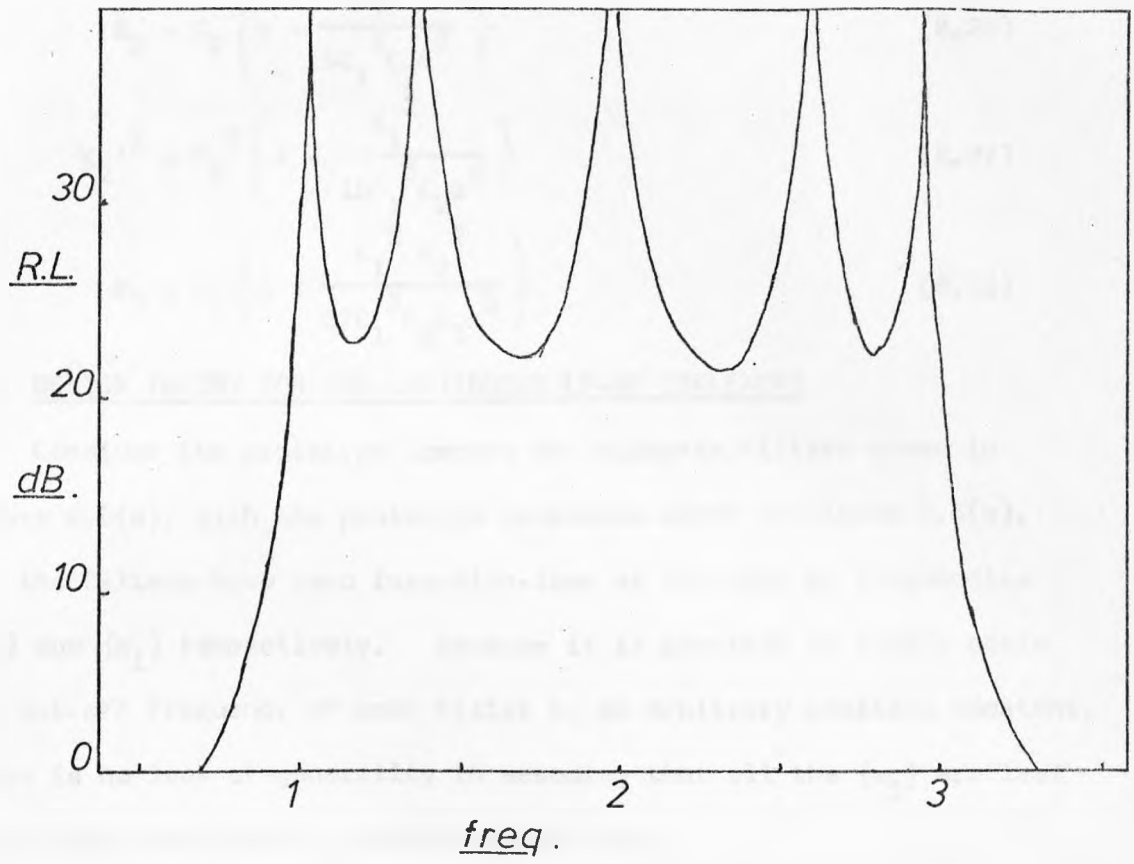

FIGURE 8.4 Diplexer Response, $\alpha = 2$.

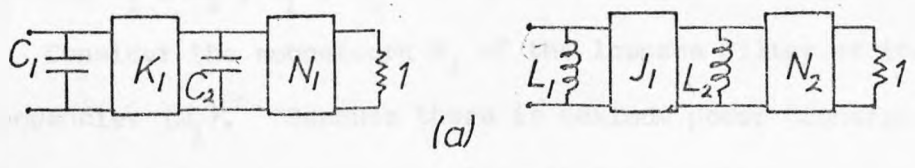

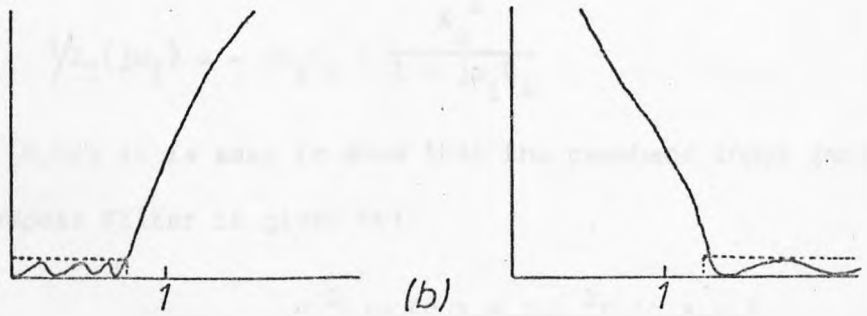

FIGURE 8.5 L.P. & H.P. Prototypes for Diplexer.

$$B_2 = C_2\left\{\alpha + \frac{K_1^2}{8C_1^3C_2\alpha^3}\right\} \tag{8.26}$$

$$K_2'^2 = K_2^2\left\{1 - \frac{K_1^2}{16C_1^3C_2\alpha^4}\right\} \tag{8.27}$$

$$B_3 = C_3\left\{\alpha + \frac{K_1^2K_2^2}{32C_1^3C_2C_3\alpha^5}\right\} \tag{8.28}$$

8.3 DESIGN THEORY FOR NON-CONTIGUOUS LP-HP DIPLEXERS

Consider the prototype lowpass and highpass filters shown in Figure 8.5(a), with the prototype responses shown in Figure 8.5(b). Let the filters have zero insertion-loss at the sets of frequencies $\{\omega_i\}$ and $\{\sigma_i\}$ respectively. Because it is possible to freely scale the cut-off frequency of each filter by an arbitrary positive constant, there is no loss of generality in assuming that all the $\{\omega_i\}$ are less than unity, and the $\{\sigma_i\}$ greater than unity.

Now the filters, which are each minimum-reactance, will be connected in series as shown in Figure 8.6 to form a diplexer, and the values of the first two elements in each filter will be modified, becoming C_1', C_2', L_1', L_2', to give optimum performance.

Consider the subnetwork N_1 of the lowpass filter at the set of frequencies $\{\omega_i\}$. Because there is maximum power transfer through the network at this set of frequencies, it follows that

$$1/Z_2(j\omega_i) = -j\omega_iC_2 + \frac{K_1^2}{1 - j\omega_iC_1} \tag{8.29}$$

Using (8.29) it is easy to show that the passband input impedance of the lowpass filter is given by:

$$Z_1(j\omega_i) = \frac{K_1^2 + j\omega_i(C_2'-C_2) + \omega_i^2C_1(C_2'-C_2)}{K_1^2 + j\omega_iK_1^2(C_1'-C_1) - \omega_i^2(C_2'-C_2) + j\omega_i^3C_1C_1'(C_2'-C_2)} \tag{8.30}$$

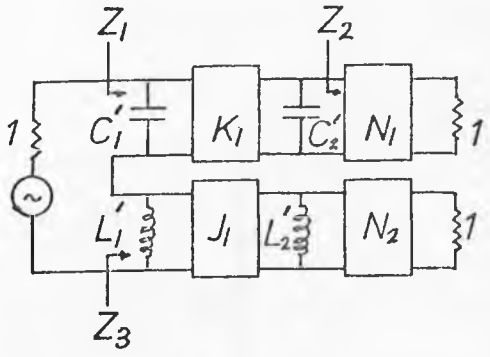

FIGURE 8.6 LP/HP Diplexer.

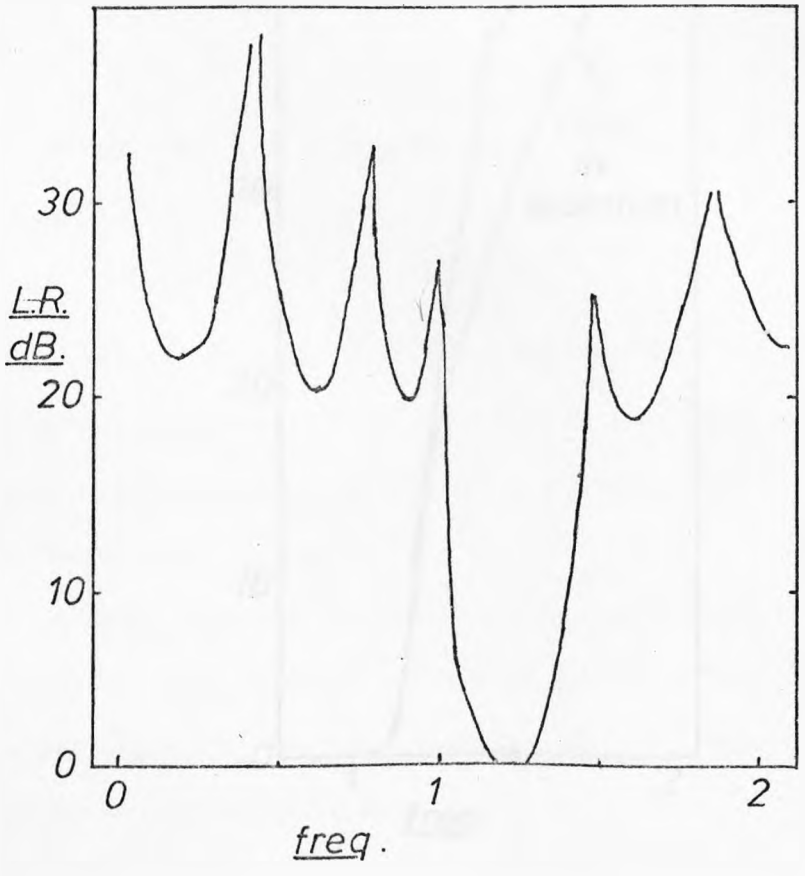

FIGURE 8.7(a) Response of Example Design.

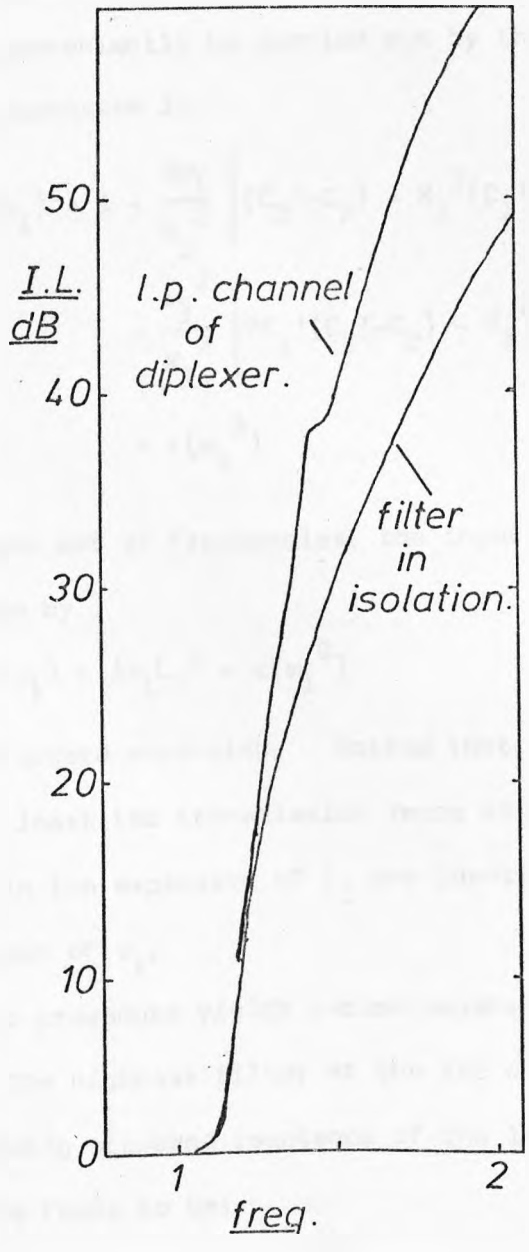

FIGURE 8.7 (continued)

Now, since the $\{\omega_i\}$ are assumed less than 1, then the impedance $Z_1(j\omega_i)$ can be expanded as a power series in ω_i about the origin. The expansion can conveniently be carried out by the method used in Chapter 6. The resulting expansion is;

$$Z_1(j\omega_i) = 1 + \frac{j\omega_i}{K_1^2}\left[(C_2'-C_2) - K_1^2(C_1'-C_1)\right] + \frac{\omega_i^2}{K_1^2}\left[2C_1'(C_2'-C_2) - K_1^2(C_1'-C_1)^2\right] + \varepsilon(\omega_i^3) \tag{8.31}$$

At the same set of frequencies, the input impedance of the highpass filter is given by

$$Z_3(j\omega_i) = j\omega_i L_1' + \varepsilon(\omega_i^3) \tag{8.32}$$

by a straightforward expansion. Notice that, because the highpass filter has at least two transmission zeros at the origin, the even-degree terms in the expansion of Z_3 are identically zero up to at least the fourth power of ω_i.

A similar procedure yields series expansions for the passband input impedance of the highpass filter at the set of frequencies $\{1/\sigma_i\}$ and the corresponding stopband reactance of the lowpass filter. These expansions are found to be;

$$Z_3(-j/\sigma_i) = 1 - \frac{j}{\sigma_i J_1^2}\left\{\left[\frac{1}{L_2'} - \frac{1}{L_2}\right] - J_1^2\left[\frac{1}{L_1'} - \frac{1}{L_1}\right]\right\} - \frac{1}{\sigma_i^2}\left\{\frac{2}{L_1'}\left[\frac{1}{L_2'} - \frac{1}{L_2}\right] - J_1^2\left[\frac{1}{L_1'} - \frac{1}{L_1}\right]^2\right\} + \varepsilon(\sigma_i^{-3}) \tag{8.33}$$

$$Z_1(-j/\sigma_i) = -\frac{j}{\sigma_i C_1'} + \varepsilon(\sigma_i^{-3}) \tag{8.34}$$

Equating the first and second-degree terms of the input impedance of

the diplexer (ie $Z_3 + Z_1$) to zero in each passband gives a set of simultaneous equations in the unknown primed element values, (8.35)-(8.38).

$$\frac{C_2'-C_2}{K_1^2} - (C_1' - C_1) + L_1' = 0 \qquad (8.35)$$

$$\frac{2C_1'(C_2'-C_2)}{K_1^2} - (C_1' - C_1)^2 = 0 \qquad (8.36)$$

$$\frac{1}{J_1^2}\left[\frac{1}{L_2'} - \frac{1}{L_2}\right] - \left[\frac{1}{L_1'} - \frac{1}{L_1}\right] + \frac{1}{C_1'} = 0 \qquad (8.37)$$

$$\frac{2}{J_1^2 L_1'}\left[\frac{1}{L_2'} - \frac{1}{L_2}\right] - \left[\frac{1}{L_1'} - \frac{1}{L_1}\right]^2 = 0 \qquad (8.38)$$

Although this set of equations is non-linear, a simple and direct solution exists. From (8.36):

$$C_2' - C_2 = \frac{K_1^2(C_1' - C_1)^2}{2C_1'}$$

Substituting in (8.35) and rearranging gives

$$C_1^2 - C_1'^2 + 2C_1' L_1' = 0 \qquad (8.39)$$

From (8.37) and (8.38), a similar procedure yields

$$L_1' C_1' = \frac{2L_1'^2 L_1^2}{L_1^2 - L_1'^2} \qquad (8.40)$$

Substituting (8.40) for the product term "$2C_1'L_1'$", and also for "C_1'", in (8.39) yields the equation:

$$C_1^2 - \frac{4L_1^4 L_1'^2}{(L_1^2 - L_1'^2)^2} + \frac{4L_1'^2 L_1^2}{L_1^2 - L_1'^2} = 0$$

$$\Rightarrow \quad C_1^2(L_1^2 - L_1'^2)^2 = 4L_1^2 L_1'^4$$

$$\Rightarrow \quad L_1^2 - L_1'^2 = \frac{2L_1 L_1'^2}{C_1}$$

$$\Rightarrow \quad L_1^2 = L_1'^2\left(\frac{2L_1}{C_1} + 1\right)$$

$$L_1' = \frac{L_1}{\sqrt{\left(\frac{2L_1}{C_1} + 1\right)}} \tag{8.41}$$

Substituting for L_1' in (8.40), we get

$$\frac{C_1'L_1}{\sqrt{\left(\frac{2L_1}{C_1} + 1\right)}} = \frac{2L_1^4}{\left(\frac{2L_1}{C_1} + 1\right)\left[1 - \frac{1}{\frac{2L_1}{C_1} + 1}\right]}$$

$$= \frac{2L_1^2}{\frac{2L_1}{C_1} + 1 - 1}$$

$$= L_1C_1$$

$$\therefore \quad C_1' = C_1\sqrt{\frac{2L_1}{C_1} + 1} \tag{8.42}$$

There are no equivalent compact explicit expressions for C_2' and L_2'; they can be found from (8.36) and (8.38) by substituting for C_1' and L_1', and are given by:

$$C_2' = C_2 + \frac{K_1^2}{2C_1'}(C_1' - C_1)^2 \tag{8.43}$$

$$\frac{1'}{L_2} = \frac{1}{L_2} + \frac{J_1^2L_1'}{2}\left(\frac{1}{L_1'} - \frac{1}{L_1}\right)^2 \tag{8.44}$$

Expressions (8.41) to (8.44) are then the design formulae for general non-contiguous lowpass-highpass diplexers.

It is in principle possible to make modifications to the first three elements of each filter, and to force the input impedance of the diplexer to be exactly unity up to the third degree in ω_i. However, the resulting set of non-linear equations corresponding to (8.35)-(8.38) has so far defied solution.

A computer program has been written which designs and analyses LP/HP diplexers using the new formulae (see Appendix 4), using conventional Chebyshev channel filters. The program assumes that the

LP channel cutoff frequency is at 1 rad/sec, and the designer can specify the HP cutoff, and the degree and return-loss ripple in each channel.

Figure 8.7(a) gives the common-port return-loss response of a diplexer where each channel has seven elements, a designed return-loss ripple of 22 dB, and the HP channel cuts off at 1.5 rads/sec. It can be seen that the inband return loss is very little degraded, being better than 20 dB, and all the return-loss peaks are preserved. Figure 8.7(b) shows the lowpass-channel insertion loss, with the insertion loss of an equivalent filter in isolation for comparison. There is an improvement of approximately 9 dB in insertion loss at the edge of the HP channel ($\omega = 1.5$), which is maintained over the entire HP channel passband.

The performance of the new HP/LP diplexer is not maintained when the channel spacing is much smaller, and it is not possible, for example, to use the new method to design contiguous diplexers. However, in such cases Wenzel's method [5.4] can be used, which is very direct and capable of excellent results. Thus this new method of design can be regarded as complementary to Wenzel's method, and useful when non-contiguous designs are required.

8.4 DESIGN FORMULAE FOR INTERDIGITAL FILTERS

Chapter 4 presented a derivation of the design formulae for interdigital filters, in which it was shown that an equivalent circuit to the interdigital structure could be drawn as in Figure 8.8. In this circuit, the shunt susceptances, B_r, have the value

$$B_r = - Y_r \cos(\theta)$$

and the frequency-variant input and output transformers have ratio

$$r = \sqrt{(\sin(\theta))}$$

where θ is the electrical length of the n-wire line and Y_r is the

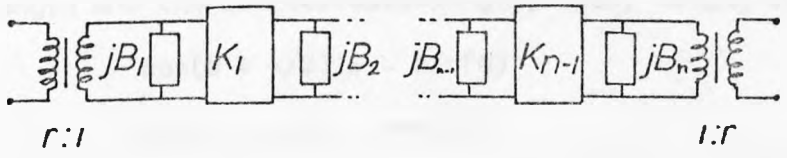

FIGURE 8.8 Interdigital Equivalent Circuit.

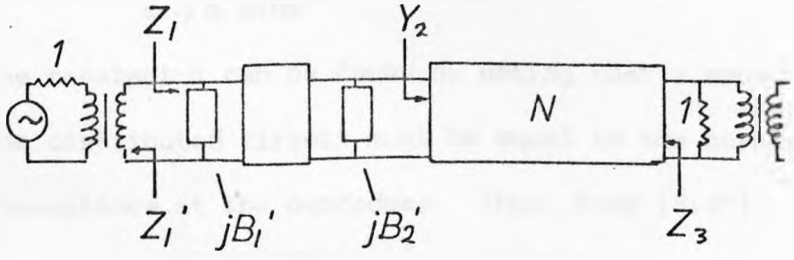

FIGURE 8.9 Modified Equivalent Circuit.

total characteristic admittance at the r'th node.

If θ is re-defined as the difference between the electrical length and the quarter-wave-length, then, noting that

$$\cos(\theta + \pi/2) = - \sin(\theta)$$

$$\sin(\theta + \pi/2) = \cos(\theta)$$

B_r and r can be written in terms of the new variable as

$$B_r = Y_r \sin(\theta) \tag{8.45}$$

$$r = \sqrt{(\cos(\theta))} \tag{8.46}$$

To a first order, the filter can be designed by equating the shunt susceptances of this circuit to the shunt susceptances in a lumped low-pass prototype, as shown in Figure 3.13,

under the transform

$$\omega \rightarrow \alpha \sin\theta \tag{8.47}$$

The constant α can be found by noting that a shunt susceptance of the distributed circuit must be equal to the corresponding lumped susceptance at the bandedge. Thus, from (8.47),

$$1 = \alpha \sin(\theta_o)$$

or $$\alpha = 1/\sin(\theta_o) \tag{8.48}$$

Thus $$C_r = Y_r \sin(\theta_o)$$

or $$Y_r = \alpha C_r \tag{8.49}$$

Consider the circuit of Figure 8.9 , where the output of the equivalent circuit has been loaded with a one-ohm resistor before the output frequency-varying transformer. Thus the input impedance Z_1 is equal to one ohm at a finite set of frequencies $\{\theta_i\}$, because of the maximum-power-transfer properties of the lumped prototype. It thus follows that

$$Y_2(j\theta_i) = - j\alpha C_1 \sin(\theta_i) + \frac{K_1^2}{1 - j\alpha C_2 \sin(\theta_i)} \tag{8.50}$$

Now, at this set of frequencies, the impedance seen looking at

the source through the input transformer is just

$$Z_1'(j\theta_i) = \frac{1}{\cos(\theta_i)}$$

$$= \frac{1}{\sqrt{(1-\sin^2(\theta_i)}} \qquad (8.51)$$

Let the first two elements of the low-pass lumped prototype be modified, becoming C_1', C_2', to approximately compensate for the variation of the source resistance in the interdigital filter. Using (8.50), it is possible to expand $Z_1(j\theta_i)$ as a power series in $\sin(\theta_i)$; from equation (8.31) the result is:

$$Z_1(j\theta_i) = 1 + \frac{ja\sin(\theta_i)}{K_1^2}\left[(C_2' - C_2) - K_1^2(C_1' - C_1)\right]$$

$$+ \frac{a^2\sin^2(\theta_i)}{K_1^2}\left[2C_1'(C_2' - C_2) - K_1^2(C_1' - C_1)^2\right] \qquad (8.52)$$

Expanding (8.51)

$$Z_1'(j\theta_i) = 1 + \tfrac{1}{2}\sin^2\theta_i + \ldots \qquad (8.53)$$

For an exact match up to the second order,

$$\frac{a}{K_1^2}\left[(C_2' - C_2) - K_1^2(C_1' - C_1)\right] = 0$$

$$\Rightarrow C_2' - C_2 = K_1^2(C_1' - C_1) \qquad (8.54)$$

and $$\frac{a^2}{K_1^2}\left[2C_1'(C_2' - C_2) - K_1^2(C_1' - C_1)^2\right] = \tfrac{1}{2} \qquad (8.55)$$

Substituting (8.54) into (8.55),

$$2C_1'(C_1' - C_1) - (C_1' - C_1)^2 = \frac{1}{2a^2}$$

$$2C_1'^2 - 2C_1'C_1 - C_1'^2 - C_1^2 + 2C_1'C_1 = \frac{1}{2a^2}$$

$$C_1'^2 = C_1^2 + \frac{1}{2a^2}$$

$$C_1' = \sqrt{(C_1^2 + \frac{1}{2a^2})} \qquad (8.56)$$

and thus, from (8.54)

$$C_2' = C_2 + K_1^2(C_1' - C_1) \qquad (8.57)$$

Having modified the first two elements in this way, the maximum power-transfer properties of the filter, and reciprocity, ensure that Z_3, the impedance looking back at the source from the output of the filter (see Figure 8.10), must be given by;

$$Z_3 = 1 + \varepsilon(\sin^3\theta_i)$$

and thus the last two elements can also be modified by the same equations, ie

$$C_n' = \sqrt{(C_n^2 + \frac{1}{2\alpha^2})} \qquad (8.58)$$

$$C_{n-1}' = C_{n-1} + K_{n-1}^2(C_n' - C_n) \qquad (8.59)$$

A computer program has been written which designs prototype inter-digital filters using these equations, based on lumped filters with Chebyshev response (see Appendix 5), and analyses the design, plotting the return loss as a function of frequency. Figure 8.10 (curve (a)) shows the response of a tenth-degree design, with a prototype ripple of 22 dB and a cutoff electrical length of 45^o. This represents a 3:1 bandwidth, and is near the attainable physical limit for the inter-digital structure. For comparison, curve (b) is the response of an unmodified filter. The improvement resulting from the modifications is clear, though the worst-case in-band return loss is degraded to 16 dB. The two highest frequency return-loss poles have been recovered, and the bandwidth is exactly as designed. The performance is considerably better than obtainable using the original design procedure, though not comparable with the results given by a design using explicit formulas [8.1]. However, these results indicate that the new method may be of value for designing broadband coupled-resonator bandpass filters where no explicit formulas are available for the structure, as is the case for example, the combline filters and

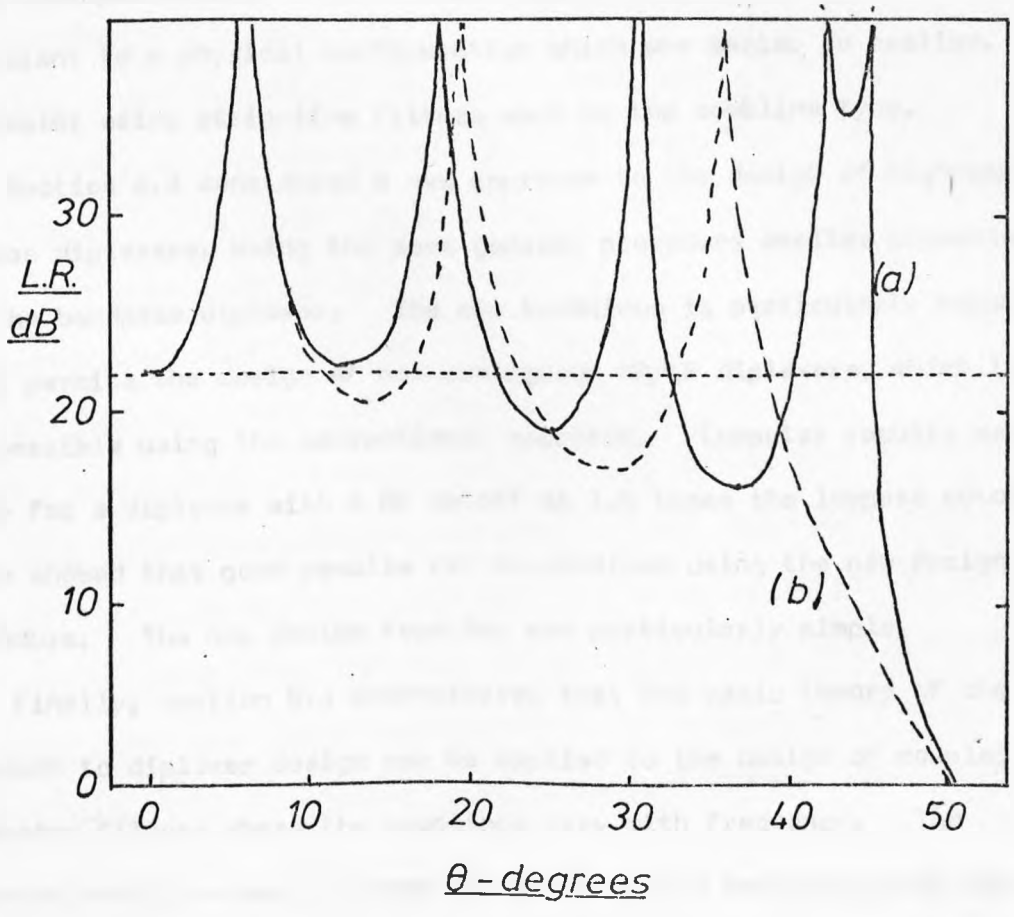

FIGURE 8.10 Response of Trial Interdigital Design.

lumped-element filters considered in Chapter 4.

8.5 CONCLUSIONS

Section 8.2 gave the derivation of alternative direct design formulas for symmetrical bandpass diplexers, where a series annulling inductor is connected in the common port. This contrasts with the original case covered in Chapter 6, where the symmetrical diplexer used no annulling components. It was shown that the new solution gave worse performance for the same channel separation, but was equivalent to a physical configuration which was easier to realise, particular using strip-line filters such as the combline type.

Section 8.3 considered a new approach to the design of highpass/lowpass diplexers, using the same general procedure earlier presented for the bandpass diplexer. The new technique is particularly valuable as it permits the design of non-contiguous HP/LP diplexers, which is not possible using the conventional approach. Computer results were given for a diplexer with a HP cutoff at 1.5 times the lowpass cutoff, which showed that good results can be obtained using the new design procedure. The new design formulae are particularly simple.

Finally, section 8.4 demonstrated that the basic theory of the approach to diplexer design can be applied to the design of coupled-resonator filters where the couplings vary with frequency. The computed results clearly showed the value of the technique when applied to the design of broadband interdigital filters, and further extensions to (for example) combline and lumped-element filters may be useful.

CHAPTER 9. Conclusions.

9·1 Bandpass Filters.

A wide range of bandpass filters can be designed by transformation of a lowpass prototype. The prototypes considered were of a class often called "all-pole" which have all their transmission zeros at infinity. The optimum response of this class for meeting amplitude specifications with minimum degree was shown to be the Chebyshev or equal-ripple response.

Five representative types of bandpass filter were considered, as far as possible from a unified viewpoint. These were of the sort sometimes known as coupled resonator filters. Design procedures were developed for a type of lumped-constant filter, for transmission-line filters of the interdigital and combline type, for direct-coupled cavity waveguide filters, and finally a new design procedure was given for quartz-crystal single sideband filters.

It is interesting to note that such apparently different types of filter can all be successfully designed by essentially the same theory. This is evidence of the great power of the underlying ideas. Indeed, the ideas can be further extended to filters using virtually any type of resonator, and these resonators need not be electrical.

The design procedures all satisfied the criterion outlined in the introduction. They can be applied by an engineer unskilled in filter theory, and translate the initial specification for the filter directly into the appropriate parameters of a physical realisation. Such design methods are called "direct". In every case the

computations needed in the design were well within the scope of an ordinary scientific calculating machine.

9.2 Diplexers.

Diplexers are linear three-ports which combine signals in two different frequency bands at two of the ports onto the third port with minimum loss, and minimum mismatch, at least within the bands. They generally use some combination of filters. The inevitable interactions between the filters can be avoided either by using additional devices to decouple them, or by designing the filters so that the interactions are necessary to the correct operation of the diplexer.

For decoupling, either circulators or hybrids can be used. Both methods were considered from a scattering matrix viewpoint. An alternative diplexing method using hybrids was also considered. This is the commutating filter which has received a lot of attention in recent years.

All these methods carry a weight penalty since they use additional passive devices. In addition, the circulator may limit the system dynamic range through nonlinear effects in the ferrite, while the performance of the hybrid methods is critically dependant on maintaining exact balance between separate transmission paths.

The traditional methods of designing diplexers using directly interacting filters are based on singly-terminated filter prototypes. The exact maximally-flat lowpass-highpass solution has been known for many years, but is not selective enough for many applications. The corresponding exact equi-ripple solution uses elliptic filters which may be difficult to realise, especially at microwave frequencies. However, Wenzel has shown that convent-

ional singly-terminated Chebyshev filters give excellent results as long as simple design rules are observed. This was confirmed by the computed response of an example design, and a direct design procedure for these lowpass-highpass diplexers indicated.

The corresponding bandpass-bandpass case is more complicated. Very similar rules for the design apply, using singly-terminated filters. However, a reactance-annulling network is needed at the common junction, and its design requires numerical (ie computer) analysis of the filters' input impedances. Thus the design of bandpass-bandpass diplexers by the traditional method is rather far from being "direct".

A common disadvantage of methods based on the use of singly-terminated filters is that the diplexer passbands are constrained to be contiguous. However, communication channels are rarely contiguous, and this leads in most cases to the degree of the filters in the diplexer being excessive to ensure sufficient isolation between the channels. This indicates the need for a non-contiguous design method for diplexers.

9·3 Direct Design of Non-Contiguous Diplexers.

A new design procedure was derived for non-contiguous bandpass diplexers. This procedure gives corrections which can be applied to a pair of bandpass filters so that they give optimum performance when "diplexed". The design formulae are given in terms of the elements of the original prototypes and a simply-defined band separation variable. The method directly optimises the common-port return loss of the diplexer, but it was shown that it simultaneously optimises the insertion-loss of each filter and the return loss at the other

ports. An interesting by-product of the procedure is a worthwhile improvement in the insertion loss of each filter over the passband of the other.

Computed responses were given for several prototype diplexers, demonstrating the high performance possible with the new technique. Then the design of waveguide diplexers was considered. First, the design of a narrow-band diplexer around 5·8 Ghz. was described. After allowing for an initial design error, the measured performance of the design was found to agree very well with theoretical predictions. Also, no special problems arose in tuning the diplexer once the initial design mistake was allowed for. Together with the earlier results reported by Rhodes this indicates that the design of narrow band diplexers can be considered routine.

It was found by computer analysis of typical designs that the new design method worked well even when applied to broadband waveguide filters. This was surprising since the derivation of the design formulae assumed a lumped prototype while broadband waveguide filters are essentially distributed networks. The method probably works because the lumped description applies fairly well to the waveguide filter at least around the passband. Whatever the reason, the result is welcome, and the design of broadband waveguide diplexers should present little problem.

A broadband diplexer has been constructed for the 7·25-8·4 Ghz. band. The theoretical performance of this diplexer was very good. It has not yet been possible to confirm the performance experimentally because of problems in aligning the filters.

Some further work on diplexers has also been reported in the thesis. Another solution of the bandpass diplexer problem was investigated, which existed only for the symmetrical case. This solution incorporated an additional inductor in series with the input port of the diplexer. It was shown that this form of the diplexer was not capable of such high performance as the first version investigated. However, in some cases it could lead to a better physical arrangement of the filters, especially in stripline systems.

Next the basic theory which had been applied to bandpass diplexers was applied to the design of lowpass-highpass diplexers. A direct design method for non-contiguous diplexers was developed, which can be regarded as complementary to Wenzel's method for contiguous types. Again, computed results were given for a typical design to demonstrate that high performance was possible.

Finally, the theory was used to obtain improved design formulae for interdigital filters of large bandwidth. This was done by modifying the first and last two elements of the filter to compensate for the apparent variation of the source and load impedances with frequency. The computed results showed that the method worked, though the improvement obtained was not enough to make the method competitive with the explicit formulas derived by Rhodes. However, it does indicate that the method may be valuable for the design of other bandpass structures for which explicit formulas are not available.

9·4 Further Work on Diplexers.

The methods developed here allow the direct design of non-contiguous bandpass-bandpass and lowpass-highpass diplexers. Other types of response are sometimes needed for special system requirements. One such arises when a diplexer is needed for two channels which are very close together and a very high isolation is needed between them. A very high degree would be needed in each channel if this specification was to be met using a conventional bandpass diplexer. If the other attenuation requirements permit, single-sided designs discussed by Rhodes in [4·12] are ideal for this sort of specification and a suitable design procedure may be developed by applying the frequency transformation developed for crystal filters to the non-contiguous lowpass-highpass diplexer prototype. Work is planned to develop an appropriate waveguide realisation.

9·5 Extension to Multiplexers.

The most obvious and urgent extension of this work is to the design of non-contiguous multiplexers having an arbitrary number of channels. Some work has been done on this, and the problem is not trivial.

If the solution to the multiplexer is attempted directly using the methods of chapter 6 it is found that the exact cancellation of all the error terms up to the third order obtained for the diplexer does not occur. There are in fact insufficient variables to allow a determinate solution to the problem. If an additional element is introduced as in chapter 8 for the diplexer, a solution is possible for the triplexer. The extension to the multiplexer will require yet more additional elements to be introduced.

BIBLIOGRAPHY.

The references below are arranged according to chapter. Some references appear in more than one context. Journal titles are generally abbreviated, but the full title is normally obvious. Particular abbreviations are:

Proc.	Proceedings
IEE	Institute of Electrical Engineers (UK).
IEEE (IRE)	Institute of Electrical and Electronic Engineers (Institute of Radio Engineers) (USA)
MTT	IEEE Transactions on Microwave Theory and Techniques.
CT	IEEE Transactions on Circuit Theory
CAS	IEEE Transactions on Circuit and Systems Theory.
Elect. Lett.	Electronics Letters (published by IEE).
BSTJ	Bell System Technical Journal.
Elec. Commun.	Electrical Communications (published by ITT corporation)

Chapter 1.

1 RV Bruce
'Bell: Alexander Graham Bell and the Conquest of Solitude.'(Chapter 9, The Multiple Telegraph.) Gollancz 1973.

Chapter 2.

1 HJ Carlin, AB Giordano
'Network Theory.' p1. Prentice-Hall 1964.

2 JO Scanlan, R Levy
'Circuit Theory' Vol1 p95. Oliver & Boyd 1970.

3 Ibid p223

4 Ibid Vol2 p300

5 EV Bohn
'The Transform Analysis of Linear Systems' p358 Addison-Wesley 1963

6 Scanlan & Levy, op cit p376-80.

7 Ibid p415-420.

8 S Darlington
'Synthesis of Reactance Four-Poles with Prescribed Insertion-Loss Characteristics.'
Jour. Math. Phys. Vol18 p257-353 Sept. 1939.

9 Carlin & Giordano, op cit p222.

10 Scanlan & Levy, op cit p383.

11 S Ramo, JR Whinnery, T Van Duzer
'Fields and Waves in Communication Electronics.' p23. John Wiley 1965.

12 PI Richards
'Resistor Transmission-Line Circuits'
Proc IRE Vol36 p217-20 Feb 1948.

13 EA Guillemin
'Synthesis of Passive Networks' p296 John Wiley 1957.

Chapter 3.

1 JD Rhodes.

'Theory of Electrical Filters' John Wiley 1976.

2 AI Zverev

'Handbook of Filter Synthesis' John Wiley 1967. Chapter 6.

3 SB Cohn

'Direct Coupled Resonator Filters.'

Proc IRE Vol45 p187-96 Feb1957

4 HJ Orchard

'Formulae for Ladder Filters'

Wireless Engineer Vol30 p3-5 Jan1953

5 H Takahasi

'On the Ladder Type Filter Network with Cnebyshev Response'. J. Inst. Elec. Comm. Engrs. Japan Vol34 p65-74 Feb 1951.

Chapter 4.

1 Cohn op cit [3.3]

2 GL Matthaei, L Young, EMT Jones

'Microwave Filters, Impedance-Matching Networks and Coupling Structures.' McGraw-Hill 1964.

3 JD Rhodes

'The Theory of Generalised Interdigital Networks.'

CT-16 No.3 Aug1969 p280-8

4 JD Rhodes

'The Generalised Interdigital Linear-Phase Filter'

MTT-18 NO.6 June1970 p301-7.

5 KK Pang

'Design of Microwave Filters by the Sine-Plane Approach' MTT-21 No10 Oct 1973 p607-11

6 MJ Sayer

'A New Design Procedure for Narrow-Band Combline Micro-

wave Filters' M.Sc. Dissertation, Leeds University 1974.

7 R Levy

'Theory of Direct-Coupled-Cavity Filters.'

MTT-15 No.6 June 1967.

8 WP Mason

'Electric Wave Filters Employing Quartz Crystals as Elements' BSTJ Vol13 p405-52 July 1934.

9 RA Sykes

'A New Approach to the Design of High-Frequency Crystal Filters' 1958 IRE Nat. Conv. Record, part2 p18-29.

10 M Dishal

'Modern Network Theory Design of SSB Crystal Ladder Filters' Proc.IEEE Vol 53 No.9 Sept.65.

11 JL Haine

'New Active Quadrature Phase-Shift Network'

Elect. Lett. Vol13 No.7 31 March 1977.

12 JD Rhodes

'Explicit Design Formulas for Waveguide Single-Sided Filters' MTT-23 No.8 Aug1975 p681-9.

13 EA Guillemin

'Synthesis of Passive Networks.' chapter 5. John Wiley 1957.

14 EG Cristal

'New Design Equations for a Class of Microwave Filters' MTT-19 p486-90 May 1971.

15 HJ Riblet

'An Explicit Derivation of the Relationship Between the Parameters of an Interdigital Structure and the Equivalent Transmission-Line Cascade.'MTT-15 No.3 March1967

16 WJ Getsinger

'Coupled Rectangular Bars Between Parallel Plates' MTT-10 p65-72 Jan 1972.

17 JD Rhodes
'Theory of Electrical Filters'
p151 John Wiley 1976
18 RJ Wenzel
'Exact Theory of Interdigital Bandpass Filters and Related Coupled Structures.' MTT-13 No.5 Sept1965 p559-75.
19 JD Rhodes
'Microwave Filters'
IEE Colloquium Digest 1976/33.
20 WL Jones
'Design of Tunable Combline Filters of Near-Constant Bandwidth' Elect. Lett. Vol1 No.6 Aug1965 p156-8.
21 CF Kurth
'Generation of SSB Signals in Multiplex Communication Systems.' CAS-23 No.1 Jan1976 p1-17.

Chapter 5.

1 CM Kudsia, V O'Donovan
'Microwave Filters for Communication Systems'
Artech House 1974
2 H Rapaport
'A Microwave Ferrite Frequency Separator'
IRE Trans MTT-6No.1 p53-8
3 PA Matthews, IM Stephenson
'Microwave Components' chapter 7
Chapman & Hall 1968
4 HD Brudy, HK Ligotky, A Nissensolu
'High Power Broad Band Microwave Link Systems'
Elec. Commun. Vol 48 No.1&2 1973
5 AF Harvey
'Microwave Engineering' p115
Academic Press 1963

6 HD Lewis, LC Tillotson

'A Non-reflective Branching Filter for Microwaves'

BSTJ Vol.27 p83-6

7 Vos, Laurent U.S. Patent 1,920,041

8 Bobis U.S. Patent 2,044,047

9 PA Reiling

'Waveguide Filters for Pulse Transmission Studies'

Bell Lab. Record Vol.29 p164-8 April1951.

10 HJ Carlin

'UHF Multiplexer uses Selective Coupler'

Electronics Vol.28 p152-5 Nov 1955

11 Klopfenstein, Epstein

'The Polarguide. A Constant Resistance Waveguide Filter'

Proc IRE Vol44 p210-8

12 SB Cohn, FS Coale

'Directional Channel-Separation Filters'

Proc IRE Vol.44 No.8 p1018-1024 Aug 1956

13 FS Coale

'A Travelling Wave Directional Filter'

MTT-4 No.4 p256-60 Oct 56.

14 FS Coale

'Application of Directional Filters for Multiplexing

Systems' MTT-6 No.4 p450-3 Oct 58.

15 O Wing

'Cascade Directional Filter'

MTT-7 No.2 p197-201 April 1959

16 L Young, JQ Owen

'A High Power Diplexing Filter'

MTT-7 No.3 p384-7 July 1959

17 Moriarty
'Resonant Ring Scattering in Forward Scatter Systems'
Electronics Vol.32 No.27 p54-56 July1959
18 Marcatili
'Circular Electric Hybrid Junction and some Channel
Dropping Filters' BSTJ Vol.40 No.1 p185-196
19 Marcatili, Bisbee
'Band Splitting Filter'
BSTJ Vol.40 No.1 p197-212
20 J Kaiser
'Ring Network Filter'
MTT-9 No.4
21 MV O'Donovan
'Microwave Branching Systems'
Radio and Electronic Engineer, Vol.25 No.5 p449-456
22 CF Kurth
'Branching Filters with an All-Stop Region'
Frequenz Vol.17 No.4 p158-64
23 G Salzmann
'New Separation Filters based on the Electromagnetic
Coupling of Transmission lines '
Acta Technica Hungarica Vol42 No.1-3 p109-122.
24 RD Standby
'Frequency Response of Strip Line Travelling Wave
Directional Filters' MTT-11 No.4 p264-5
25 Possenti, Porta
'Branching Filters in the Technique of Radio Links'
Alta Frequenza Vol.33 No.4 p209-226
26 G Craven, DW Stopp, RR Thomas
Resonant-Slot Hybrid Junction and Channel-Dropping
Filters' Proc IEE Vol12 No.4 P669-80 April 1965

28 AL Saha, HM Barlow
'Channel-Dropping Filters for Millimetre Waves in Circular Waveguide.' Proc IEE Vol.116 No.6 p941-6 June1969

29 WB Weir, DK Adams
'Wideband Multiplexers using Directional Filters' Microwaves Vol.8 No.5 p44-50 May1969

30 Shimada et al.
'Millimetre Wave Directional Filter' MTT-18 No.1 p61-2 Jan 1970

31 U Unrau, H-G Unger
'Quasi Optical Band Splitting Filter with Extended Bandwidth' Proceedings of Conference on Trunk Telecomms. by Guided Wave, IEE 1970 p62-8

32 U Unrau
'Periodic-Band Multiplexer for a TE_{01} Telecomm. System' Arch. Elek. Ubertrag. Vol25 No.1 p56-7 Jan 1971

33 E Kuhn
'Broadband 3-Cavity Ring-Type Channel Dropping Filter' Proc. 1971 Euro. Microwave Conference B12/3 August 1971

34 Chung-li Ren
'Design of a Channel Diplexer for Millimetre Wave Applications' MTT-20 No.12 p820-7 Dec 1972

35 U Unrau
'Bandsplitting Filter in Oversized Rectangular Waveguide' Elect. Lett.Vol.9 No.2 p30-1 25 Jan 1972

36 BK Watson
'A Band-Branching Unit for use over the 32-110 Ghz Band based on Broadband Centre-Excited Couplers' Proc. 1973 Euro. Microwave Conference Vol II B13/4

37 JI Smith, RE Fisher
A Low Loss, Wideband Transmitter Multiplexer.'
1973 IEEE G-MTT Int. Microwave Symposium Digest
p213-3 June 1973
38 E Corli, T Corzani, GB Stracca
'Design and Characteristics of Waveguide Interferential
Branching Filters' Alta Frequenza Vol.42 No.10 p519-28
Oct 1973
39 N Suzuki
'A 40-120 GHz Michelson Interferometer Type Band Splitting
Filter' MTT-22 No.5 p565-6 May 1974
40 AL Saha, RK Singh
'A Channel Dropping Filter for Millimetre Waves in Circ-
ular Waveguide' Indian Journal of Pure and Applied Phys-
ics Vol.11 No.10 p750-4 Oct1973
41 AAM Saleh
'Quasi-Optical Diplexers'
IEEE M/wave Symposium Digest p12-14 June 1974
42 CB Cotner
'Suspended Substrate Stripline Directional Filters for
Receiver Demultiplexing at 4 GHz.' Comsat Tech. Review
Vol5 No.1 p179-98 Spring 1975
43 J Bodonyi
'Channelling Filters for Trunk Waveguide Communication
at Millimetre Wavelengths' Marconi Review Vol36 No.190
1973
44 J Bodonyi
'Development of Channelling Filters for the Millimetre
wave Multiplexing System.' Marconi Review Vol37 No.193
p69-92 1974

45 CS Barham
'Review of Design and Performance of Microwave Multiplexers' Marconi Review Vol35 No.184 1972

46 EA Guillemin
'Synthesis of Passive Networks' John Wiley 1957 p311

47 EL Norton
'Constant Resistance Networks with Applications to Filter Groups' BSTJ Vol.16 p178 1937

48 Guillemin op cit p296

49 RJ Wenzel
'Application of Exact Synthesis Methods to Multichannel Filter Design' MTT-13 No.1 p5-15 Jan 1965

50 HJ Orchard
'Formulae for Ladder Filters'
Wireless Engineer Vol30 p3-5 Jan 1953

51 RJ Wenzel
'Wideband High Selectivity Diplexers Using Digital Elliptic Filters.' MTT-15 No.12 p669-80 Dec 1967

52 GL Matthaei, EG Cristal
'Multiplexer Channel-Separating units using Interdigital and Parallel-Coupled Filters' MTT-13 p328-34 May 1965

53 TA Abele
'A High Quality Waveguide Directional Filter'
BSTJ Vol.46 No.1 p81-104 Jan 1967

54 RD Standley
'Millimetre Wavelength Diplexing Filters using Circular TE_{011} Mode Resonators.'MTT-16 No.1 p50-1 Jan 1968

55 EA Guillemin
'Communication Networks' Vol.2

56 EG Cristal, GL Matthaei
'A Technique for the Design of Multiplexers Having Contiguous Channels' MTT-12 p88-93 Jan 1964
57 RJ Wenzel, WG Erlinger
'Narrowband Contiguous Multiplexing Filters with Arbitrary Amplitude and Delay Responses' Proc. 1976 IEEE MTT-S International M/wave Symposium June 1976 p116-8
58 AE Atia
'Computer Aided Design Of Waveguide Multiplexers' MTT-22 No.3 p332-6 March 1974
59 G Pfitzenmaier
'A Waveguide Multiplexer with Dual Mode Filters for Satellite Use.' Proc 5th Euro. M/wave Conference p407-11 Sept 1975
60 MH Chen, F Assal,C Mahle
'A Contiguous Band Multiplexer'
Comsat Tech. Review Vol6 No.2 Fall 1976
61 Foldes, Thompson
'Waveguide Quadruplexer System'
MTT-9 No.4
62 GL Matthaei, EG Cristal
in 'Advances in Microwaves', 2, editor L Young. Academic Press 1967
63 CK Mok
'Design of Evanescent Mode Waveguide Diplexers' MTT-21 No.1 p43-8 Jan 1973
64 RJ Wenzel
'Printed-Circuit Complementary Filters for Narrow-Bandwidth Multiplexers' MTT-16 No.3 March 1968 p147-157

Chapter 6.

1 JD Rhodes

'Direct Design of Symmetrical Interacting Bandpass Channel Diplexers' IEE Journal of Microwaves, Optics and Acoustics. Vol.1 No.1 September 1976

2 JL Haine, JD Rhodes

'Direct Design Formulas for Asymmetric Bandpass Channel Diplexers' To be published in IEEE Trans. on MTT, October 1977.

Chapter 7.

1 M Dishal

'Alignment and Adjustment of Synchronously Tuned Multiple Resonant Circuit Filters'

Proc. IRE Nov. 1951

Chapter 8.

1 JD Rhodes, op cit [3.1], p154-6

Papers Published.

'New Active Quadrature Phase-Shift Network'
Electronics Letters, 31 March 1977, Vol. 13 No. 7.
p216-218

Haine & Rhodes
'Direct Design Formulas for Asymmetric Bandpass Channel Diplexers'.
IEEE Transactions on MTT, Vol. 25 No. 10. p807-813
October 1977

'Simple Design Procedure for Single-Sideband Crystal Filters.'
Electronics Letters, 10 November 1977, Vol.13 No. 23.
p687-688.

APPENDIX ONE.

```
10 ;"DESIGNS WENZEL TYPE HP/LP DIPLEXER."
20 DIM C(20),L(20),K(20),J(20),A$(80)
25 DIM A(20),D(20),G(20)
30 ;"N,LR?"
40 INPUT N,L
50 E=SQR((10↑(L/20)-1)/2)
60 B=LOG(E+SQR(E*E-1))
70 B=EXP(B/N)
80 B=(B+1/B)↑2/4
85 ;"CROSSOVER FREQUENCY=";SQR(B)
90 E=LOG(E+SQR(E*E+1))/N
100 E=EXP(E)
110 E=(E-1/E)/2
115 P=3.14159
120 FOR I=1 TO N
130 A(I)=SIN((2*I-1)*P/2/N)
140 D(I)=(E*E+SIN(P*I/2/N)↑2)*COS(I*P/2/N)↑2
150 K(I)=1
160 J(I)=1
170 NEXT I
180 G(1)=A(1)/E
190 FOR I=2 TO N
200 G(I)=A(I)*A(I-1)/D(I-1)/G(I-1)
210 C(N+1-I)=G(I)
220 NEXT I
230 C(N)=G(1)
240 FOR I=1 TO N
250 L(I)=1/B/C(I)
260 NEXT I
270 N1=N
280 N2=N
300 ;"F1,DEL.F,F2?"
310 INPUT F1,X,F2
311 ;"PLOT OF LR=1:"
312 INPUT Q
313 ;"SCALE FACTOR?"
314 INPUT D
315 GOSUB 1480
320 M=0
330 F=F1+M*X
340 A1=1
350 A2=0
360 A3=F*C(1)
370 A4=1
380 FOR I=2 TO N1
390 B1=-F*C(I)/K(I-1)
400 B2=1/K(I-1)
410 B3=K(I-1)
420 B4=0
430 S=A1*B1-A2*B3
440 A2=A1*B2+A2*B4
450 A1=S
460 S=A3*B1+A4*B3
470 A4=A4*B4-A3*B2
480 A3=S
```

```
490 NEXT I
500 B1=1
510 B2=0
520 B3=-1/F/L(1)
530 B4=1
540 FOR I=2 TO N2
550 C1=1/J(I-1)/F/L(I)
560 C2=1/J(I-1)
570 C3=J(I-1)
580 C4=0
590 S=B1*C1-B2*C3
600 B2=B1*C2+B2*C4
610 B1=S
620 S=B3*C1+B4*C3
630 B4=B4*C4-B3*C2
640 B3=S
650 NEXT I
660 Z1=(B1*B4+B2*B3)/(B3↑2+B4↑2)
670 Z2=(B2*B4-B1*B3)/(B3↑2+B4↑2)
680 V1=A1+A4*Z1-A3*Z2
690 V2=A2+A4*Z2+A3*Z1
700 S1=((V1+A4)↑2+(V2+A3)↑2)/((V1-A4)↑2+(V2-A3)↑2)
710 V1=(V1+A4)↑2+(V2+A3)↑2
720 S2=4.3429*LOG(V1/4)
730 S1=4.3429*LOG(S1)
731 IF G=1 GOTO 734
732 Y=INT(S2/D+.5)
733 GOTO 735
734 Y=INT(S1/D+.5)
735 IF Y>70 GOTO 738
736 ;"I";TAB(Y),"."
737 GOTO 750
738 ;"I"
750 IF F<F2 GOTO 770
755 GOSUB 1480
760 GOTO 300
770 M=M+1
780 GOTO 330
1480 FOR I=0 TO 6
1490 FOR J=1 TO 10
1500 K=10*I+J
1510 A$(K,K)="*"
1520 NEXT J
1530 K=10*(I+1)
1540 A$(K,K)="I"
1550 NEXT I
1560 ;A$
1570 RETURN
1580 END
BASIC
*
```

```
10 ;"THIS PROGRAM DESIGNS AND ANALYSES A PROTOTYPE DIPLEXER."
20 ;"CHANNEL 1 IS ASSUMED TO HAVE A BANDWIDTH OF 2 RADS/SEC."
30 ;"TYPE IN THE BANDWIDTH OF CHANNEL 2:"
40 INPUT B
45 B=B/2
50 ;"TYPE IN DEGREE& RIPPLE LEVEL OF CH.1."
60 INPUT N1,L1
70 ;"TYPE IN DEGREE & RIPPLE LEVEL OF CH.2."
80 INPUT N2,L2
90 ;"TYPE IN THE BAND SEPARATION."
100 INPUT S
110 A=S/2
120 DIM C(20),D(20),K(20),J(20)
125 DIM A$(80)
130 E=SQR(10↑(L1/10)-1)
140 E=LOG(E+SQR(E*E+1))
150 E=EXP(E/N1)
160 E=.5*(E-1/E)
165 P=3.14159
170 FOR I=1 TO N1
180 C(I)=2*SIN((2*I-1)*P/2/N1)/E
190 IF I=N1 GOTO 210
200 K(I)=SQR(E*E+SIN(I*P/N1)↑2)/E
210 NEXT I
220 E=SQR(10↑(L2/10)-1)
230 E=LOG(E+SQR(E*E+1))
240 E=EXP(E/N2)
250 E=.5*(E-1/E)
260 FOR I=1 TO N2
270 D(I)=2*SIN((2*I-1)*P/2/N2)/E
275 D(I)=D(I)/B
280 IF I=N2 GOTO 300
290 J(I)=SQR(E*E+SIN(I*P/N2)↑2)/E
300 NEXT I
310 C1=C(1)
320 C2=C(2)
330 C3=C(3)
340 K1=K(1)
350 K2=K(2)
360 D1=D(1)
370 D2=D(2)
380 D3=D(3)
390 J1=J(1)
400 J2=J(2)
410 DIM A(20),B(20)
420 A(1)=-C1*(A+1/2/C1/C1/A+(J1↑2/D2-1/C1)/(8*D1↑2*C1*A↑3))
430 A(2)=-C2*(A+K1↑2/(8*C1↑2*C2*D1*A↑3))
440 A(3)=-C3*(A+K1↑2*K2↑2/(32*C1↑2*C2↑2*C3*D1*A↑5))
450 FOR I=4 TO N1
460 A(I)=-C(I)*A
470 NEXT I
480 R1=SQR(1+(1/C1-1/D1)/(4*C1*A↑2)-(J1↑2/D2-1/D1)/(16*C1*D1↑2*A↑4))
```

```
490 T=1-1/4/C1/D1/A↑2
500 T=T-((K1↑2/C2-1/C1-2/D1)/C1+(3*J1↑2/D2-1/D1)/D1)/16/C1/D1/A↑4
510 K(1)=K1*SQR(T)
520 K(2)=K2*SQR(1-K1↑2/(16*C1↑2*C2*D1*A↑4))
530 B(1)=D1*(A+1/2/D1/D1/A+(K1↑2/C2-1/D1)/(8*C1↑2*D1*A↑3))
540 B(2)=D2*(A+J1↑2/(8*D1↑2*D2*C1*A↑3))
550 B(3)=D3*(A+J1↑2*J2↑2/(32*D1↑2*D2↑2*D3*C1*A↑5))
560 FOR I=4 TO N2
570 B(I)=D(I)*A
580 NEXT I
590 R2=SQR(1+(1/D1-1/C1)/(4*D1*A↑2)-(K1↑2/C2-1/C1)/(16*D1*C1↑2*A↑4))
600 T=1-1/4/C1/D1/A↑2
610 T=T-((J1↑2/D2-1/D1-2/C1)/D1+(3*K1↑2/C2-1/C1)/C1)/16/C1/D1/A↑4
620 J(1)=J1*SQR(T)
630 J(2)=J2*SQR(1-J1↑2/16/D1↑2/D2/C1/A↑4)
640 ;"LISTING OF ELEMENT VALUES? (1=YES)"
650 INPUT Q
660 IF Q=1 GOTO 680
670 GOTO 840
680 ;"CHANNEL 1:"
690 ;"R1=";R1
700 ;"CAPACITOR","SUSCEPTANCE","ADMITTANCE INVERTER"
710 FOR I=1 TO N1
720 ;C(I),A(I)
730 IF I=N1 GOTO 750
740 ;" ",," ",K(I)
750 NEXT I
760 ;"CHANNEL 2:"
770 ;"R2=";R2
780 ;"CAPACITOR","SUSCEPTANCE","ADMITTANCE INVERTER"
790 FOR I=1 TO N2
800 ;D(I),B(I)
810 IF I=N2 GOTO 830
820 ;" ",," ",J(I)
830 NEXT I
834 ;"ANNULLING REACTANCE=";X0
840 ;"RESPONSE ANALYSIS: TYPE IN START, STEP, FINISH FREQUENCIES."
850 INPUT F1,D,F2
860 ;"PLOT OF CH.1 RETURN OR INSERTION LOSS? (1=RL.)"
870 INPUT Q
875 GOSUB 1480
880 M=0
890 F=F1+M*D
900 A1=1
910 A2=0
920 A3=F*C(1)+A(1)
930 A4=1
940 FOR I=1 TO N1-1
950 B=A(I+1)+F*C(I+1)
960 K=K(I)
970 B1=-B*A1/K-K*A2
980 B2=A1/K
990 B3=-B*A3/K+K*A4
1000 B4=-A3/K
1010 A1=B1
1020 A2=B2
1030 A3=B3
1040 A4=B4
1050 NEXT I
1060 A1=R1*A1
1070 A2=R1*A2
```

```
1080 A3=A3/R1
1090 A4=A4/R1
1100 B1=1
1110 B2=0
1120 B3=F*D(1)+B(1)
1130 B4=1
1140 FOR I=1 TO N2-1
1150 B=B(I+1)+F*D(I+1)
1160 J=J(I)
1170 C1=-B*B1/J-J*B2
1180 C2=B1/J
1190 C3=-B*B3/J+J*B4
1200 C4=-B3/J
1210 B1=C1
1220 B2=C2
1230 B3=C3
1240 B4=C4
1250 NEXT I
1260 B1=R2*B1
1270 B2=R2*B2
1280 B3=B3/R2
1290 B4=B4/R2
1300 Z1=(B1*B4+B2*B3)/(B3↑2+B4↑2)
1320 V1=A1+A4*Z1-A3*Z2
1330 V2=A2+A3*Z1+A4*Z2
1340 S1=((V1+A4)↑2+(V2+A3)↑2)/((V1-A4)↑2+(V2-A3)↑2)
1342 V1=V1+A4
1343 V2=V2+A3
1350 S2=(V1↑2+V2↑2)/4
1360 IF G=1 THEN 1380
1370 Y=INT(4.3429*LOG(S2))
1375 GOTO 1390
1380 Y=INT(4.3429*LOG(S1))
1390 IF Y>70 GOTO 1410
1400 ;"I";TAB(Y+1),"."
1405 GOTO 1420
1410 ;"I"
1420 IF F<F2 GOTO 1440
1430 GOTO 1460
1440 M=M+1
1450 GOTO 890
1460 GOSUB 1480
1470 GOTO 840
1480 FOR I=0 TO 6
1490 FOR J=1 TO 10
1500 K=10*I+J
1510 A$(K,K)="*"
1520 NEXT J
1530 K=10*(I+1)
1540 A$(K,K)="I"
1550 NEXT I
1560 ;A$
1570 RETURN
1580 END
BASIC
*
```

```
10 ;"THIS PROGRAM DESIGNS AND ANALYSES A SYMMETRICAL DIPLEXER"
20 ;"USING A SERIES ANNULLING INDUCTOR."
30 ;"DEGREE?"
40 INPUT N
50 ;"RIPPLE?"
60 INPUT L
70 ;"BAND SEPARATION?"
80 INPUT S
90 A=S/2
100 E=SQR(10↑(L/10)-1)
110 E=LOG(E+SQR(E*E+1))
120 E=EXP(E/N)
130 E=.5*(E-1/E)
140 P=3.14159
150 DIM C(20),K(20),B(20)
155 DIM A$(80)
160 FOR I=1 TO N
170 C(I)=2*SIN((2*I-1)*P/2/N)/E
175 B(I)=A*C(I)
180 IF I=N THEN 200
190 K(I)=SQR(E*E+SIN(I*P/N)↑2)/E
200 NEXT I
210 C1=C(1)
220 C2=C(2)
230 C3=C(3)
240 K1=K(1)
250 K2=K(2)
260 B(1)=C1*(A+1/4/C1↑2/A+(K1↑2/C2-9/4/C1)/8/C1↑3/A↑3)
270 B(2)=C2*(A+K1↑2/8/C1↑3/C2/A↑3)
280 B(3)=C3*(A+(K1*K2/C1/C2)↑2/32/C3/A↑5/C1)
285 N1=N
290 N=1-7/16/C1↑2/A↑2-(K1↑2/C2-1/C1)/4/C1↑3/A↑4
300 R=SQR(N)
305 N=N1
310 K(2)=K(2)*SQR(1-K1↑2/16/C1↑3/C2/A↑4)
320 K=1-1/2/C1↑2/A↑2-(K1↑2/C2-27/16/C1)/4/C1↑3/A↑4
330 K(1)=K(1)*SQR(K)
340 L2=1/4/C1/A/A
350 ;"LIST OF ELE. VALUES? 1=YES."
360 INPUT Q
370 IF Q=1 GOTO 380
375 GOTO 460
380 ;" CAPACITOR","SUSCEPTANCE","INVERTER"
390 FOR I=1 TO N
400 ;C(I),B(I)
410 IF I=N THEN 430
420 ;" ","  ",K(I)
430 NEXT I
440 ;"INPUT TRANSFORMER=";R
450 ;"SERIES INDUCTOR=";L2
460 ;"F1, DEL. F, F2?"
470 INPUT F1, D, F2
471 ;"SCALE FACTOR?"
472 INPUT G
473 ;"L.R. OR LA? 1=L.R."
474 INPUT Q
475 GOSUB 1480
480 M=0
```

```
490 F=F1+M*D
500 A1=R
510 A2=0
520 A3=(-B(1)+F*C(1))/R
530 A4=1/R
540 FOR I=2 TO N
550 C1=-(F*C(I)-B(I))/K(I-1)
560 C2=1/K(I-1)
570 C3=K(I-1)
580 C4=0
590 S=A1*C1-A2*C3
600 A2=A1*C2+A2*C4
610 A1=S
620 S=A3*C1+A4*C3
630 A4=A4*C4-A3*C2
640 A3=S
650 NEXT I
660 B1=R
670 B2=0
680 B3=(B(1)+F*C(1))/R
690 B4=1/R
700 FOR I=2 TO N
710 C1=-(F*C(I)+B(I))/K(I-1)
720 C2=1/K(I-1)
730 C3=K(I-1)
740 C4=0
750 S=B1*C1-B2*C3
760 B2=B1*C2+B2*C4
770 B1=S
780 S=B3*C1+B4*C3
790 B4=B4*C4-B3*C2
800 B3=S
810 NEXT I
820 Z1=(B1*B4+B2*B3)/(B3↑2+B4↑2)
830 Z2=F*L2+(B2*B4-B1*B3)/(B3↑2+B4↑2)
840 V1=A1+A4*Z1-A3*Z2
850 V2=A2+A4*Z2+A3*Z1
860 S1=((V1+A4)↑2+(V2+A3)↑2)/((V1-A4)↑2+(V2-A3)↑2)
870 V1=(V1+A4)↑2+(V2+A3)↑2
880 S2=4.3429*LOG(V1/4)
890 S1=4.3429*LOG(S1)
895 IF Q=1 GOTO 898
896 Y=INT(G*S2+.5)
897 GOTO 900
898 Y=INT(G*S1+.5)
900 IF Y>70 GOTO 903
901 ;"I";TAB(Y),"."
902 GOTO 910
903 ;"I"
910 IF F<F2 GOTO 930
920 GOTO 950
930 M=M+1
940 GOTO 490
950 GOSUB 1480
955 GOTO 460
```

```
1480 FOR I=0 TO 6
1490 FOR J=1 TO 10
1500 K=10*I+J
1510 A$(K,K)="*"
1520 NEXT J
1530 K=10*(I+1)
1540 A$(K,K)="I"
1550 NEXT I
1560 ;A$
1570 RETURN
1580 END
BASIC
*
```

APPENDIX FOUR.

```
10 ;"THIS PROGRAM DESIGNS AND ANALYSES A LP/HP DIPLEXER."
20 ;"THE LP CHANNEL CUTOFF IS AT 1 RAD/SEC."
30 ;"INPUT HP CUTOFF:"
40 INPUT B
50 ;"LP CHANNEL:N,LR.?"
60 INPUT N1,L1
70 ;"HP CHANNEL:N,LR?"
80 INPUT N2,L2
85 DIM C(20),L(20),K(20),J(20)
86 DIM A$(80)
90 E=SQR(10↑(L1/10)-1)
100 E=LOG(E+SQR(E↑2+1))/N1
110 E=.5*(EXP(E)-EXP(-E))
115 P=3.14159
120 FOR I=1 TO N1
130 C(I)=2*SIN((2*I-1)*P/2/N1)/E
140 K(I)=SQR(E↑2+SIN(I*P/N1)↑2)/E
150 NEXT I
160 E=SQR(10↑(L2/10)-1)
170 E=LOG(E+SQR(E↑2+1))/N2
180 E=.5*(EXP(E)-EXP(-E))
190 FOR I=1 TO N2
200 L(I)=E/2/SIN((2*I-1)*P/2/N2)/B
210 J(I)=SQR(E↑2+SIN(I*P/N2)↑2)/E
220 NEXT I
230 L1=L(1)
240 C1=C(1)
250 K=SQR(1+2*L1/C1)
260 L(1)=L1/K
270 C(1)=C1*K
280 C(2)=C(2)+K(1)↑2*(C(1)-C1)↑2/2/C(1)
290 L(2)=1/(1/L(2)+J(1)↑2*L(1)*(1/L(1)-1/L1)↑2/2)
300 ;"F1,DEL.F,F2?"
310 INPUT F1,X,F2
311 ;"PLOT OF LR=1:"
312 INPUT Q
313 ;"SCALE FACTOR?"
314 INPUT D
315 GOSUB 1480
320 M=0
330 F=F1+M*X
340 A1=1
350 A2=0
360 A3=F*C(1)
370 A4=1
380 FOR I=2 TO N1
390 B1=-F*C(I)/K(I-1)
400 B2=1/K(I-1)
410 B3=K(I-1)
420 B4=0
430 S=A1*B1-A2*B3
440 A2=A1*B2+A2*B4
450 A1=S
460 S=A3*B1+A4*B3
470 A4=A4*B4-A3*B2
480 A3=S
```

```
490 NEXT I
500 B1=1
510 B2=0
520 B3=-1/F/L(1)
530 B4=1
540 FOR I=2 TO N2
550 C1=1/J(I-1)/F/L(I)
560 C2=1/J(I-1)
570 C3=J(I-1)
580 C4=0
590 S=B1*C1-B2*C3
600 B2=B1*C2+B2*C4
610 B1=S
630 B4=B4*C4-B3*C2
640 B3=S
650 NEXT I
660 Z1=(B1*B4+B2*B3)/(B3↑2+B4↑2)
670 Z2=(B2*B4-B1*B3)/(B3↑2+B4↑2)
680 V1=A1+A4*Z1-A3*Z2
690 V2=A2+A4*Z2+A3*Z1
700 S1=((V1+A4)↑2+(V2+A3)↑2)/((V1-A4)↑2+(V2-A3)↑2)
710 V1=(V1+A4)↑2+(V2+A3)↑2
720 S2=4.3429*LOG(V1/4)
730 S1=4.3429*LOG(S1)
731 IF G=1 GOTO 734
732 Y=INT(S2/D+.5)
733 GOTO 735
734 Y=INT(S1/D+.5)
735 IF Y>70 GOTO 738
736 ;"I";TAB(Y),"."
737 GOTO 750
738 ;"I"
750 IF F<F2 GOTO 770
755 GOSUB 1480
760 GOTO 300
770 M=M+1
780 GOTO 330
1480 FOR I=0 TO 6
1490 FOR J=1 TO 10
1500 K=10*I+J
1510 A$(K,K)="*"
1520 NEXT J
1530 K=10*(I+1)
1540 A$(K,K)="I"
1550 NEXT I
1560 ;A$
1570 RETURN
1580 END
BASIC
*
```

```
10 ;"THIS PROGRAM DESIGNS A BROADBAND INTERDIGITAL FILTER"
20 ;"USING APPROXIMATE MODIFICATIONS."
30 ;"N,LR?"
40 INPUT N,L
50 DIM C(20),K(20)
55 DIM A$(80)
60 E=SQR(10↑(L/10)-1)
70 E=LOG(E+SQR(E↑2+1))/N
80 E=EXP(E)
90 E=.5*(E-1/E)
100 ;"CUTOFF ELECTRICAL LENGTH (DEGREES)?"
110 INPUT W
120 P=3.14159
130 W=1/SIN(W*P/180)
140 FOR I=1 TO N
150 C(I)=2*SIN((2*I-1)*P/2/N)/E
160 K(I)=SQR(E↑2+SIN(I*P/N)↑2)/E
170 NEXT I
180 C(N)=C(1)*SQR(1+1/2/W↑2/C(1)↑2)
190 C(N-1)=C(2)+K(1)↑2*(C(N)-C(1))
200 C(1)=C(N)
210 C(2)=C(N-1)
211 FOR I=1 TO N
212 C(I)=C(I)*W
213 NEXT I
220 ;"F1,DEL.F,F2?"
230 INPUT F1,D,F2
270 GOSUB 1480
280 M=0
290 F=F1+M*D
300 C=COS(F*P/180)
310 S=SIN(F*P/180)
320 A1=1
330 A2=0
340 A3=C(1)*S
350 A4=1
360 FOR I=2 TO N
370 B1=-C(I)*S/K(I-1)
380 B2=1/K(I-1)
390 B3=K(I-1)
400 B4=0
410 X=A1*B1-A2*B3
420 A2=A1*B2+A2*B4
430 A1=X
440 X=A3*B1+A4*B3
450 A4=A4*B4-A3*B2
460 A3=X
470 NEXT I
480 A2=A2*C
490 A3=A3/C
500 S=((A1+A4)↑2+(A2+A3)↑2)/((A1-A4)↑2+(A2-A3)↑2)
510 Y=INT(.5+4.3429*LOG(S))
520 IF Y>70 GOTO 550
540 ;"I";TAB(Y),"."
545 GOTO 560
```

```
550 ;"I"
560 IF F>F2 GOTO 600
570 M=M+1
580 GOTO 290
600 GOSUB 1480
610 GOTO 220
1480 FOR I=0 TO 6
1490 FOR J=1 TO 10
1500 K=10*I+J
1510 A$(K,K)="*"
1520 NEXT J
1530 K=10*(I+1)
1540 A$(K,K)="I"
1550 NEXT I
1560 ;A$
1570 RETURN
1580 END
BASIC
*
```

APPENDIX SIX.

```
10 ;"DESIGN AND ANALYSIS OF WAVEGUIDE DIPLEXER."
12 ;"VERSION NO. 3 11/5/77 WITH 4'TH&5'TH ORDER CORRECTIONS."
20 GOTO 800
21 ;"PLOT OF INSERTION(=1) OR RETURN(=0) LOSS?"
22 INPUT Q1
31 ;"ENTER START, STEP, FINISH FREQUENCIES:"
32 INPUT F1, D, F2
33 GOSUB 670
34 M=0
35 F=F1+M*D
36 L=.3/SQR(F*F-T)
45 Q=-.5*ATN(2/B1(1))*L1/L
50 A1=COS(Q)
60 A2=SIN(Q)
70 A3=A2
80 A4=A1
90 FOR I=1 TO N1
100 C=COS(C1(I)*L1/L)
110 S=SIN(C1(I)*L1/L)
120 B=B1(I)*L/L1
130 A=A1*C-A2*(S-B*C)
140 A2=A1*S+A2*(B*S+C)
150 A1=A
160 A=A3*C+A4*(S-B*C)
170 A4=A4*(B*S+C)-A3*S
180 A3=A
190 NEXT I
200 B=B1(N1+1)*L/L1
210 A1=A1+A2*B
220 A3=A3-B*A4
230 Q=-.5*ATN(2/B(1))*L2/L
240 B1=COS(Q)
250 B2=SIN(Q)
260 B3=B2
270 B4=B1
280 FOR I=1 TO N2
290 C=COS(C(I)*L2/L)
300 S=SIN(C(I)*L2/L)
310 B=B(I)*L/L2
320 A=B1*C-B2*(S-B*C)
330 B2=B1*S+B2*(B*S+C)
340 B1=A
350 A=B3*C+B4*(S-B*C)
360 B4=B4*(B*S+C)-B3*S
370 B3=A
380 NEXT I
390 B=B(N2+1)*L/L2
400 B1=B1+B*B2
410 B3=B3-B*B4
550 Z1=(B1*B4+B2*B3)/(B3*B3+B4*B4)
560 Z2=(B2*B4-B1*B3)/(B3*B3+B4*B4)
565 X=X0*(L1+L2)/2/L
570 V1=A1+A4*Z1-A3*(Z2+X)
580 V2=A2+A3*Z1+A4*(Z2+X)
590 S1=((V1+A4)↑2+(V2+A3)↑2)/((V1-A4)↑2+(V2-A3)↑2)
600 V1=V1+A4
610 V2=V2+A3
```

```
620 S2=(V1↑2+V2↑2)/4
630 Y=INT(4.3429*LOG(S1))
631 X=INT(4.3429*LOG(S2))
632 IF 01=0 GOTO 634
633 Y=X
634 IF Y>70 GOTO 638
635 ;"I";TAB(Y),"."
636 GOTO 640
638 ;F,Y
640 M=M+1
650 IF F<F2 GOTO 35
652 GOSUB 670
655 GOTO 21
670 FOR I=0 TO 6
680 FOR J=1 TO 10
690 K=10*I+J
700 A$(K,K)="*"
710 NEXT J
720 K=10*I+10
730 A$(K,K)="I"
740 NEXT I
750 ;A$
760 RETURN
770 E=SQR(10↑(L/10)-1)
772 E=LOG(E+SQR(E*E+1))/N
774 E=EXP(E)
776 E=.5*(E-1/E)
778 FOR I=1 TO N
780 Y(I)=2*SIN((2*I-1)*P/2/N)/E/A
782 Y(I)=Y(I)-A*(E*E+SIN(I*P/N)↑2)/(4*E*SIN((2*I+1)*P/2/N))
784 Y(I)=Y(I)-A*(E*E+SIN((I-1)*P/N)↑2)/(4*E*SIN((2*I-3)*P/2/N))
786 NEXT I
788 FOR I=1 TO N-1
790 K(I)=SQR(E*E+SIN(I*P/N)↑2)/E
792 NEXT I
794 RETURN
800 REM                              ..............THE PROGRAM STARTS
810 DIM A$(80),B(40),C(40),B1(40),C1(40)
820 DIM Y(40),K(40),Y1(40),K1(40),Y2(40),K2(40)
830 ;"WAVEGUIDE WIDTH?"
840 INPUT T
850 T=(5.906/T)↑2
860 P=3.14159
870 ;"CHANNEL 1: F1,F2,DEGREE,RIPPLE?(HF. CHANNEL!)"
880 INPUT F1,F2,N1,R1
890 L1=.3/SQR(F2*F2-T)
900 L2=.3/SQR(F1*F1-T)
910 X=P*(L2-L1)/(L2+L1)
920 X=1/(1/X+X/6)
930 A=X
940 L=R1
950 N=N1
960 GOSUB 770
970 FOR I=1 TO N1
980 Y1(I)=Y(I)*A
990 IF I=N1 GOTO 1010
1000 K1(I)=K(I)
1010 NEXT I
1020 ;"CHANNEL 2: F1,F2,DEGREE,RIPPLE?(LF. CHANNEL)"
1030 INPUT F1,F2,N2,R2
1040 L3=.3/SQR(F2↑2-T)
```

```
1050 L4=.3/SQR(F1*F1-T)
1060 Y=P*(L4-L3)/(L4+L3)
1070 Y=1/(1/Y+Y/6)
1080 A=Y
1090 L=R2
1100 N=N2
1110 GOSUB 770
1120 FOR I=1 TO N2
1130 Y2(I)=Y(I)*X
1140 IF I=N2 GOTO 1160
1150 K2(I)=K(I)
1160 NEXT I
1170 S=(L3+L4-L1-L2)/2
1171 B=L2-L1
1172 L1=(L1+L2)/2
1174 L2=(L3+L4)/2
1180 A=S/B
1190 D1=Y1(1)
1200 D2=Y1(2)
1205 D3=Y1(3)
1220 C2=Y2(2)
1225 C3=Y2(3)
1230 E1=1/(2*D1*D1*A*A)+1/(8*C1*C1*D1*A↑4)*(K2(1)↑2/C2-1/D1)
1235 E1(1)=-S*P/2/L1*E1
1240 E1(2)=-S*P*K1(1)↑2/(16*L1*D1*D1*D2*C1*A↑4)
1245 E1(3)=K1(1)↑2*K1(2)↑2/(32*D1↑2*D2↑2*D3*C1*A↑6)
1246 E1(3)=-S*P*E1(3)/2/L1
1250 E2=1/(2*C1*C1*A*A)+1/(8*D1*D1*C1*A↑4)*(K1(1)↑2/D2-1/C1)
1255 E2(1)=S*P/2/L2*E2
1260 E2(2)=S*P*K2(1)↑2/(16*L2*C1*C1*C2*D1*A↑4)
1262 E2(3)=K2(1)↑2*K2(2)↑2/(32*C1↑2*C2↑2*C3*D1*A↑6)
1263 E2(3)=S*P*E2(3)/2/L2
1265 X0=(1/D1-1/C1)/2/A
1266 X0=-X0
1270 R1=1+(1/D1-1/C1)/(4*D1*A*A)
1272 R1=R1-(K2(1)↑2/C2-1/C1)/(16*C1↑2*D1*A↑4)
1274 R1=SQR(R1)
1280 R2=1+(1/C1-1/D1)/(4*C1*A*A)
1282 R2=R2-(K1(1)↑2/D2-1/D1)/(16*D1↑2*C1*A↑4)
1284 R2=SQR(R2)
1290 Z=1-1/(4*C1*D1*A*A)
1291 X1=(K1(1)↑2/D2-1/D1-2/C1)/4/D1+(3*K2(1)↑2/C2-1/C1)/4/C1
1292 X1=-X1/4/C1/D1
1300 X2=(K2(1)↑2/C2-1/C1-2/D1)/4/C1+(3*K1(1)↑2/D2-1/D1)/4/D1
1301 X2=-X2/4/D1/C1
1303 Y1=(-1)*K1(1)↑2/(16*D1↑2*D2*C1)
1304 Y2=(-1)*K2(1)↑2/(16*C1↑2*C2*D1)
1305 K1(1)=K1(1)*SQR(Z+X1/A↑4)
1306 K1(2)=K1(2)*SQR(1+Y1/A↑4)
1307 K2(1)=K2(1)*SQR(Z+X2/A↑4)
1308 K2(2)=K2(2)*SQR(1+Y2/A↑4)
1320 Y1(1)=Y1(1)/R1/R1
1330 Y2(1)=Y2(1)/R2/R2
1340 K1(1)=K1(1)/R1
1350 K2(1)=K2(1)/R2
1360 K1(0)=1
1370 K1(N1)=1
1380 K2(0)=1
1390 K2(N2)=1
1400 Y1(0)=X
```

```
1410 Y1(N1+1)=X
1420 Y2(0)=X
1430 Y2(N2+1)=X
1440 FOR I=0 TO N1
1450 Y=SQR(Y1(I)*Y1(I+1))/X/K1(I)
1460 B1(I+1)=Y-1/Y
1470 IF I=0 GOTO 1510
1480 C1(I)=P-.5*(ATN(2/B1(I))+ATN(2/B1(I+1)))
1490 IF I>=4 GOTO 1510
1500 C1(I)=C1(I)+E1(I)
1510 NEXT I
1540 FOR I=0 TO N2
1550 Y=SQR(Y2(I)*Y2(I+1))/X/K2(I)
1560 B(I+1)=Y-1/Y
1570 IF I=0 GOTO 1610
1580 C(I)=P-.5*(ATN(2/B(I))+ATN(2/B(I+1)))
1590 IF I>=4 GOTO 1610
1600 C(I)=C(I)+E2(I)
1610 NEXT I
1612 ;"PRINTOUT OF VALUES? 1=YES"
1614 INPUT Q
1616 IF Q=1 GOTO 1620
1618 GOTO 21
1620 ;"CH. 1:MIDBAND GUIDE WAVELENGTH=";L1*100;"CMS."
1630 ;"SUSC.","LENGTH"
1640 FOR I=1 TO N1+1
1650 ;B1(I)
1660 IF I=N1+1 GOTO 1680
1670 ;" ",C1(I)*L1*6.2659
1680 NEXT I
1690 ;"CH. 2:MIDBAND GUIDE WAVELENGTH=";L2*100;"CMS."
1700 ;"SUSC","LENGTH"
1710 FOR I=1 TO N2+1
1720 ;B(I)
1730 IF I=N2+1 GOTO 1750
1740 ;" ",C(I)*L2*6.2659
1750 NEXT I
1770 ;"ANULLING REACTANCE=";X0
1780 GOTO 21
1790 END
BASIC
*CLOSE1
*
```